Quantitative aspects of affinity adsorption

Mayes, Andrew Geoffrey

Award date:
1992

Awarding institution:
University of Bath

QUANTITATIVE ASPECTS OF AFFINITY ADSORPTION

submitted by **ANDREW GEOFFREY MAYES**

for the degree of PhD

of the University of Bath

1992

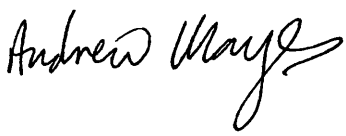

ProQuest LLC
789 East Eisenhower Parkway
P.O. Box 1346
Ann Arbor, MI 48106-1346

ACKNOWLEDGEMENTS

I should like to thank my supervisors Dr. Robert Eisenthal and Dr. John Hubble who allowed me freedom to roam but were always available with help, advice and encouragement when I became lost. Their complementary skills and characteristics provided an excellent environment in which to grow and learn.

My thanks are also due to the Biochemistry Department as a whole for providing a happy environment in which to work, and to its technical staff in particular for their help in finding solutions to many problems, both large and small.

I should also like to acknowledge the generosity of the Department of Chemical Engineering in making equipment available to me, and the S.E.R.C. for providing financial support with grant GR/E 32717 and an instant studentship award.

DEDICATION

To my family

for their constant support and encouragement

ABSTRACT

This thesis addresses two aspects of ligand density effects in affinity adsorption.

Theory (Hubble (1987) Biotech. Bioeng. **30** 208 - 215) predicted that small but finite concentrations of free ligand should enhance the binding of a positively cooperative protein to an immobilised ligand. This was investigated experimentally using two model systems.

i) With yeast glyceraldehyde-3-phosphate dehydrogenase binding to immobilised NAD^+ or AMP Sepharose matrices no evidence for enhanced binding was apparent as NAD^+ concentration was increased. Using an AMP cellulose matrix, however, an approximately 4 fold enhancement was observed. Possible explanations for the differing behaviour of the cellulose and Sepharose matrices are discussed.

ii) With bovine liver fructose bisphosphatase binding to phosphocellulose matrices, no evidence for enhancement of binding was observed as a function of AMP concentration, using frontal analysis to measure capacity.

The second aspect explored is the effect of immobilised ligand density on protein binding characteristics for ligands immobilised on soluble polymers. The binding of lysozyme to Cibacron Blue 3G - dextran conjugates was used as a model system.

Dye-dextran conjugates with different ligand densities were synthesised and characterised. Methods were developed using gel-permeation chromatography and spectral titration to enable liquid phase protein adsorption isotherms to be measured. Results for lysozyme binding indicated that no steric hindrance occurred even at the highest dye density tested (1 dye residue per 16 glucosyl residues) hence a constant fraction of the immobilised dye bound specifically to lysozyme regardless of dye density. The operational affinity of conjugates for lysozyme increased with increasing dye density. The possible mechanisms for this effect and its implications are

discussed.

The effect of buffer composition and ionic strength on lysozyme binding to dye dextran-conjugates was also investigated, and preliminary data is presented to demonstrate the feasibility of using spectral titration for kinetic as well as equilibrium studies of protein binding.

TABLE OF CONTENTS

CHAPTER 5

CHAPTER 1

A BRIEF HISTORICAL PERSPECTIVE

The early history of affinity chromatography might be considered more as one of affinity adsorption and dates back to the study of the effect of chloride ion on amylase, both free and bound to starch particles, by Starkenstein (1910). It was probably better demonstrated by Ambard (1921) who observed a selective removal of amylase from solution by starch particles and Holmbergh (1933) who found that α-amylase was adsorbed by starch particles in aqueous ethanol whereas β-amylase was not. These observations were used by Hockenhull and Herbert (1944) to achieve a 300 fold purification of amylase from *Clostridium acetobutylicum*. This was one of the earliest examples of deliberate purification using bio-specific adsorption and it was rapidly realised that the technique had general utility if an insoluble substrate was available. Thus Lineweaver *et al.* (1949) achieved a purification of polygalacturonidase by adsorption/desorption using alginic acid, Schwimmer and Balls (1949) purified malt α-amylase on wheat starch and purified porcine elastase was obtained using powdered elastin (Grant and Robbins 1957; Hall 1957).

A major advance was made by Campbell *et al.* (1951) with the deliberate synthesis of an insoluble adsorbent by immobilising a protein antigen on cellulose particles in order to purify the corresponding anti-protein antibodies. This report should have been a watershed for the technique and two reviews from 1953 attest to the growing understanding of its mechanism and importance. Taylor (1953) wrote of amylase purification on starch:

> "....to test the attractive suggestion that the adsorption is related to the same forces which operate in the attraction of the enzyme for its substrate. Further extension of this work would be highly desirable. Insoluble polymers, of known composition, should prove to be

particularly suitable for the separation of proteins with specific 'affinities' ".

Zittle (1953) demonstrated a clear vision of the emerging method of affinity chromatography when he wrote:

> "....It would be desirable to have an adsorbent of absolute specificity such that a single adsorption would suffice to remove the wanted protein from a mixture... The binding of substrate and enzyme which is highly specific might provide the desired specific forces. It would be necessary to have a solid resemble the substrate sufficiently so that it could be the site of enzyme-substrate bonding and yet useable under conditions that it would not be altered by the enzyme."

A contemporaneous report by Lerman (1953) attests to the validity of this vision. Mushroom Tyrosinase was purified using a substrate analogue covalently coupled to cellulose and is the first report of the deliberate chemical synthesis of an enzyme specific adsorbent.

While the technique of Campbell continued to be used in immunological research (Silman and Katchalski, 1966) the work of Lerman appears to have been overlooked for a number of years and it was not until the early 1960's that McCormick's group reported the preparation of flavin-cellulose to purify rat liver flavokinase (Arsenis and McCormick, 1964). They extended this work (Arsenis and McCormick, 1966) by preparing a flavin-phosphate cellulose to purify several flavin mononucleotide-dependent enzymes, the first example of the use of a 'group specific' adsorbent.

The paper by Axén *et al.* (1967) on the activation of polysaccharides using cyanogen halides, together with the availability of beaded agarose (Hjerten, 1964)) heralded a new era in affinity chromatography and the simplicity of the method made it easily accessible to those with little knowledge of synthetic organic chemistry. This resulted in an explosion of interest in the technique in the early 1970's where the groundwork in the understanding of the parameters affecting the performance of affinity

separations was laid.

In the preface to their book on affinity Chromatography Lowe and Dean (1974a) stated:

> "The inherent advantages of this technique over classical procedures have resulted in an extremely diverse literature, the exponential growth of which must surely present a daunting task to any worker in this field."

The volume of literature is indeed daunting. Nishikawa (1983) published a brief review of the reviews on affinity chromatography and the table has 70 entries up to 1981. I cannot hope, therefore, to be comprehensive in these introductory chapters and have, instead, tried to select for discussion those aspects of the technique which impinge most directly on the experimental work presented in later chapters.

More comprehensive reviews can be found in Cuatrecasas and Anfinson (1971), Jakoby and Wilchek (1974), Lowe and Dean (1974a), Mosbach *et al.* (1976), Turkova (1978), Scouten (1981), Yang and Tsao (1982), Dean *et al.* (1985) and Horvath (1988).

CHAPTER 2

SOME PARAMETERS AFFECTING THE PERFORMANCE OF AFFINITY MATRICES

2.1 The Composition and Properties of the Support Matrix

In order to provide an appropriate support for ligand immobilisation a matrix must possess a number of properties. The essential properties of an ideal matrix can be summarised as follows:

i) High permeability and large surface area

ii) A physical structure with good hydrodynamic properties

iii) negligible non-specific protein adsorption to, or denaturation by, the matrix surface

iv) high density of chemically derivatisable groups

v) physical and chemical stability under conditions required for derivatisation and operation including resistance to microbial and enzymatic degradation.

To date no matrix has been designed which combines all of the above properties so in practice a compromise has to be reached by selecting a matrix which has the best combination of properties for a particular application. The structure and properties of those matrices used in this thesis will be briefly reviewed here. Much more detailed considerations of available matrices and their properties can be found in a number of books on affinity chromatography (Lowe and Dean, 1974a; Turkova, 1978a; Scouten, 1981a; Dean *et al.*, 1985a) and in commercial product guides.

Cellulose

This is a naturally occurring linear β-1,4-D-glucan with occasional 1-6 linkages. Its structure is dominated by hydrogen bonding which causes chain aggregation into linear sheets which also bond to one another by Van der Waals interactions to form three dimensional elementary fibrils. Cellulose fibres are composed of bunches of such fibrils which aggregate randomly but with their axes running approximately along the fibre axis. Chain-end dislocations and irregular branch points lead to less ordered amorphous regions which show higher reactivity towards activating chemicals (Krassig, 1985). The extent of amorphous regions depends on the source and treatment of the cellulose which thus shows batch-to-batch variability. Due to the high degree of hydrogen bonding on accessible fibrilar surfaces cellulose is highly resistant to chemical attack, with the exception of strong acids and reducing agents, except at sites of dislocations and in amorphous regions. This tends to lead to low levels of derivatisation at widely spaced substitution sites (Kremer and Tabb, 1989). Cellulose has good hydrophillic character, but the lack of porosity and structural uniformity and non-ideal particle shape make it generally unsatisfactory in comparison with modern alternatives. The introduction of regenerated beaded cellulose matrices (Chen and Tsao, 1976;1977) has partially overcome some of these objections. It has considerable importance in the history and development of affinity chromatography, however, and is still widely used as a low cost ion exchanger.

Agarose

This is an alternating linear polymer of 1-3 linked β-D-galactopyranose and 2-4 linked 3-6-anhydro-α-L-galactopyranose. It is a natural product extracted from certain seaweeds and marine algae. It is readily formed into uniform spherical particles of a desired size (Hjerten, 1964) which show excellent porosity and very low non-specific adsorption. The much more open structure renders it much more reactive than cellulose for derivatisation although this can be complicated by its incompatibility with many organic solvents. Indeed its major drawback is its sensitivity to organic and chaotropic solvents, and heat, which break down the hydrogen-bonds holding the triple helix agarose strands together in a three dimensional network. This causes the structure to collapse and the beads to solubilise. This tendency can be greatly reduced

by covalent cross linking using epichlorohydrin (Porath *et al.*, 1971) which yields much more rigid but still highly permeable gels, such as the Sepharose products of Pharmacia. These have excellent general properties, hence their ubiquitous use at laboratory scale but their lack of resistance to high pressures and flow rates renders them less attractive for industrial scale operations. To try to overcome this problem Superose was introduced. This has uniform small particle size and is highly cross-linked rendering it more rigid and greatly improving its hydrodynamic properties.

Dextran

Dextran is an α-1,6-D-glucopyranose polymer with occasional α-1,3 linked branches produced by fermentation of *Leuconostoc mesenteroides* and other related species with sucrose used as carbon source. About 5% of the total residues appear as branches, around 85% of which are short, consisting of only one or two residues. The remaining 15% have an average length of 33 with a maximum of about 50 (Sidebotham, 1974). Crude dextran has a molecular weight of about 50 million. Lower molecular weight fractions are produced by partial acid, base or enzyme hydrolysis or various physical methods. Due to the flexibility of the α-1,6 bond soluble dextran forms random coil structures in solution.

Cross linked dextran gels would be attractive candidates for an affinity support as they possess most of the required characteristics and are more hydrophillic and more chemically stable than agarose. Unfortunately, rigidity can only be obtained by sacrificing porosity due to the high degree of cross-linking required. This renders porous gels hydrodynamically weak and inferior to agarose for affinity applications although they are useful in gel-permeation chromatography due to their well defined exclusion characteristics.

2.2 Activation Chemistry

The lack of a simple and reliable method for the activation of available matrices was undoubtedly one of the main reasons why affinity chromatography was not used more widely following the pioneering work of Lerman and McCormick. It was following the publication of the cyanogen bromide method of Axen *et al.* (1967) that the sudden explosion of interest in the technique occurred. This method has subsequently been modified and improved (Wilchek *et al.*, 1984) and is probably still the most widely used activation protocol. It is very successful for immobilisation of proteins which bind via exposed surface groups (usually lysine and cysteine residues) to several matrix sites but has a drawback for small ligands since the mainly isourea linkages formed are not especially stable to hydrolysis. This leads to a slow but finite leakage of ligand from the column (Tesser *et al.*, 1972) and can lead to major problems in, for example, purification of hormone receptor proteins (Sica, 1973) and manufacture of therapeutic products. Leakage is discussed by Turkova (1978c).

Cyanogen bromide activation does not provide a universally applicable method for ligand immobilisation and many alternative methods have been introduced. With a few exceptions such as periodate oxidation of vicinal diols and the addition reaction with divinylsulphone (Porath *et al.*, 1975) these methods essentially fall into two groups, acylation reactions and alkylation reactions. The former includes use of carbonyldiimidazole (Bethell *et al.*, 1979), and activated sulphonyl chlorides such as tresyl chloride and tosyl chloride (Nilsson and Mosbach, 1980). Alkylations include reactions with epihalohydrins (Porath *et al.*, 1971), haloacetates (Sober and Peterson, 1954), bisoxiranes (Sundberg and Porath, 1974) and halotriazines (Kay and Crook, 1967; Hodgins and Levy, 1980). Halotriazines are worthy of especial mention since, as well as providing an activation mechanism in their own right, they also form the basis of the direct coupling of triazine dyes used in dye ligand chromatography (see chapter 4). Activation and coupling chemistry is discussed in many books and reviews on affinity chromatography including Jackoby and Wilchek (1974), Lowe and Dean (1974c), Turkova (1978b), Scouten (1981b), Dean *et al.* (1985b), Horvath (1988b).

2.3 Spacer Arms

The need for spacer arms to project immobilised ligands away from the matrix surface was recognised early in the development of affinity chromatography (Cuatrecasas *et al.*, 1968; Cuatrecasas, 1970). The optimum length of the spacer was systematically investigated by Lowe *et al.* (1973a) using homologous series of ATP and NAD^+ derivatives with increasing numbers of methylene groups in the spacer. They found that the optimum was 6 - 8 carbon atoms (about 1nm), with higher molecular weight enzymes requiring longer spacers than those of lower molecular weight. Enzymes with weaker affinity for the ligand also required longer spacers. Using glycine oligomers as spacers for NAD^+ showed essentially no difference in binding strength in the series glycine to tetraglycine for lactate dehydrogenases (Lowe and Dean, 1974b). This may be due to increased hydrophillicity or rigidity compared with oligomethylene spacers and it emphasises the importance of the nature as well as the length of the spacer.

It is now recognised that the nature of the spacer may cause considerable modulation of the affinity interaction. The classic example of this is the work of Steers *et al.* (1971) who found that a very long (2.1nm) spacer was optimal when purifying β-galactosidase on p-aminophenylthiogalactoside, giving very tight binding and preventing bio-elution. O'Carra *et al.* (1973) showed that a very similar interaction occurred with a matrix containing the spacer alone and attributed the tight binding to a non-biospecific interaction between protein and spacer. Hence the apparent benefit of a long spacer had little to do with steric effects as surmised by Steers. Such specific hydrophobic interaction of proteins with spacers was used by Er-el *et al.* (1972) to purify phosphorylase b. They prepared a homologous series of alkyl matrices and found that the enzyme was retarded by the C_3 derivative, bound by the C_4 derivative and irreversibly adsorbed by the C_6 derivative such that recovery could only be achieved with denaturing buffers. A number of other enzymes were not retained by these adsorbents. That such hydrophobic interactions contributed to binding in affinity chromatography was confirmed by Barry and O'Carra (1973) who investigated binding of dehydrogenases to a variety of hydrophillic and hydrophobic

spacers. These gave varying results for different enzymes which was interpreted in terms of specific and non-specific interactions. It was work on the hydrophobic binding of proteins to ligand spacers used in affinity chromatography which lead to the realisation that this process was specific but non-bioselective and that it could provide a useful technique in its own right, that of hydrophobic interaction chromatography.

2.4 The Choice and Orientation of the Ligand

The choice of an appropriate ligand is dictated firstly by the need for a molecule that shows a high degree of bio-selectivity for the target protein and binds with high affinity. This may show unique specificity for a particular protein but in general the so-called 'group selective' ligands i.e. those which bind a wide range of related proteins are more popular, since this avoids the need to synthesise a new matrix for the purification of each protein. These include cofactors or their derivatives such as NAD^+ and AMP, various lectins (for particular groups of glycoproteins) and synthetic 'pseudo-ligands' such as the much used dye-ligands. Nucleotide and triazine dye ligands are discussed in chapter 4. With group selective ligands some selectivity is achieved during adsorption with the remainder coming from careful choice of elution conditions including consideration of mechanistic details such as ternary complex formation.

The orientation in which the ligand is coupled to the spacer is clearly crucial to the successful design of an affinity adsorbent. It is essential that those groups on the ligand involved in the 'docking' to the protein should be unimpeded in order to alter the nature of the interaction as little as possible. Also required is a chemical group susceptible to attack, not intimately involved in protein binding, which can be used for ligand attachment. If the nature of the binding site is unknown then this information must be obtained by trial and error using ligand binding and/or enzyme kinetic methods.

Orientation effects are probably best exemplified by work with nucleotide ligands for dehydrogenase and kinase purification. It has been shown that such ligands coupled via N^6 and to a lesser extent C^8 of the adenine moiety are generally more effective than those coupled via the ribose or phosphate. This work has been reviewed by Scouten (1981d), and the empirical observations have been rationalised by X-ray diffraction studies which show that the adenine moiety is the least constrained part of the molecule when nucleotides bind to the nucleotide cleft of dehydrogenases (Branden and Eklund, 1980). The need for immobilised cofactors both for purification and as active and regeneratable entities in enzyme biotransformations has lead to a large base of literature on the chemical derivatisation and coupling of nucleotide cofactors. This has recently been reviewed by Buckmann and Carrea (1989).

2.5 Immobilised Ligand Density

From a simple quantitative consideration of affinity chromatography (see equation 8 of chapter 3) it is clear that for a system with low affinity eg. $K_d = 1 \times 10^{-3}M$ an immobilised ligand concentration approaching $1 \times 10^{-2}M$ would be required in order to achieve sufficient retardation to separate the required product from the tail of the non-adsorbed protein (10 column volumes for this calculation). $1 \times 10^{-2}M$ is roughly the upper limit of practically achievable ligand densities (at least for beaded agarose supports); hence if 10 column volumes is assumed to be the minimum retardation required then an interaction with a K_d of $10^{-3}M$ represents the lowest affinity interaction for which an effective affinity adsorbent can be designed.

It is generally assumed that the highest achievable ligand density is desirable in all cases since this will tend to tip the equilibrium between free and bound protein in favour of the bound state and increase the apparent affinity of the interaction. This was observed by Harvey *et al.* (1974) for lactate dehydrogenase binding to AMP-Sepharose with different ligand concentrations. They also noted that ligand distribution was important since Sepharose with a high ligand density diluted with blank Sepharose bound lactate dehydrogenase more tightly than did uniformly

distributed ligand with the same bulk-average concentration.

Since a dynamic equilibrium is set up as the enzyme passes down a column the geometry of the column is also important. With high affinity systems binding is tight and bed height is of little importance. In this case a short bed is preferable due to increased flow rates etc.. With low affinity systems a large bed height is preferable to maximise protein ligand interactions (Lowe *et al.*, 1974).

Contrary to expectation the highest achievable ligand density is not always desirable and can lead to a variety of problems. Such a problem was experienced by Kalderon *et al.* (1970) and Schmidt and Raftery (1973). Both these groups were using positively charged ligands, quaternary ammonium compounds, to purify acetylcholine binding proteins.

Kalderon purified acetylcholinesterase on a column containing 0.16 μmoleml^{-1} ligand and achieved acceptable results. When the ligand density was increased however, the specific activity of the product progressively decreased, presumably due to the ligand acting as an anion exchanger and binding other proteins non-specifically. These were then eluted with the product by the non-selective elution using 1M NaCl. A matrix with 1.4 μmoleml^{-1} yielded a product with only half the specific activity of that from the matrix with 0.16 μmoleml^{-1}.

Schmidt and Raftery used a similar method to purify acetylcholine receptors from *Torpedo californica* electroplax with similar problems. With a ligand density of 0.4 μmoleml^{-1} a specific interaction was achieved leading to a reasonably pure product but at 2 μmoleml^{-1} the binding was dominated by non-specific interactions. It was calculated that the critical ligand density was about 1 μmoleml^{-1} which corresponded to a nearest neighbour distance of 10nm assuming a uniform ligand distribution and ligands at the intersections of a cubic lattice. At this ligand density it would be expected that protein molecules could bind only one ligand at a time and that only the specific interaction with the acetylcholine binding site would be sufficiently strong to retain the protein. At higher ligand densities multiple non-specific interactions could

collectively be sufficient to retain a protein molecule. This highlights the desirability of specific elution protocols when possible.

When preparing adsorbents for the purification of hepatic glucokinase using 2-amino-2-deoxy-glucopyranose Holroyde *et al.* (1976) found that increasing ligand density lead not only to tighter binding of the target protein, but also to increased non-specific binding of unwanted proteins, presumably by hydrophobic or ionic interactions with the ligand/spacer/matrix. The increased affinity of glucokinase necessitated the use of more rigorous elution conditions (including 0.5M KCl at the highest ligand density) which in turn eluted more of the non-specifically bound protein leading to a product of lower purity. Hence the optimum separation was achieved using an intermediate ligand density.

Use of too high a ligand density may lead to multiple binding of oligomeric proteins to the matrix. If the affinity is low this may prove beneficial but for high affinity systems it may cause considerable problems in the elution stage. This is discussed further in chapter 3. High ligand densities also offer the possibility of simultaneous specific and non-specific interactions with adjacent ligands. This is especially likely with complex ligands having both charged and hydrophobic regions eg. triazine dyes, and with the high ligand densities often achieved with these matrices the effects on desorption could be profound.

Another potential problem with high ligand densities is that the absolute amount of ligand leakage will be increased, both intrinsically and due to the more rigorous elution conditions required as a consequence of the tighter binding obtained.

2.6 Possible Routes to Maximisation of Protein Ligand Interaction

Calculations by many workers, eg. Liu *et al.*, (1984), have indicated that at saturation only a small fraction, typically from 0.1% to 5%, of the total bound ligand is participating in binding. Clearly matrix occlusion can only account for a small

fraction of the remainder in most affinity matrices so the question arises as to why the remaining accessible ligand is not binding protein.

Steric hindrance of adjacent ligands such that binding of protein to one leads to masking of others is a possibility and the calculation by Schmidt and Raftery (see above) suggests that this may occur to some degree at immobilised ligand concentrations above about 10^{-3}M. Since this is in the range of typical concentrations for an immobilised ligand, the effect is unlikely to account for the inaccessibility of the majority of the unbound ligand.

It must also be remembered that the equilibrium is dynamic and not static so, although only a small fraction of the total ligand may be binding protein at any instant in time, a much larger fraction may be occupied at some stage during a particular time interval. Thus a situation where a protein molecule may 'oscillate' between a number of ligands in a particular microenvironment can be envisaged and their orientation and spacing, as well as the intrinsic affinity of the protein ligand interaction, will account for the observed operational capacity and affinity of the system.

Maximisation of ligand usage involves two principles:

i) maximisation of the intrinsic affinity constant for the interaction such that the 'off' constant is lower and hence 'oscillation' between adjacent ligands is reduced making more of them available for simultaneous protein binding.

ii) manipulation of ligand density and, most importantly, distribution such that adjacent ligands are optimally spaced and oriented to retain a protein in a microenvironment with minimal steric masking.

Maximisation of affinity could be achieved in two ways. Most obvious is the selection of the ligand with the highest affinity for the protein (other considerations such as ease of coupling being equal) and optimisation of its orientation and immobilisation. The alternative is to artificially increase the affinity by making use

of biological phenomena such as ternary complex formation and intrinsic cooperativity, and may or may not be compatible with selection of the ligand of highest affinity. This principle is discussed in chapter 3.

Manipulation of ligand density is clearly possible but at present we only have a general understanding of its effects, which will also be very dependent on distribution. Ligand distribution can only be altered in a very non-specific manner by making use of the different structures of different polymeric matrices or other physical effects such as exclusion. There is little opportunity to alter ligand distribution at the microenvironmental level except for a general reduction of bulk average ligand density. This situation will remain until matrices and chemistry become available to allow adsorbents with precisely defined ligand distribution to be synthesised. These will make possible the quantitative investigation of the effects of ligand distribution.

CHAPTER 3

INTERACTIONS BETWEEN PROTEIN AND IMMOBILISED LIGANDS

3.1 Basic Considerations

The effectiveness of any affinity-based separation depends first and foremost on the affinity of the interacting pair for one another. When the ligand is immobilised on a solid phase the affinity of the interaction will dictate whether or not the protein of interest will be retarded by, or tightly bound to, the matrix. The interaction is in a state of dynamic equilibrium:

$$[P]+[M] \underset{k_{-1}}{\overset{k_1}{\rightleftharpoons}} [PM] \tag{3.1}$$

where P is the protein, M is the immobilised ligand, k_1 is the "on" constant and k_{-1} is the "off" constant. The dissociation constant K_d is given by the ratio of the "off" constant to the "on" constant i.e.

$$K_d = \frac{k_{-1}}{k_1} = \frac{[P][M]}{[PM]} \tag{3.2}$$

The conservation equations for protein and ligand give:

$$\begin{aligned} [P]_T &= [P] + [PM] \\ [M]_T &= [M] + [PM] \end{aligned} \tag{3.3}$$

where $[P]_T$ and $[M]_T$ represent total protein and matrix ligand concentrations

respectively. Hence:

$$K_d = \frac{([P]_T - [PM])([M]_T - [PM])}{[PM]} \qquad (3.4)$$

Using the simplifying assumption familiar in enzyme kinetics that $[M]_T > [P]_T$ this simplifies to:

$$K_d = [M]_T\left(\frac{[P]_T - [PM]}{[PM]}\right) \qquad (3.5)$$

The partition coefficient, σ, between solid and liquid phases is given by:

$$\sigma = \frac{bound\ protein}{free\ protein} = \left(\frac{[PM]}{[P]_T - [PM]}\right) = \frac{[M]_T}{K_d} \qquad (3.6)$$

and the elution volume, V_e, for the protein by:

$$V_e = V_0 + \sigma V_0 \qquad (3.7)$$

where V_0 is the void volume of the column. Thus the retardation of the protein due to its interaction with immobilised ligand can be expressed as a column volume ratio by:

$$\frac{V_e}{V_0} = 1 + \frac{[M]_T}{k_d} \qquad (3.8)$$

Although this equation includes a number of assumptions it is very simple and provides an immediate indication as to whether or not a particular affinity ligand is likely to give sufficient retardation to be useful, bearing in mind that typical immobilised ligand concentrations are generally of the order of a few millimolar. The possible alteration of the dissociation constant for the interaction as a result of immobilisation should also be considered. In general this is likely to be increased (i.e. lower affinity) due to steric effects but in some circumstances it may be reduced (i.e. higher affinity) due to additional favourable interactions with the chemical groups introduced by the spacer and/or activation chemicals. A good example of this is the favourable interaction between spacer and β-galactosidase discussed in chapter 2.

3.2 Quantitative Affinity Chromatography

In the early 1970's it was realised by a number of workers (Andrews *et al.*, 1973; Dunn and Chaiken, 1974; Nichol *et al.*, 1974) that, by analysing the equilibria existing in an affinity column using more rigorous mathematical models, analytical data could be obtained to describe the equilibria quantitatively in terms of association (or dissociation) constants for the protein-immobilised ligand interaction and also association (or dissociation) constants for free ligands which modulated the binding of protein to immobilised ligand.

The effects of various types of free ligand interaction with protein on its elution from an affinity column were described qualitatively by Akanuma *et al.* (1971) who predicted, and demonstrated, three types of effect according to the following scheme:

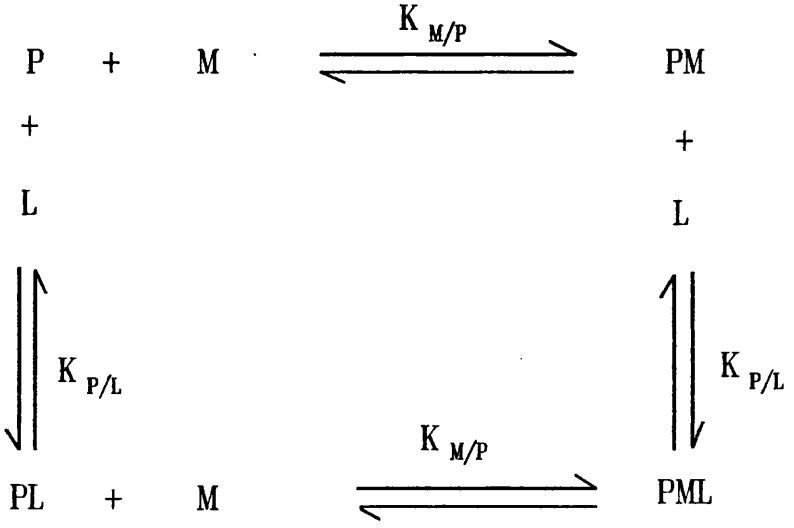

where L represents free ligand, PML represents the ternary complex formed between protein and both free and immobilised ligand, $K_{M/P}$ is the dissociation constant for the binding of protein (whether or not it has free ligand bound) to immobilised ligand and $K_{P/L}$ is the dissociation constant for the binding of free ligand to protein (whether or not it is bound to matrix ligand).

The three possible effects are as follows:

1) **Competitive effect** (where PM or PML is less stable than PL): In this case, the increase in the concentration of L will displace the equilibrium towards free P and reduce the retardation of P. This will also apply if L competes directly for the same binding site as M.

2) **Noncompetitive effect** (where the stability of PML is the same as that of PL): In this case there is no observable effect when L is increased.

3) **Uncompetitive effect** (where PML is more stable than PL): In this case the increase in L will displace the equilibrium towards the solid phase and increase the retardation of P.

The first paper on quantitative affinity chromatography by Andrews *et al.* (1973) studied the interaction of lactose synthetase with α-lactalbumin-Sepharose in the presence of glucose and N-acetylglucosamine. They used the method of zonal elution where a small pulse of protein is loaded onto an affinity column pre-equilibrated with buffer containing the desired concentration of free effector. The column is then eluted isocratically with the same buffer and the centre of the emerging protein peak is detected. From this data, knowing a number of column parameters, association constants can be calculated. The same method was used by Dunn and Chaiken (1974) to study the interaction of staphylococcal nuclease and thymidine-3'-p-aminophenyl-Sepharose. Both groups derived equivalent equations to describe the equilibria and used them to determine affinity constants (either association or dissociation) for interactions with free and immobilised ligand. A clear step by step derivation of the equation can be found in Swaisgood and Chaiken (1987).

The final equation is:

$$\frac{V_0 - V_m}{V - V_0} = \frac{K_{M/P}}{[M]_T} + \frac{K_{M/P}\,[L]}{K_{L/P}\,[M]_T} + \left(1 + \frac{[L]}{K_{L/P}}\right)\frac{[P]}{[M]_T} \qquad (3.9)$$

where: V_0 is the elution volume in the absence of [M]

V_m is the liquid phase volume ($V_0 = V_m$ if there is no gel partitioning)

V is the measured elution volume in the presence of [L]

$K_{M/P}$ is the dissociation constant for protein binding immobilised ligand

$K_{L/P}$ is the dissociation constant for protein binding free ligand

If $[P] \ll [M]_T$ and [P] is small such that $[L] \gg [LP]$, the final term in equation (3.9) can be ignored and $[L]_T$ substituted for [L]. Both of these conditions normally apply to zonal elution experiments so the equation may be simplified to :

$$\frac{V_0 - V_m}{V - V_0} = \frac{K_{M/P}}{[M]_T} + \frac{K_{M/P}\,[L]}{K_{L/P}\,[M]_T} \qquad (10)$$

or more usually:

$$\frac{1}{V - V_0} = \frac{K_{M/P}}{[M]_T\,(V_0 - V_m)} + \frac{K_{M/P}\,[L]_T}{K_{L/P}\,[M]_T\,(V_0 - V_m)} \qquad (3.11)$$

Thus knowing V_0, V_m and $[M]_T$ the dissociation constants $K_{M/P}$ and $K_{L/P}$ can be determined from y-intercept and gradient by plotting $1/(V_0 - V_m)$ against $[L]_T$.
This equation has been used successfully to measure affinity constants in several experimental systems. The results of several studies are summarised in table 1 of Chaiken (1979) (and an extended table in Swaisgood and Chaiken, 1987) and compared with values measured by other biochemical techniques. The results show excellent agreement confirming the validity of the method.

The problem with zonal chromatography is that the protein concentration cannot be defined since it varies across the zone. In cases where [P] is not small relative to $[M]_T$ and [L] the above simplification does not hold and the term in equation (3.9) including [P] must be considered.

Since:

$$[P] = \frac{[P]_T}{\left(1 + \frac{[L]}{K_{L/P}}\right)} \qquad (3.12)$$

equation (3.9) can be rewritten as:

$$\frac{V_0 - V_m}{V - V_0} = \frac{K_{M/P} + [P]_T}{[M]_T} + \frac{K_{M/P}\,[L]}{K_{L/P}\,[M]_T} \qquad (3.13)$$

Since $[P]_T$ cannot be defined in zonal-elution chromatography an alternative method of continuous elution or frontal analysis was developed. A general equation was derived by Nichol *et al.* (1974) to describe all possible equilibria between a protein and free and immobilised ligands binding at the same or different sites. They also showed how this could be simplified for specific cases in which only some of the possible equilibria actually occurred. A similar equation was derived by Kasai and Ishii (1975) and applied to the interaction of trypsin with various substituted arginine derivatives. Nichol *et al.* (1974) also considered the possibility of multiple binding sites on the protein but made the assumption, present in all quantitative considerations up to this time, that the protein could only interact with one immobilised ligand.

This methodology was used by Dunn and Gilbert (1979) who demonstrated, and quantitatively measured, the three possible free ligand effects as described by Akanuma *et al.* (1971) using α-chymotrypsin and immobilised 4-phenylbutylamine. Benzyloxycarbonyl derivatives of aromatic amino acids were found to increase elution volumes whereas benzyloxycarbonyl-ala-ala decreased elution volume. Some other ligands known to bind to the active site of the enzyme had no effect on elution volume. This lead the authors to suggest that "affinity chromatography could be 'fine

tuned' by appropriate selection of cosolutes". This will be addressed further later in this chapter. Similar results were obtained by Danner *et al.* (1979) for carboxypeptidase B.

3.3 Solute Multivalency and Multiple Matrix Interactions

The assumption that proteins could only bind to a single matrix ligand, even when they were oligomeric in structure and had the potential for multivalent interactions, was made for convenience in order to simplify the equations such that quantitative data could be obtained. Practical methodology included the limitation of operational ligand densities such that the situation where matrix ligands were spaced too far apart to permit multiple interactions obtained. The fact that the assumption was explicitly stated suggests that the possibility of multiple interactions was recognised from the beginning, but comparison of association constants calculated from quantitative affinity chromatography with those from other techniques showed good agreement (Dunn and Chaiken, 1975), attesting to the validity of the assumption and hence avoiding the necessity to address the more complex case.

The first qualitative indication of multiple matrix interactions probably appears in the work of Harvey *et al. (1974)* when studying the effect of ligand density on the binding of lactate dehydrogenase to AMP-Sepharose. They prepared a series of adsorbents with different ligand densities and measured the strength of binding. This showed a sigmoid response which probably represents the transition from binding to a single ligand to binding to multiple ligands as the immobilised ligand density increased. This sigmoid behaviour was not observed when ligand density was reduced by diluting a highly derivatised preparation with blank Sepharose. This is as might be expected since this approach does not change microenvironmental ligand densities; hence ligand spacing will still favour multiple interactions.

A qualitative observation that Glutamate dehydrogenase could not be competitively eluted from an immobilised antipsychotic drug matrix with a very high ligand density

was also attributed to multiple matrix interactions (Veronese *et al.*, 1979) although no direct evidence for this was presented.

Quantitative consideration of multiple matrix interaction first appeared in the work of Eilat and Chaiken (1979). They studied the binding of a bivalent IgA monomer to a hapten, phosphorylcholine, by zonal chromatography on an immobilised hapten column. They used columns with different concentrations of immobilised ligand and found that while the binding of IgA to a column with a low ligand density could be adequately described by existing theory assuming a single interaction with matrix ligand, the interaction with a column of higher ligand density could not. In this case plots of $1/(V - V_0)$ against [L] showed pronounced curvature. This was attributed to bivalent binding of IgA to the matrix since results from monovalent Fab fragments of the same antibody did not display curvature when chromatographed on the high ligand density matrix. In the appendix to their report the equation describing bivalent binding to a matrix ligand was derived. This equation:

$$\frac{1}{V - V_o} = \frac{1 + 2\left(\frac{[L]}{K_{P_2/L}}\right) + \left(\frac{[L]}{K_{P_2/L}}\right)^2}{(V_0 - V_m)\left[2\left(\frac{[M]_T}{K_{M/P_2}}\right) + \left(\frac{[M]_T}{K_{M/P_2}}\right)^2 + 2\left(\frac{[L][M]_T}{K_{P_2/L}K_{M/P_2}}\right)\right]} \quad (3.14)$$

was derived for the scheme which is described diagrammatically on the next page. The terms used have the same meaning as in previous equations and the subscript "2" is used to emphasise the fact that the protein is bivalent. P_2M_2 and P_2L_2 represent protein binding two immobilised ligand molecules simultaneously and two free ligand molecules simultaneously.

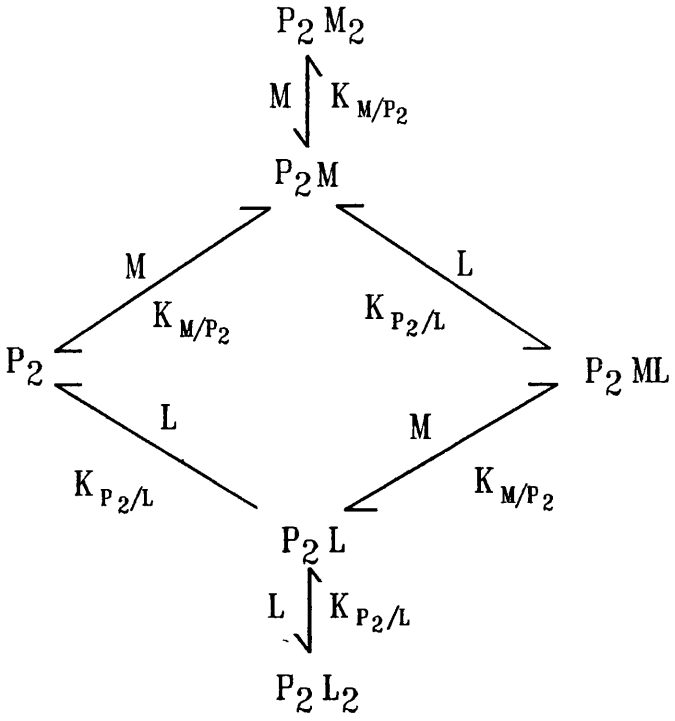

Values for the parameters were determined by non-linear least squares curve fitting of the data using the above equation. Use of the equation describing monovalent interaction gave an estimate of the operational affinity of the system as a function of ligand density which could be compared with the microscopic association constants obtained using the bivalent equation and with the association constant for the Fab fragment (which were very similar as would be expected). At the higher ligand density (5×10^{-5}M) the functional affinity was about 30 fold higher than the microscopic association constant as a result of bivalent binding.

It should, perhaps, not be surprising that a bivalent antibody should bind in a bivalent manner to immobilised ligands. The structure of the hinge region of an antibody allows considerable flexibility of the two Fab 'arms' such that they can move relative to one another (Burton, 1987). The degree of flexibility varies with the type, subtype and species of the antibody but occurs to a greater or lesser extent in virtually all antibodies. The most flexible examples such as human IgG_3 can attain conformations

with the angle between the Fab arms ranging from almost nothing (acute Y-shaped) to 180° (T-shaped). The hinge structure also allows rotation of the Fab arms. This means that the relative spatial configuration of two closely opposed immobilised ligands is probably not that critical in bivalent antibody binding since, once one Fab binding site has interacted with matrix ligand the other site, due to its flexibility, can 'explore' the conformational space within a certain maximum radius and therefore potentially interact with any immobilised ligand within this space.

Analogous bivalent binding of antibodies to 'immobilised ligands' on the surface of invading cells or viruses leads to a higher binding avidity *in vivo*, often of the order of 10^3 - 10^4 relative to the intrinsic affinity for a single interaction (Karush, 1978b) and is an important aspect of antibody function in, for example, activation of the classical complement pathway. It thus seems likely that antibodies have evolved in order to favour multiple binding and that the manifestation of such behaviour in affinity chromatography is simply a reflection of this ability.

Such behaviour of antibodies on immobilised antigen columns may have profound implications in the design of appropriate affinity columns for antibody purification. The general observation that binding affinity is enhanced by use of high ligand densities may lead one to suppose that the highest achievable ligand density will be optimal. Due to the generally high microscopic association constants for antigen / antibody interaction (typically in the range 10^5 to 10^{10} M^{-1} (Karush 1978a) this could lead to matrices with incredibly high operational affinity that will give excellent adsorption characteristics but make the antibody almost impossible to elute without the use of extreme treatments such as very low pH or denaturation by chaotropic agents. Careful consideration of these factors should lead to design of a process which minimises such problems.

The theory of multiple interactions with matrix ligand was extended by Nichol *et al.* (1981) and Winzor *et al.* (1982) to describe the more general case of a multivalent protein in partition equilibrium or frontal analysis experiments. The validity of their theoretical treatment was demonstrated using aldolase binding to cellulose phosphate.

This allowed them to measure association constants for both free and immobilised phosphate. Interestingly the constant for interaction with immobilised phosphate was found to be 150 fold greater than that for the free ligand. To explain this they proposed that a 'cluster' of closely spaced immobilised ligands form the matrix interaction site for an aldolase binding site. A similar conclusion was reached by Kyprianou and Yon (1982) from studies of the elution of Lactate dehydrogenase from 10-carboxydecylamino Sepharose: "..a single adsorption site must contain several 10-carboxydecylamino groups oriented in a precise three-dimensional array, a condition that would be satisfied by a very small proportion of these groups." This idea will be examined in more detail shortly.

It may seem surprising that aldolase and lactate dehydrogenase should bind to immobilised ligands simultaneously at multiple sites since, unlike the antibodies discussed above, the three dimensional structure, and hence the geometric spacing and orientation of the binding sites will be fixed. This in turn will mean that the orientation and spacing of immobilised ligands will need to be equally precise, thus lowering the probability of such a binding site occurring. It is perhaps significant that these observations were made with rather small and non-specific ligands at very high total matrix ligand concentrations. This will clearly increase the possibility of ligand clusters with the correct characteristics occurring.

It was also noted by Nichol *et al. (1981)* that the assumption that all protein matrix interactions could be described by the same site binding constant should be treated with caution. Such an assumption appears to be valid for the specific case studied but, "the possibility cannot be discounted that some steric limitations in relation to the cross-linking interactions may have been operative, which would necessitate consideration of additional site binding constants".

3.4 Multiple Matrix Interactions and Surface Cooperativity

The possibility that a single association constant might be insufficient to describe all protein-immobilised ligand interactions was explored in the work of Hogg and Winzor (1985). In their introduction they stated:

> "the constraint imposed on the solute's movement after the initial attachment to the matrix, coupled with consideration of the fixed placement of the surrounding immobilised reactant groups, raises the real possibility that the intrinsic binding constants governing additional solute-matrix links may differ from that pertaining to formation of the singly linked solute-matrix complex. Two probable situations arise: that in which subsequent interaction is hindered by unfavourable placement of the immobilised reactant groups; and that in which such interaction is enhanced because of the enforced location of the solute in the immediate vicinity of the matrix group."

This could be considered to be *negative* and *positive* surface 'cooperativity' although not in the traditional biochemical sense, since the effect is due to a shift in equilibria due to a localised concentration effect rather than an intrinsic change in the protein structure as a result of ligand binding.

In analysing results for the binding of horse liver alcohol dehydrogenase to Blue Sepharose, it was found that the data was best described by a model taking account of surface cooperativity. This yielded affinity constants indicating that there was an enhancement of 3-4 fold in the binding affinity for the second matrix ligand as a result of binding of the first. This was the first direct evidence that this effect could occur in affinity chromatography but had been recognised for some time in the field of immunology when considering binding of antibodies to polyvalent antigens eg. viruses and bacterial cells. Crothers and Metzger (1972) derived a theory to describe such systems based on statistical arguments.

The system considered by Hogg and Winzor was bivalent i.e. the simplest case in which surface cooperative behaviour could occur. They noted that the same approach

could in principle be used to analyse systems with more than 2 binding sites but that the practical problem of determining more intrinsic binding constants would make quantitative analysis unlikely.

Multivalent binding of protein to Cibacron Blue Sepharose was also noted for lactate dehydrogenase by Liu and Stellwagen (1987) when they studied the effect of immobilised ligand concentration on ligand accessibility and affinity (see also Stellwagen and Liu 1987b). As might be expected from probability considerations, they found that the degree of multiple binding increased as the immobilised ligand density increased but that within the range of total immobilised dye concentration studied their data showed no evidence of positive surface cooperativity, being adequately described by the model assuming multiple independent interactions.

3.5 Binding of Intrinsically Cooperative Proteins to Immobilised Ligands

In considering the binding of polyvalent proteins to immobilised ligands in the presence of free ligands it is assumed in all the models previously discussed that ligand binding sites are equivalent and independent. For many proteins this is indeed so but it is clearly not valid for intrinsically cooperative proteins. This problem was addressed theoretically by Hubble (1987) who considered the effect of free ligand on the binding of a positively cooperative protein to an immobilised ligand. In order to simplify the model it was assumed that matrix ligand was uniformly distributed throughout the system such that partitioning and exclusion effects could be ignored and that protein could only interact with a single matrix ligand. Using these assumptions the possibility of multiple matrix interactions and of surface cooperativity were excluded since to include them would have made the equations too complex to allow even semi-quantitative analysis. An equation was derived to describe the fraction of a tetrameric protein bound as a function of free ligand concentration according to the following equilibria:

$$[P] + [L] \overset{4K_1}{\rightleftharpoons} [PL]$$

$$[PL] + [L] \overset{\frac{3}{2}K_2}{\rightleftharpoons} [PL]_2$$

$$[PL]_2 + [L] \overset{\frac{2}{3}K_3}{\rightleftharpoons} [PL]_3$$

$$[PL]_3 + [L] \overset{\frac{1}{4}K_4}{\rightleftharpoons} [PL]_4$$

where K_1 to K_4 are the microscopic association constants for successive binding of L to P, PL, PL_2 and PL_3.

$$[P] + [M] \overset{4Kb_1}{\rightleftharpoons} [PM]$$

$$[PL] + [M] \overset{3Kb_2}{\rightleftharpoons} [PML]$$

$$[PL]_2 + [M] \overset{2Kb_3}{\rightleftharpoons} [PML]_2$$

$$[PL]_3 + [M] \overset{Kb_4}{\rightleftharpoons} [PML]_3$$

where Kb_1 Kb_2 Kb_3 and Kb_4 represent the microscopic association constants for binding of P, PL, PL_2 and PL_3 to M and:

$$\psi_1 = K_1 \quad \frac{\psi_2}{\psi_1} = K_2 \quad \frac{\psi_3}{\psi_2} = K_3 \quad \frac{\psi_4}{\psi_3} = K_4$$

The final equation is:

$$Y_m = \frac{4Kb_1[M] + 12Kb_2\psi_1[L][M] + 12Kb_3\psi_2[L]^2[M] + 4Kb_4\psi_3[L]^3[M]}{1 + 4\psi_1[L] + 6\psi_2[L]^2 + 4\psi_3[L]^3 + \psi_4[L]^4 + 4Kb_1[M] + 12Kb_2\psi_1[L][M] + 12Kb_3\psi_2[L]^2[M] + 4Kb_4\psi_3[L]^3[M]} \quad (3.15)$$

Using this equation simulations were carried out which showed that as the concentration of free ligand increased there was an increase in the fraction of protein

bound due to the partial saturation of the protein with ligand and the concomitant increase in the intrinsic affinity constant for the protein ligand (free or matrix bound) interaction. This was only true up to a certain free ligand concentration after which the fractional binding of protein decreased again due to competition of free ligand for matrix ligand sites ie. the protein is biospecifically eluted. For a non-cooperative protein biospecific elution would be progressively observed for all free ligand concentrations. The simulations also demonstrated that as the matrix ligand concentration was increased the enhancement in binding became less pronounced. In reality this observation would probably be accentuated by multiple matrix interactions, and surface as well as intrinsic cooperativity leading to very complex composite behaviour which would be difficult to analyse even theoretically.

In contrast to the other models discussed in this chapter no experimental evidence was presented to support this model of the behaviour of intrinsically cooperative proteins in the presence of both free and immobilised ligand.

3.6 The Co-operative Cluster Model

In 1988 the idea of positive surface cooperativity was further developed by Yon (1988a,b,c). Until this time it was always assumed, either explicitly or implicitly, that all the accessible matrix ligand was uniformly distributed and that all sites on the protein had access to the same concentration of matrix ligand. This is most unlikely to be the case with a rigid matrix where there is no possibility of translational motion for a covalently bound ligand. In the co-operative cluster model it was assumed that matrix ligands were distributed in clusters containing from 1 to N groups within the volume occupied by an N-valent protein, that the distribution of clusters followed a Poisson distribution and that within a ligand cluster the binding of ligands to protein occurred in a highly cooperative manner due to proximity.

Simulations showed that under typical conditions encountered in affinity chromatography only a small fraction of available ligand was present in clusters, over

95% being 'seen' as single isolated ligands by a typical protein of 4nm radius. The relatively small concentrations of dimeric and trimeric clusters are only really significant at low protein concentrations, and then only because of the very high operational affinity constant as a result of the high degree of cooperativity in the clusters. Tetravalent clusters occur at such low concentration that they can effectively be ignored.

At relatively high protein levels data is generally described equally well by both the multivalent and the co-operative cluster models, ie. the small concentration of clusters present has negligible effect on the binding. At very low protein concentrations, however, the curvature of Scatchard plots (Scatchard, 1949) predicted by the theory is clearly visible in practice, as demonstrated for the aldolase / phosphocellulose system described by Yon, where the cooperative cluster model gave a non-linear least squares fit which was an order of magnitude better than the multivalent binding model.

Clearly there are still problems and assumptions associated with this model. The distribution of immobilised ligand may not be random and therefore not described by the Poisson distribution. Examination of the structure of a cellulose or agarose matrix will quickly show that since this is non-uniform it is very likely to affect ligand distribution. The nature of the ligand itself may also influence the distribution, for example the known tendency of aromatic dyes to self associate may lead to preferential clustering over and above what would be expected from the random distribution. The assumption that all ligands in a cluster bind to protein ignores the geometric and spatial requirements of the relatively rigid protein molecule, effectively implying that the immobilised ligand has a great deal of local flexibility and freedom.

These objections notwithstanding, the cooperative cluster model probably represents the most sophisticated model to date for describing binding of multivalent proteins to immobilised ligand matrices. With the advent of high performance affinity chromatography as an analytical technique, modelling of these interactions is likely to become even more rigorous. The greater uniformity of HPLC packing materials

and the precision of the instrumentation should lend themselves well to this task.

CHAPTER 4

A MORE DETAILED CONSIDERATION OF SOME GROUP SELECTIVE LIGANDS

4.1 General Considerations

The attraction of group selective ligands lies mainly in their ability to interact with a whole class of proteins which contain some common structural feature, rather than with a single specific protein. This is often a common substrate binding site but may equally well be a structural motif anywhere on the protein surface which acts as a recognition site for a particular ligand.

In most cases the only useful common substrates are the various cofactors required by particular classes of enzymes. These include nucleotides, dinucleotides, coenzyme A, pyridoxal phosphate etc.. Such cofactors are invariant in structure although they cannot necessarily be assumed to bind to all proteins with which they interact in exactly the same orientation. Various nucleotide cofactor ligands are considered in section 4.2.

Other substrates are likely to have only very limited utility as group selective ligands due to the high degree of substrate specificity exhibited by most enzymes. This means that, except for a few core metabolites common to many pathways, most substrates will only be recognised by a very small number of enzymes and thus cannot be used for group selective adsorbents.

Many group selective ligands rely on recognition of common structural motifs remote from the active site of the protein. Such ligands may be small molecules or quite complex macromolecules. For example, boronate groups can complex with vicinal diols in the carbohydrate portion of many glycoproteins. A higher degree of sugar selectivity is shown by various plant and animal lectins. Concanavalin A from Jack beans, for instance, will recognise α-D-mannopyranosyl and α-D-glucopyranosyl residues (Lis and Sharon, 1973), whereas that from the haemolymph of the Horseshoe crab *Limulus polyphemus* recognises only N-acetylneuraminic acid residues (Marchalonis and Edelman, 1968). Classes of lectins are often affinity purified on immobilised sugar columns prior to their use as immobilised ligands themselves.

Other well known group selective adsorbents are Protein A and Protein G. These bind specifically to the Fc regions of particular classes of immunoglobulins. This property makes immobilised protein A and protein G columns particularly useful for antibody purification and also for 'capturing' antibodies in a favourable orientation such that they can efficiently bind antigen.

Another class of group selective ligands comprises a range of synthetic chemical 'pseudo-ligands' such as the triazine fabric dyes. These are not specifically designed to interact with proteins but many do so in a more or less specific manner. This is clearly not a true case of biological recognition but represents an interaction based on the same physical principles ie. complementarity of charge distribution, hydrogen bonding potential etc. between the pseudo-ligand and a particular part of a protein surface. Triazine dye pseudo-ligands are discussed in section 4.3.

4.2 Ligands Based on Nucleotide Cofactors

Group specific adsorbents based on nucleotide cofactors, mainly NAD(P)(H) and AMP (also ADP, ATP), have been extensively studied due to their utility in purifying two large groups of enzymes, the dehydrogenases and the kinases. Interest in biotechnological applications of these enzymes has lead to a large body of research

into producing active immobilised coenzymes for synthetic applications. This generally imposes similar constraints, in terms of method and orientation of attachment, as those encountered for affinity chromatography so the technology overlaps although the emphasis may be different. For example, precise orientation of the cofactor is critical if it is required to react with, rather than simply to bind to, an enzyme, whereas non-specific binding may be of little importance in a synthetic application where purified enzyme will probably be used. Synthesis of soluble immobilised coenzymes has recently been extensively reviewed (Bückmann and Carrea, 1989). The optimisation and scale-up of the reactions to give N^6-carboxyethyl NAD(H) (Sakamoto *et al.*, 1986) and N^6-aminoethyl NAD(H) (Bückmann, 1988) may be valuable in the synthesis of cost effective affinity adsorbents.

The structure of $NAD(P)^+$ is shown in figure 4.1. There are three potential sites for the chemical coupling of spacers/linkers: i) the ribose hydroxyl groups, ii) C^8 of the adenine ring, iii) N^1 of the adenine ring. The N^1 derivatives are unstable and undergo spontaneous Dimroth rearrangement at alkaline pH to yield compounds with substitutions on the C^6 amino group of the adenine ring (termed N^6 throughout this thesis).

Methods which involve direct coupling of NAD^+ to matrices include the diazonium method and carbodiimide promoted condensation with carboxyl groups on the matrix. The diazonium method involves incorporation of an aromatic amine functional group followed by diazotisation and direct coupling of NAD^+ at mildly alkaline pH. This method leads to an NAD^+ matrix thought to be coupled through C^8. This method was used by Barry and O'Carra (1973), Chaffotte *et al.* (1977) and Gennis (1976).

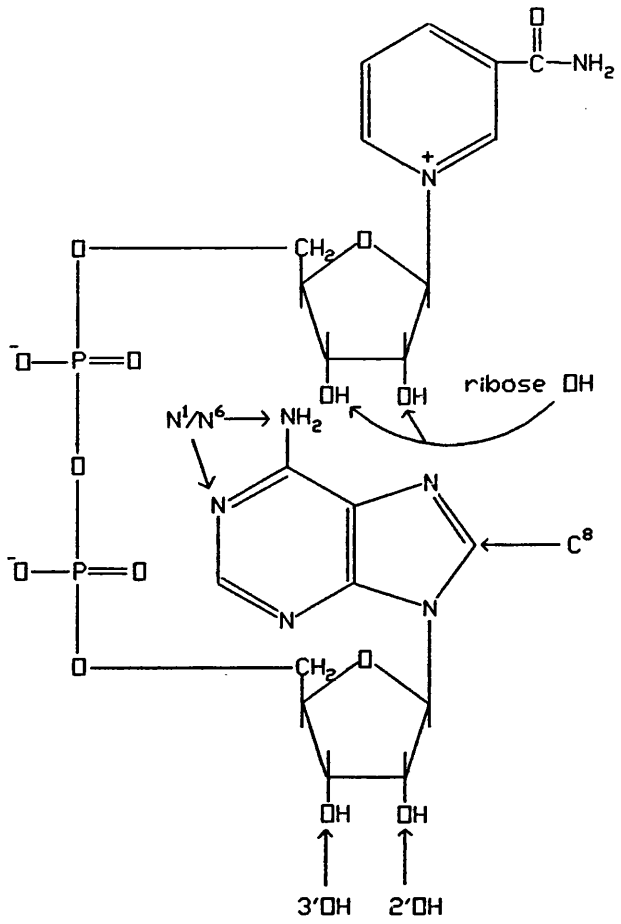

Figure 4.1

The structure of NAD^+.

$NADP^+$ has a phosphate group instead of the 2' hydroxy group on the adenine ribose ring. The arrows indicate the potential points of attack for attachment of linker groups.

Chaffotte *et al.* purified sturgeon muscle GAPDH using adsorbents with a 6-carbon hydrophobic spacer and a 3-carbon hydrophillic spacer. The structures of these are shown in figure 4.2

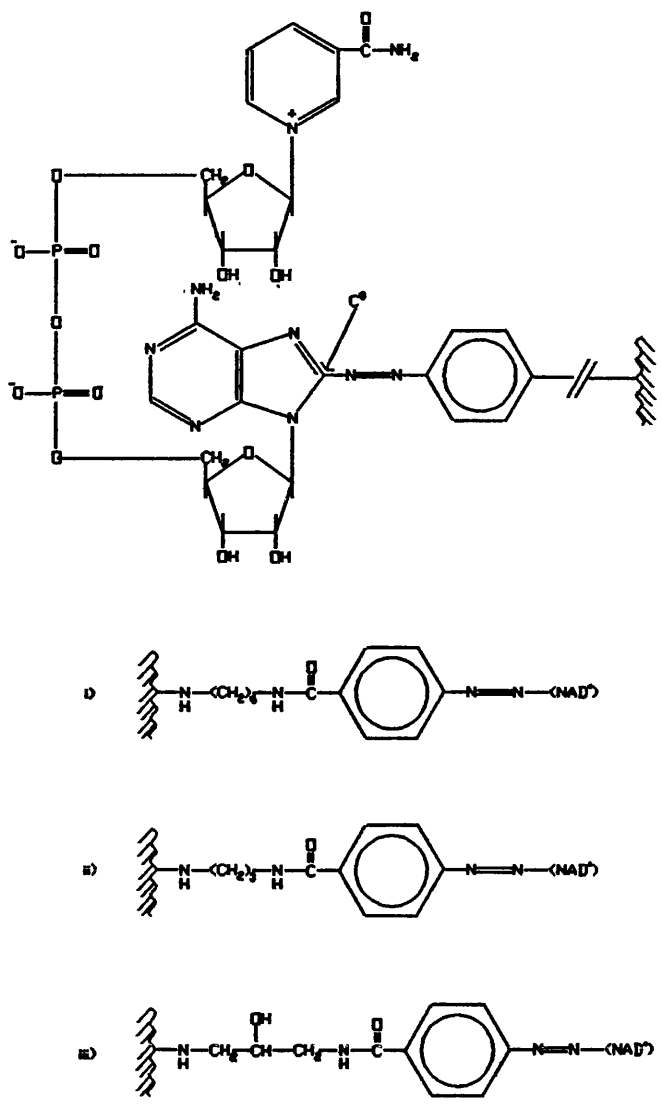

Figure 4.2

The structures of some diazo coupled NAD^+ matrices. The top structure shows the diazo coupling via C^8 of the adenine ring. Structures i and iii were synthesised by Chaffotte *et al.* (1977) and structure ii by Gennis (1976)

Structures i and iii both adsorbed the muscle enzyme but elution was much easier from the matrix with the hydrophilic spacer. Neither of these matrices bound yeast GAPDH. Barry and O'Carra (1973) prepared similar matrices with hydrophobic spacers of different lengths. These bound LDH, ADH and xanthine dehydrogenase. Rabbit muscle GAPDH bound to the diazo NAD^+ matrix with a hexamethylene spacer such that it could be quantitatively recovered if eluted immediately. However, recovery decreased as the time for which the enzyme was on the column increased, suggesting a slow secondary rearrangement of the enzyme/ligand/spacer complex. Gennis used a diazo NAD^+ derivative with a propyl spacer (structure ii in figure 4.2) to purify yeast GAPDH.

Carbodiimide promoted coupling of $NAD(P)^+$ to carboxyl containing matrices is another cheap and simple method of synthesis (Larsson and Mosbach, 1971). Unfortunately this reaction appears to lead to a heterogeneous adsorbent with NAD^+ coupled through both N^6 and ribose hydroxyl groups (Lowe *et al.*, 1973a). Calculations suggested that tight binding sites only represented 0.1% of NAD^+ present, similar to the fraction displaying coenzymic activity. This was interpreted by Lowe *et al.* as the fraction coupled via N^6 due to the similarity of the binding behaviour of enzymes to that with N^6-(6-aminohexyl)AMP matrices. While the heterogeneity of carbodiimide coupled matrices clearly poses a problem for the quantitative interpretation of binding data the adsorbent has been shown to be useful for the purification of a range of dehydrogenases (Lowe *et al.*, 1973b). The general applicability of this method to any adenine based compound allowed Lowe and Dean (1973) to assess the relative binding strength of lactate dehydrogenase on a range of adenine nucleotide derivatives and fragments without the need for complex synthesis of the many derivatives tested.

An attempt was made by Gilham (1971) to prepare an adsorbent by periodate oxidation of the vicinal diol on the ribose ring of NAD^+ to generate aldehyde groups, then Schiff base formation with amine groups on a matrix. Coupling of NAD^+ was achieved but the resulting matrix showed little affinity for dehydrogenases as would have been expected from the above argument.

In order to avoid the uncertainties caused by heterogeneity of cofactor coupling, chemically defined, homogeneous, cofactor-spacer conjugates have been produced by what has been termed the "preassembly" approach. These conjugates are then attached to activated matrices eg. by the CNBr method. Mosbach *et al.* (1972) prepared N^6-(6-aminohexyl)-5'-AMP (figure 4.3). This bound GAPDH and could resolve GAPDH and LDH. The same matrix was used by Chaffotte *et al.* (1977) for the large-scale preparation of yeast GAPDH.

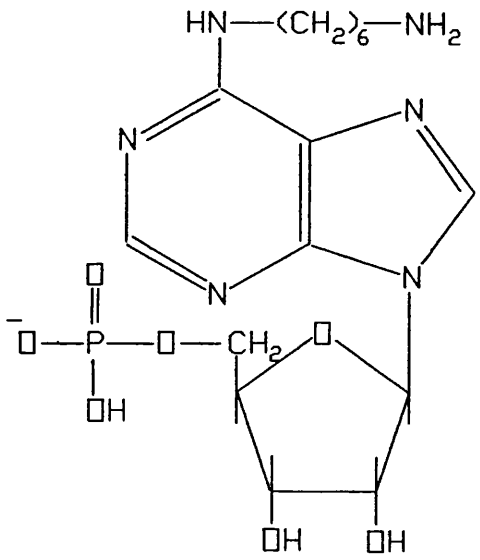

Figure 4.3

The structure of N^6-(6-aminohexyl)-5'-AMP

N^6-(6-aminohexyl)-adenosine-2',5'-bisphosphate was synthesised by Brodelius *et al.* (1974). This adsorbent bound $NADP^+$ dependent enzymes but had little affinity for the NAD^+ dependent enzymes which bound well to N^6-(6-aminohexyl)-5'-AMP

derivative. Wermuth and Kaplan (1976) used 8-(6-aminohexyl)amino-2'-AMPagarose (figure 4.4), synthesised according to their earlier procedure (Lee *et al.*, 1974) to purify pyridine nucleotide transhydrogenase from ***Pseudomonas aeruginosa***. This adsorbent appears to be specific for $NADP^+$ requiring enzymes and shows no affinity towards kinases and NAD^+ dependent dehydrogenases. Thus AMP analogues are available for NAD^+ and $NADP^+$ requiring enzymes. These have the advantage of easier synthesis and greater stability than the full dinucleotide cofactors.

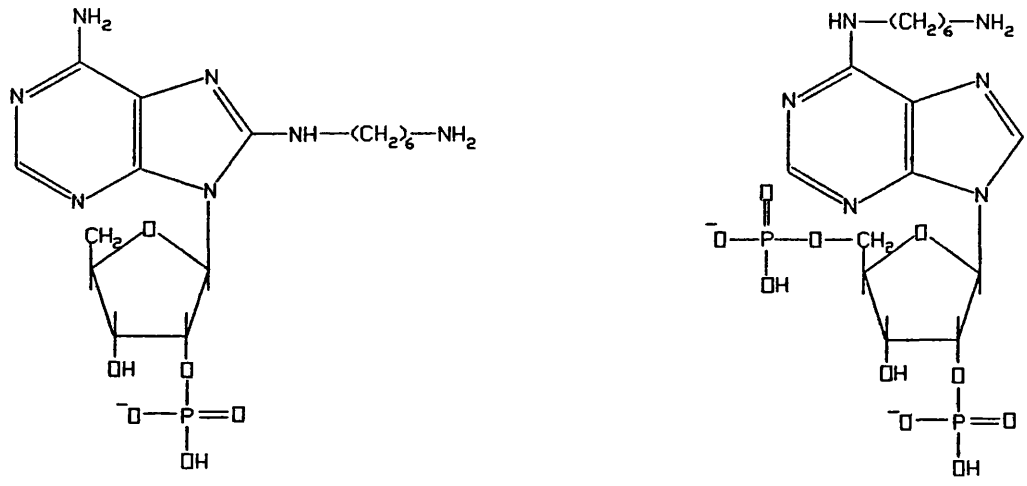

Figure 4.4

The structure of 8-(6-aminohexyl)amino-2'-AMP and N^6-(6-aminohexyl) adenosine 2',5'-bisphosphate.

While successful for the purification of dehydrogenases, N^6 coupled 5'AMP shows little affinity for most kinases suggesting that the amino group of the adenine ring is important in binding of nucleotides to these enzymes. Several alternative supports

have been prepared and shown to be useful for kinase purification. Lee *et al.* (1977) found that creatine kinase, pyruvate kinase, adenylate kinase and aldolase bound to 8-azoATP agarose. Trayer *et al.* (1974) synthesised 8-(6-aminohexylamino)ATP agarose and P^1-(6-aminohex-1-yl)-P^2-5'ADP agarose (figure 4.5) and showed that glucokinase and myosin ATPase fragments bound to both adsorbents.

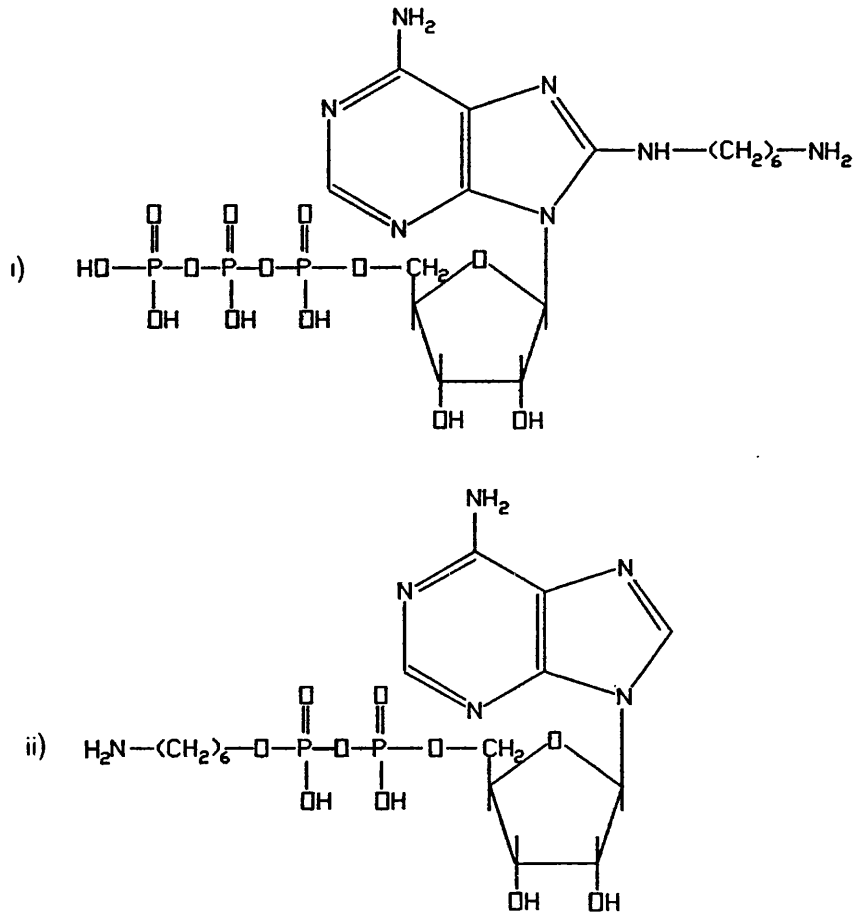

Figure 4.5

The structures of i) 8-(6-aminohexylamino)-ATP
and ii) P^1-(6-aminohex-1-yl)-P^2-5'-ADP

In contrast with the general lack of success with N^6 substituted ligands for purifying kinases, Ramadoss *et al.* (1976) found that N^6-(6-aminohexyl)- carbamoylmethyl ATP agarose was at least 90 times more effective than N^6-(6-aminohexyl) ATP agarose at binding phosphofructokinase.

The specificity of group selective adsorbents is achieved at both the adsorption and desorption stages. During adsorption the group selective character of the matrix is used to bind a certain group of enzymes. The number of such enzymes present in a crude preparation may need to be reduced by some prior treatment such as ammonium sulphate fractionation or ion exchange chromatography. This could be particularly important if the target enzyme is a minor component in a mixture of similar enzymes, when the capacity of the column may be greatly reduced by competitive binding. Such a situation was described by Andersson *et al.* (1975) when purifying and separating the isomers of equine liver ADH on N^6-(6-aminohexyl)-5'-AMP.

Once bound to the ligand a number of elution strategies may be employed, both to elute the target enzyme and to elute potential contaminants while leaving the target enzyme bound prior to its specific elution.

The simplest elution strategy is to increase the ionic strength of the buffer, either stepwise or by use of a gradient (eg. Lowe *et al.*, 1973a). The latter gives better resolution. The method is not very specific and is usually only applicable if the highest purity is not required or if the starting material is already reasonably pure.

Use of free nucleotides as competitive inhibitors is a very effective method of displacing enzymes. Either pulses (Mosbach *et al.*, 1972) or gradients of free nucleotide may be used. The former gives recovery in a small volume of buffer, the latter may give higher purity and recovery (Lowe *et al.*, 1973a), especially when purifying directly from crude supernatants when more enzymes will be specifically bound to the column. NAD(P)H is often a more effective displacer than $NAD(P)^+$ for dehydrogenases (Lowe and Dean, 1973) since the reduced cofactor generally has a higher affinity than the oxidised form when forming a binary complex.

The use of ternary complex formation by addition of a substrate or substrate analogue in the presence of cofactor has also been employed. Ohlsson *et al.* (1972) used NAD^+ and pyruvate to elute LDH from N^6-(6-aminohexyl) AMP Sepharose and NAD^+ and hydroxylamine to elute ADH although none of these compounds could effect elution alone.

The preparation and use of nucleotide cofactors as general ligands has been reviewed by Mosbach (1972), Lowe and Dean (1974e), Mosbach *et al.* (1976) and Scouten (1981c).

4.3 Triazine Dye Ligands

The triazine dyes are a class of fibre reactive dyes manufactured for the dyeing of cloth and for use in the printing trade. The best known are the 'Procion' range made by ICI and the 'Cibacron' range of Ciba-Geigy.

The structural basis of these dyes is the trichloro-s-triazine ring to which a wide variety of chromophores may be attached by displacement of the reactive chlorine groups. Either one (as in the Procion MX series) or two (as in the Procion H series) of the chlorine groups may be substituted with chromophores. The remaining active chlorine acts as a leaving group in the chemical reaction which covalently couples the dye to the fibre substrate (eg. a glucose hydroxyl group of cotton cellulose). The structures of some common triazine dyes are shown in figure 4.6.

Biochemical interest in triazine dyes began when it was observed (Kopperschläger *et al.*, 1968) that several enzymes co-chromatographed with Blue-Dextran when this was used as a void volume marker in gel-permeation chromatography.

The potential use of this interaction in protein separation was soon realised and Blue Dextran (Ryan and Vestling 1974), or the dye component of blue dextran, Cibacron Blue F3G-A, was coupled to solid supports to make specific adsorbents (Bohme *et al.*, 1972; Easterday and Easterday, 1974; Heyns and DeMoor, 1974).

There has arisen in the literature a degree of confusion concerning the exact isomeric structures of samples of Cibacron blue F3G-A and its ICI equivalent Procion Blue H-B. These dyes are often referred to by the general name Reactive Blue 2 although this term strictly only refers to dye containing a mixture of the meta and para isomers of the sulphoanilino ring i.e. Procion Blue H-B. Such a mixture is undesirable in analytical terms since the two isomers may interact differently with a target molecule (Beillmann *et al.*, 1979).

i)

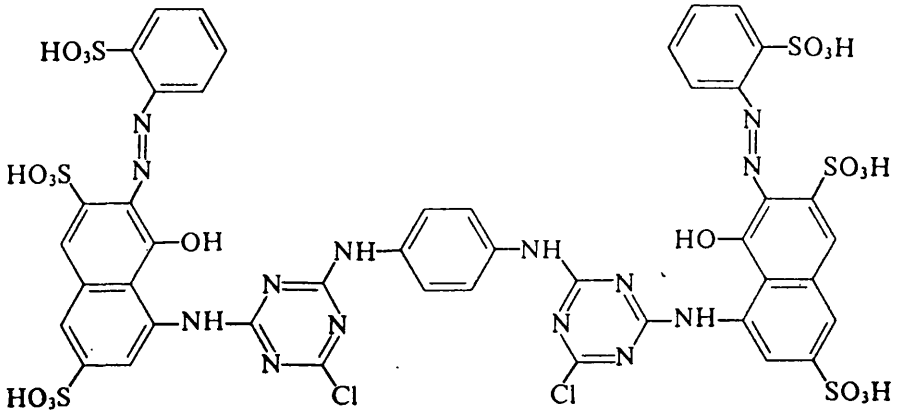

Procion Red HE-3B

ii)

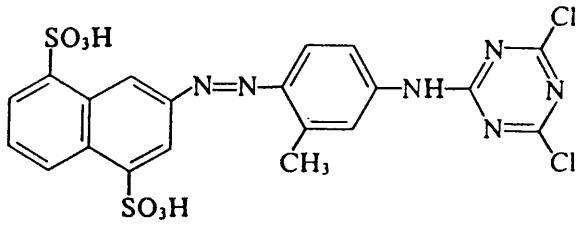

Procion Yellow MX-R

iii)

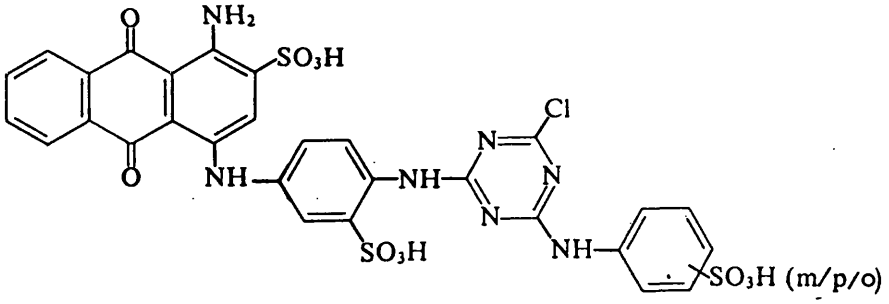

Procion Blue H-B (Cibacron Blue F3G-A)

Figure 4.6

Structures of some commonly used triazine dyes.

All three isomers (ortho, meta and para) isomers of the sulphoanilino ring of structure iii have appeared in the literature with various names.

Samples of Cibacron blue from several sources have been identified as the ortho isomer (Burton *et al.*, 1988; Sigma, 1989). Thus in order to avoid ambiguity it seems desirable to test the dye sample being used to identify the isomer(s) present and to explicitly state this information.

There has been much interest in the nature of the dye-protein interactions taking place in an attempt to explain the selectivity of dye adsorbents. Early work, using Cibacron blue as an affinity ligand (Thompson *et al.*, 1975) and as a spectral probe (Thompson and Stellwagen, 1976) suggested that the dye bound in the dinucleotide fold of dehydrogenases and that this explained its specificity for enzymes utilising nucleotide ligands. While the above was eventually directly confirmed by X-ray crystallographic studies of the alcohol dehydrogenase/dye complex (Beillmann *et al.*, 1979) it became apparent that many proteins which did not contain the dinucleotide fold also showed a very high affinity for Cibacron Blue. This lead to the proposal of a much more general picture of dye/protein interactions. For instance Beissner *et al.* (1979) stated:

> "These dye columns are not probes for the dinucleotide fold nor affinity columns in the strictest sense, but localised cation exchangers having some hydrophobic interactions as well. This does not preclude the protein from interacting at other sites on the protein by hydrophobic forces, electrostatic forces, or a combination of both."

A similar conclusion was reached by Subramanian and Kaufman (1980) who proposed, from studies on dihydrofolate reductase using Cibacron Blue as a spectral probe, that:

> "the blue dye is capable of binding specifically to any protein possessing a cluster of aromatic and other apolar groups and/or geometrically spaced positively charged groups for proper interaction with the aromatic rings and/or sulphonate groups of the dye molecule. The so-called specificity of the blue dye for the nucleotide binding proteins is thus a special case of the above mentioned requirements and not diagnostic of the dinucleotide fold."

This explains why the huge range of different triazine dyes, containing different chromophores with varying charge distributions, show differing affinities for

particular proteins depending on the degree of complementarity between the ligand and the protein surface with which it is interacting. For instance Procion red HE3B generally shows a higher affinity for $NADP^+$ dependent dehydrogenases than does Cibacron Blue F3G-A (Watson *et al.*, 1978). Lowe *et al.* (1986) demonstrated that various analogues of Cibacron Blue F3G-A bound to horse liver alcohol dehydrogenase with affinities that varied by several orders of magnitude.

In order to find out which dye is most suitable for any particular separation an empirical approach based on screening a range of dye adsorbents under varying conditions is usually adopted. A general approach has been suggested by Scopes (1986) and a rapid small scale screening method by Berg and Scouten (1990).

Dye-ligand columns usually bind a larger proportion of the proteins present in a crude mixture than would a more specific bio-ligand. In order to achieve a high degree of purification, elution conditions must be carefully controlled, especially if non-specific methods of elution such as increasing ionic strength are to be used. If the dye binding site on a protein overlaps with a ligand or effector binding site, or is perturbed by binding of an effector to a distant site, then desorption by specific displacement may be achieved. This generally gives the most satisfactory results where applicable.

Dye-ligands have many potential advantages in affinity chromatography when compared with bio-ligands. These were summarised by Dean and Qadri (1983) who highlighted the most important factors as being the saving of expense, both directly and indirectly due to the ease and safety of adsorbent synthesis, the stability of the resulting adsorbent to chemical and microbial attack (although the stability of the matrix material itself is still an important consideration) and the high levels of selectivity which can be achieved by careful choice of conditions. Another feature of note is the very high ligand densities which can be achieved. This may or may not be advantageous but it can lead to very high capacities in some cases eg. $50mgml^{-1}$ for human serum albumin (Travis *et al.*, 1976). In other cases high ligand densities may hamper washing and elution stages by increasing the range and frequency of non-specific binding interactions.

Dye-ligand chromatography is now well established as a powerful laboratory-scale technique in protein purification. Its advantages, however, suggest that the method should be applicable to large-scale operations and that it will have an increasingly important role in future industrial processes.

Dye ligand Chromatography has been reviewed by Kopperschlager *et al.* (1982), Dean and Qadri (1983), Lowe and Pearson (1984), Clonis (1988) and quantitative aspects by Stellwagen and Liu (1987).

CHAPTER 5

MATERIALS AND METHODS

5.1 Materials

The following came from Sigma Chemical Co., Poole, Dorset.

long fibrous cellulose, phosphocellulose, dextran of various molecular weights CNBr, diaminopropane HCl, sodium trinitrobenzenesulphonate, N^6-(6-aminohexyl)AMP (A8518), N^6-([6-aminohexyl]-carbamoylmethyl)NAD^+ (A5265), N^6-AMP agarose (A3019), C^8-AMP agarose (A1271), NAD^+ agarose (N1008), NAD^+ (N7004), $NADP^+$ (N0505), NADH (N8129) AMP (A2002), fructose-1-6-diphosphate (752-1), glyceraldehyde-3-phosphate diethylacetal (monobarium salt) (G5376), GAPDH (yeast G8380), G6PDH (*Leuconostoc* G5760), PGI (yeast P5381), ADH (yeast A7011), BSA (A6003), Lysozyme (L6876)

The following were obtained from Pharmacia LKB, Upsalla, Sweden

Sephadex G50(coarse) and G75(medium), Sepharose 4B and CL6B, PD10 prepacked desalting columns, precast 8-25% polyacrylamide gradient gels and buffer strips for electrophoresis.

p-nitrobenzoylazide came from Eastman-Kodak,Liverpool, CTMB (analar) from BDH,Poole and Cibacron blue 3G from Ciba,Manchester. Cibacron Blue Sepharose CL6B was a gift from Andy Booth, Department of Chemical Engineering.

All other chemicals were of analytical grade and were supplied by a variety of manufacturers.

5.2 METHODS

5.2.1 Activation of Cellulose and Sepharose matrices

Matrices were activated using the cyanogen bromide activation method of Axen *et al.* (1967) as modified by March *et al.* (1974).

Solid cyanogen bromide was dissolved in dry acetonitrile at a concentration of $2gml^{-1}$. 1 volume of 2M Na_2CO_3 was mixed with 1 volume of 50% (v/v) matrix in distilled water. The suspension was stirred gently on a magnetic stirrer using a stir bar with a central ridge to minimise matrix degradation by physical grinding. The rate of stirring was increased and 0.05 volumes cyanogen bromide in acetonitrile added all at once. The suspension was stirred vigorously for 90 seconds then washed rapidly on a sintered glass funnel with 10 volumes of 0.1M $NaHCO_3$ pH 9.5 followed by 10 volumes of distilled water. The activated matrix was used immediately for coupling of ligands or further derivatisation.

5.2.2 Preparation of p-Aminobenzamidopropyl-Sepharose

The aminopropyl spacer arm was added using the method of Barry and O'Carra (1973) and further derivatised to yield p-aminobenzamidopropyl Sepharose essentially as by Cuatrecasas (1970).

Freshly prepared cyanogen bromide activated matrix was washed with 20 volumes ice cold 0.5M diaminopropane HCl pH10.0 and then added to 1 volume 2M diaminopropane HCl pH10.0 and gently mixed at 4°C overnight. The matrix was washed with 20 volumes 0.2M boric acid/NaOH buffer pH9.3 and then with a mixture of 20:80 (v/v) buffer and DMF. Solid p-nitrobenzoyl azide was added to give a concentration of 0.07M and gently stirred at room temperature for 1 hour. The slurry was washed with 20 volumes 20:80 buffer/DMF and then 50:50 water/DMF until the washings were colourless. The moist gel was added to 2

volumes 0.5M sodium bicarbonate pH8.5 containing 0.1M sodium dithionite and allowed to react at 40°C for 40 minutes. The matrix was washed with 20 volumes 0.5M HCl and then either used immediately for coupling of NAD^+ or washed with water and stored at 4°C until required.

The success of the stages in the derivatisation was assessed qualitatively using the colour test with 3% aqueous sodium trinitrobenzenesulphonate (TNBS) (Inman and Dintzis 1969). A few drops of sodium TNBS solution were added to a small sample of matrix suspended in saturated sodium borate. This produced a pale lemon yellow colour with unsubstituted Sepharose, orange with aminopropyl sepharose and a red orange with p-aminobenzamidopropyl sepharose.

5.2.3 Coupling of NAD^+ to p-Aminobenzamidopropyl Sepharose

This step was carried out according to Barry and O'Carra (1973).

A 50% slurry of p-aminobenzamidopropyl Sepharose in 0.5M HCl was treated with sodium nitrite to 0.1M for 7 minutes at 4°C to induce diazotisation. NAD^+ in ice cold saturated sodium borate was added to give 40mg per ml Sepharose and the pH immediately adjusted to 8.0 using sodium hydroxide. The suspension was mixed gently overnight then washed with a large volume of 0.1M NaCl. The resulting matrix was mustard yellow in colour. It was stored in the dark at 4°C.

5.2.4 Coupling of Preformed Nucleotide Ligands to CNBr Activated Matrices

Sepharose 4B or long fibrous cellulose was activated with cyanogen bromide using the above method. The final wash was with 0.1M sodium bicarbonate pH8.9 (buffer A). Matrix was resuspended in an equal volume of buffer A and sufficient N^6-(6-aminohexyl)AMP or N^6-([6-aminohexyl]-carbamoylmethyl)NAD^+ added to give the

desired concentration of matrix ligand. This was agitated gently for 16 hours at 4°C. The matrix was washed with buffer A and the washings retained for spectrophotometric determination of unbound ligand. The washed matrix was added to 1M ethanolamine, adjusted to pH8.5 with HCl, and left at room temperature for 2 hours to block any remaining reactive groups, then washed with water, 1M sodium chloride and water again before storage at 4°C as a moist cake.

5.2.5 Preparation of Ethanolamine Sepharose Control Matrix

Ethanolamine Sepharose was prepared by CNBr activation followed by immediate blocking with 1M ethanolamine (final concentration) adjusted to pH8.5 with HCl, rather than addition of ligand.

5.2.6 Estimation of Bound Nucleotide

a) by mass balance

Nucleotide bound to the matrices was estimated by calculation of the difference between ligand added and ligand remaining in the washings. Absorbance was measured at 267nm and an extinction coefficient of $17.7 mM^{-1}cm^{-1}$ used for the N^6-AMP derivative and $21.7 mM^{-1}cm^{-1}$ for N^6-NAD^+ derivative.

b) by direct spectroscopy

Ligand bound to Sepharose was estimated by direct spectroscopy of a 10% suspension of matrix in 50% w/w glycerol/water using a similar suspension of underivatised Sepharose as a blank. Difference spectra were measured using a Pye SP8 400 double beam spectrophotometer. The extinction coefficient of the coupled ligand was assumed to be the same as for the free ligand. For the azo-linked NAD^+ derivative p-aminobenzamidopropyl sepharose was used as the blank. The absorbance maximum had shifted to 275nm due to the coupling of NAD^+ but its extinction coefficient at the new wavelength was assumed to be unchanged in calculating bound nucleotide.

c) by hydrolysis and adenine determination

The method used was that of Larsson and Mosbach (1971). 0.25g moist matrix was hydrolysed in 5ml 0.5M HCl for 15 minutes in a boiling water bath. The volume was made up to exactly 10ml and the absorbance of the adenine moities measured at 260.5nm. A standard curve was constructed by hydrolysing known amounts of NAD^+ or AMP together with 0.25g blank Sepharose in the same way as for the experimental samples. The Nucleotide content of the matrix was read directly form the standard curve.

All three methods were tried for nucleotide Sepharose derivatives and found to give very similar estimates. The mass balance method was used routinely since it was the easiest method and was the only one which worked reliably for cellulose derivatives. Coupling efficiencies were routinely found to be 94 - 96% for Sepharose matrices and 50 - 60% for cellulose matrices.

5.2.7 Determination of Protein Concentration

For crude protein solutions the Bio-Rad dye binding assay based on the Bradford (1976) method was used with standard curves constructed using thyroglobulin in the range 0-20μg protein. Samples were diluted as required into a final volume of 200μl and 800μl of Bio-Rad reagent, diluted 1 in 4 with double distilled water, added. After 15 minutes incubation the absorbance of each was measured at 595nm against a zero protein blank.

For pure protein preparations absorbance at 280nm was measured and concentrations determined using the following extinction coefficients:

Protein	Source	$E^{1\%}$
Albumin	Bovine serum	6.7
Alcohol dehydrogenase	Yeast	14.7
Fructose bisphosphatase	Bovine liver	8.9
Glyceraldehyde-3-phosphate dehydrogenase	Yeast	9.3
Lysozyme	Hen egg white	22.2

5.2.8 Nucleotide removal from GAPDH

Nucleotides were removed by charcoal treatment using the method of Gennis (1976). GAPDH was spun out of an ammonium sulphate suspension and resuspended in 50mM sodium pyrophosphate buffer pH8.5 containing 1mM EDTA and 1mM 2-mercaptoehtanol. Activated charcoal was added to $50mgml^{-1}$ and the suspension gently stirred for 5 minutes. The suspension was filtered through a $0.2\mu m$ filter to remove the charcoal then buffer exchanged into the same buffer using a PD10 column. Treated GAPDH had an A280nm/A260nm ratio of about 2.

5.2.9 Preparation of Glyceraldehyde-3-Phosphate Solution

Glyceraldehyde-3-phosphate was liberated from its monobarium diethylacetal using the protocol supplied with the product by Sigma. 200mg diethylacetal was dissolved in 12ml water and 3g Dowex 50X8 H^+ resin added. The mixture was heated for 3 minutes in a boiling water bath, mixing periodically, then rapidly cooled in an ice bath. The solution was decanted from the resin beads which were then washed twice with 4ml water and the washings combined with the solution to give a total of about 20ml of approximately 20mM DL-glyceraldehyde-3-phosphate solution. This was frozen in aliquots until required.

To check that hydrolysis was substantially complete the solution was assayed using GAPDH by the supplied Sigma protocol. Two cuvettes were prepared containing 1.5ml 0.2M tris pH8.5, 0.3ml 0.17M sodium arsenate pH8.5, 0.05ml 0.2M L-cysteine (freshly adjusted to pH7), 0.6ml 0.1M sodium fluoride, 0.05ml 0.2M NAD^+ and 0.1ml GAPDH solution containing 5I.U. 0.4ml water was added to the blank cuvette and 0.4ml containing about 0.3μmole GAP was added to the experimental cuvette. The change in absorbance at 340nm was measured against the blank cuvette until the reaction had reached completion, and the concentration of the GAP solution calculated assuming that 1μmole NADH is produced when 1μmole D-GAP is oxidised. L-GAP is not oxidised by GAPDH.

5.2.10 Assay of GAPDH

GAPDH was assayed at pH8.5 and 25°C in 1ml of a buffer containing (final concentrations) 50mM sodium pyrophosphate, 5mM EDTA, 10mM sodium dihydrogen orthophosphate, 0.1M potassium chloride, 10mM cysteine, 1mM NAD^+, and 1mM D-glyceraldehyde-3-phosphate (2mM DL racemate) which was added last to initiate the reaction. Enzyme (about 0.005 I.U.) was preincubated for 8 minutes in the assay buffer to ensure complete reduction of active site thiol groups. Increase in absorbance at 340nm was followed using a Cecil 272 UV spectrophotometer fitted with a jacketed cuvette holder. Temperature was maintained using a recirculating water bath and cuvettes were left for 15 minutes to equilibrate prior to use.

5.2.11 Assay of Fructose Bisphosphatase (FBPase)

The coupled assay described by Nimmo and Tipton (1975a) was used. This method couples fructose-6-phosphate production to NADH generation via the enzymes phosphoglucose isomerase (PGI) and glucose-6-phosphate dehydrogenase (G6PDH). FBPase was assayed in 1ml of a buffer containing 50mM triethanolamine pH7.4 or

50mM glycine-KOH pH9.6, plus 100mM KCl, 0.1mM EDTA, 2.1mM $MgSO_4$, 100μM fructose 1-6 diphosphate, 0.15mM $NADP^+$, 5 units PGI, 3 units G6PDH and FBPase. G6PDH (1μl of 10mgml^{-1}) and PGI (2μl of 2.5mgml^{-1}) were added directly from ammonium sulphate suspensions for operational convenience. The small amount of ammonium sulphate did not interfere with the assay and the technique has been used by many other workers for FBPase assay (e.g. MacGregor *et al.*, 1982). Enzyme was incubated for 10 minutes at 30°C in a cuvette containing all components except fructose-1-6-bisphosphate which was added last to initiate the reaction. Increase in absorbance was followed at 340nm and rates estimated from the linear part of the progress curve which was reached about 20 seconds after initiation of the reaction.

5.2.12 Purification of Fructose Bisphosphatase

The purification protocol was based on that of Nimmo and Tipton (1975) but with the latter stages simplified by substituting dye ligand chromatography, as introduced for this enzyme from other sources by a number of workers (Han and Johnson, 1982; MacGregor *et.al.*, 1982; Marcus *et.al.*, 1982; Tashima and Mizunuma, 1982), for the ion exchange and gel filtration steps of the original method.

Bovine liver from a freshly slaughtered animal was collected from an abattoir and transported to the lab on ice where it was immediately processed. 500g liver was roughly chopped and blended in 100g portions with about 350ml 0.1M KCl for 30 seconds in a waring blender. The combined homogenates were strained through two layers of muslin to remove any large lumps of tissue and centrifuged at 20000g for 60 minutes. The supernatant was collected and its pH adjusted to 4.55 by dropwise addition of 5M acetic acid while stirring. The pH was then immediately raised to 6.5 by addition of 5M NaOH. The resulting turbid suspension was centrifuged at 20000g for 60 minutes. The supernatant was filtered through glass wool to remove a yellow lipid layer and solid ammonium sulphate was slowly added to give 52% saturation. The suspension was stirred gently for 30 minutes then centrifuged for 60 minutes at

20000g. The supernatant was raised to 62% saturation with ammonium sulphate and again stirred for 30 minutes before centrifugation at 20000g for 60 minutes. The supernatant was discarded and the pellet redissolved in about 125ml 10mM tris pH7.6 (buffer A). This solution was desalted by passage through a 1000cm^3 column of Sephadex G50 equilibrated with buffer A, and loaded at a flow rate of 60$mlhr^{-1}$ onto two columns (2.6cm diameter × 40cm long) of Cibacron blue Sepharose CL6B connected in series and equilibrated with buffer A. These columns were washed with buffer A until the absorbance of the eluate at 280nm was less than 0.01. Bound FBPase was then eluted with buffer containing 0.5mM AMP and 10ml fractions collected. The enzyme was eluted as a sharp band with the AMP front. The bulk of the activity appeared in 5 fractions. These were combined and dialysed against buffer A then against 5 volumes of saturated ammonium sulphate. The precipitated enzyme was spun down and stored as an ammonium sulphate suspension at about 5$mgml^{-1}$.

Samples from various stages of the purification were analysed by SDS PAGE using preformed 5% to 25% gradient gel on a Pharmacia Fast gel system using supplied protocols for running the gel and staining with Coomassie Blue.

5.2.13 Testing Affinity Matrices for GAPDH Binding

About 1ml of the matrix to be tested was packed into a small column and equilibrated with the required buffer by pumping at least 10ml buffer through. GAPDH was removed from an ammonium sulphate suspension by centrifugation, resuspended in the required buffer and desalted using a PD10 column equilibrated with the same buffer. About 100U activity was then loaded onto the 1ml test column and the column washed with buffer until the absorbance at 280nm returned to baseline. Bound enzyme was then eluted using 5ml 1mM NAD^+. Fractions of 1 - 2ml were collected and assayed for activity.

5.2.14 Testing Matrices for FBPase Binding

The apparatus used was as described for the determination of batch adsorption kinetics by Horstmann *et al.* (1986). A water jacketed vessel, maintained at 25°C, was set up with an overhead stirrer and a small 20μm porosity filter leading to an external loop containing a flow cell in a Cecil 272 spectrophotometer and a peristaltic pump. FBPase (20μgml^{-1}) in buffer (50mM triethanolamine/KOH, 10μM EDTA, 1mM $MgSO_4$ and 0.2mM DTT pH7.2) was added to the vessel and the solution pumped around the recycle loop until a stable plateau was obtained on a chart recorder connected to the spectrophotometer. The volume of the external loop was minimised and a high flow rate used to minimise the response time of the system. At time zero about 1ml settled volume of the matrix to be tested was added and the system left until a new stable plateau was achieved. The protein bound can be determined from the difference between the plateaus since the volume of the system and the extinction coefficient of FBPase are known.

5.2.15 Equilibrium batch adsorption

A suspension of matrix was allowed to settle in a measuring cylinder and its volume measured. The matrix was then filtered to a moist cake on a sintered glass funnel and weighed. A mass of this moist matrix equal to 4 ml settled volume was added to 20ml 50mM sodium pyrophosphate buffer pH 8.5 containing 1mM 2-mercaptoethanol and 1mM EDTA (buffer A). The total volume was measured and the suspension added to a water jacketed vessel maintained at 25°C $\pm$ 0.3°C, stirred with an overhead stirrer to minimise physical matrix degradation. A known amount of GAPDH was added and allowed to equilibrate for about 10 minutes. A 100μl sample was withdrawn, spun briefly to sediment the matrix and 20μl samples of supernatant removed for triplicate enzyme assays. The total added ligand concentration in the vessel was increased by adding a small volume of NAD^+ solution and the system allowed to re-equilibrate for 8 minutes before repeating the cycle. This was continued until the desired range of added ligand had been covered.The concentration of free

enzyme is found from the assays so, knowing the total amount of enzyme initially added and the system volume (recalculated after each cycle), bound enzyme can be calculated from the enzyme mass balance for each concentration of added ligand.

5.2.16 Batch Binding using Separate Incubations for Each NAD^+ Concentration

GAPDH was not sufficiently stable at 40°C for the above protocol to be used so an alternative method was used which only necessitated the enzyme being at 40°C for about 15 minutes.

A small cylindrical vessel was maintained at 40°C using a recirculating water bath. AMP-Sepharose was washed with buffer A then filtered on a sintered glass funnel to a moist cake and divided into 225mg $\pm$2mg aliquots. 650μl buffer A was mixed with an aliquot of matrix in the vessel and 100μl buffer A containing 0.3U GAPDH added. 10μl of an NAD^+ solution of appropriate concentration was added to give the required final NAD^+ concentration and the mixture stirred using a small magnetic stirring bar for 10 minutes. 200μl was removed, centrifuged briefly to remove the matrix and 20μl aliquots of the supernatant assayed in triplicate to determine the amount of free enzyme. The total volume of each incubation was 1ml so the amount of enzyme bound to the matrix could be calculated from the mass balance as a function of NAD^+ concentration.

5.2.17 Frontal Analysis of FBPase Binding to Phosphocellulose

50mg phosphocellulose was swollen in running buffer (50mM triethanolamine pH7.2 containing 1.01mM $MgSO_4$, 10μM EDTA and 0.2mM DTT) containing AMP at the appropriate concentration. This was packed into a column 6.6mm diameter by 13mm maintained at 30°C by a water jacket and a recirculating water bath. The column was washed with running buffer at a flow rate of 35μlmin^{-1} for at least 1 hour before use.

FBPase was removed from an ammonium sulphate suspension by centrifugation, resuspended in running buffer without AMP and desalted into the same buffer on a PD10 column. The concentration was adjusted to 100μg/ml (A280=.089). 6ml of this solution was mixed with 6ml running buffer containing twice the required concentration of AMP to make up the feedstock solution. This was loaded continuously at a flow rate of 35μlmin^{-1} and 4 minute fractions collected for enzyme assay to determine the position of the emerging protein front. The assay of Nimmo and Tipton (1975) was used (see section 5.2.11).

5.2.18 Characterisation of Cibacron Blue 3G Dye

This was carried out using the paired ion reverse phase HPLC method of Burton *et al.* (1988) with the gradient profile adjusted due to the use of a shorter column with a smaller particle size silica.

A 150mm Hypersil ODS column with 3μm particle size was equilibrated with methanol - 0.1% (w/v)aqueous CTMB (80:20) (buffer A) for about 2 hours at a flow rate of 1mlmin^{-1}. Samples of dye were made up in distilled water at about 1mM and diluted 20 fold with buffer A. 20μl samples were injected and eluted using the following gradient:

Buffer A - 80% methanol / 20% 0.1% (w/v) CTMB						
Buffer B - 95% methanol / 5% 0.1% (w/v) CTMB						
Time (min)	0	3	5	6	15	18
% B	0	0	33.3	33.3	66.7	100

Peaks were detected by absorbance at 280nm.

Since no pure dye samples were available as standards, Basilen blue from Sigma, which was stated to be a mixture of meta and para isomers, was used.

5.2.19 Coupling of Cibacron Blue to Dextran

a) Initial protocol

The coupling was performed by a method modified from that of Bohme *et al.* (1972). A solution of 20g of dextran in 600ml water was mixed with solutions of 2g of Cibacron blue in 200ml water and 20g of Na_2CO_3 in 200ml water. The mixture was then stirred at 45°C. whilst samples of 100ml were withdrawn at various time intervals. After 75 hours another 2g of Cibacron blue was added to the mixtures. An equal volume of ethanol was added to each sample which was then allowed to stand at -20°C. for at least 60 min. The precipitate was spun down and the pellet resuspended in 50 ml of water. The precipitation and resuspension procedure was repeated a further two times. The final resuspension of the dextran-Cibacron blue conjugates was in 40ml of water. These solutions were dialysed against a large volume of distilled water for 24 hours to remove any remaining dye before storage at 4°C. with a few crystals of sodium azide to inhibit the growth of microorganisms.

b) Improved protocol

20g Na_2CO_3 and 20g dextran of M.W. 5×10^5 or 2×10^6 were dissolved in 1l distilled water and sufficient dye added to achieve the lowest desired loading at completion assuming that 30% of the mass of crude dye added coupled to the dextran. This was incubated at 45°C for 24 hours. A 100ml aliquot was removed and more dye added to the remainder to obtain the next highest loading. This cycle was repeated a further 8 times to give a range of 10 conjugates. The dye dextran conjugates were recovered and washed as above.

On the basis of gel filtration experiments, no low molecular weight material of high absorbance was present in the conjugate solutions. This indicated that the free dye was separated from that bound to dextran by the preparation method. Similar analysis showed that no release of dye occurred over a two-month storage period and that the conjugates were stable two months after production.

5.2.20 Characterisation of Dye-Dextran Conjugates

a) Dry Weight Determination

1ml samples of dialysed dye-Dextran conjugate solutions were pipetted in triplicate into dry preweighed glass test-tubes. These were dried in an oven at 80°C and weighed periodically until they reached constant weight. All tubes were then reweighed and the mass of conjugate in each tube calculated. These figures were then used together with spectroscopic measurements of the same conjugate solutions in the calculation of dye loading.

b) Absorbance Measurement

Doubling dilutions of free dye and conjugates 20D2 and 20D10 were made up in distilled water. The absorbance of each solution was measured at 610nm and 257nm and the results used to calculate deviations from the Beer-Lambert Law as a function of concentration.

c) Hydrolysis of Dye-Dextran Conjugates

The method developed by Chambers (1977) for estimation of dye substitution in Blue Dextran and Blue Dextran-Sepharose was used.

1ml concentrated HCl was added to 1ml blue dextran solution in small glass test-tubes. The tubes were incubated in a water bath at 40°C. 0.5ml samples were removed after various time intervals. These samples were diluted by doubling dilution in 6M HCl and used to determine the effect of hydrolysis time on the nature of the dye spectrum and deviation from the Beer-Lambert law. Free dye controls were carried out in parallel using dye concentrations of 25μM, 75μM, 150μM and 500μM dye to check the stability of the dye chromophore under the hydrolysis conditions used.

5.2.21 Laser Light Scattering Measurements

These were carried out using an Oros Instruments M801 Molecular Size Detector. Solutions of underivatised dextran of different molecular weights and dye dextran conjugates were filtered through 0.2μm filters to remove dust particles etc. Samples were injected into the sampling cell of the instrument through a 0.2μm filter and at least 10 readings taken for each conjugate tested. From the data the mean diffusion coefficient D_T was determined. The callibration graph constructed with the underivatised dextran samples was then used to calculate an apparent molecular weight for each conjugate tested. Samples were measured in distilled water and in 1M NaCl solution.

5.2.22 Gel Permeation Binding Experiments

a) Using a conventional Sephadex G75 column

A column (50 x 0.66 cm i.d.) was packed with Sephadex-G75 under gravity. Sephadex was chosen because Cibacron blue does not interact with the dextran matrix under the experimental conditions, and the pore size allowed adequate separation of lysozyme (molecular weight, 14400) and the conjugates (average molecular weight $>2 \times 10^6$); the latter were completely excluded and eluted at the void volume of the column. The column was equilibrated with 'running buffer' (50mM NaCl, 10mM tris, and lysozyme as appropriate adjusted to pH 8.0 with HCl) until a stable plateau was observed on a chart trace (at least two column volumes of running buffer were required). Typical flow rates were 20 to 25 ml/hour. Column temperature was maintained at 24°C by the use of a water jacket and a thermostatically controlled recirculating water bath. Running buffers were degassed by helium sparging and pre-equilibrated to the column temperature before use. The samples for loading were prepared by diluting aqueous dye-dextran conjugate solutions with an equal volume of double-strength buffer which contained lysozyme at twice the concentration of that in the equlibration buffer. The dye-dextran conjugate sample was loaded

using a precalibrated injection loop of 36.25 μl volume. The column eluate was passed through a quartz flow cell in a spectrophotometer connected to a chart recorder, with absorbance monitored at 280 nm. From the chart trace, extinction coefficient of lysozyme (see below) and the flow rate, troughs could be integrated to determine the amount of bound lysozyme.

An operational extinction coefficient for lysozyme was determined by equilibrating the column with running buffer in the absence of lysozyme and then in the presence of a known concentration of lysozyme. The difference between the baseline and the plateau on the chart trace could then be used to relate pen displacement and lysozyme concentration in subsequent measurements.

b) Using a Superose 12HR column on an FPLC system

The method used was essentially the same as a) above except that a 50μl injection loop was used and the flow rate was 36mlhour^{-1}. The plastic air filled jacket normally fixed to the column was removed and replaced with a glass water jacket in order to achieve more precise temperature control. An in-line filter was added just before the top of the column in an attempt to trap any aggregates before they blocked the top frit of the column.

The trough areas were estimated by photocopying the chart traces and cutting out and weighing the troughs since this was considered to be more accurate than direct calculation since the enhanced resolution of the column relative to the Sephadex G75 column yielded much sharper, deeper troughs.

5.2.23 Spectral Titration

a) Equilibrium studies

Sample and reference cuvettes each containing a solution of approximately 70μM (with respect to dye) conjugate in 10mM tris 50mM NaCl pH8.0 were equilibrated at 25°C in a Cecil 272 spectrophotometer with a thermostatted cuvette holder. Small

volumes of 5mM lysozyme solution were added to the sample cuvette and equal volumes of buffer added to the reference cuvette. The contents of the cuvettes were mixed in situ using small plastic paddles which could be left in the cuvettes without obstructing the light path. The absorbance difference was measured at 595nm after each addition of lysozyme. Lysozyme concentrations in the range 0 - 250μM were used. All conjugate solutions were normalised for total dextran content by adding underivatised dextran of the appropriate molecular weight to adjust the concentration of dextran to that of the one with the lowest dye/dextran ratio used in the titrations i.e. 2D2 or 5D1 (see figure 1 for definitions of nomenclature). Difference spectra were produced using the same method but scanning across the wavelength range 400 - 750nm using a Cecil 588 scanning spectrophotometer after each lysozyme addition. ϵ_f was calculated for each conjugate from absorbance at 595nm. Values varied slightly due to different degrees of dye stacking, but were all within the range 9000-9800 $M^{-1}cm^{-1}$.

b) Kinetic studies

Reaction kinetics were followed using a stopped flow apparatus with associated computerised data capture model SF51 (Hi-Tech Scientific, Salisury, U.K.).

Solutions of dye or dye dextran conjugate, and lysozyme were made up at twice the required final concentration and loaded into the two syringes of the apparatus. Injection was carried out using a pneumatic ram which achieved very efficient mixing and consequently small dead times. Data was captured by a PC fitted with a rapid (1MHz) analogue to digital conversion card and stored and displayed using software supplied with the instrument. Readings were taken at intervals over the time scale 0-2 seconds for most runs except for free dye mixed with lysozyme where the time scale was increased to 100 seconds for some runs.

5.2.24 Computer Curve Fitting

For the cooperative binding work a curve fitting program based on the simplex method (Caceci *et al.*, 1984), written in Turbo Basic, was used. For later work, including all the work with dye-dextran conjugates, the Pfit curve fitting program supplied with the FigP (Biosoft) scientific graph plotting program was used. This was faster and much more convenient due to the interactive nature of the interface and the ease of visually checking the 'goodness of fit' given by the calculated parameters. Pfit is based on the Marquardt curve fitting algorithm, which is generally recognised to offer the best compromise between robustness and speed. In the few cases where the results determined by Pfit were compared with those obtained from the Simplex method the parameter values showed close agreement (as would be expected).

CHAPTER 6

COOPERATIVE BINDING PHENOMENA - RESULTS

6.1 Selection of an Appropriate System for the Study of Cooperative Binding

In order to make a rational decision regarding which protein/ligand system would be most appropriate for this study the attributes of an ideal system were defined and available systems assessed with regard to these ideals. Attributes of an ideal system include the following:

1) The protein must display positive homotropic cooperativity for its ligand within an experimentally practical concentration range. This cooperative behaviour would ideally be well documented and demonstrated by ligand binding rather than kinetic measurments.

2) The protein should be stable over a reasonably long period of time under experimental conditions and stable for weeks or months under appropriate bulk storage conditions.

3) The protein should be available commercially at reasonable cost or be easily purified to homogeneity from a readily available starting material using a published protocol.

4) The protein should have a history of use as a model protein in affinity chromatography research so that development does not have to be pursued from scratch in order to construct an appropriate experimental matrix ligand system.

5) The protein should have a simple, reliable and specific assay which would ideally be spectrophotometrically based.

Possible Systems Considered

i) Albumin / Alizarin Yellow G

Alizarin yellow G was reported to bind cooperatively to albumin when studied by equilibrium dialysis (Nissani *et al.*, 1983). This would be a very attractive system in terms of cost and the dye would be easy to monitor. It is probably unsuitable from a chromatographic viewpoint due to the known tendency of albumin to bind non-specifically to many matrix/ligand combinations. Computer simulation of theoretical binding curves for this system using the published affinity constants showed little enhancement of binding so it was dismissed from further consideration.

ii) Fructose Bisphosphatase E.C. 3.1.3.11

Fructose bisphosphatase has been purified from many sources by a number of workers (Sarngadharan *et al.*, 1970; Nimmo and Tipton, 1975a; DeMaine *et al.*, 1982; Han and Johnson, 1982; Macgregor *et al.*, 1982). Nimmo and Tipton used beef liver and have published a reasonably large scale purification protocol together with kinetic and binding studies which indicate that the negative effector AMP binds in a strongly positively cooperative manner while at the same time displaying 'half site reactivity' i.e. only two molecules of AMP bind per tetramer at saturation (Nimmo and Tipton 1975b). Fresh beef liver is easy to obtain in large quantities if required. Fructose bisphosphatase is reasonably stable for a few hours at room temperature and is stable for several months when stored as an ammonium sulphate suspension at 4°C. No affinity purifications on nucleotide ligands have been published for this enzyme but it may bind to AMP ligands for which there is much data. The enzyme has been purified by specific substrate or effector elution from both phosphocellulose and various blue dye matrices (Han and Johnson, 1982; MacGregor *et al.*, 1982) so these may serve as suitable pseudo-affinity ligands. It has been shown that chicken liver

fructose bisphosphatase binds to blue Sepharose specifically at the AMP binding site (Cruz *et al.*, 1979) and this may well also be true of the beef liver enzyme. Fructose bisphosphatase has a spectrophotometric assay but this is complicated by the requirement for two coupling enzymes and the fact that AMP, the ligand in question, acts as a powerful inhibitor of the enzyme. This might limit the experimental approaches which can be used in studies on the binding of this enzyme to matrices.

iii) Glyceraldehyde-3-phosphate Dehydrogenase E.C. 1.2.1.12

This was one enzyme considered in the theoretical modelling using the data of Cook and Koshland (1970). This data suggested mixed cooperativity for NAD^+ binding; positive between sites 1 and 2 but negative thereafter. It was later claimed by Gennis (1976) that this apparent mixed cooperativity was a result of protein affinity heterogeneity. Partially denatured protein retained NAD^+ binding capability but with altered association constants compared with the native enzyme. It was also shown that freshly prepared affinity purified glyceraldehyde-3-phosphate dehydrogenase showed only positive cooperativity with 4 mole NAD^+ bound per mole enzyme at saturation (i.e. 1 mole NAD^+ per subunit). The binding of NAD^+ to glyceraldehyde-3-phosphate dehydrogenase has been studied by equilibrium dialysis and other techniques and the results have been reported by a number of workers (Sloan and Velick, 1973; Velick *et al.*, 1972). The stability of glyceraldehyde-3-phosphate dehydrogenase may be a potential problem since loss of activity can be considerable over 24 hours. Denaturation may be kept within acceptable limits, however, by careful choice of conditions and the timescale of the experiments. It is probably also more stable in the presence of NAD^+, a condition which will be satisfied for the majority of the time during affinity chromatography studies. The enzyme is reported to be relatively stable as a cold ammonium sulphate suspension but does lose activity at a measurable rate under these conditions (Mosbach *et al.*, 1972). The affinity purification described by Gennis is rapid (total time about 3 hours) so it should not be necessary to store enzyme for a long period of time. The starting material is dried yeast which is cheap and easy to store. Glyceraldehyde-3-phosphate dehydrogenase has been used in model affinity chromatography systems both with NAD^+ based

ligands and with other related group specific adsorbents (Barry and O'Carra, 1973; Mosbach, 1972). In most cases Glyceraldehyde-3-phosphate dehydrogenase behaves as a model enzyme and has been shown to elute quantitatively from a number of different matrices by a pulse of NAD^+. One concern regarding the behaviour of glyceraldehyde-3-phosphate dehydrogenase in affinity chromatography is a report (Barry and O'Carra, 1973) that elution of the rabbit muscle enzyme from certain matrices is time dependant, recovery decreasing with time. This, it was suggested, was due to a further non-specific binding effect occuring between the enzyme and the spacer arm after the primary affinity interaction with the ligand. It was later found (O'Carra *et al.*, 1974) that use of a more hydrophilic spacer arm illiminated this problem. Similar behaviour may not be apparent for the yeast enzyme but must be considered when deciding which immobilisation chemistry should be adopted if this system is selected. Glyceraldehyde-3-phosphate dehydrogenase has a simple spectrophotometric assay (Stallcup *et al.*, 1972).

iv) Isocitrate Dehydrogenase (NAD^+ linked) E.C.1.1.1.41

The characterisation of isocitrate dehydrogenase has been reported for enzymes from many sources. The NAD^+ linked enzymes from pea mitochondria (Davies, 1969; Cox and Davies, 1970), swede (Coultate and Dennis, 1969), *Neurospora crassa* (Cook and Sanwal, 1969), *Blastocladiella emersonii* (Ingebretsen and Sanner, 1974) and yeast (Barnes *et al.*, 1971) all show positive cooperativity for isocitrate binding and those from pea mitochondria, *Blastocladiella* and yeast are also reported to be cooperative with respect to NAD^+ in kinetic studies. A report on the yeast enzyme (Kuehn *et al.*, 1971) indicated that the apparent cooperative binding of NAD^+, measured by equilibrium dialysis, was lost during purification. This is clearly of concern from an experimental viewpoint since most of the kinetic data was obtained from crude or partially purified enzyme preparations. NAD^+ would be a more convenient ligand than isocitrate to use in model studies due to the large amount of information on affinity chromatography of dehydrogenases on immobilised nucleotides. Isocitrate almost certainly binds cooperatively but it has rather poor affinity constants and any isocitrate like affinity column would also be a good ion exchange column (analogous

to a CM ion exchange column) leading to the possibility of much non-specific binding.

Other aspects of isocitrate which render it unattractive as a model system are the generally complex purification protocols which fail to yield homogeneous material and its probable lack of stability in dilute solution when purified. The starting materials for some of these enzymes would need to be cultured, further complicating the aquisition of the enzyme. It is reported to be fairly stable when stored in 50% glycerol at -20°C.

v) Lactate Dehydrogenase E.C. 1.1.1.27

This was one of the enzymes considered in the theoretical predictions which gave rise to this practical investigation (Hubble, 1987). The data of Klinov *et al.* (1979) for NADH binding to the porcine M4 isoenzyme was used. Although still valid for the computer modelling it appears that this enzyme only becomes cooperative when adsorbed onto dextran sulphate. In free solution all the available evidence from gel filtration and fluorescence quenching studies (Holbrook and Stinson, 1970; Stinson and Holbrook, 1973), indicates that NADH binding is characterised by four independent sites with identical microscopic association constants. For this reason lactate dehydrogenase is clearly inappropriate as a model system in this study.

It would thus appear that of the enzymes considered above GAPDH is the most promising system for study with FBPase also offering some possibility of success.

6.2 Simulation of Binding Curves for GAPDH

The data for binding of NAD^+ to GAPDH at 25°C were read from the graph published by Gennis (1976) and fitted to a 4 site Adair equation by non-linear least squares curve fitting in order to determine the values for the successive site binding constants (microscopic association constants) in this system, which was claimed to show pure positive cooperativity. The results of this fitting are shown below:

K_1 $2.6 \times 10^3 M^{-1}$

K_2 $1.5 \times 10^4 M^{-1}$

K_3 $1.9 \times 10^5 M^{-1}$

K_4 $5.7 \times 10^3 M^{-1}$

These constants are similar to those published by and Cook and Koshland (1970) and Mockrin *et al.* (1975) but are inconsistent with the claim of Gennis that the data showed pure positive cooperativity.

The values for the four site binding constants above were used in simulations of binding curves as carried out by Hubble (1987). In these simulations it was assumed:

i) that binding to immobilised ligand was described by the same constants as for binding of free ligand

ii) that the immobilised ligand was all accessible to the protein and uniformly distributed throughout the system volume

iii) that each protein molecule could only bind to a single matrix ligand

Simulated curves of fractional binding (i.e. bound enzyme / total enzyme in the system) against free ligand concentration were produced for a range of matrix ligand concentrations. These are presented in figure 6.1 which clearly shows the predicted enhancement of binding as the free ligand concentration increases up to a critical concentration, after which the enzyme is progressively biospecifically eluted. It is also clear that as the matrix ligand concentration increases the enhancement of binding due to free ligand becomes swamped due to the high levels of binding observed in the absence of added ligand.

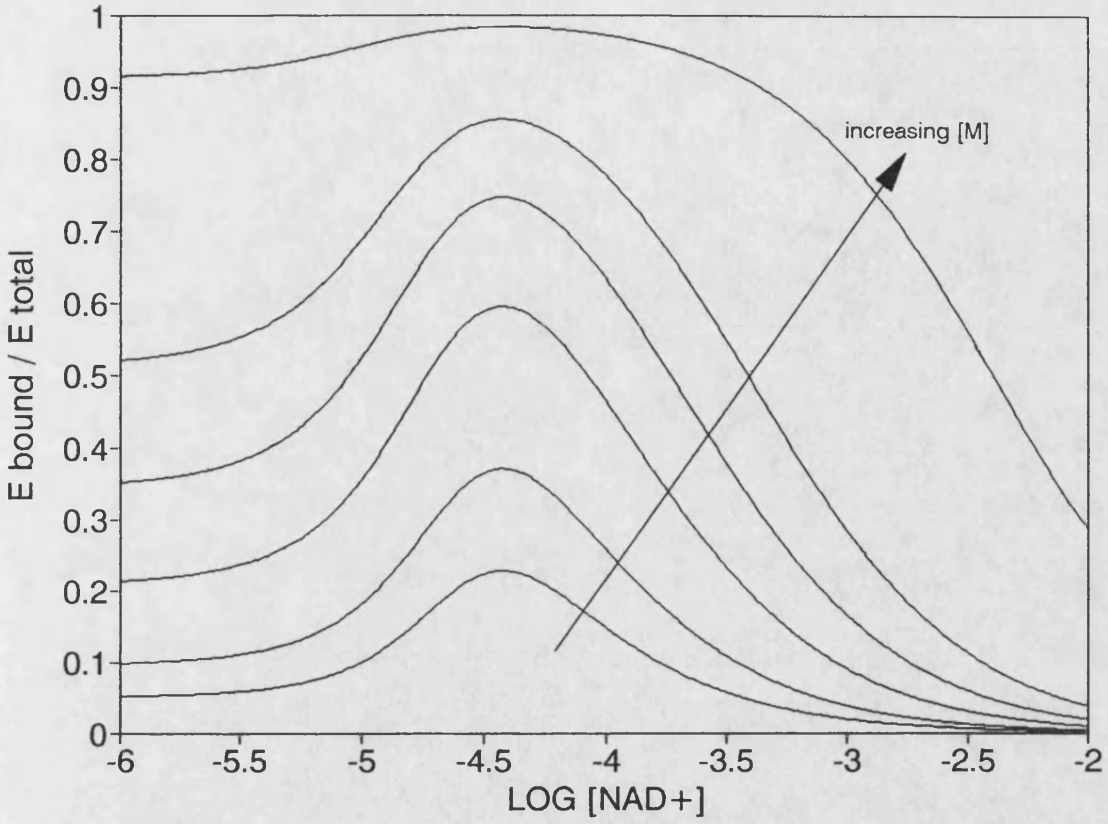

Figure 6.1

The predicted effect of matrix ligand concentration on the relationship between free ligand concentration and the fraction of GAPDH bound. The affinity constants used were derived from the data of Gennis (1976) and were:

$K_1 = 2.6\times10^3M^{-1}$; $K_2 = 1.5\times10^4M^{-1}$; $K_3 = 1.9\times10^5M^{-1}$; $K_4 = 5.7\times10^3M^{-1}$

The matrix ligand concentrations were: 5×10^{-6}M, 1×10^{-5}M, 2.5×10^{-5}M 5×10^{-5}M, 1×10^{-4}M, 1×10^{-3}M

A simulation was also carried out for the binding data at 40°C from Niekamp *et al.* (1977) since, although the affinity constants are lower at the higher temperature, the degree of cooperativity between the first two binding sites is greater. The constants used were:

$K_1 = 137M^{-1}$, $K_2 = K_3 = K_4 = 8.3 \times 10^3M^{-1}$

This simulation is compared with an equivalent curve at 25°C in figure 6.2.

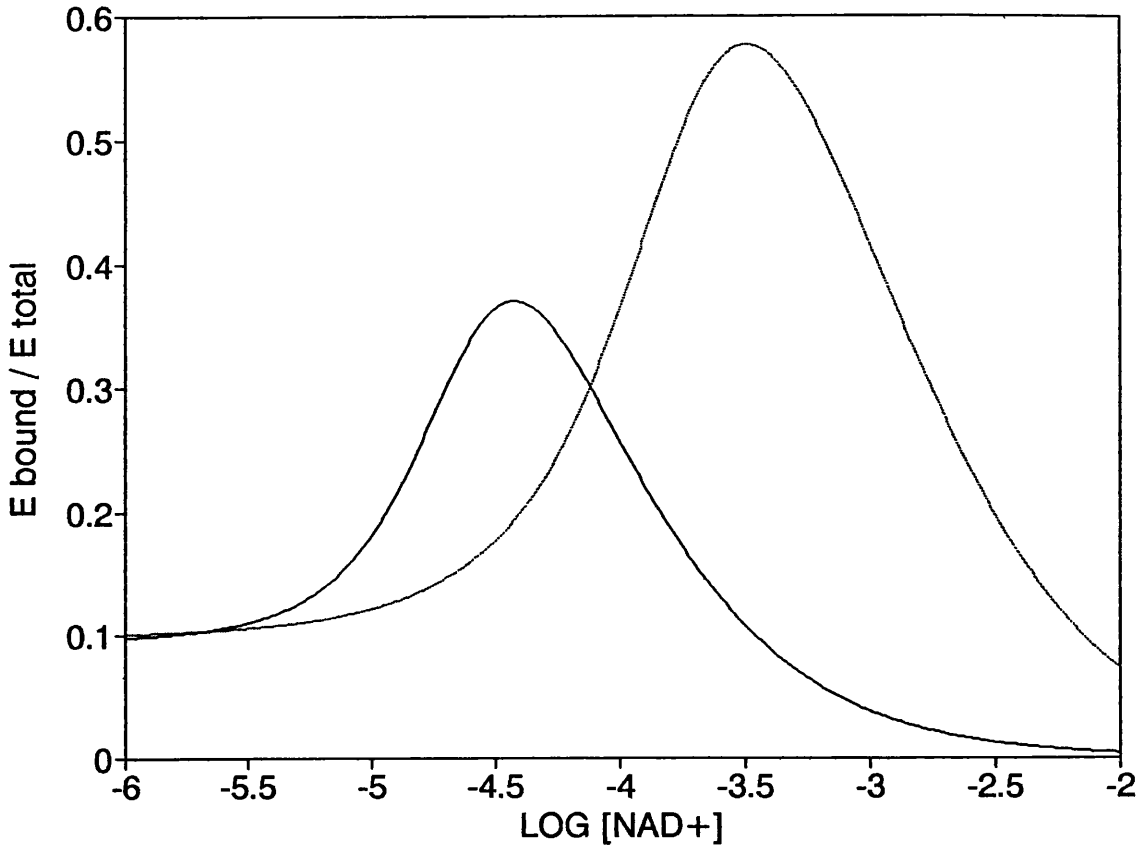

Figure 6.2

The effect of temperature on the predicted effect of free ligand on the fractional binding of GAPDH to an immobilised ligand. The association constants used were: at 25°C $K_1 = 2.6\times10^3M^{-1}$; $K_2 = 1.5\times10^4M^{-1}$;$K_3 = 1.9\times10^5M^{-1}$; $K_4 = 5.7\times10^3M^{-1}$; at 40°C $K_1 = 137$, $K_2 = K_3 = K_4 = 8.3 \times 10^3$

The matrix ligand concentrations were 1×10^{-5}M at 25°C (solid line) and 2×10^{-4}M at 40°C (dotted line)

6.3 Simulation of Binding Curves for FBPase

The data for binding of AMP to FBPase were extracted from the Scatchard plot at 0.5mM Mg^{2+} and from the Hill plot at 1mM Mg^{2+} published by Nimmo and Tipton (1975b). Both sets of data were fitted to a two site Adair equation to determine the microscopic site binding constants for the interaction. The results are summarised in the table below.

	$[Mg^{2+}]$	K_1	K_2
data from	mM	M^{-1}	M^{-1}
Hill plot	1	1.24×10^{3}	1.00×10^{6}
Scatchard plot	0.5	1.30×10^{3}	1.02×10^{6}

table 6a.
Summary of association constants obtained by non-linear least squares curve fitting of data extracted from graphs presented by Nimmo and Tipton (1975b).

The constants obtained by fitting the AMP binding data to a 2 site Adair equation were very similar irrespective of whether the data from the Hill plot or the Scatchard plot were used. Since the data set extracted from the Hill plot contained more data points these constants were used for the simulation which follows although the difference would be minimal if the constants from the Scatchard plot had been used.

The equation describing the binding of a two site protein to immobilised ligand in the presence of free ligand was derived as follows:

$$\begin{aligned} [P] + [L] &\overset{2K_1}{\rightleftharpoons} [PL] \\ [PL] + [L] &\overset{\frac{1}{2}K_2}{\rightleftharpoons} [PL]_2 \\ [P] + [M] &\overset{2Kb_1}{\rightleftharpoons} [PM] \\ [PM] + [L] &\overset{Kb_2}{\rightleftharpoons} [PML] \end{aligned} \qquad (6.1)$$

where [P] is protein, [L] free ligand and [M] matrix ligand.
From these equilibria:

$$\begin{aligned} [PL] &= 2K_1[P][L] \\ [PL_2] &= K_1K_2[P][L]^2 \\ [PM] &= 2Kb_1[P][M] \\ [PML] &= 2Kb_1Kb_2[P][M][L] \end{aligned} \qquad (6.2)$$

The fractional binding of protein is given by:

$$\bar{Y} = \frac{[PM] + [PML]}{[P] + [PM] + [PML] + [PL] + [PL_2]} \qquad (6.3)$$

Hence by substituting from equation (6.2) above the final equation is:

$$\bar{Y} = \frac{2Kb_1[M]\,(1 + Kb_2[L])}{1 + 2Kb_1[M]\,(1 + Kb_2[L]) + 2K_1[L]\,(1 + K_2[L])} \qquad (6.4)$$

Simulations were carried out for a range of matrix ligand concentrations by substitution of parameter values in equation (6.4). The result, shown in figure 6.3, is very similar in general form to the simulations for GAPDH, showing an enhancement in binding up to a critical free ligand concentration followed by a reduction in binding due to competitive elution. The swamping of the effect by high matrix ligand concentrations is also clearly demonstrated.

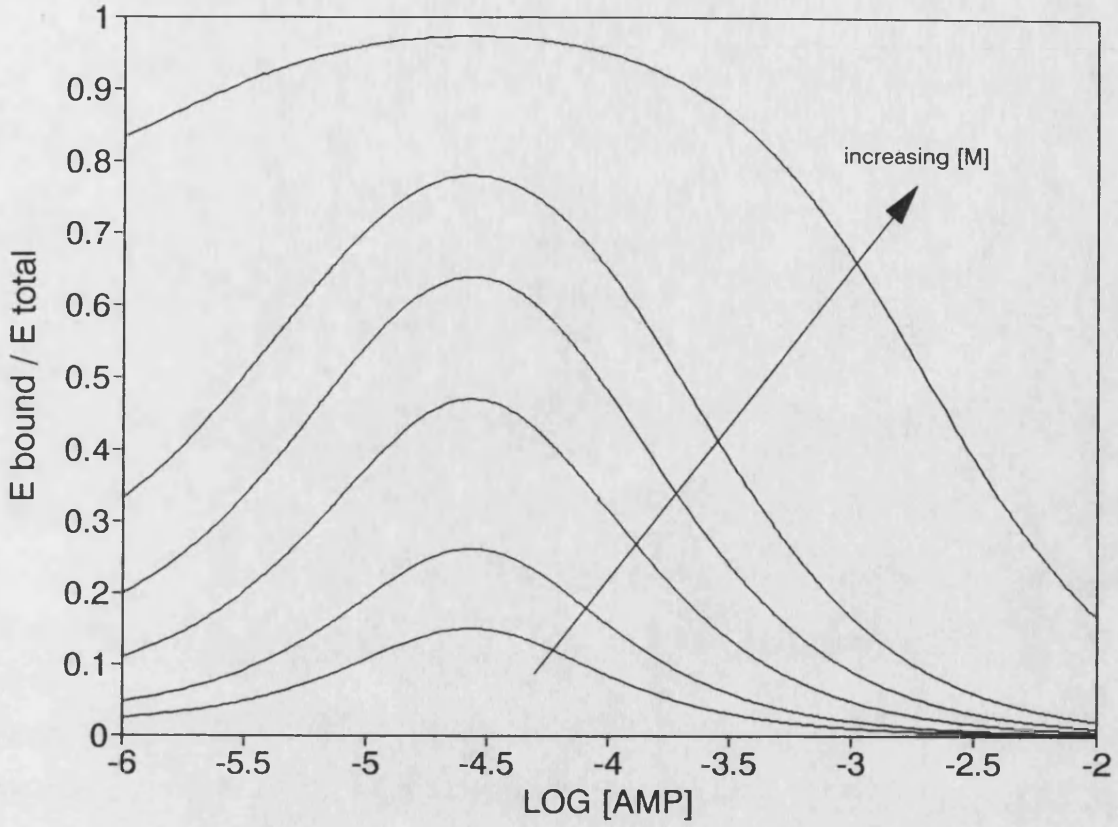

Figure 6.3

The predicted effect of matrix ligand concentration on the relationship between free ligand concentration and the fraction of FBPase bound. The affinity constants used were: $K_1 = 1.24 \times 10^3$, $K_2 = 1.00 \times 10^6$

The matrix ligand concentrations were:

5×10^{-6}M, 1×10^{-5}M, 2.5×10^{-5}M, 5×10^{-5}M, 1×10^{-4}M, 1×10^{-3}M.

6.4 Purification of FBPase

The results of a typical purification of FBPase are summarised in table 6b. The specific activity of the final product was similar to or slightly higher than that obtained by Nimmo and Tipton (1975a) using the original protocol on which this method is based. The yield was very similar as were the other parameters used to assess the purity of the product (the ratio of the activities of the enzyme measured at pH 7.2 and 9.5 which was about 2 and the % inhibition by 15μM AMP which was 52%). The SDS PAGE gel shown in figure 6.4 confirmed that the final product was almost pure and that the subunit had the correct molecular weight of 35000. The advantage of the modifications to the original protocol was the simplification and the consequent saving in time achieved.

An attempt was made to incorporate a heat treatment step before the blue Sepharose column in order to reduce the protein concentration and remove the residual haemoglobin from the preparation. This could have considerably reduced the washing time required for the blue Sepharose column. Although successful for FBPase from several other sources, the beef liver enzyme proved to be heat labile even in the presence of substrate. Considerable losses of activity occured at temperatures high enough to achieve worthwhile protein aggregation; hence this step was not included in the final protocol.

step	volume ml	enzyme activity U/ml	protein concn. mg/ml	specific activity U/mg	total activity U	yield %
crude supernatant	1920	2.32	101	0.02	4454	100
pH treatment	1620	2.02	62	0.03	2372	73
ammonium sulphate pellet*	320	6.37	35	0.18	2038	46
blue Sepharose eluate	35	39.1	1.46	26.8	1369	31
* after resuspension and desalting						

TABLE 6b

Summary of the stages in the purification of fructose bisphosphatase from beef liver

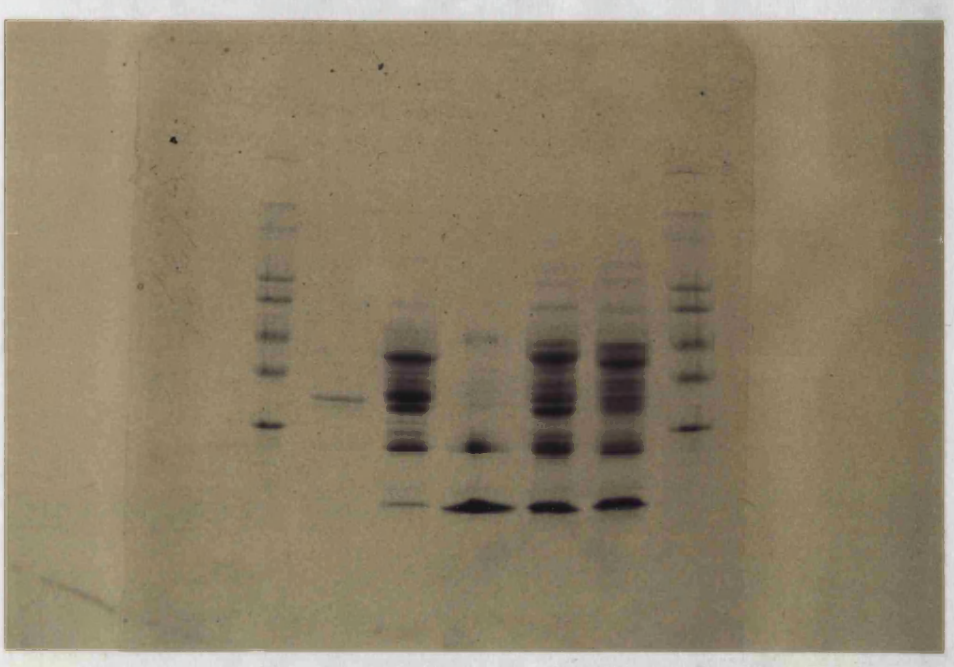

Figure 6.4

Photograph of an SDS PAGE gel showing the protein composition of the various stages in the purification of beef liver FBPase.

Track 1	molecular weight markers (205k, 116k, 97k, 68k, 43k, 29k)
Track 2	crude supernatant
Track 3	supernatant after pH treatment
Track 4	52% ammonium sulphate supernatant
Track 5	desalted ammonium sulphate pellet
Track 6	Eluate from blue Sepharose column
Track 7	molecular weight markers (as for track 1)

6.5 Testing Matrices for Binding of GAPDH

The binding of GAPDH to three immobilised nucleotide matrices under a variety of conditions is summarised in table 6c. From this it is clear that little binding is apparent for the azo NAD^+ matrix at pH8.5 but that both the N^6 coupled matrices showed reasonable binding at this pH. Of the two N^6 linked matrices the NAD^+ appears to bind GAPDH better since the same capacity was achieved with a ligand density which was only 40% of that of the AMP matrix.

matrix	[ligand]	temp	pH	buffer	GAPDH bound
	mM	°C			$mgml^{-1}$
I	1.8	25	7.0	10mM EDTA	0.52
		4	8.5	50mM tris	0.08
		25	8.5	50mM tris	0.03
II	4.4	20	7.0	50mM TES 0.1M KCl	0.57*
		20	8.5	50mM tris 0.1M KCl	0.72
III	1.8	20	8.5	50mM pyro-phosphate	0.71
matrix I - p-azo-benzamidopropyl NAD^+ Sepharose					
matrix II - N^6-(6-aminohexyl)AMP Sepharose					
matrix III - N^6-(6-aminohexyl)carbamoylmethyl NAD^+ Sepharose					

* This matrix was probably not saturated.

Table 6c

Summary of binding conditions and capacity for binding of GAPDH to 3 nucleotide Sepharose matrices.

6.6 Testing Matrices for Binding of FBPase

The binding of FBPase to various matrices was measured using a batch adsorption rig with a recycle loop containing a flow cell for monitoring of protein concentration. Four matrices were tested for binding, namely Cibacron Blue Sepharose CL6B, phosphocellulose, N^6(6-aminohexyl)AMP agarose and C^8(6-aminohexyl)aminoAMP agarose. Progress curves for binding of FBPase to the first two matrices are shown in figures 6.4 and 6.5. Neither of the AMP matrices tested showed any binding of FBPase at all.

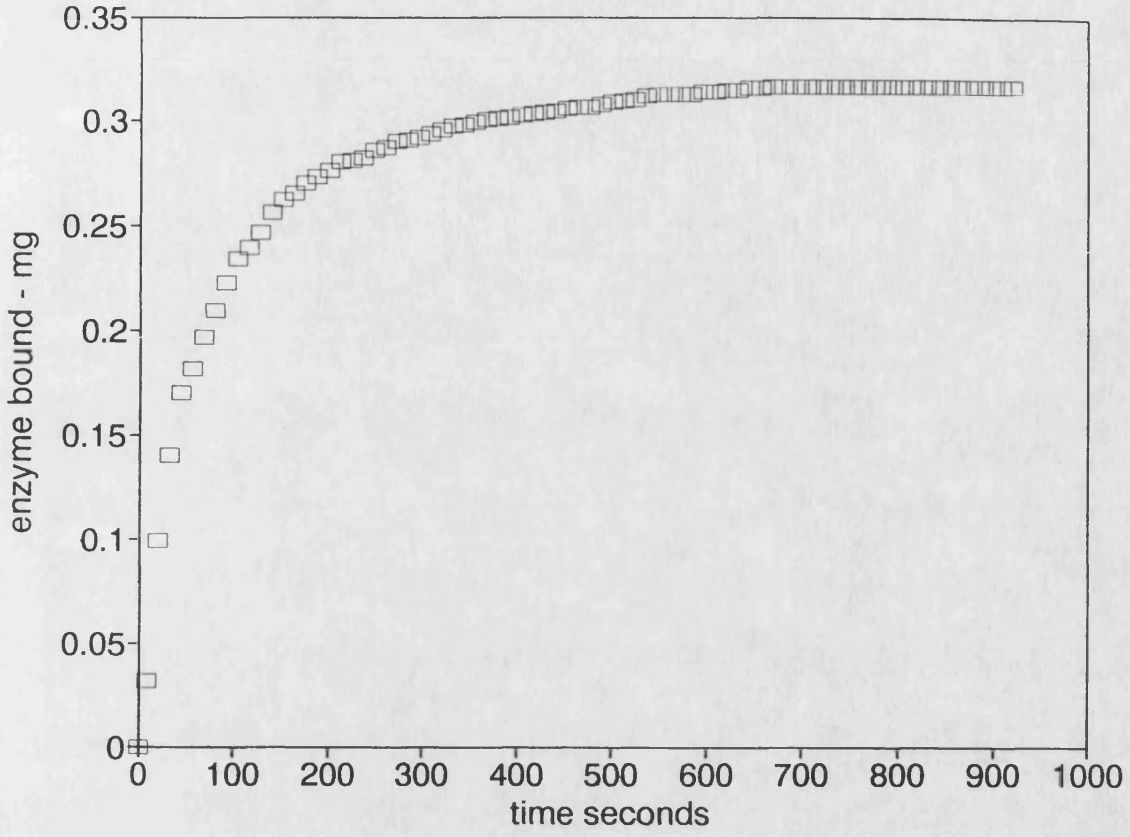

Figure 6.5

Progress curve for batch adsorption of FBPase onto Cibacron Blue Sepharose at 30°C in 50mM triethanolamine/KOH, 10μM EDTA, 1mM $MgSO_4$ and 0.2mM DTT. At time = zero 0.87ml (settled volume) blue Sepharose was added to 21.83ml buffer containing FBPase at 20μgml^{-1}. Protein concentration was monitored by measuring absorbance at 280nm in the external loop.

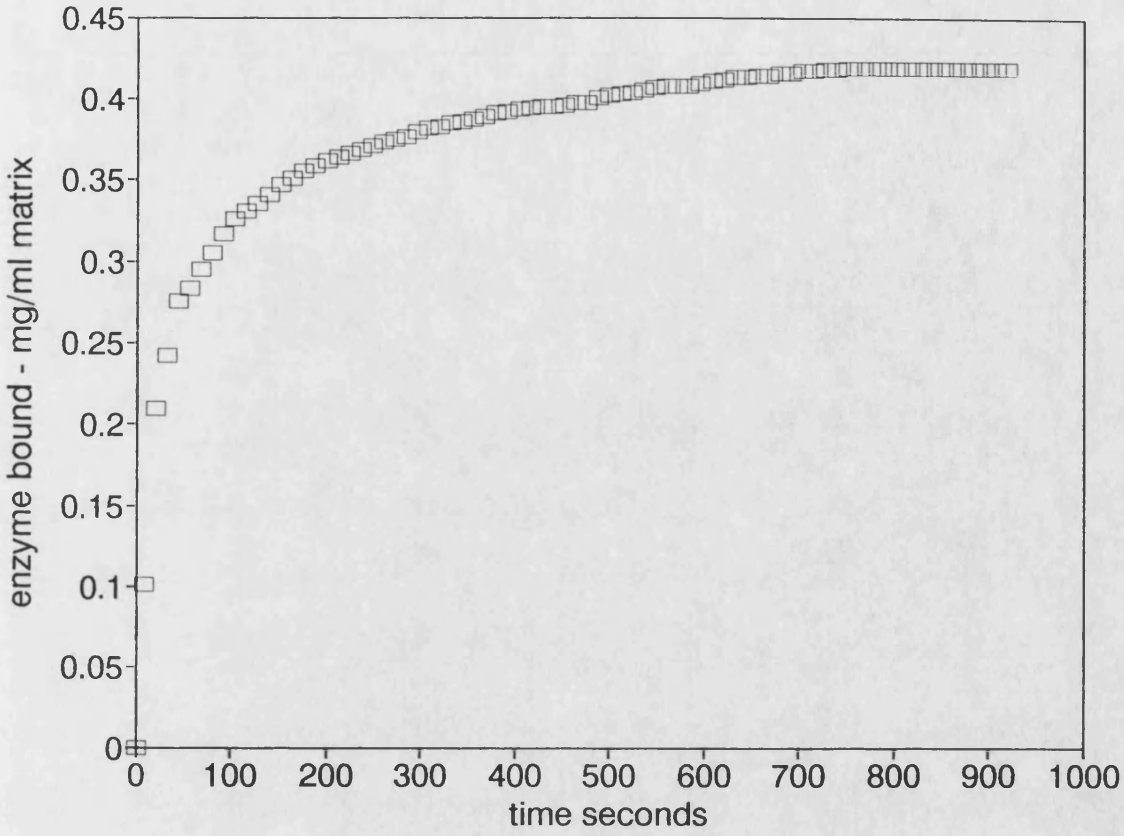

Figure 6.6

Progress curve for batch adsorption of FBPase onto phosphocellulose at 30°C in 50mM triethanolamine/KOH, 10μM EDTA, 1mM $MgSO_4$ and 0.2mM DTT. At time = zero 0.82ml (settled volume) phosphocellulose was added to 21.83ml buffer containing FBPase at 20μgml^{-1}. Protein concentration was monitored by measuring absorbance at 280nm in the external loop.

6.7 Equilibrium Batch Adsorption of GAPDH using Sepharose Matrices

Figure 6.7 shows a typical result for binding of GAPDH to N^6-(6-aminohexyl) carbamoylmethyl NAD^+ Sepharose. There was no obvious enhancement of binding on progressively adding NAD^+ but biospecific elution of the enzyme from the matrix was clearly observed as the NAD^+ concentration reached higher levels. A control experiment using underivatised Sepharose indicated that there was no non-specific binding of the enzyme to the Sepharose beads alone and that the enzyme was stable under the conditions adopted for the duration of the experiment (about 90 minutes).

Figure 6.8 shows the result of a similar experiment carried out at pH6.5 where GAPDH exhibits no cooperativity when binding NAD^+. Under these conditions the binding of the enzyme to the matrix-ligand appears to be more favourable than at pH8.5 in the absence of NAD^+, but it also appears to be more easily eluted, only 30μM NAD^+ being required to swamp the enzyme interactions with matrix-ligand.

Figures 6.9, 6.10 and 6.11 are plots of bound enzyme / total enzyme for batch adsorption experiments using AMP Sepharose matrices with different immobilised ligand densities. The volume of the matrix with the highest density used was reduced to keep the bulk average ligand densities comparable. This avoided too much of the enzyme in the system being bound in the absence of NAD^+ which would prevent any possible enhancement of binding on adding NAD^+ from being observed. The fractional binding of GAPDH increased with increasing immobilised ligand density in the absence of added NAD^+ (arbitrarily plotted at -6.5). No enhancement of binding was observed for any of these matrices under the experimental conditions adopted when NAD^+ was progressively introduced into the system.

An attempt was made to investigate the binding of GAPDH to AMP-Sepharose at pH8.5 and 40°C. Unfortunately the enzyme was not sufficiently stable under these conditions for the usual 'sequential' equilibrium batch adsorption method to be used. Instead an alternative protocol was adopted where a separate incubation was set up for each NAD^+ concentration studied. Using this method the enzyme was only

required to be stable for 15 minutes rather than for more than 90 minutes as required for the 'sequential' method. The result of an experiment using this modified method is shown in figure 6.9. As for the studies at 25°C competitive elution is clearly demonstrated but there is still no evidence of any enhancement of binding at low added NAD^+ concentrations.

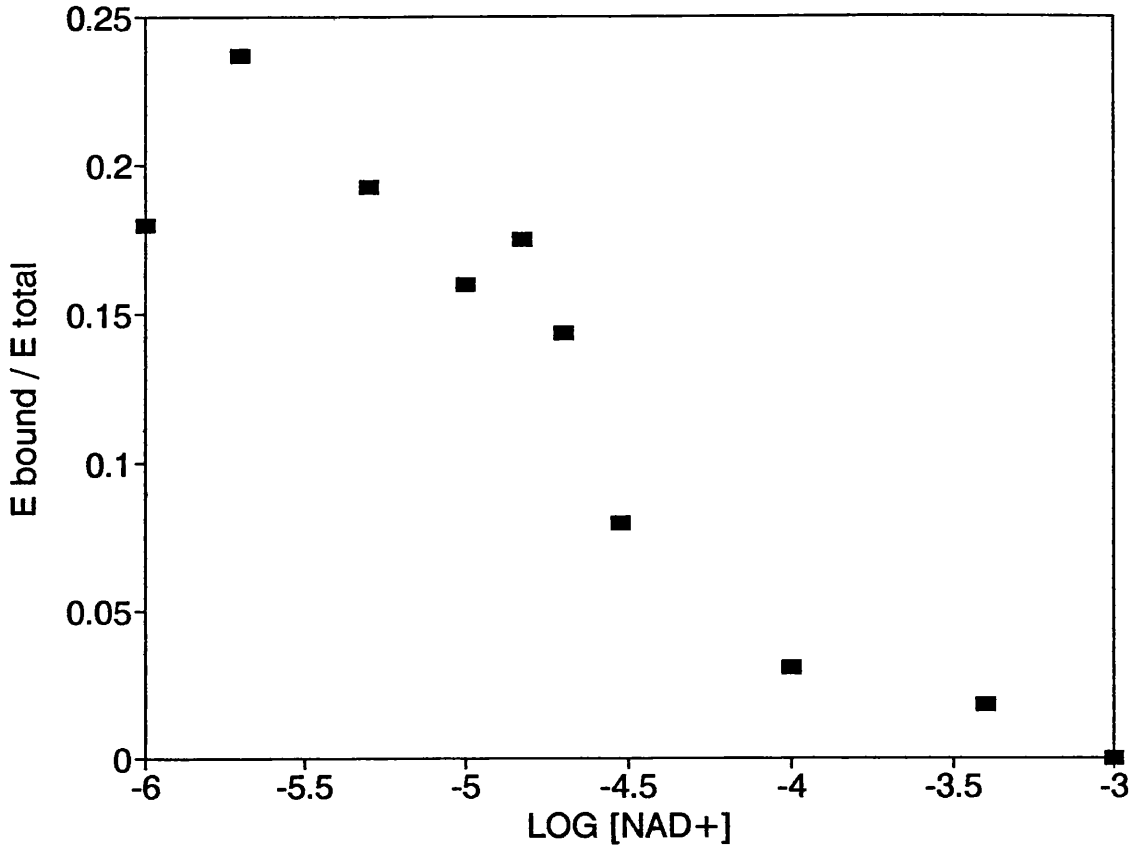

Figure 6.7

The effect of added NAD^+ on the fraction of GAPDH bound to NAD^+-Sepharose in 50mM sodium pyrophosphate buffer pH8.5 containing 1mM 2-mercaptoethanol and 1mM EDTA at 25°C. The bulk average matrix-ligand concentration was 4.4×10^{-5}M and the matrix volume 25% of total (matrix ligand concentration 1.76×10^{-4}M). The value at zero added NAD^+ is arbitrarily plotted at -6.

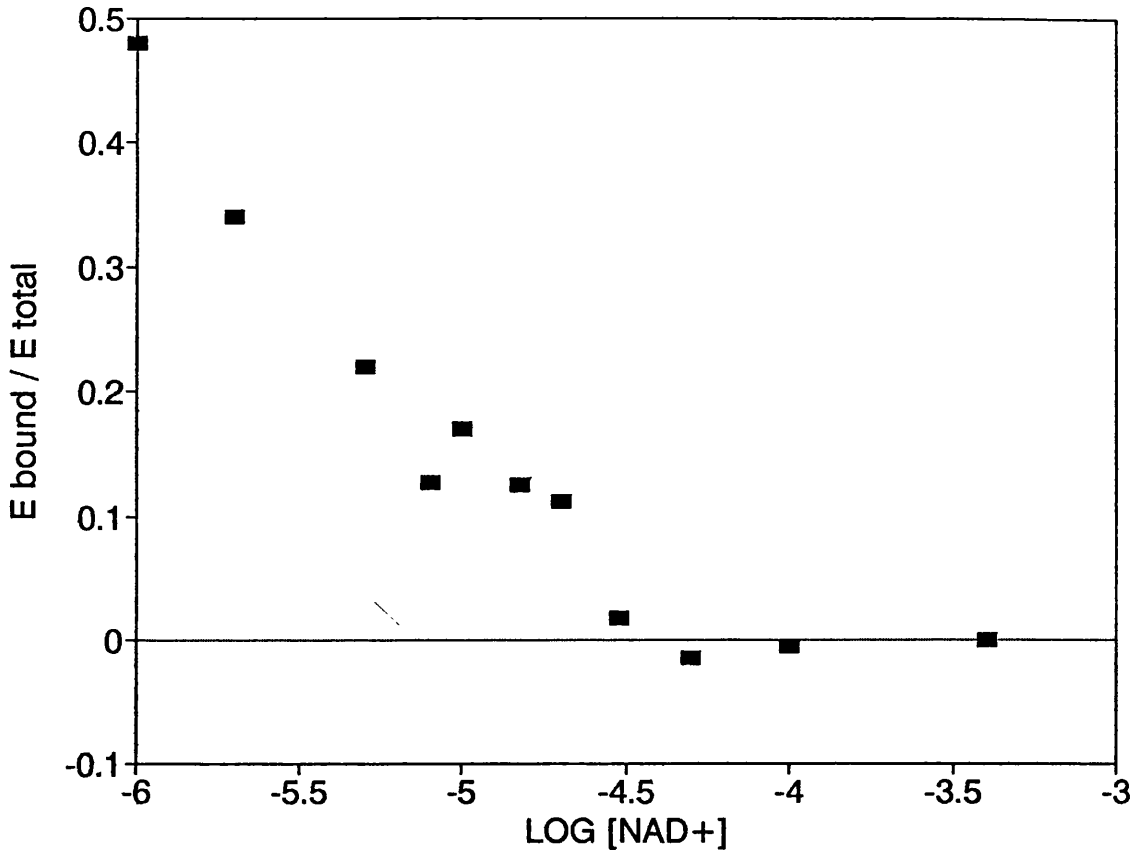

Figure 6.8

The effect of added NAD^+ on the fraction of GAPDH bound to NAD^+-Sepharose in 50mM sodium phosphate buffer pH6.5 containing 1mM 2-mercaptoethanol and 1mM EDTA at 25°C. The bulk average matrix-ligand concentration was 4.4×10^{-5}M and the matrix volume 25% of total (matrix ligand concentration 1.76×10^{-4}M). The value at zero added NAD^+ is arbitrarily plotted at -6.

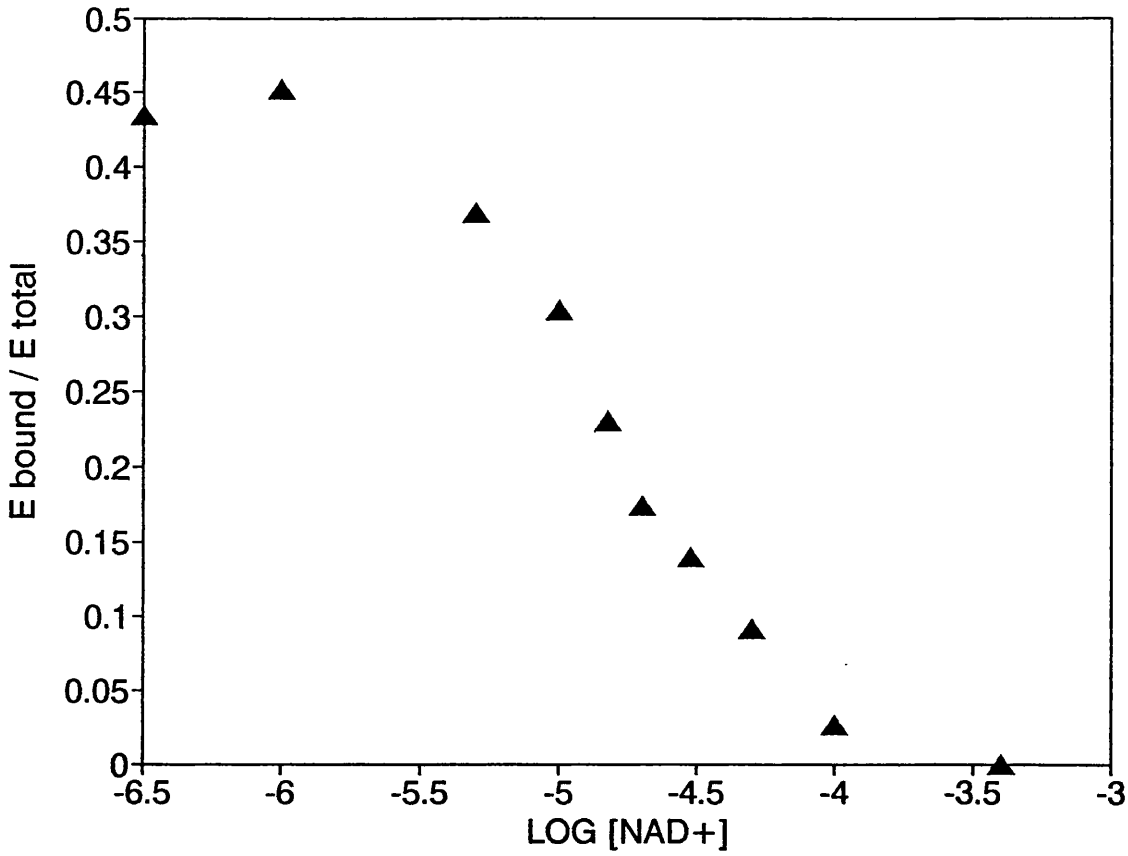

Figure 6.9

The effect of added NAD^+ on the fraction of GAPDH bound to 'high density' AMP-Sepharose in 50mM sodium phosphate buffer pH8.5 containing 1mM 2-mercaptoethanol and 1mM EDTA at 25°C. The bulk average matrix-ligand concentration was 1.0×10^{-4}M and the matrix volume 6.5% of total (matrix ligand concentration 1.5×10^{-3}M). The value at zero added NAD^+ is arbitrarily plotted at -6.5.

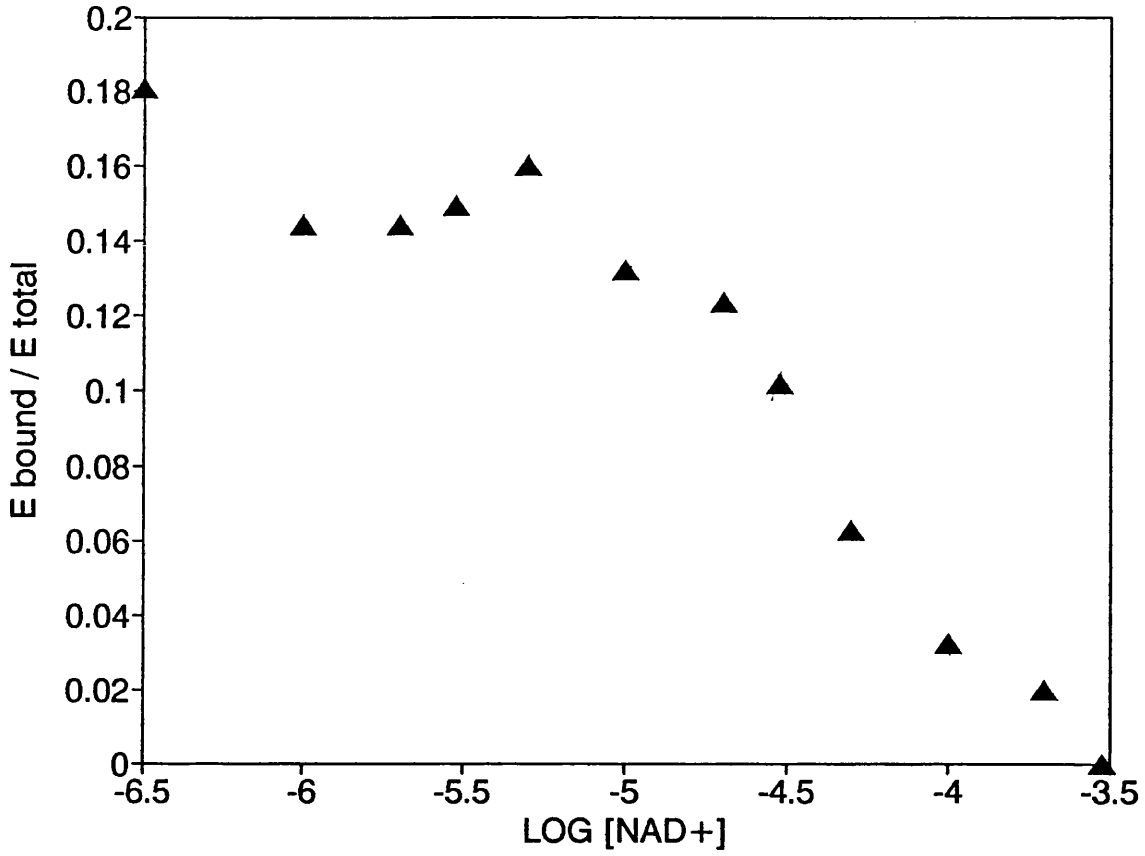

Figure 6.10

The effect of added NAD^+ on the fraction of GAPDH bound to 'medium density' AMP-Sepharose in 50mM sodium phosphate buffer pH8.5 containing 1mM 2-mercaptoethanol and 1mM EDTA at 25°C. The bulk average matrix-ligand concentration was 9.3×10^{-5}M and the matrix volume 18% of total (matrix ligand concentration 5.2×10^{-4}M). The value at zero added NAD^+ is arbitrarily plotted at -6.5.

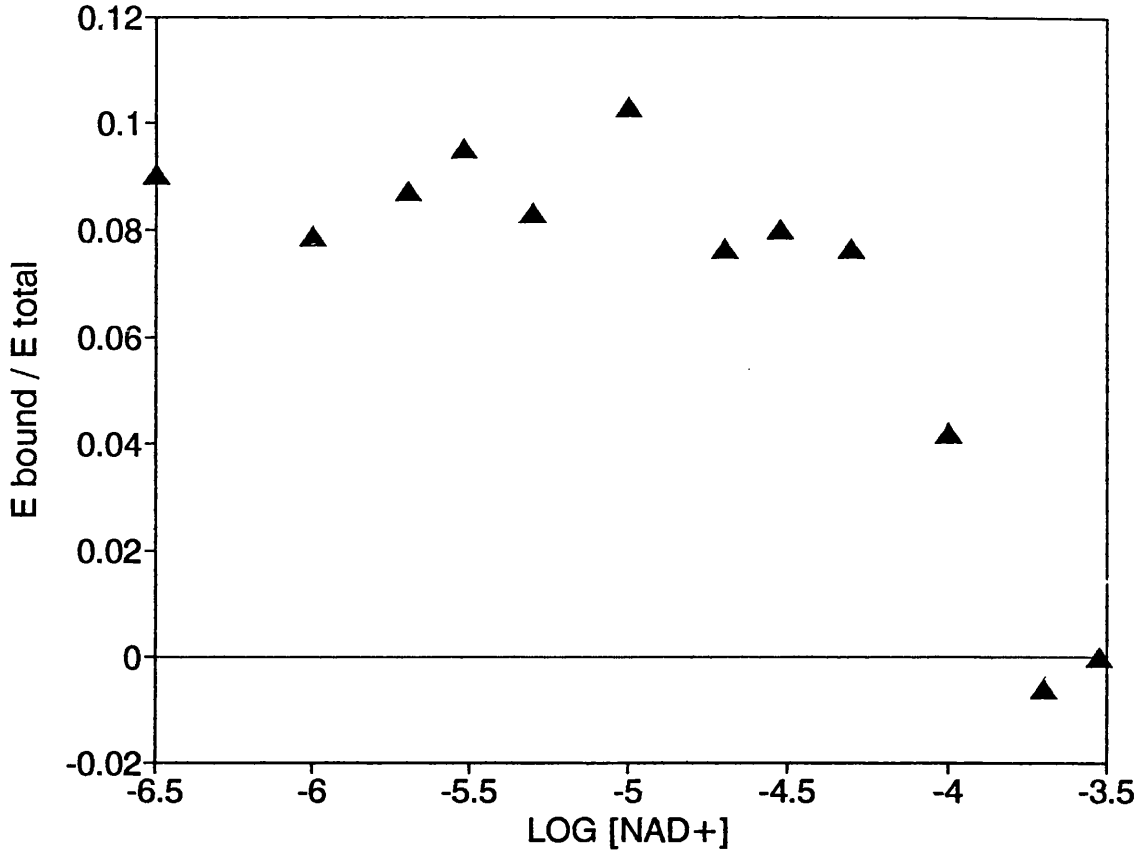

Figure 6.11

The effect of added NAD^+ on the fraction of GAPDH bound to 'low density' AMP-Sepharose in 50mM sodium phosphate buffer pH8.5 containing 1mM 2-mercaptoethanol and 1mM EDTA at 25°C. The bulk average matrix-ligand concentration was 2.5×10^{-5}M and the matrix volume 18% of total (matrix ligand concentration 1.4×10^{-4}M). The value at zero added NAD^+ is arbitrarily plotted at -6.5.

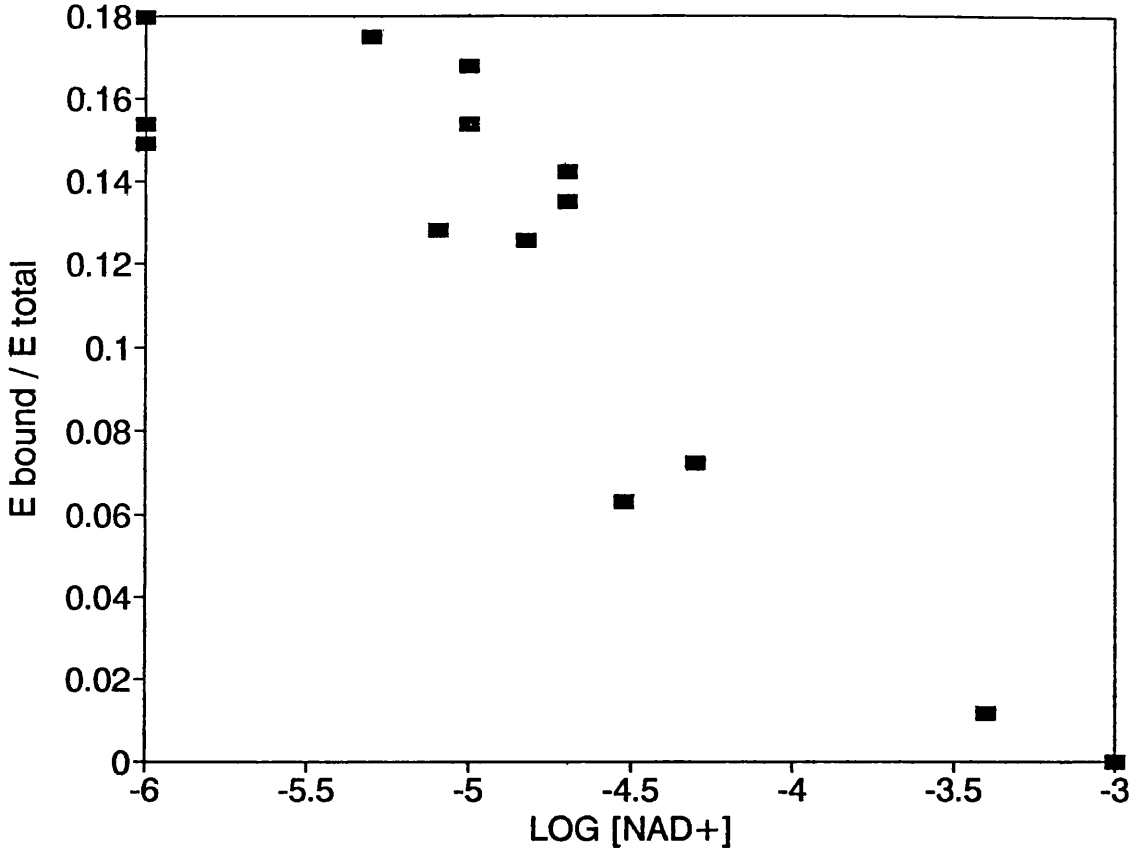

Figure 6.12

The effect of added NAD^+ on the fraction of GAPDH bound to AMP-Sepharose in 50mM sodium phosphate buffer pH8.5 containing 1mM 2-mercaptoethanol and 1mM EDTA at 40°C. A separate incubation was used to determine each point. The bulk average matrix-ligand concentration was 5×10^{-5}M and the matrix volume 25% of total (matrix ligand concentration 2×10^{-4}M). The value at zero added NAD^+ is arbitrarily plotted at -6.

6.8 Equilibrium Batch Adsorption of GAPDH using AMP Cellulose

Due to the low levels of binding observed when carrying out equilibrium batch adsorption experiments with AMP cellulose the scatter of points in individual experiments was greater than that for the Sepharose experiments. The changes in the concentration of bound enzyme were smaller than those observed in the Sepharose experiments and similar to the dimensions of the errors in the enzyme assay. A number of individual experiments all suggested that some enhancement of binding was apparent however, and by combining the data from several runs the enhancement effect was quite clearly seen. A plot of bound enzyme / total enzyme against log added NAD^+ is shown in figure 6.13. An approximately four-fold increase in binding was apparent on adding free ligand. No such effect was observed in control experiments using blank cellulose or ethanolamine derivatised cellulose.

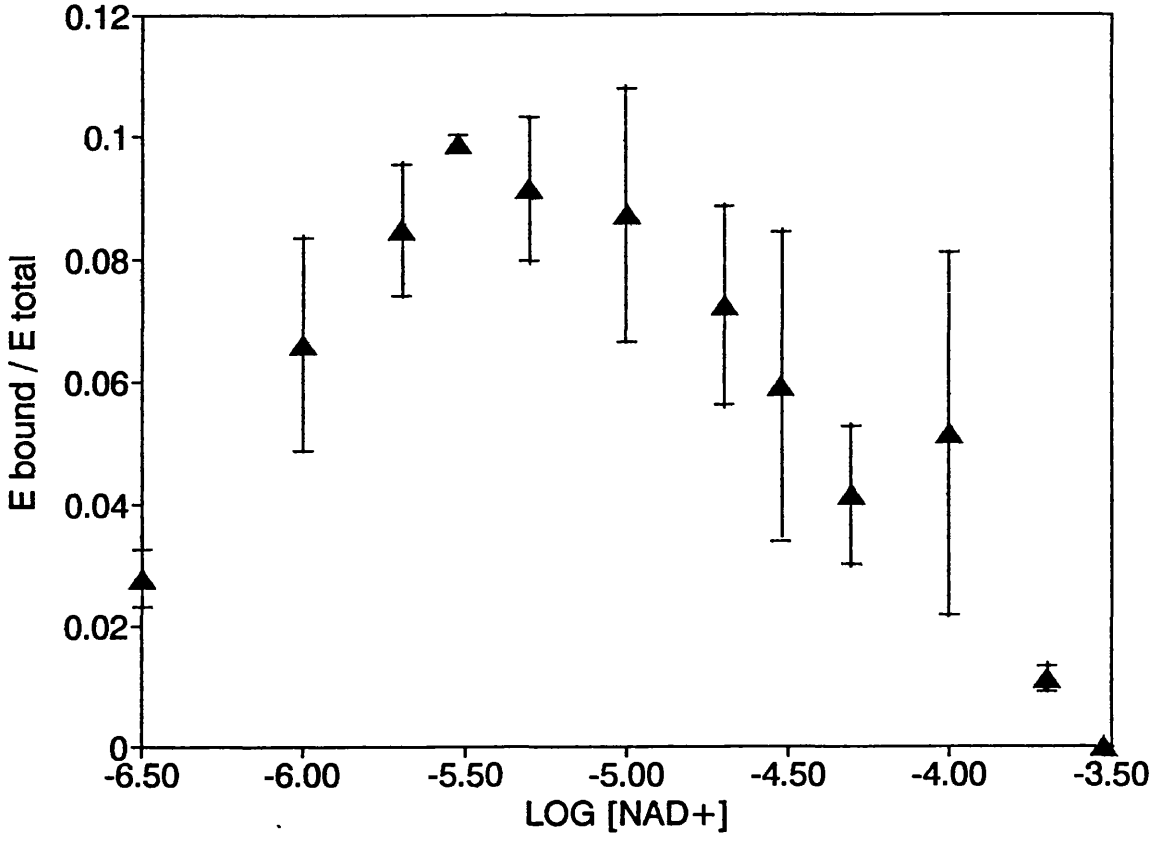

Figure 6.13

The effect of added NAD^+ on the fraction of GAPDH bound to AMP cellulose in 50mM sodium phosphate buffer pH8.5 containing 1mM 2-mercaptoethanol and 1mM EDTA at 25°C. The bulk average ligand concentration was 7.8×10^{-5}M and the matrix volume 20% of total volume (matrix ligand concentration 3.9×10^{-4}M). The values plotted are means ± standard errors for 3 experiments using separate aliquats of matrix from the same batch. The value in the absence of added NAD^+ is arbitrarily plotted at -6.5.

6.9 Frontal Chromatography of FBPase on Phosphocellulose

The results of frontal chromatography runs using different concentrations of AMP are shown as graphs of fractional saturation of the column against the volume of FBPase solution loaded in figure 6.14. The effective capacity of the column at each AMP concentration was estimated as the volume, V, of FBPase solution loaded when the concentration in the eluate reached 50% of that in the load. Using the capacity in the presence of 250μM AMP (which should swamp any matrix interactions) as an estimate of V_0, the liquid volume of the system including flow cell, pump tubing etc., values of $1/(V - V_0)$ were calculated for each AMP concentration. These are shown in figure 6.15 plotted against AMP concentration. The data indicate a linear dependence of $1/(V - V_0)$ on AMP concentration. The line shown on the graph is a regression line; the y intercept is 0.242 ml^{-1} and the gradient 8360$ml^{-1}M^{-1}$.

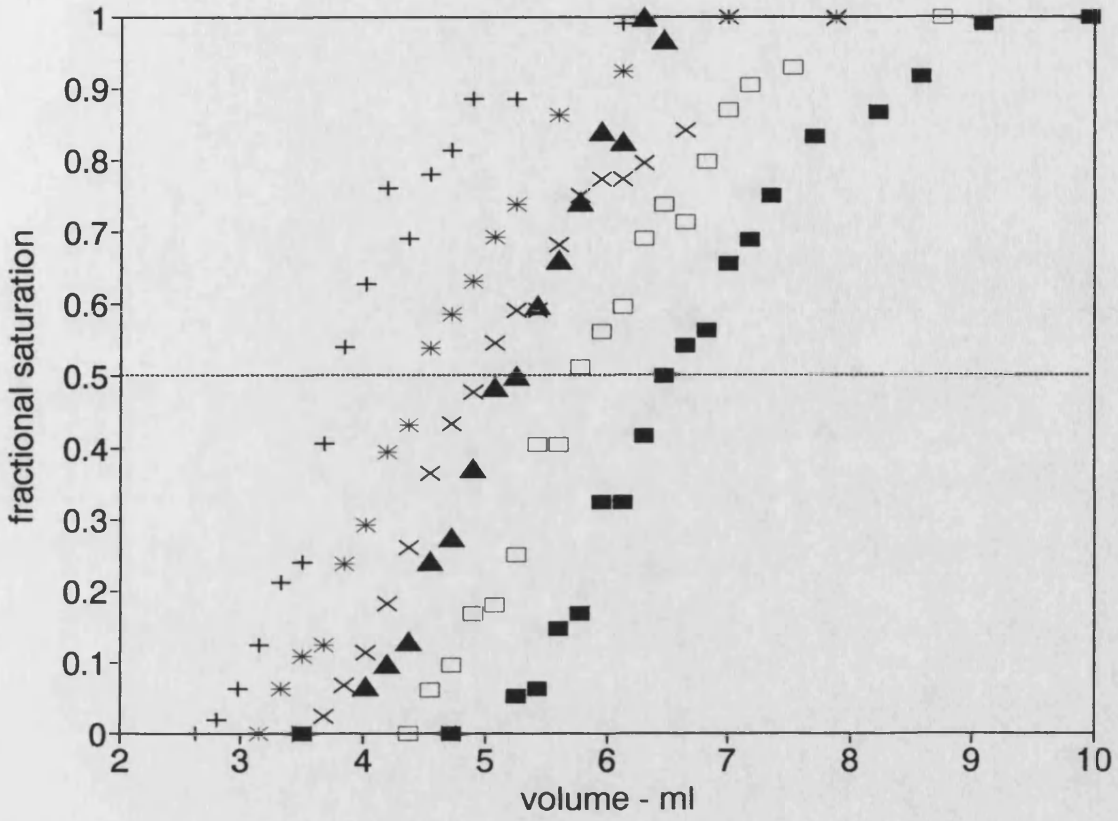

Figure 6.14

Frontal chromatography of 50μgml^{-1} FBPase in 50mM triethanolamine pH7.2 containing 1.01mM $MgSO_4$, 10μM EDTA, 0.2mM DTT and the required concentration of AMP. The protein solution was loaded at a flow rate of 35μlmin^{-1} onto a 0.66cm diameter by 1.3cm column of phosphocellulose equilibrated with the same buffer. 5 minute fractions were collected and the concentration of FBPase measured by enzymatic assay. The elution volume, V, at each AMP concentration was estimated from the point where the emerging protein front reached a fractional saturation of 0.5. AMP concentrations were:

0μM (■), 5μM (□), 10μM (▲), 15μM (×), 20μM (*), 50μM (+).

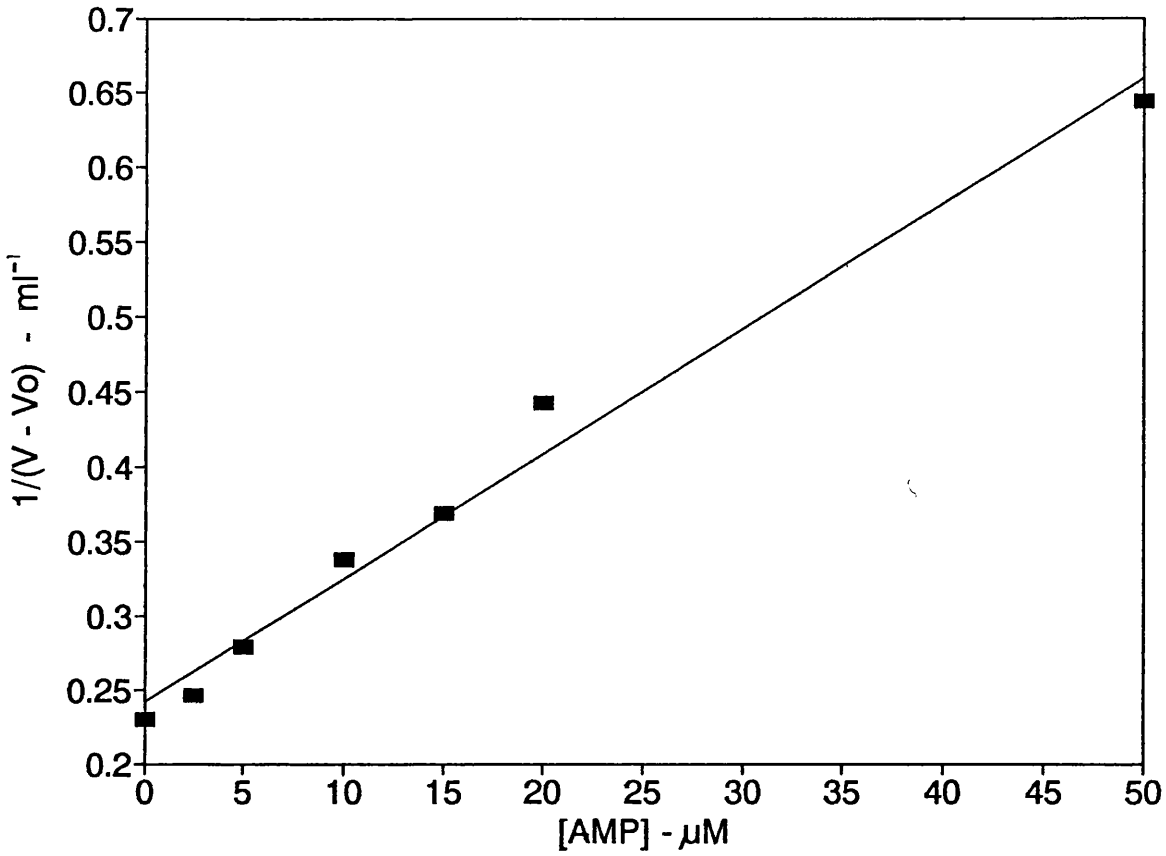

Figure 6.15

Plot of $1/(V - V_0)$ against AMP concentration for frontal analysis of FBPase on phosphocellulose. V_0 was taken as the midpoint of the breakthrough curve in the presence of 250μM AMP. The line through the data is a regression line giving a gradient of $8360ml^{-1}M^{-1}$ and a y-intercept of $0.242ml^{-1}$.

CHAPTER 7

COOPERATIVE BINDING PHENOMENA - DISCUSSION

7.1 The Simulated Binding Curves

The simulated binding curves for the two systems studied both show the same basic form. Addition of free ligand up to an optimum concentration progressively increases the fractional binding to matrix ligand due to the 'switching' of the enzyme to a higher affinity state by the cooperative effect. Further increasing the free ligand concentration beyond this point leads to a decline in fractional binding due to an increasing proportion of the enzyme sites being occupied by free ligand. This causes competition between free and matrix-bound ligand for the enzyme sites which outweighs the increased affinity of the sites due to the cooperative effect and leads to biospecific elution.

The assumptions used in deriving the equations on which the simulation is based (see section 6.2) are clearly approximations. In view of the results of other investigators discussed in chapters 2 and 3 it seems unlikely that any of the assumptions is correct in detail. The reasons for the breakdown of the assumptions are discussed later in the light of the experimental findings. While the inaccuracy of the assumptions suggests that quantitative analysis of these simulations might be inappropriate, they still provide valuable qualitative information about the behaviour of such cooperative binding systems. Firstly the simulations demonstrate the validity of the basic hypothesis that addition of free ligand to a cooperatively binding system should enhance the binding of protein to matrix ligand. Secondly they indicate that at high matrix ligand densities the effect is swamped due to the high fractional binding in the absence of free ligand.

Finally they indicate the free ligand concentration range over which the effect is likely to be apparent. The latter two points proved to be of value in the design of the experimental systems used for practical investigations.

7.2 Binding of GAPDH to Nucleotide Matrices

From the results obtained and presented in sections 6.4 and 6.6 of chapter 6 several observations can be made which require discussion:

i) Binding of GAPDH to immobilised nucleotide matrices was more favourable at near neutral pH than at pH 8.5

ii) NAD^+ matrices bound more GAPDH per μmole of immobilised ligand than AMP matrices in both the column and batch adsorption experiments.

iii) The fractional binding measured in the batch adsorption experiments was always much lower than that predicted in the simulations for the same bulk average ligand concentration.

iv) In the absence of added NAD^+, AMP-cellulose showed much lower fractional binding than a similar Sepharose matrix.

v) GAPDH showed enhanced binding to AMP-cellulose on addition of free NAD^+. No such behaviour was apparent for nucleotide-Sepharose matrices.

vi) The concentration of NAD^+ required to achieve maximum enhancement of binding of GAPDH to AMP-cellulose was lower than the optimum predicted from the simulations.

Reference to published binding data for GAPDH and free NAD^+ under various conditions of pH and temperature (Velick *et al.*, 1971; Niekamp *et al.* 1977) indicates that binding is tighter and less positively cooperative as either the temperature or the pH is lowered. At pH 6.5 and 7.3 the binding data at 25°C is well described by binding to 4 independent sites, with an affinity constant roughly 10 fold higher than the most favourable affinity constant of the cooperative binding observed at pH8.5. This explains why GAPDH bound better to nucleotide matrices at pH values around neutral than at pH8.5 (particularly evident when comparing figures 6.7 and 6.8).

In an attempt to explain tighter NAD^+ binding at neutral pH in terms of molecular interactions the 3-dimensional structure of GAPDH was viewed with NAD^+ bound. Since the structure of the yeast enzyme has not been determined the lobster enzyme (Buehner *et al.*, 1974) was used as a model. This is clearly not ideal but the NAD^+ binding region of this enzyme has been shown to be very similar in sequence to that of yeast and it seems reasonable to suppose that this will also be true of the 3-dimensional structure of the yeast enzyme. A photograph of part of the GAPDH structure with NAD^+ bound is shown in figure 7.1 and in close-up in figure 7.2. The most obvious candidates for an explanation of a change between pH6.5 and pH8.5 are ionising groups with pK_a values in this range which might be involved in ionic or hydrogen bonding interactions between cofactor and enzyme. Examination of the structure indicated that neither of the phosphate groups in NAD^+ had any obvious near-neighbours, with which to interact by hydrogen or ionic bonds, which could be disrupted by the ionisation state of the phosphate groups. Neither were any protein histidine residues involved directly in NAD^+ binding. It thus appears that this is far too naive a view of the differences in binding affinity at pH6.5 and 8.5. Much more complex changes in the protein conformation are probably responsible, bringing about subtle changes in the conformation of the NAD^+ binding site which collectively account for the observed differences.

One aspect of ligand binding which is well explained by the molecular structure is the observation that most dehydrogenases bind well to N^6 and C^8 derivatives of NAD^+ and AMP but not to phosphate or ribose coupled derivatives. The photograph in figure 7.2 shows the adenine ring in a hydrophobic cleft of the protein but with the plane of the ring orientated such that both N^6 and C^8 both protrude out of the ends of the cleft into solution. Spacers attached to these two sites can be accommodated without perturbing the protein structure in the vicinity of the binding site. The hydrophobicity of the residues surrounding the adenine binding cleft may also explain the anomalous binding of NAD^+ derivatives with hydrophobic spacers to muscle GAPDH observed by Barry and O'Carra (1973).

Figure 7.1

Photograph of NAD^+ bound in the active site of lobster GAPDH. The X-ray coordinates used to generate the model were those of Buehner *et al.* (1974). The two domains which form the binding site are coloured yellow and blue. NAD^+ is coloured pink.

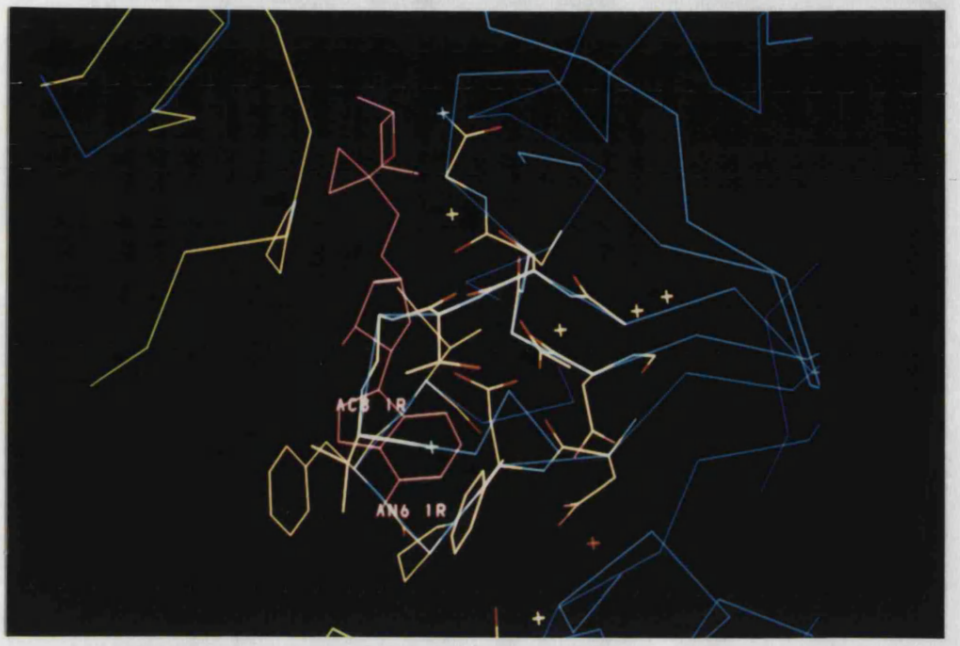

Figure 7.2

Enlargement of the NAD^+ binding site from figure 7.1. N^6 and C^8 of the adenine ring are identified to emphasise their solvent accessibility. The hydrophobic residues between which N^6 gains access to solvent are also clearly visible.

The tighter binding of GAPDH to NAD^+ matrices compared with AMP matrices is presumably simply due to the larger number of interactions taking place between ligand and protein in the former case. Table 3 of Bräden and Eklund (1980) lists a number of hydrogen bond interactions with the nicotinamide ribose and hydrophobic interactions with the nicotinamide ring itself. These would additionally reinforce the binding to the adenine ring and the adenine ribose moieties common to both ligands.

That the fractional binding observed in the batch adsorption experiments was lower than that predicted by the simulations may be a result of restrictions imposed on ligand accessibility by the support matrix, and changes in binding constants arising from the chemical effects of immobilisation.

In the simulations it was assumed that the immobilised ligand was all accessible. In reality this is unlikely to be the case. Investigation of the use of similar immobilised nucleotide ligands in coenzyme regeneration systems suggests that about 40% of the bound nucleotide may be enzymatically available to liver ADH (Schmidt and Grenner 1976). This was determined for matrices with typical ligand loadings of 1 - 3μmolml^{-1} gel. Clearly the ability to act as a coenzyme imposes a greater constraint on the coupling and geometry of the ligand than does the requirement simply to bind to the enzyme. However, the figure of 40% 'sequential' accessibility measured in this way is probably a better estimate of the ligand availability than the values estimated from saturation of matrices with enzyme. This technique generally yields values of 0.1 - 5% 'simultaneous accessibility' for matrices with typical ligand loadings of 1 - 3μmolml^{-1} but is probably strongly influenced by steric hindrance and pore plugging. This is unlikely to be a major consideration in these experiments where the enzyme concentration used was very low.

The effect of immobilisation on the affinity constant for the protein-nucleotide interaction is also difficult to assess since it cannot be separated from the physical constraints imposed by the matrix. Again some clues can be obtained from measurements of catalytic efficiency of coenzyme-spacer conjugates in enzyme assays. Table 3 of Bückmann and Carrea (1989) lists the K_m values for a range of such

conjugates with 10 different dehydrogenases, together with the K_m of the unmodified nucleotide. The values for the modified coenzymes are mostly in the range 0.3 to 10 times the value for the native coenzyme. While these are K_m values and not true binding constants they nevertheless give some indication of the expected effect of modifying the coenzyme such that it can be coupled to a solid support. The simulation shown in figure 7.3 gives an indication of the likely effect of changing the affinity constants for protein interactions with matrix-ligand to 50% and 10% of those for binding of free ligand. As expected this leads to a reduction in the fractional binding of the protein to the matrix but **does not** alter the concentration of NAD^+ required to give the maximum enhancement of binding. A reduction in the affinity of the protein-immobilised ligand interaction may in part explain the low fractional binding measured in the equilibrium batch adsorption experiments.

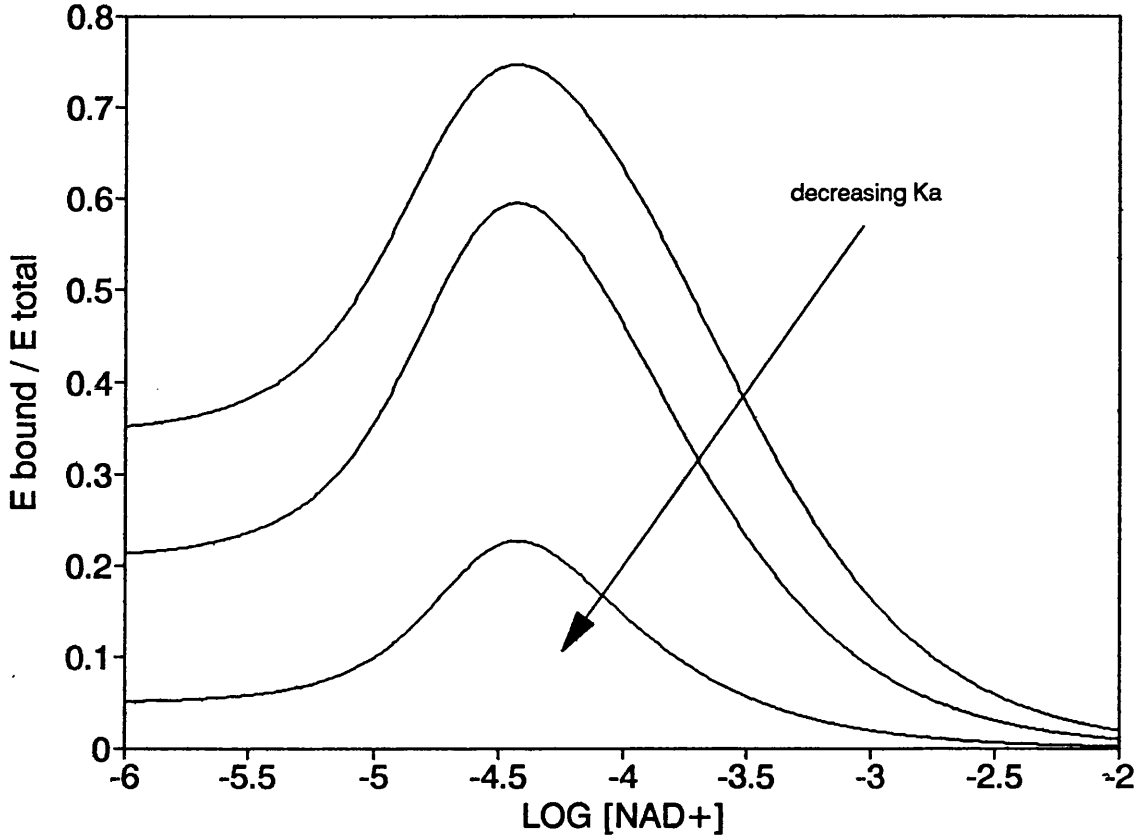

Figure 7.3

A simulation showing the influence of the affinity constants for interaction of GAPDH with matrix ligand on the fraction of enzyme bound . The constants for interaction with matrix ligand were reduced to 50% and 10% of those for equivalent interactions with free ligand. The matrix ligand concentration was 5×10^{-5}M.

The difference between the behaviour of the cellulose and Sepharose matrices probably arises from their differing physical structures and consequent differences in the pattern of derivatisation. Sepharose beads are approximately spherical with a size range of 60 - 140μm. The beads are highly porous, being only 4% agarose. The coupled ligand will thus be restricted to the small fraction of the total bead volume occupied by the agarose chains themselves leading to very high microenvironmental

ligand densities at agarose surfaces, especially where the agarose triple helices come together to form the small areas of two-dimensional surface typical of the internal structure of Sepharose.

In addition, Since both activating chemicals and coupling ligands must diffuse into the particle from the liquid phase it is likely that the end product will not be a uniformly derivatised particle but one with a 'shell' of high ligand density at the surface and a concentration gradient running to a minimum at the centre of the particle. Such 'shell' effects have been observed when coupling protein ligands to Sepharose (Lasch *et al.*, 1982; Mullon *et al.*, 1988) but might be expected to be less pronounced for small ligands due to their higher diffusion rates.

Taken together these two effects will ensure that Sepharose beads have microenvironmental ligand densities which might be up to two orders of magnitude higher than the bulk average.

Fibrous cellulose approximates to cylinders of length 100 - 250μm and diameter about 25μm. Thus the surface area is very approximately 3 times greater for cellulose compared with an equal volume of Sepharose. Cellulose is largely non-porous due to the very high packing density of the carbohydrate chains resulting from inter-chain and intra-chain hydrogen bonding and Van der Waals forces between adjacent layers. This gives cellulose its rigid crystalline structure but renders the hydroxyl groups rather unreactive. Cellulose fibres also have some less ordered amorphous regions which are more permeable than the micro-crystalline regions. Non-hydrogen-bonded hydroxyl groups occur only in these amorphous regions and at the sites of various chain end dislocations eg. 1-6 glycosidic bonds or due to twisting and crossing of chains (Kremer and Tabb, 1989). It is only at these dislocations that activation and coenzyme coupling will occur. The physical surface of the cellulose fibres will dictate the distribution and spacing of immobilised ligands and will minimise the occurrence of clusters of immobilised ligand except possibly in the amorphous regions. The microenvironmental ligand density for cellulose will thus be higher than the bulk average since derivatisation is largely at the surface of fibres rather than throughout

their volume but the effect will be less pronounced than for Sepharose and, unlike Sepharose, clusters of very high ligand density will be minimised.

For a given bulk average ligand density this would have two possible repercussions in terms of the behaviour of the cellulose and Sepharose matrices in batch adsorption experiments:

i) The Sepharose matrix, and to a lesser extent the cellulose matrix, will behave as one with a higher ligand density thus tending to swamp out the cooperative effect.

2) The higher local ligand densities in the Sepharose matrix will lead to an increased probability of multivalent interactions between protein and immobilised ligand.

This behaviour has been observed for a number of proteins with multiple binding sites (Eilat and Chaiken, 1979; Hogg and Winzor, 1985; Liu and Stellwagen, 1987), and was discussed in chapter 4. A bivalent interaction will have a higher affinity constant than a monovalent one and if this is greater than or equal to the enhanced affinity of enzyme molecules partially saturated with free ligand then this will also swamp out any enhancement which might have been achieved due to the cooperative effect. The effect of localised high concentrations of matrix ligand together with the consequences of multivalent interaction between macromolecule and resin can be considered qualitatively using an extension to the model described by Hubble (1987). In the original theoretical assessment of liquid phase cooperativity the assumption was made that with low matrix ligand densities only monovalent interactions would be possible between adsorbate and support. However, if localised high concentrations of immobilised ligand occur the possibility of mulitivalent interactions between enzyme and support cannot be discounted. The original model can easily be extended to consider all theoretically possible interactions between a tetravalent enzyme and both free and immobilised ligand. The broader model can be used to give a qualitative indication of the effects that these multivalent surface interactions might be expected to have on observed binding enhancements. Development of the revised model leads to the formulation of fourteen equilibria describing interactions between individual

complex species: For interaction with soluble ligand(using macroscopic association constants:

$$[E]+[L] \overset{K_1}{\rightleftharpoons} [EL] \qquad [EL]+[L] \overset{K_2}{\rightleftharpoons} [EL_2]$$

$$[EL_2]+[L] \overset{K_3}{\rightleftharpoons} [EL_3] \qquad [EL_3]+[L] \overset{K_4}{\rightleftharpoons} [EL_4]$$

A similar set of equilibria can be formulated for the interactions of E with immobilised ligand (M) using macroscopic association constants K_{m1} - K_{m4}. Binding between enzyme and both soluble and immobilised ligand can be described in terms of 6 further association constants:

$$[EM]+[L] \overset{K_{l1}}{\rightleftharpoons} [EML] \qquad [EML]+[L] \overset{K_{l2}}{\rightleftharpoons} [EML_2]$$

$$[EML_2]+[L] \overset{K_{l3}}{\rightleftharpoons} [EML_3] \qquad [EM_2]+[L] \overset{K_{l4}}{\rightleftharpoons} [EM_2L]$$

$$[EM_2L]+[L] \overset{K_{l5}}{\rightleftharpoons} [EM_2L_2] \qquad [EM_3]+[L] \overset{K_{l6}}{\rightleftharpoons} [EM_3L]$$

Binding of enzyme to the affinity support can be described in terms of:

$$Y_m = \frac{\sum [EM_i] + \sum [EM_iL_j]}{[E] + \sum [EL_j] + \sum [EM_i] + \sum [EM_iL_j]}$$

where i denotes number of sites bound to immobilised ligand and j denotes number of sites bound to free ligand (for a tetramer $1 \leq (i+j) \leq 4$).

This equation can be expressed in terms of the equilibrium concentrations of L and M together with appropriate products of the individual association constants. Where the association constants are known this relationship can be used to predict the effect

of free ligand concentrations on fractional binding as previously described. However, the more general form allows the effect of permitting progressively more complex multiple interactions between enzyme and adsorbate to be predicted. An example of a prediction of this type is given in figure 7.4 using the same association constants for GAPDH as detailed for figure 6.1.

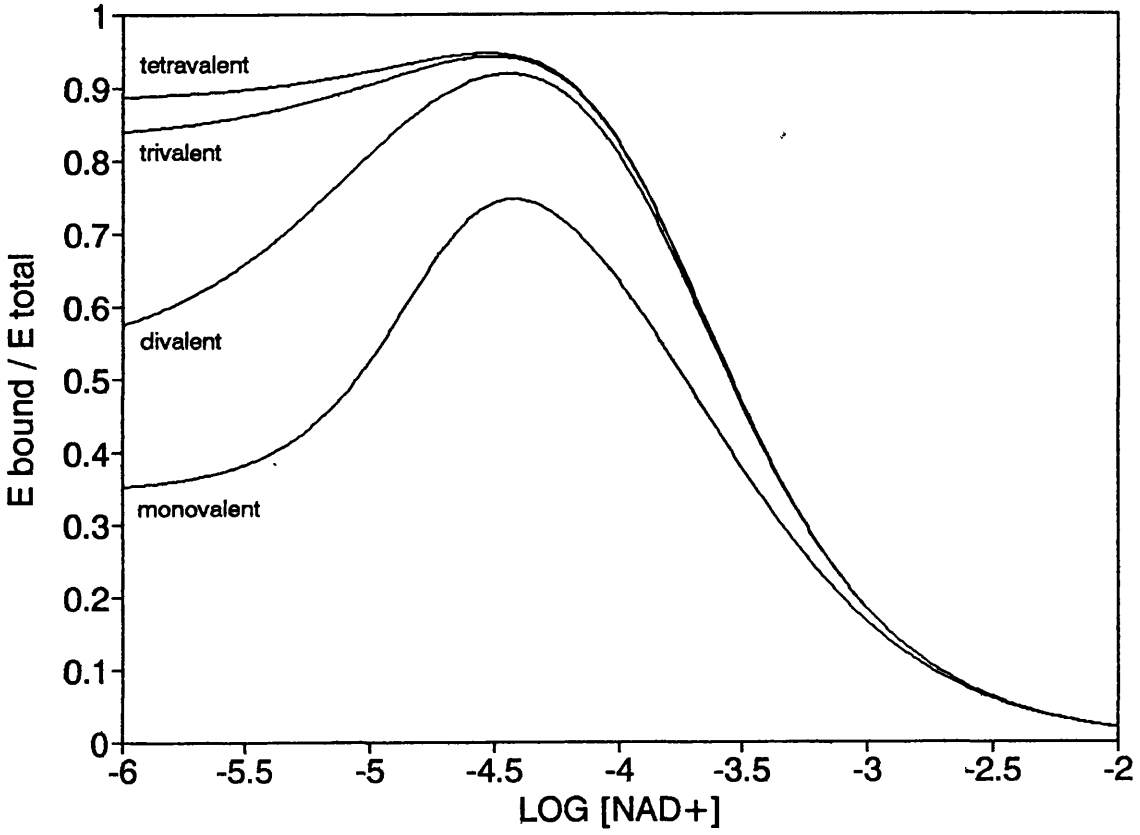

Figure 7.4

The predicted effect of multivalent interactions between enzyme and matrix ligand on the relationship between free ligand concentration and fractional binding. The association constants used for GAPDH were as in figure 6.1. The bulk average ligand concentration was 5×10^{-5}M.

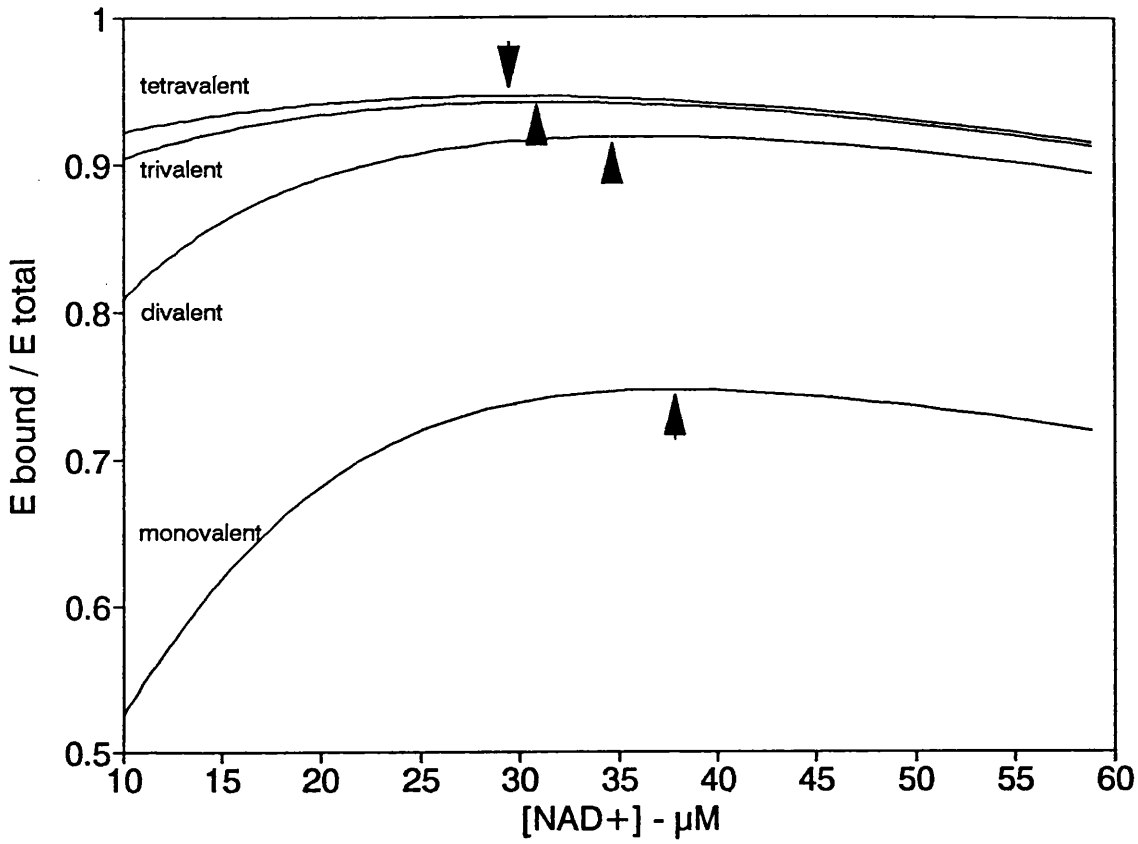

Figure 7.5

Expansion of sections of the graphs shown in figure 7.4 to indicate the change in the NAD^+ concentration required to achieve maximum enhancement of binding as a result of allowing multiple protein-immobilised ligand interactions in the model.
The optima are indicated by arrow heads.

As the number of permitted interactions with immobilised ligand is increased from 1 to 4, the curves obtained clearly show a smaller enhancement effect due to the increased binding in the presence of low NAD^+ concentrations and the consequent flattening out of the binding curves. This behaviour is consistent with the results observed in the Sepharose experiments where no clear evidence of enhanced binding could be observed. Consideration of the cooperative cluster theory presented in chapter 4, suggests that in general the concentrations of ligand clusters with the correct spatial geometry to permit multiple interactions will be quite low. For the bulk average ligand concentrations used in these studies the concentration of dimeric sites would be of the order of 2×10^{-8}M, with higher order sites having even lower concentrations. Since the protein concentration in the batch adsorption experiments was also 2×10^{-8}M, however, this could make a significant contribution to the overall binding. Given the arguments for non-uniform ligand distribution discussed previously, the actual concentrations of clusters with the correct spatial geometry for divalent and higher order binding will probably be much higher than that calculated statistically by the cooperative cluster theory, and it seems likely that multiple interaction may account for most of the observed protein binding and hence explain the lack of cooperative effects in experiments with Sepharose matrices.

The expanded section of figure 6.2 presented in figure 6.3 clearly indicates that the presence of multiple interactions has only a small effect on the optimum free ligand concentrations required to achieve maximum enhancement of binding, so this cannot provide an adequate explanation of why the observed optimum in the AMP-cellulose experiments was lower than that predicted. More likely is that the affinity constants used in the simulations were inappropriate for the particular GAPDH preparation and precise conditions used in the experiments. Repeating some of these simulations using the binding data of Cook and Koshland (1970) instead of those of Gennis indicated that this could make a considerable difference to the simulated curves. Three such simulations using the two different sets of binding data are compared in figure 7.6

Using the data of Cook and Koshland the simulations show optima at about 10μM, much closer to the observed optimum in the cellulose experiments than the 40μM

predicted by the data of Gennis. It is possible that the GAPDH supplied by Sigma is more comparable to the conventionally isolated enzyme of Cook and Koshland than to the freshly affinity purified material of Gennis but since binding of free NAD^+ was not actually measured for the Sigma enzyme this is unproven.

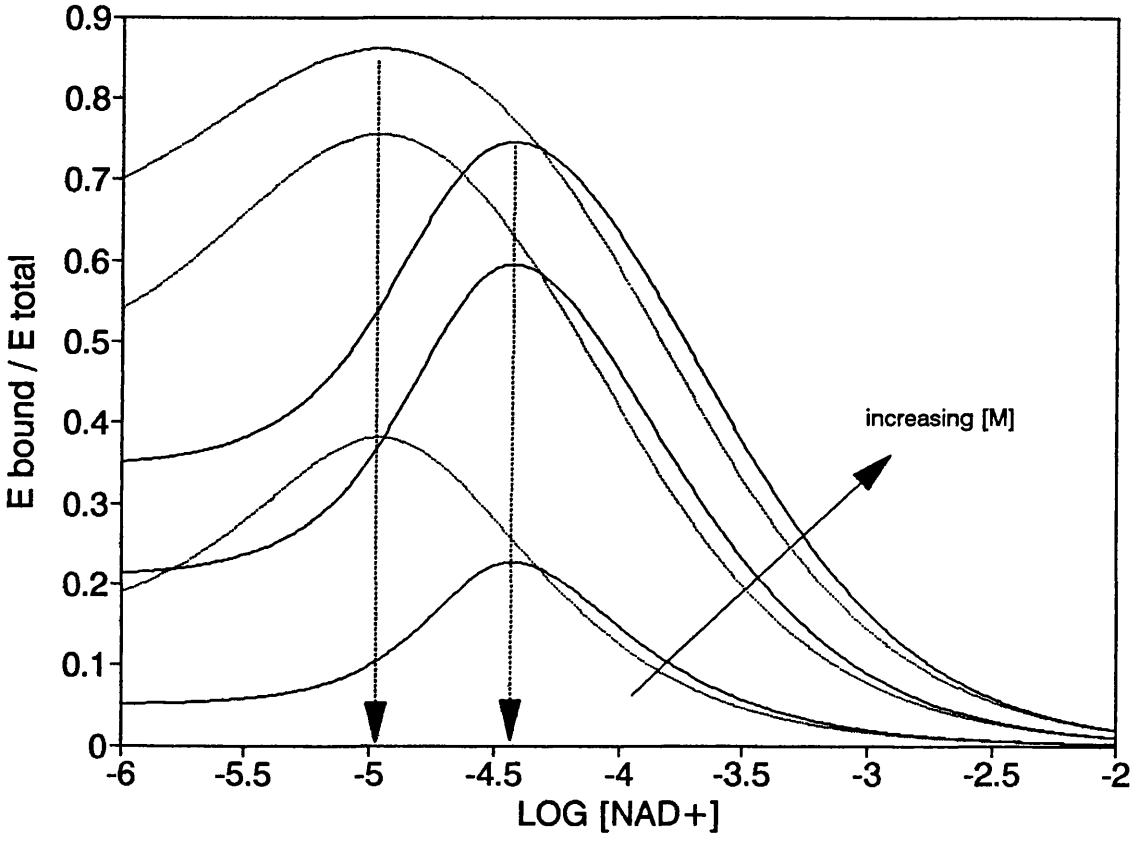

Figure 7.6

Comparison of simulations of fractional GAPDH binding as a function of added NAD^+ for three different matrix ligand concentrations using the binding constants of Gennis (1976) (solid lines) and Cook and Koshland (1970) (broken lines). The matrix ligand concentrations used were: 5×10^{-6}M, 2.5×10^{-5}M, 5×10^{-5}M

7.3 Binding of FBPase to Immobilised Ligands

The lack of interaction between FBPase and immobilised AMP ligands was somewhat surprising although in retrospect the lack of any published purification protocols making use of these matrices might have provided a pointer to this behaviour. AMP immobilised via its phosphate group was not investigated since protein chemical information on the enzyme (Schiff base formation with pyridoxal phosphate - see below) suggested that the phosphate group had a strong ionic interaction at the AMP binding site (probably to a lysine residue). Since neither of the anticipated immobilised ligands could be used for cooperative binding studies this left only phosphocellulose and Blue-Sepharose/cellulose. Clearly both of these potential ligands are far from ideal. The phosphoryl group of phosphocellulose is analogous to part of the natural ligand but may be too small and limited in its interactions at the binding site to be affected by allosteric alteration of the conformation of the site. The binding of blue dye may well be rather less specific in terms of mimicking natural ligand interactions and may well also interact with areas of the protein adjacent to, but not part of, the effector site. Phosphocellulose was chosen as the matrix to study in binding experiments.

Due to the fact that the effector ligand AMP is also an enzyme inhibitor the batch adsorption techniques used in the GAPDH work could not be utilised due to the difficulty of accurately assessing the enzyme concentration in the liquid phase in the presence of increasing concentrations of inhibitor. For this reason the technique of frontal chromatography was adopted as an alternative.

There appears to be some doubt from the published literature on FBPase as to the exact nature of the binding of this enzyme to phosphocellulose. FBPase can be specifically eluted from this matrix either by FBP or by its allosteric inhibitor AMP. The question arises as to whether each of the binding sites for AMP and FBP is interacting with phosphoryl groups on the matrix or whether only one site interacts with phosphoryl groups while binding of substrate or effector to the other site elutes the protein allosterically by changing protein conformation such that it weakens the

binding of the other site to phosphoryl groups.

Review of the FBPase purification literature indicates that in general FBP is used for substrate elution of FBPase from both CM-cellulose and phosphocellulose although in some cases both AMP and FBP are used together. It is not clear whether this reflects the relative efficiency of the two compounds, the lack of prior knowledge about the effects of AMP on a particular enzyme, or simply a matter of operational convenience in avoiding adding a known enzyme inhibitor to the preparation which would then have to be removed. Mendicino and Abou-Issa (1974) found that both AMP and FBP were effective for elution of pig kidney FBPase from phosphocellulose and that at low concentrations the two appeared to act cooperatively to achieve more efficient elution. This can be explained if it is assumed that FBPase binds to phosphocellulose at both the FBP and AMP binding sites. AMP will compete at its own binding site to displace FBPase bound to the matrix through this site. It will also allosterically affect the substrate binding site, weakening interactions and allowing FBP to compete more effectively with matrix phosphoryl groups bound at this site.

There are two pieces of evidence which suggest that the enzyme binds to phosphocellulose primarily through the AMP binding. Covalent coupling of pyridoxal phosphate to the enzyme in the presence of FBP results in an active enzyme derivative which contains about 4 moles of pyridoxal phosphate per mole of enzyme. The catalytic activity of the derivative remains unaltered by this treatment but the sensitivity to AMP inhibition is greatly reduced (Colombo *et al.*, 1972), as is its ability to bind to phosphocellulose. FBPase bound to phosphocellulose showed almost the same enzyme activity as free enzyme when assayed in the presence of a coupling system which regenerated FBP (Mendicino and Abou-Issa, 1974), and had almost the same kinetic properties. This was taken as evidence for binding primarily to the AMP site since no significant reduction in accessibility of the FBP sites was apparent.

The balance of evidence thus suggests that FBPase binds to phosphocellulose primarily through the AMP binding site. If this is the case, however, it seems strange that FBP acts as such an effective eluting substrate since there is no evidence of the 'reverse'

allosteric effect i.e. binding of FBP weakening the binding of AMP to the inhibitor site.

Whatever the mode of binding it is clear, from the results of the frontal chromatography experiments in section 6.8, that the cooperative binding of AMP to the enzyme did not sufficiently change the conformation of the binding site(s) such that the phosphate group alone had a higher affinity for that binding site. Hence the data gave a straight line in the reciprocal plot (see figure 6.15) typical of simple competitive binding between free and bound ligands for the same enzyme binding site. By making some approximations the association constants for interaction of FBPase with AMP and matrix phosphoryl groups were calculated to be $4.7 \times 10^5 M^{-1}$ and $3 \times 10^4 M^{-1}$ respectively. These are presumably operational 'average' constants which may represent separate interactions with different sites having different affinities. This is clearly the case for the AMP constant; the calculated value falls midway between the two constants determined for the cooperative binding of AMP by curve fitting to equilibrium dialysis data (see section 6.2).

The mode of binding of FBPase to blue-Sepharose is somewhat clearer. Most purification protocols using blue dye matrices use AMP as the eluting ligand, although both FBP and AMP have been used in a few cases. AMP alone gave satisfactory results for the beef liver enzyme as detailed in this thesis.

Bumble-bee FBPase, which shows no AMP inhibition, does not bind to blue-Sepharose whereas the chicken liver enzyme, which does show AMP inhibition, binds well to this matrix (Leyton *et al.*, 1980). Also, treatment of chicken liver enzyme with pyridoxal phosphate in the presence of FBP gives an AMP insensitive product which no longer binds to blue-Sepharose (Cruz *et al.*, 1979). Coupled with the fact that chicken liver enzyme cannot be eluted from blue-Sepharose with FBP, the evidence points to the enzyme binding only at the AMP binding site(s).

It is interesting that the chromophore of blue-Sepharose can bind tightly to the AMP binding site of FBPase whereas the immobilised natural ligands N^6 and C^8 derivatised AMP showed no binding at all. This suggests that the orientation of and/or the nature of the nucleotide binding cleft is somewhat different to that found, for instance, in a typical dehydrogenase. It would be interesting to know the manner of interaction of the blue dye. Does it bind in its known NAD^+ mimicking conformation or in some other way?

CHAPTER 8

PROTEIN BINDING TO DYE-DEXTRAN CONJUGATES RESULTS

8.1 The Synthesis and Characterisation of Dye-Dextran Conjugates

8.1.1 Characterisation of the Dye Sample used in Subsequent Experiments

The dye isomer used was identified by paired ion reverse-phase HPLC. Figures 8.1 and 8.2 show elution profiles for Basilen Blue and Cibacron Blue 3G respectively. Clearly the retention times for the two major peaks in the Cibacron Blue trace differ from both of those in the Basilen Blue trace. According to Sigma (1990), Baselin Blue is a mixture of the meta and para isomers of the sulphoanilino ring (see chapter 4 for the dye structures) so it is clear that Cibacron Blue contains neither of these isomers. It is therefore tentatively proposed that the major peak of the Cibacron Blue trace is the ortho isomer. This would be consistent with the elution order of the isomers reported by Burton *et al.* (1988) and the structure of Cibacron Blue 3GA sold by Sigma. The other main peak was thought to be the hydrolysis product of the ortho isomer with the active chlorine group cleaved from the triazine ring. This was confirmed by heating a sample of dye at pH11.3 in a boiling water bath. Samples were removed at various times and analysed by HPLC after neutralising with HCl. A time dependant transfer of material from the peak at 12.24 minutes to that at 11.13 minutes was clearly observed.

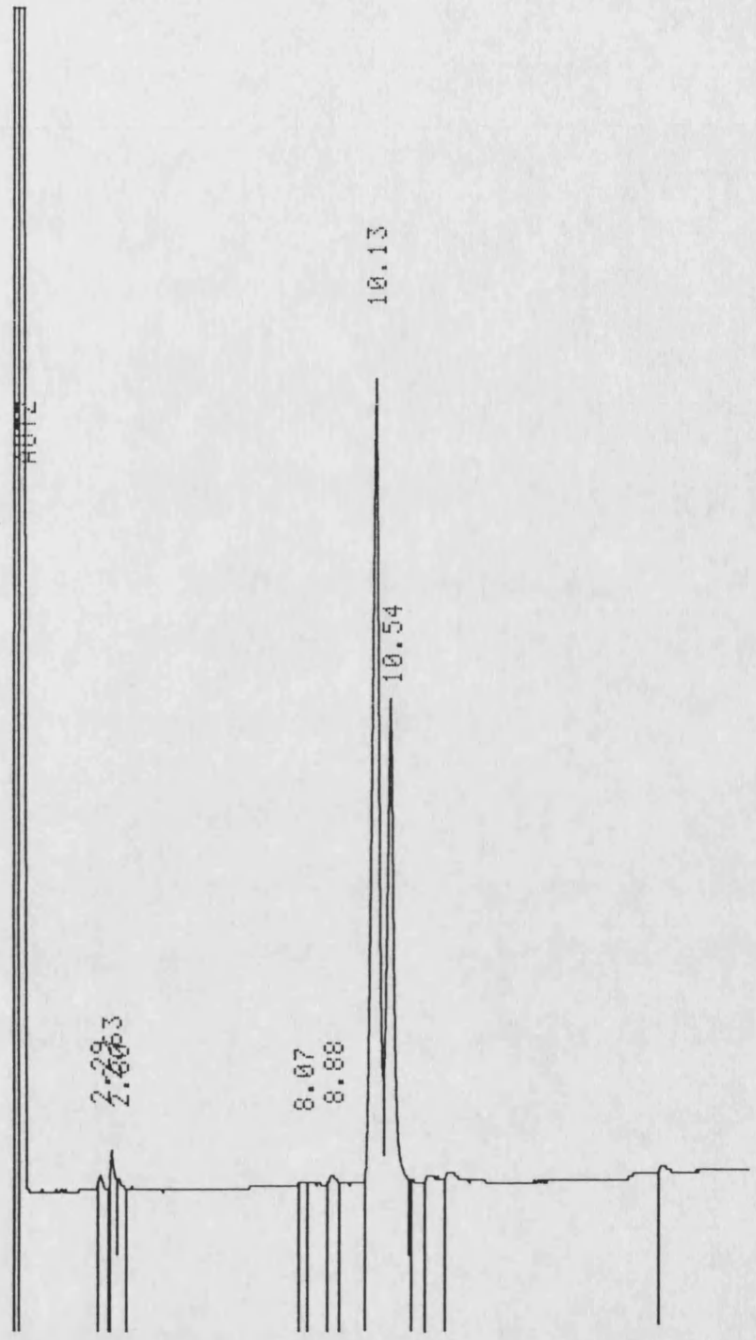

Figure 8.1

Elution profile at 280nm for HPLC of Basilen Blue on a 3μm Hypersil ODS column (150mm $\times$ 4.6mm ϕ) eluted on a solvent gradient of methanol-0.1% aqueous CTMB rising in 5 steps from (80:20 v/v) to (95:5 v/v) at a flow rate of 1mlmin^{-1}.

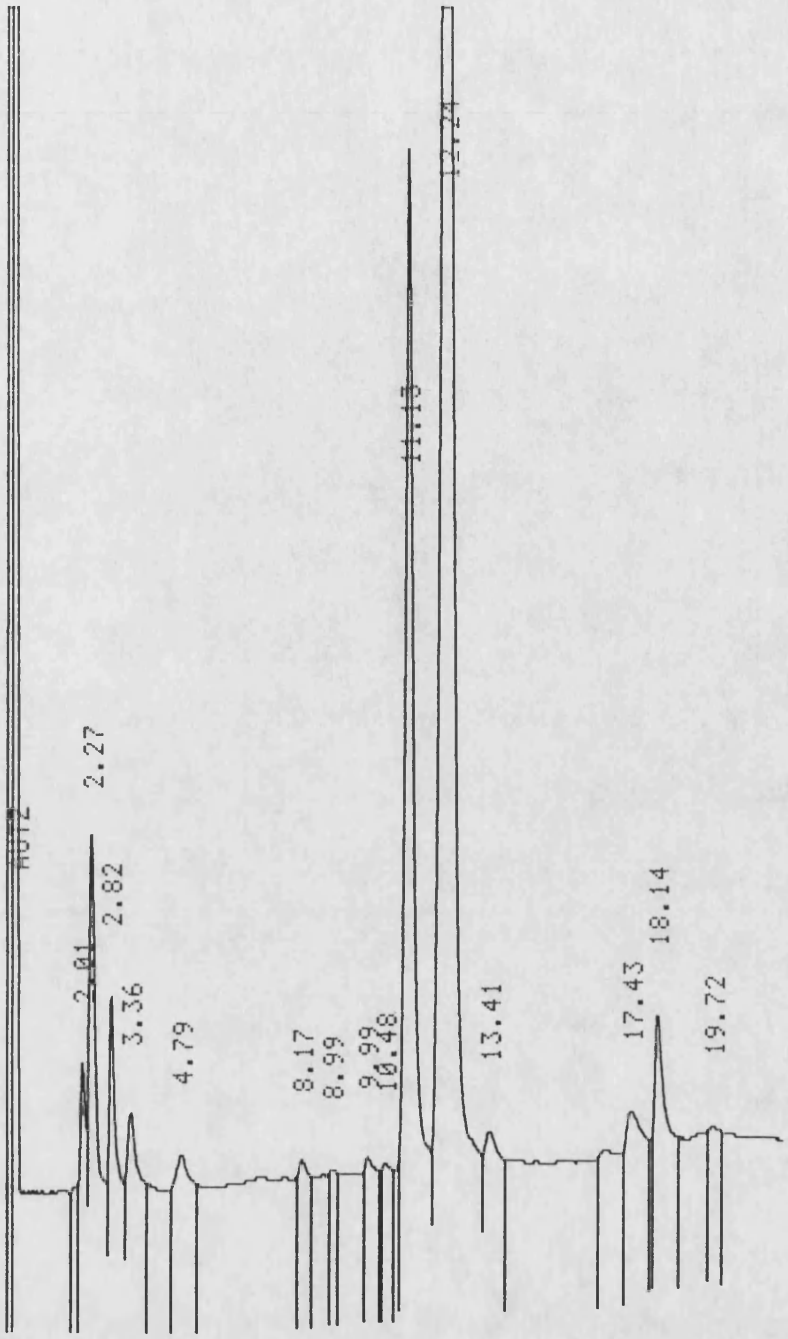

Figure 8.2

Elution profile at 280nm for HPLC of Cibacron Blue on a 3μm Hypersil ODS column (150mm $\times$ 4.6mm ϕ) eluted on a solvent gradient of methanol-0.1% aqueous CTMB rising in 5 steps from (80:20 v/v) to (95:5 v/v) at a flow rate of 1mlmin^{-1}.

8.1.2. Synthesis of Dye-Dextran Conjugates

A progress curve for the coupling of Cibacron Blue 3G to dextran with a molecular weight of 2×10^6 is shown in figure 8.3. As expected the rate of increase in dye coupling to the dextran decreases with time as all the free reactive dye is consumed, either by reaction with the dextran or by deactivation caused by reaction of dye with hydroxide ion in solution.

While both the initial (method 5.2.18a) and improved (method 5.2.18b) protocols for conjugate synthesis gave adequate results the latter is preferred since, although it is more protracted, it it gives much better control over the final dye:dextran ratios obtained. Also, since the reaction is left to proceed to completion all the samples removed can be stored and processed in one batch at the end which is more convenient than having to process each sample immediately after it is taken. The method of recovery was the same for both methods so the product yield was the same in either case being typically about 60% based on total mass recovery. This was considered to be quite acceptable for a laboratory scale synthesis so no attempt was made at optimisation.

8.1.3. Spectrophotometric Measurement of Conjugates

Measurement of absorbance as a function of concentration for free dye and for dye-dextran conjugates indicated that none of these materials obeyed the Beer-Lambert law. The nature and magnitude of the deviation from linearity depended on the wavelength used and the dye dextran conjugate being measured. At 257nm deviations were negative (i.e. decreasing extinction coefficient as concentration increased) wheras at 610nm the deviations were positive (i.e. increasing extinction coefficient as concentration increased). At concentrations below 5μM dye, deviation was negligible for both free dye and dye-dextran conjugates, consistent with the findings of Stellwagen and Liu (1987). Since the degree of deviation varies with dye loading, use of standard curves to estimate conjugate concentrations is unsatisfactory. Also,

although dilution of dye dextran conjugates to below 5μM avoids the deviation caused by intermolecular dye stacking (between dye molecules coupled to different dextran chains), it takes no account of the possibility of intramolecular dye stacking (between dye molecules coupled to the same dextran chain) which could be considerable.

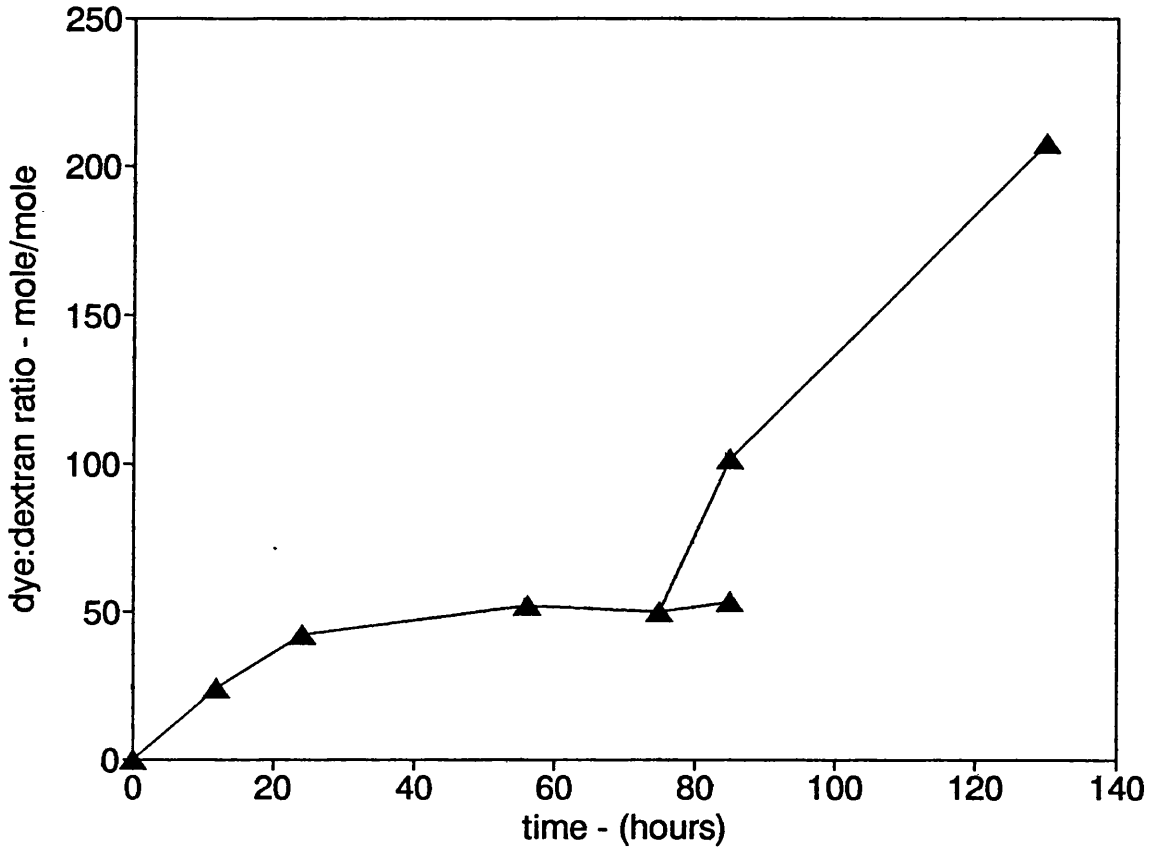

Figure 8.3

Time course for reaction of 2g Cibacron Blue 3G with 20g dextran (M.W. 2 × 10^6) in 1000ml water containing 20g sodium carbonate at 45°C. 100ml Aliquats were removed at the indicated times and coupling estimated by absorbance and dry weight measurements after removal of unbound dye. The branch point indicates the addition of 2g fresh dye to the remaining 500ml of reaction mixture.

8.1.4 Hydrolysis of Dye-Dextran Conjugates

Hydrolysis of dye-dextran conjugates in 6M HCl at 40°C caused a shift in the dye spectrum. Typical spectra at various times during hydrolysis of conjugate DCB206 are shown in figure 8.4. The peak shifted from about 505nm towards 485nm with a concomitant increase in amplitude. The shoulder associated with this peak at about 650nm gradually disappeared as hydrolysis time increased until the spectrum resembled that of free dye under the same conditions.

Comparison of spectra for several conjugates at different times during hydrolysis indicated the presence of an isosbestic point at 541nm. Absorbance measurements of free dye solutions at 541nm in 6M HCl confirmed that absorbance was proportional to concentration under these conditions at least up to 100μM (the maximum concentration checked). The extinction coefficient, E_m, was determined to be $3985M^{-1}cm^{-1}$. Incubation of free dye controls under the same hydrolysis conditions indicated that the dye chromophore was stable under these conditions for up to 3 hours at concentrations below 150μM. At 500μM, however, some dye precipitation was observed. Measurement of absorbance of a dye or dye-dextran conjugate solution in 6M HCl at 541nm thus gives an estimate of dye concentration independent of the effects of dye stacking and microenvironment. This method was used routinely for determination of conjugate concentrations in all subsequent work.

A visual impression of the differences in the spectra of the dye-dextran conjugates in 6M HCl as a function of dye loading is shown in the photograph in figure 8.5a. As loading increased the colour of the solution changed from rose pink to mauve as a result of the increasing absorbance in the red region of the spectrum due to the increasing amplitude of the shoulder at 650nm. After hydrolysis all the solutions were the same rose pink colour as free dye (figure 8.5b) .

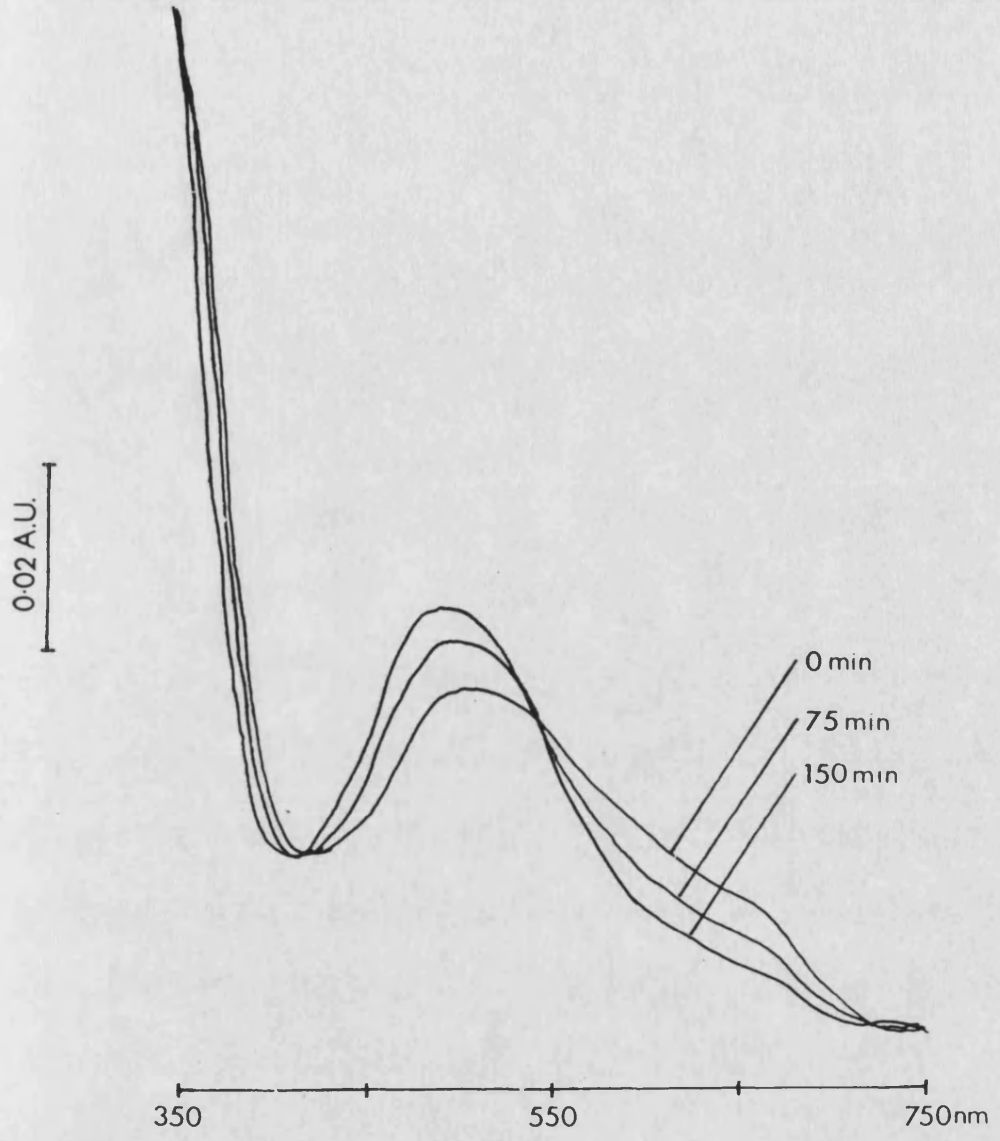

Figure 8.4

The effect of hydrolysis time on the spectrum of dye-dextran conjugate DCB206. 10μM (with respect to dye) conjugate DCB206 was hydrolysed in 6M HCl at 40°C for the indicated time. The absorbance spectrum of the sample was then recorded (still in 6M HCl) using a scanning spectrophotometer. This revealed an isosbestic point at 541nm.

Figure 8.5a

Figure 8.5b

The visible colour of 50μM dye-dextran conjugates with increasing dye:dextran ratios in 6M HCl a) before and b) after hydrolysis for 3 hours at 40°C. The conjugates are (left to right) 20D2, 20D5, 20D7, 20D9, 20D10, 5D7, 5D9, 5D10.

The dye:dextran ratios of the conjugates synthesised were determined from absorbance measurement at the isosbestic point of 541nm in 6M HCl from which the mass of dye could be calculated, together with total dry weight measurements which allowed the mass of dextran to be calculated by difference.

An indication of the degree of intramolecular dye stacking in the conjugates was obtained by comparison of estimates of dye loading from absorbance measurements at 257nm in water with those obtained at 541nm in 6M HCl. These results are compared in the bar graphs for the 20D series and the 5D series of conjugates shown in figures 8.6 and 8.7. The ratio of the loadings estimated from the measurements at 257nm and 541nm are plotted against the loadings estimated from the measurements at 541nm (the 'true values') in the insets to figures 8.6 and 8.7.

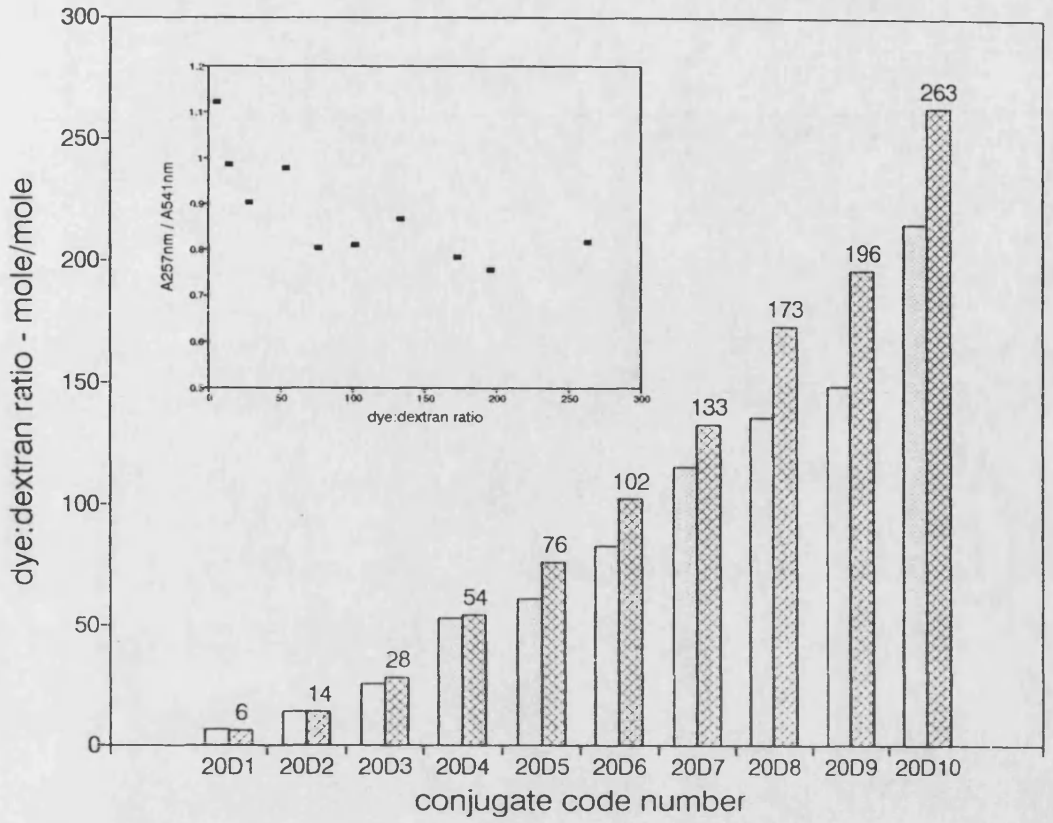

Figure 8.6

Bar graph showing the effect of intramolecular dye stacking on estimates of dye:dextran ratio made using absorbance measurements at 257nm in water (stippled bars) and 541nm in 6M HCl (cross hatched bars) for the 20D series of conjugates. The numbers over the bars are the 'true' values for loading used in all subsequent calculations.

Inset: The ratio of the loadings estimated from the measurements at 257nm and 541nm plotted against the 'true' estimate from the 541nm value.

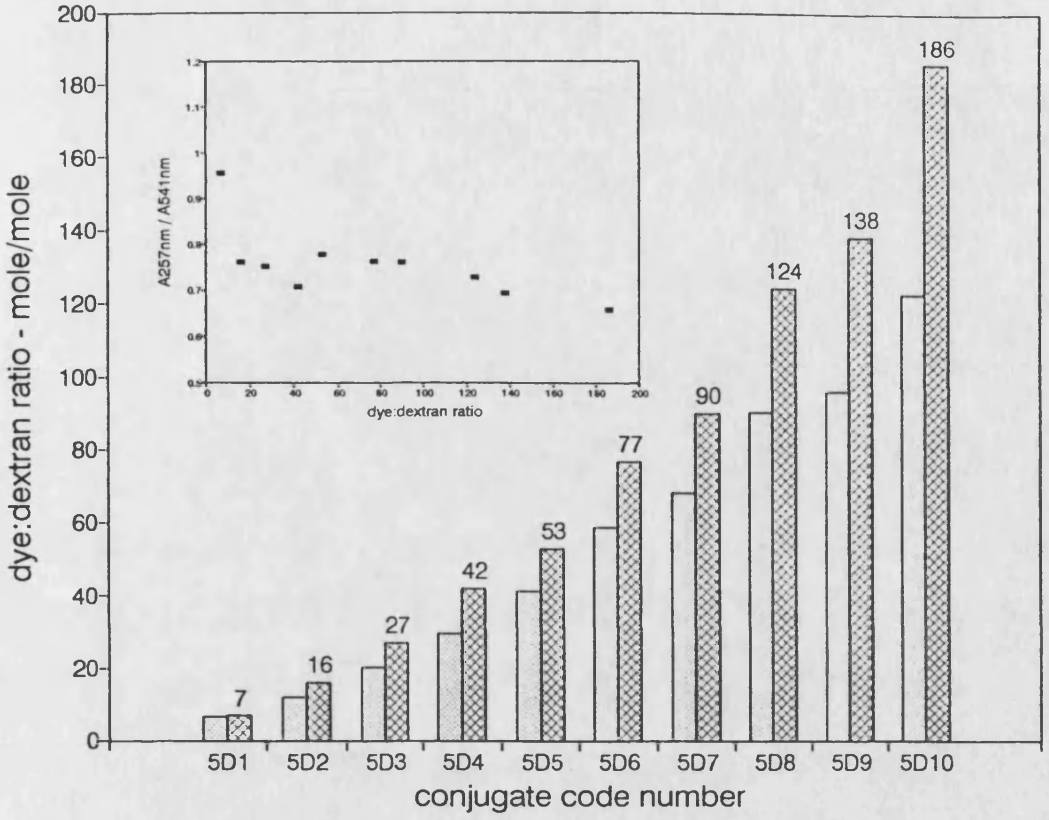

Figure 8.7

Bar graph showing the effect of intramolecular dye stacking on estimates of dye:dextran ratio made using absorbance measurements at 257nm in water (stippled bars) and 541nm in 6M HCl (cross hatched bars) for the 5D series of conjugates. The numbers over the bars are the 'true' values for loading used in all subsequent calculations.

Inset: The ratio of the loadings estimated from the measurements at 257nm and 541nm plotted against the 'true' estimate from the 541nm value.

The loadings of the conjugates synthesised using the initial protocol are summarised in table 8a together with their respective identification codes which are used in subsequent results and discussion.

Based on dextran M.W. 2×10^6		Based on dextran M.W. 5×10^5	
code	dye:dextran ratio	code	dye:dextran ratio
DCB201	23.9	DCB51	6.6
DCB202	42.0	DCB52	16.2
DCB205	53.4	DCB55	20.1
DCB206	101.5	DCB56	30.7
DCB207	207.9	DCB57	72.8

Table 8a

Identification codes and dye:dextran ratios of dye-dextran conjugates synthesised using the initial protocol.

8.1.5. Laser Light Scattering Measurements

The diffusion coefficient D_T was measured for each of a range of conjugates from the 5D series. The values presented in table 8b below are the means and standard deviations from a series of measurements on each conjugate.

dextran standards			dye-dextran conjugates			
M.W.	mean D_T	S.D.(n)	code	mean D_T	S.D.(n)	"M.W."
40	498	8.5(16)	5D1	142	6.0(13)	586*
70	383	3.3(11)	5D3	155	4.1(20)	480
124	312	7.7(13)	5D5	165	7.6(17)	438
480	155	2.2(14)	5D8	179	19.9(19)	362
2000	141	6.2(11)	5D10	234	20.6(14)	204

* extrapolated value

Table 8b

Values for the diffusion coefficients of various dextran standards and dye-dextran conjugates in distilled water determined by laser light scattering measurements. The molecular weight values are quoted in 1000's of KDa. The diffusion coefficients are quoted with dimensions of $m^2s^{-1} \times 10^{13}$. The 'M.W.' values of the conjugates were calculated from the regression line through the linear portion of a log M.W. against log D_T callibration graph using the data from the dextran standards. The 2×10^6 dextran standard did not fall on the line through the other 4 points so the 'M.W.' of 5D1 was determined by extrapolation of the line. The 2×10^6 standard may have given an anomalous result since some of the readings gave two values for D_T indicating that more than one normally distributed population of sizes may be present. Hence the single D_T values measured may have been eroneous.

8.2 Quantitation of Protein Binding by Gel-Permeation Chromatography

8.2.1 Technical Development and Control Experiments

For the experiments using the Sephadex G75 column, trough areas were calculated by measuring the deviation of the trace from the stable plateau line at 2mm intervals and integrating using the trapezium rule. A typical eluate trace is shown in Figure 8.8.

Dye-dextran conjugates DCB201-207 and DCB51-57 were used for the binding experiments. Each of the dye-dextran conjugates was used for binding measurements at lysozyme concentrations in the range 0.5 - 0.0052mgml^{-1}.

The amount of lysozyme bound to each conjugate at each concentration of free lysozyme was calculated using the formula:

$$lysozyme\ bound = \frac{L_f \times A \times FR}{CS \times PLATEAU} \quad moles \qquad (8.1)$$

where L_f = *molar concentration of lysozyme in running buffer*
A = *area of trough in mm*
FR = *flow rate in l hour*$^{-1}$
CS = *chart speed in mm hour*$^{-1}$
$PLATEAU$ = *difference in mm between baseline in the absence of lysozyme and plateau in the presence of lysozyme*

For the experiments carried out using the FPLC system with a Superose 12HR column the trough areas were determined by photocopying the chart traces and cutting and weighing the trough regions. This was considered to be more accurate than measurement, since, particularly at high lysozyme concentrations the troughs were quite short and deep. A typical trace from this column is shown in fig 8.9.

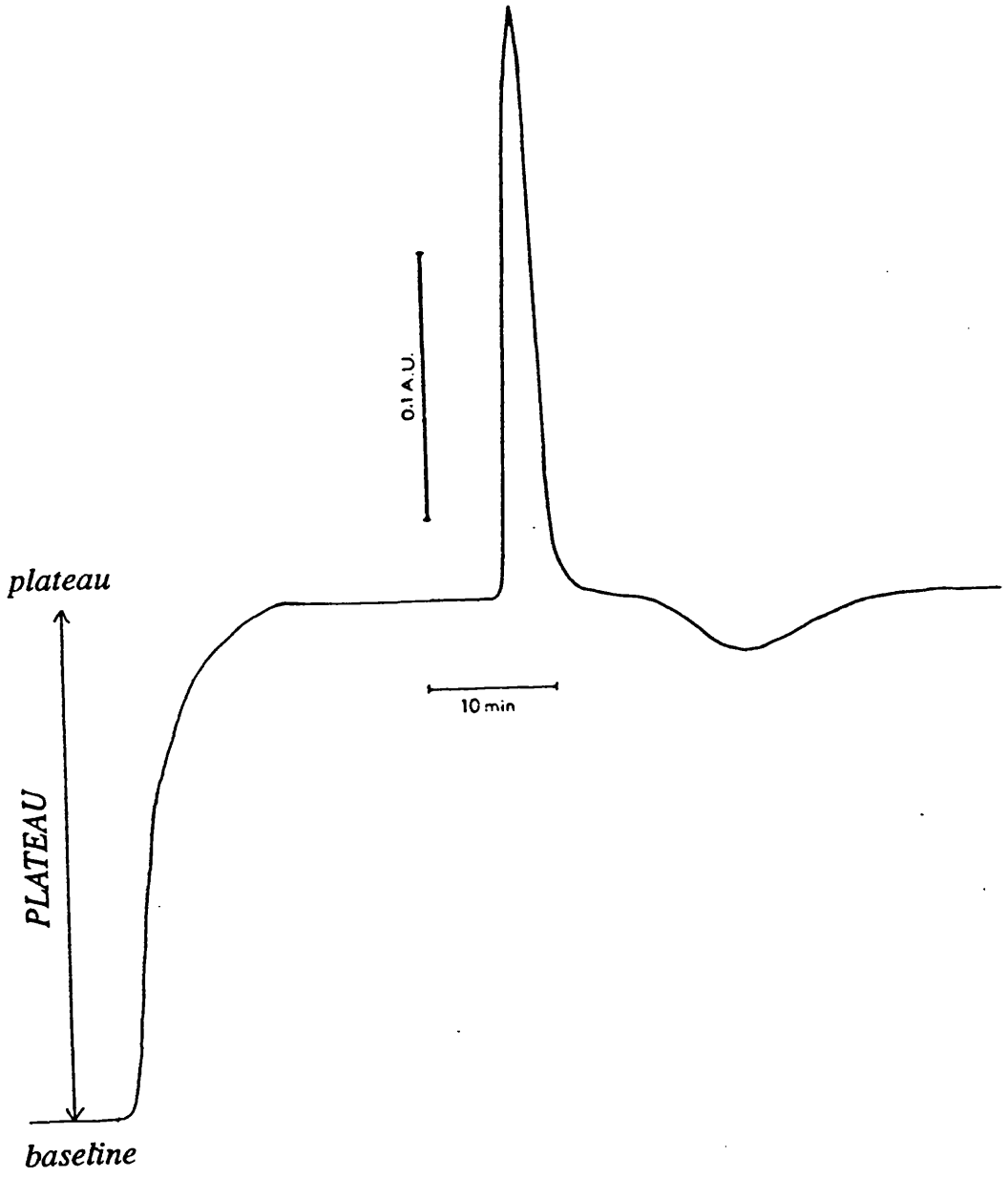

Figure 8.8

A typical chart trace for a gel permeation binding experiment. Dye-dextran conjugate DCB205 at a concentration of 69μM (with respect to dye) in the presence of lysozyme (62.5mgl^{-1}) at 24°C. The flow rate was 24mlhr^{-1}; absorbance was monitored at 280nm. The column was 50cm by 0.66cm and was packed with Sephadex G75.

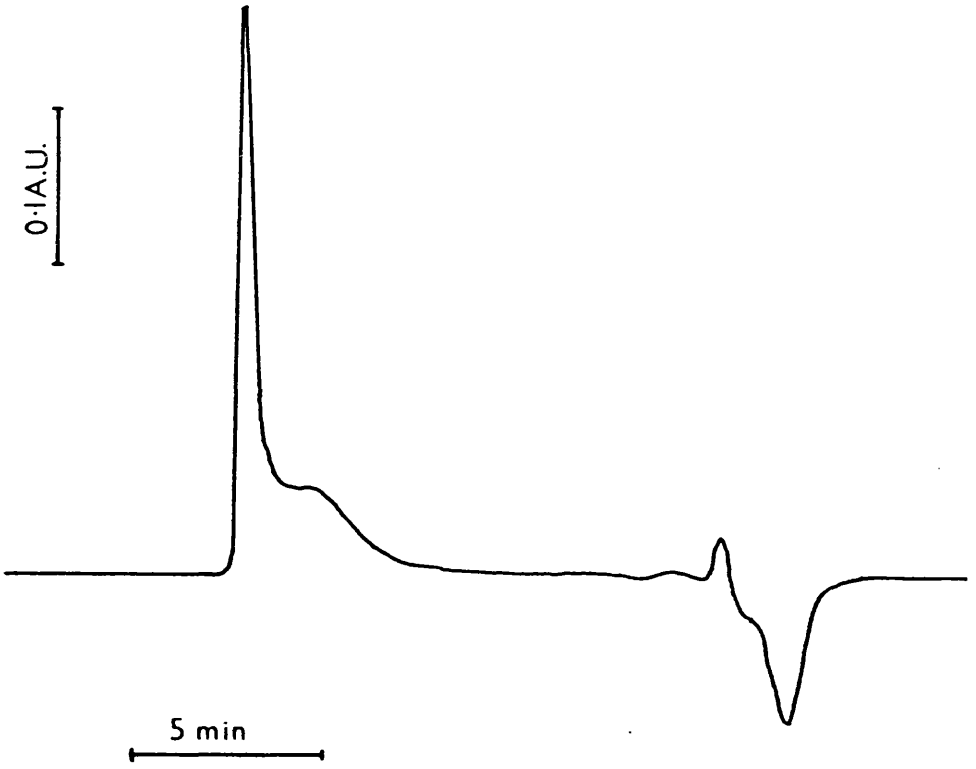

Figure 8.9

Typical chart trace for a Superose 12HR gel-permeation binding experiment using 69μM 5D7 (with respect to dye) in the presence of 125mgl^{-1} lysozyme. The flow rate was 48mlhr^{-1}; absorbance was monitored at 280nm. The column dimensions were 30cm by 1cm diameter.

Considerable problems were encountered with increasing back pressure when using the Superose column. This appeared to be due mainly to buildup of aggregates of dye-dextran conjugate and lysozyme, mostly on the top and bottom frits but also to a certain degree in the top part of the gel bed. Various washing procedures were assessed for removal of the aggregates including 1M NaCl, 20% aqueous ethanol, 0.1M sodium borate pH7.0, 50mM HCl and 50mM NaOH. Only the latter two proved to be really effective. 50mM HCl was used routinely to clean the column. In severe cases the replacement of the frits proved to be a more efficient solution than extensive washing.

In all the gel-permeation experiments the amount of dye used in each run was kept constant so the amount of dye-dextran conjugate varied in inverse proportion to its dye loading. Some control experiments were run in which the dextran concentration was also kept constant by the inclusion of appropriate amounts of blank dextran. These indicated that the total dextran concentration had no effect on lysozyme binding in the range used here (0.07 to 0.5% w/w).

In the absence of dye ligands no binding was observed between dextran and lysozyme even at the highest dextran concentration examined (5% w/w). However, a dextran concentration of 5% w/w had a considerable effect on lysozyme binding to dye-dextran conjugates, reducing the binding of lysozyme to 20D10 (110μM with respect to dye) by 10% at 0.25mgml^{-1} lysozyme and by 37% at 0.025mgml^{-1} lysozyme.

8.2.2 Lysozyme Binding to the DCB20 Series of Conjugates

Data from gel permeation binding measurements for the DCB20 series is presented in semi-log form in figure 8.10. The data clearly indicate the presence of high affinity 'specific' saturable sites and lower affinity 'non-specific' sites which showed no approach to saturation over the range of ligand concentration studied. Data points corresponding to the saturable part of these binding curves were used to determine operational values for the half saturation constant $K_{0.5}$ (a dissociation constant) and the value of n, together with their standard errors, using a computer program based on the method of Wilkinson (a non-linear least squares fit to a hyperbolic function). Plots of these data points and the fitted curves are presented as graphs of L_b/M against $[L_f]$ in figure 8.11.

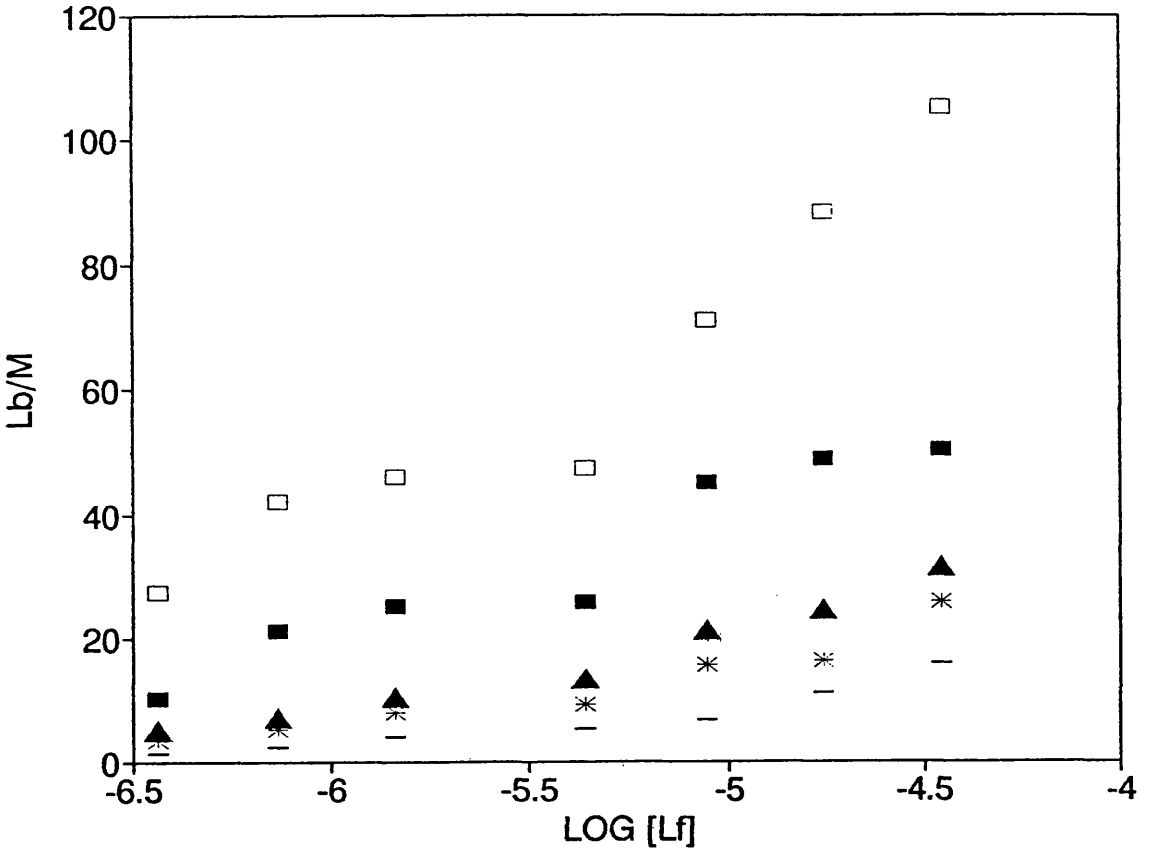

Figure 8.10

Semi-logarithmic plots of L_b/M against log $[L_f]$ for binding of lysozyme to conjugates DCB 201(-), 202(*), 205(▲), 206(■), 207(□) at 24°C.

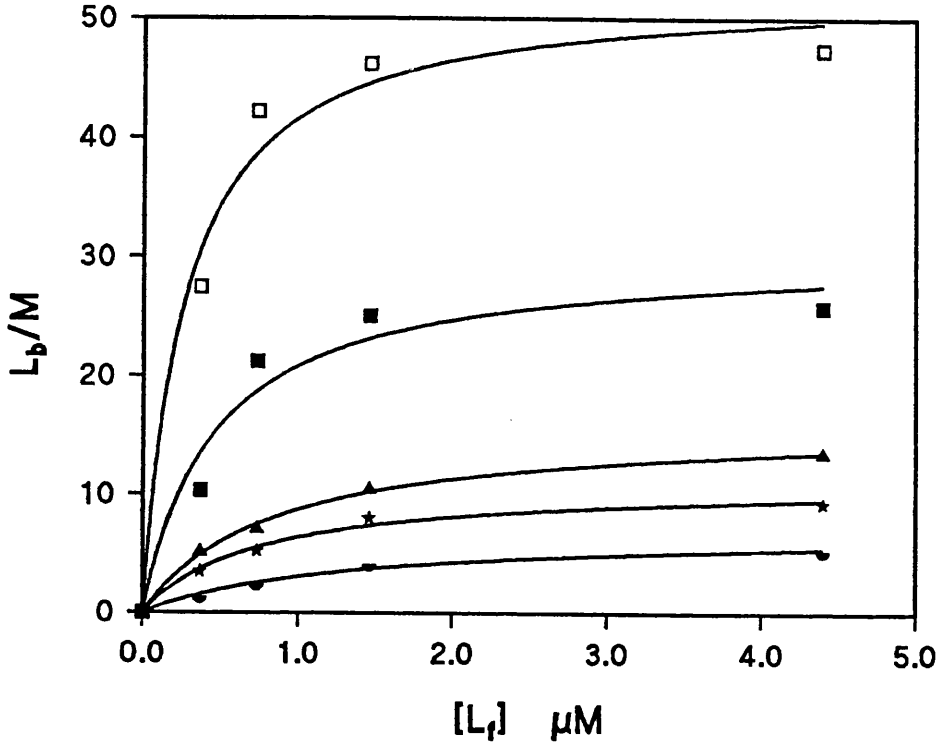

Figure 8.11

Graphs of L_b/M against L_f for the 'saturable' part of the binding curves shown in figure 8.9: DCB 201(-), 202(★), 205(▲), 206(■), 207(□).
The solid line through each set of data was generated using the values for $K_{0.5}$ and n obtained from curve fitting to a hyperbolic adsorption isotherm.

Values of n and $K_{0.5}$ are plotted against the ligand loadings of the corresponding dye-dextran conjugates in Figure 8.12 and 8.13. From these figures it is apparent that specific binding capacity is directly proportional to the dye loading on the dextran up to a loading of 101 moles dye per mole dextran, i.e. the function is linear and passes through the origin. The gradient of the line indicates that approximately 30% of the total conjugated dye is available for specific binding. At the highest loading (208 moles dye per mole dextran) the proportionality no longer holds and the fraction of conjugated dye available for binding is reduced by 20% compared with the values observed for the other dye-dextran conjugates studied.

The relationship of specific binding affinity to dye loading is more complex but a general decrease of $K_{0.5}$ with increasing loading is apparent. It should be stressed that these are operational constants and do not represent the true values of K_d and n because of the contribution made by the lower affinity system.

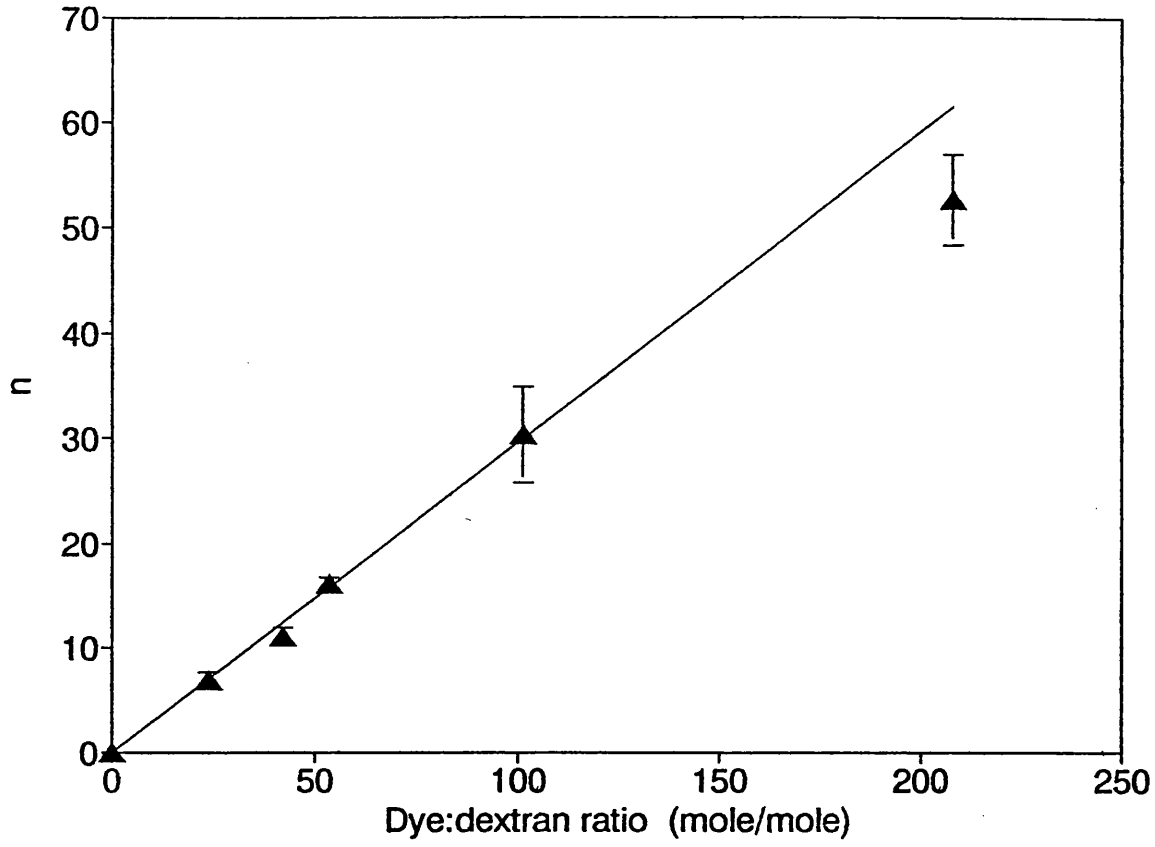

Figure 8.12a

The effect of ligand loading on n for the DCB20 series of conjugates. The graph shows means ± standard errors obtained from the estimation of n by the method of Wilkinson. The line is a regression line through the five lower points.

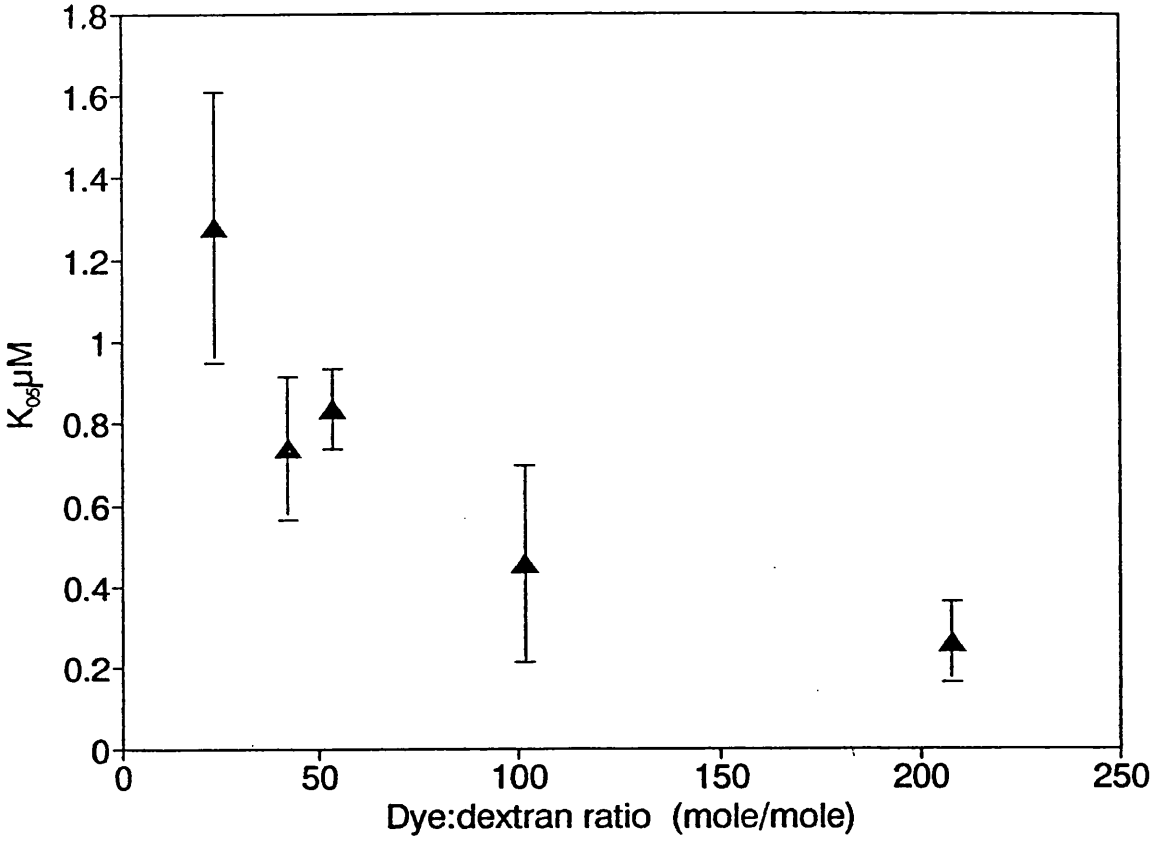

Figure 8.13

The effect of ligand loading on the value of $K_{0.5}$ for the DCB20 series of conjugates. The graph shows means $\pm$ standard errors obtained from the estimation of $K_{0.5}$ by the method of Wilkinson.

8.2.3 Lysozyme Binding to the DCB5 Series of Conjugates

Visual examination of the results for the DCB5 series of conjugates, shown in figure 8.14, indicates that the binding curves show the same general form as those presented above. A similar treatment of the data yields the same general trends in the results although the values obtained from the curve fits shown in figure 8.15 should be treated with some caution since each fit was calculated using only 4 data points (including the origin). The graph of n against loading is presented in fig 8.16. The value for n, obtained from the curve fit to the data for DCB51, was 25% greater than the total amount of dye present on this conjugate. This seems unlikely in view of the values for the other conjugates, and by omitting this point the regression line passes almost through the origin (actually through 0,-0.3). Since the origin is a known point this should be weighted to ensure that the line passes through it hence the dotted line in figure 8.16 is probably more realistic than the solid line, although the difference in the estimates of the fraction of dye participating in binding at saturation of the high affinity interaction is small, the estimates being 28% (from the solid line) including the dubious data point and 31% (for the broken line) omitting it.

A plot of $K_{0.5}$ against loading is shown in figure 8.17 and shows the same increase in operational affinity and approach towards a maximum affinity (minimum $K_{0.5}$) as the dye loading increases as was observed for the DCB20 series.

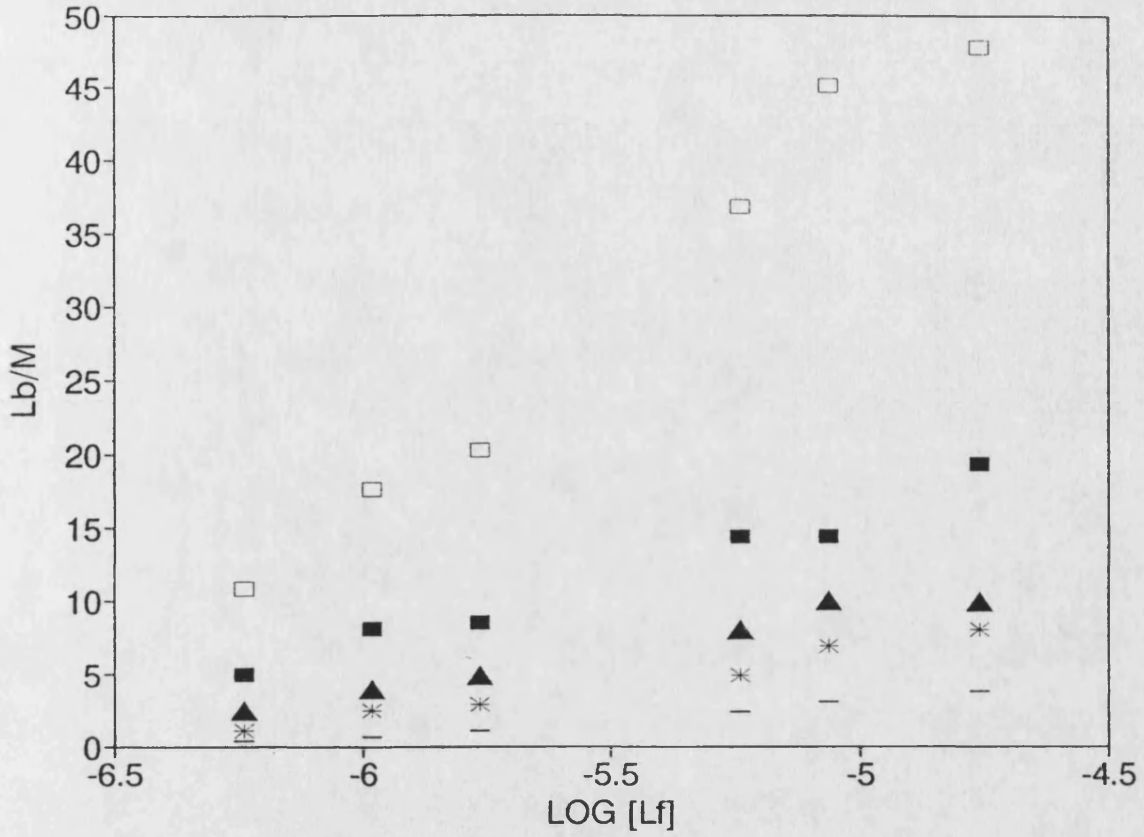

Figure 8.14

Semi-logarithmic plots of L_b/M against log $[L_f]$ for binding of lysozyme to conjugates DCB 51(-), 52(★), 55(▲), 56(■), 57(□) at 24°C.

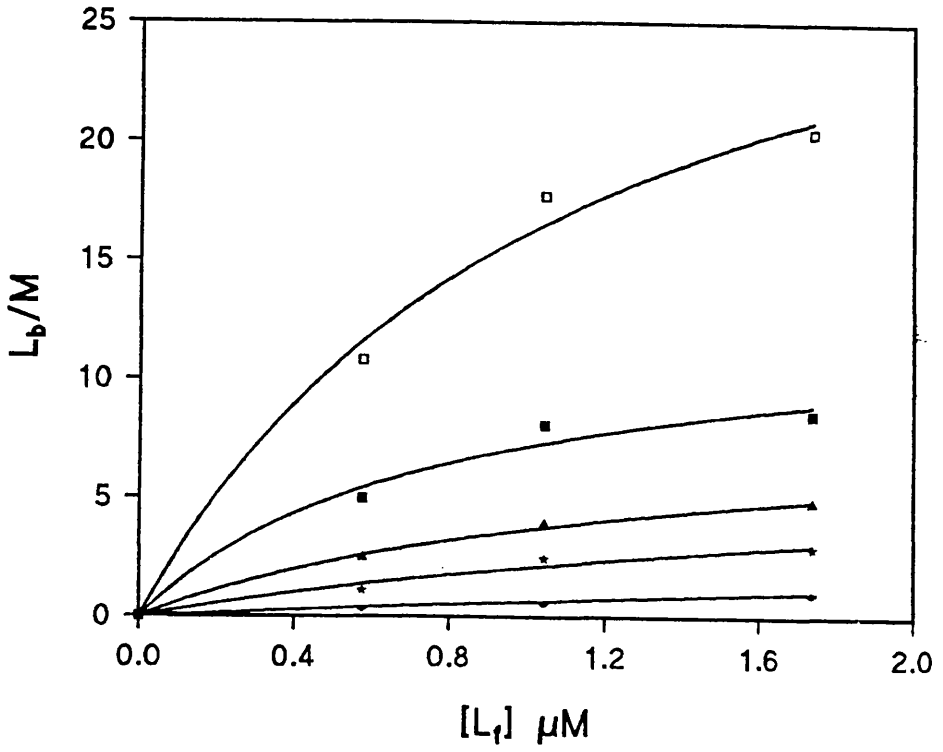

Figure 8.15

Graphs of L_b/M against L_f for the saturable part of the binding curves for the DCB5 series of conjugates shown in figure 8.13: DCB 51(-), 52(★), 55(▲), 56(■), 57(□). The solid line through each set of data was generated using the values for $K_{0.5}$ and n obtained from curve fitting to a hyperbolic adsorption isotherm.

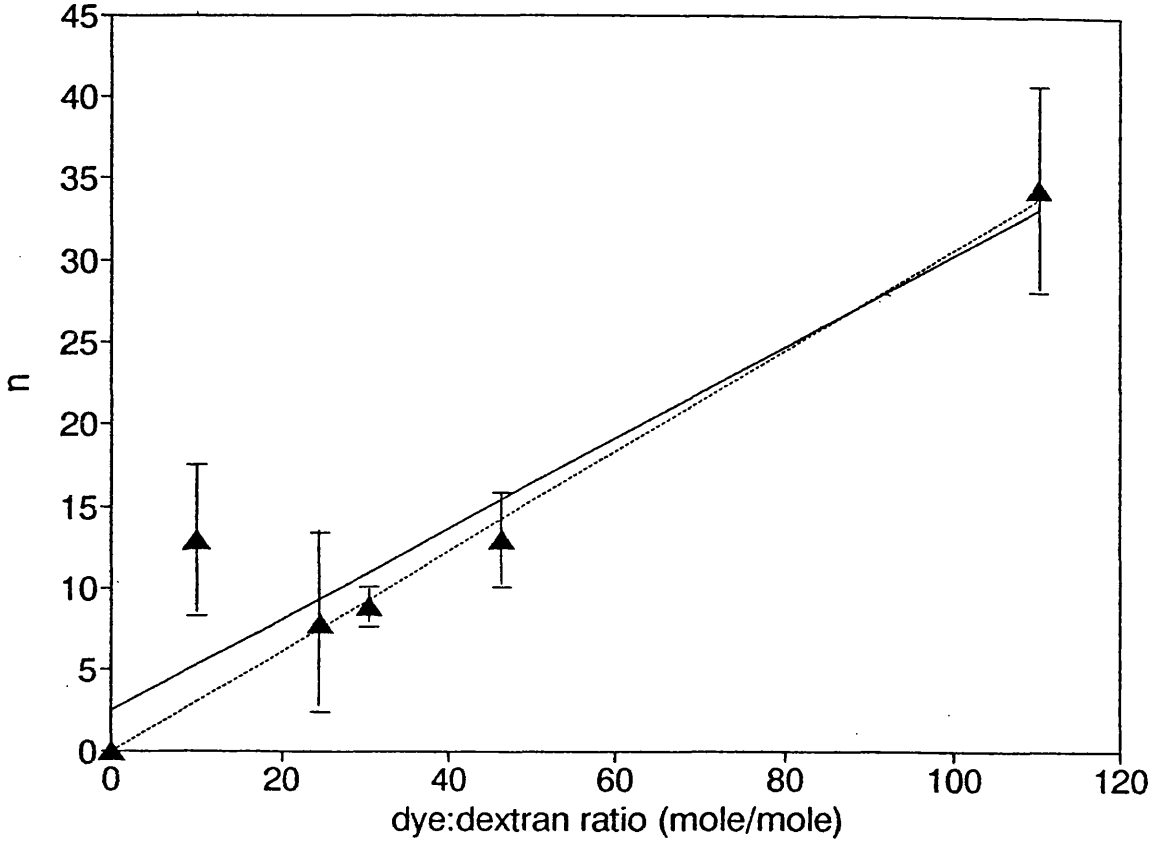

Figure 8.16

The effect of ligand loading on n for the DCB5 series of conjugates . The graph shows means ± standard errors obtained from the estimation of n by the method of Wilkinson. The solid line is a regression line through all of the data points. The broken line is a regression line omitting the point for conjugate DCB51.

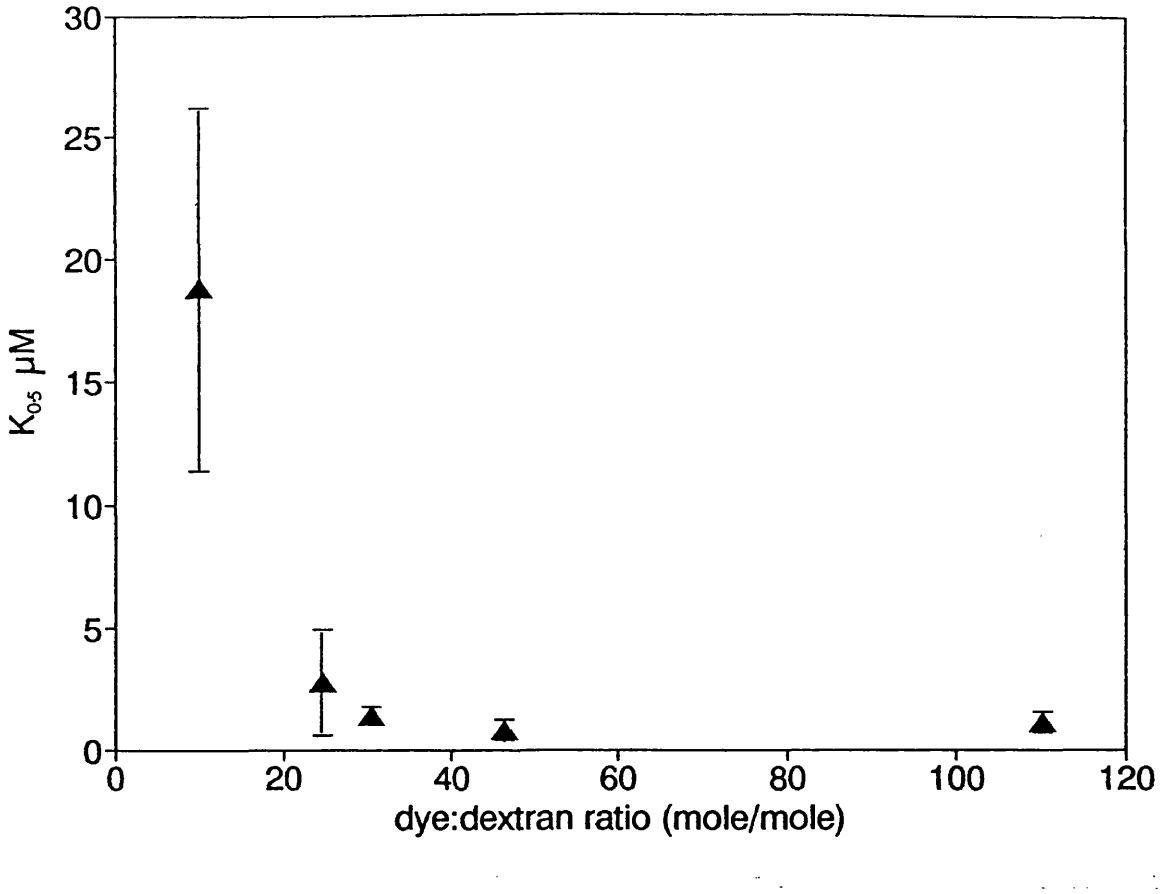

Figure 8.17

The effect of ligand loading on the value of $K_{0.5}$ for the DCB5 series of conjugates. The graph shows means $\pm$ standard errors obtained from the estimation of $K_{0.5}$ by the method of Wilkinson.

8.2.4 Lysozyme Binding to the 5D series of Conjugates using the FPLC System and Superose 12HR Column.

In the experiments conducted using a Superose 12HR gel permeation column on a FPLC system the data obtained did not in general show the same clearcut biphasic behaviour observed in the previous data, except perhaps in the saturation curves for 5D1 to 5D3 (see figure 8.18a. This observation was confirmed by comparing the constants obtained when the first 5 points on each saturation curve or all the data points were fitted to a hyperbolic function. The discrepancy between the two sets of constants thus calculated decreased with increasing loading such that by 5D8 there was effectively no difference i.e. the entire data sets could be described adequately by the same hyperbolic function as that determined from the first five points. Semi-log plots of the data are shown in figure 8.18 a and b.

8.2.5 Use of the Superose 12HR Column for Binding Measurements with Larger Proteins.

The feasibility of using this column for similar binding determinations with larger proteins was tested using BSA (M.W. 67000) and yeast ADH (M.W. 145000). The traces in fig 8.19 a to c clearly show that the peaks and troughs are adequately separated and hence that the method is potentially useable for proteins of these molecular weights, providing the dextran is prefractionated to remove the lower molecular weight material. This forms a large shoulder on the peak and prevents complete resolution from the trough as seen in figure 8.19a for a run with BSA.

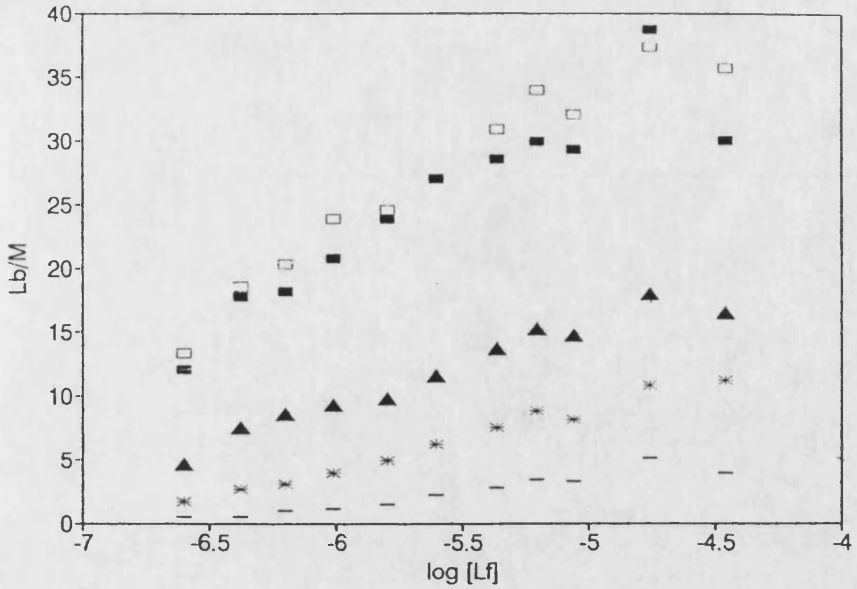

Figure 8.18a

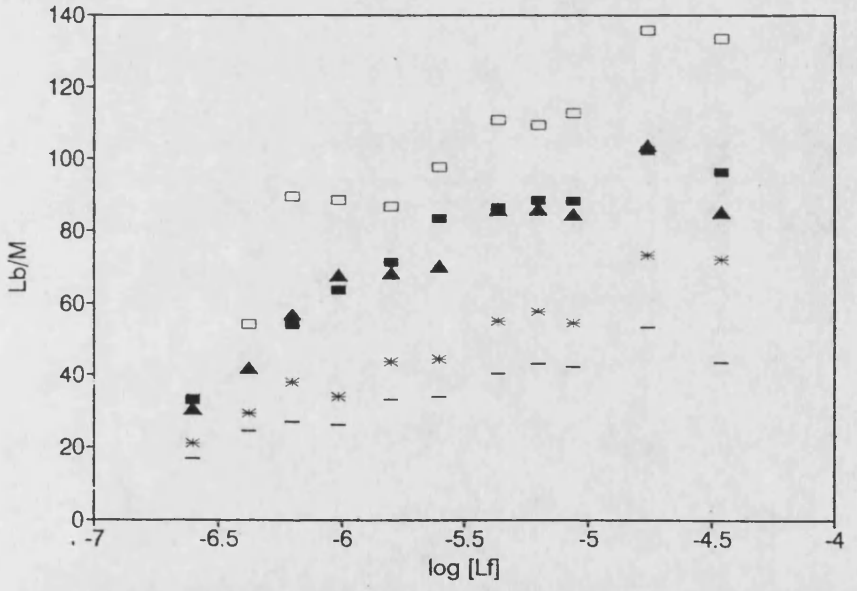

Figure 8.18b

Semi-log plots of L_b/M against log $[L_f]$ for binding of lysozyme to the 5D series of conjugates at 25°C measured using a Superose 12HR column on a FPLC system: a) 5D1(-), 5D2(★), 5D3(▲), 5D4(■), 5D5(□): b) 5D6(-), 5D7(★), 5D8(▲), 5D9(■), 5D10(□).

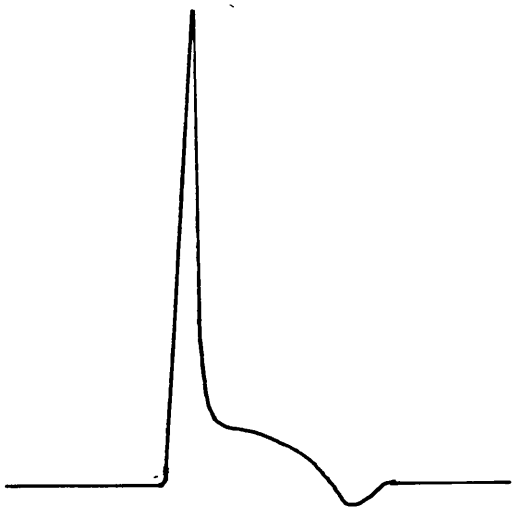

Figure 8.19a

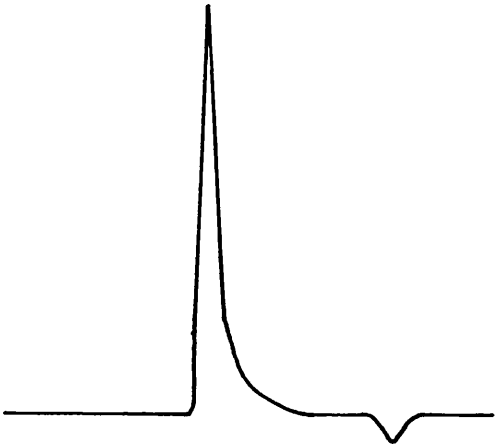

figure 8.19b

Chart traces from a Superose 12HR column eluted at 0.5mlmin^{-1} for gel permeation binding measurements:

a) loading 50μl of 69μM unfractionated DCB205 with the column equilibrated with 67μgml^{-1} BSA in 10mM tris 50mM NaCl pH8.0.

b) as for a) but with 50μl 16μM DCB205 fractionated on a Superose 12 column to remove the lower molecular weight material.

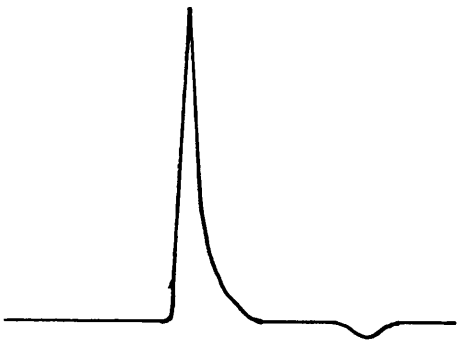

Figure 8.19c

c)loading 50μl of 16μM fractionated DCB205 with the column equilibrated with 35μgml^{-1} yeast ADH in 10mM malonate 50mM NaCl pH6.0.

8.3 Quantitation of Protein Binding by Spectral Titration

8.3.1 Binding of Lysozyme to the 20D and 5D series of Conjugates

Difference spectra obtained when a dye-dextran conjugate is titrated with increasing concentrations of lysozyme are shown in figure 8.20. They comprise a peak with a maximum at about 700nm and a trough with a minimum at 595nm. Since the magnitude of the trough is greater than that of the peak all fixed wavelength titrations with lysozyme were carried out at 595nm.

Titration curves for the 20D and 5D series of conjugates with lysozyme are shown in figures 8.21 and 8.22 respectively.

In order to determine D_a, the concentration of occupied dye sites at saturation, and K_d, the dissociation constant for the dye lysozyme interaction, an equation was derived as follows to relate these constants to the absorbance difference.

At any point in the titration the observed absorbance can be attributed to to the sum of the absorbances of the individual species in the system. At 595nm the contributions will be limited to free and bound Cibacron Blue since the protein has no absorbance at this wavelength. As the aim is to relate the spectral shift to changes in the fractional saturation of the adsorbent, calculation is complicated by the presence of immobilised dye which is in an orientation which precludes binding. For this reason the immobilised dye is divided into two populations (i) available: D_a and (ii) unavailable: D_u. The observed absorbance in the absence of added protein (lysozyme) can now be expressed in terms of the absorbtion coefficient for the uncomplexed dye and the concentration of each sub-population in the system:

$$A_{595} = ef(D_a + D_u) \tag{8.2}$$

where *ef* is the absorption coefficient of uncomplexed dye

The introduction of lysozyme into the system leads to two competing effects on the observed absorbance.

i) a lowering of the uncomplexed dye concentration

ii) formation of a dye-protein complex which has a modified absorbtion coefficient (*eb*) due to the spectral shift which occurs on binding.

The observed absorbance can be described mathematically by:

$$A_{595} = ef((D_a - D_b) + D_u) + ebD_b \tag{8.3}$$

where D_b is the concentration of complexed dye.

In practice the relative concentrations of D_a and D_u will not be known in advance of the titration, and may vary between different batches of adsorbent. To overcome this problem the difference in absorbance between solutions of equal dye concentration with and without lysozyme are determined. Hence subtraction of equation 8.2 from equation 8.3 gives:

$$\Delta A_{595} = D_b(eb - ef) \tag{8.4}$$

The concentration of D_b can be calculated from the equilibrium between complexed and free species:

$$K_d = \frac{(D_a - D_b)(L_t - D_b)}{D_b} \tag{8.5}$$

where L_t is the total concentration of added lysozyme.

Solving equation 8.5 for D_b gives the physically significant root:

$$D_b = \frac{(D_a + K_d + L_t) - \sqrt{(D_a + K_d + L_t)^2 - 4D_aL_t}}{2} \qquad (8.6)$$

This expression can be substituted into equation 8.3 to give the following expression relating the change in A_{595nm} to K_d, D_a and *eb*.

$$\Delta A_{595nm} = (e_b - e_f)\frac{(D_a + K_d + L_t) - \sqrt{(D_a + K_d + L_t)^2 - 4D_aL_t}}{2} \qquad (8.7)$$

The measured difference absorbances at 595nm were corrected for the small volume change caused by addition of lysozyme solution. The exact total lysozyme concentration present after each lysozyme addition was calculated from the total volume of lysozyme solution added and the resulting cumulative volume in the cuvette.

The curve fits to equation 8.7 for the titration data are indicated by dotted lines in figures 8.21 and 8.22. Equation 8.7 clearly describes the data well and all the titration curves gave similarly good fits with comparable sum of squares residuals. Knowing the total dye concentration in each titration, the number of dye molecules participating in binding at saturation, n, (asssuming a 1:1 interaction) can be calculated from:

$$n = \frac{D_a}{D_t} \,.\, loading$$

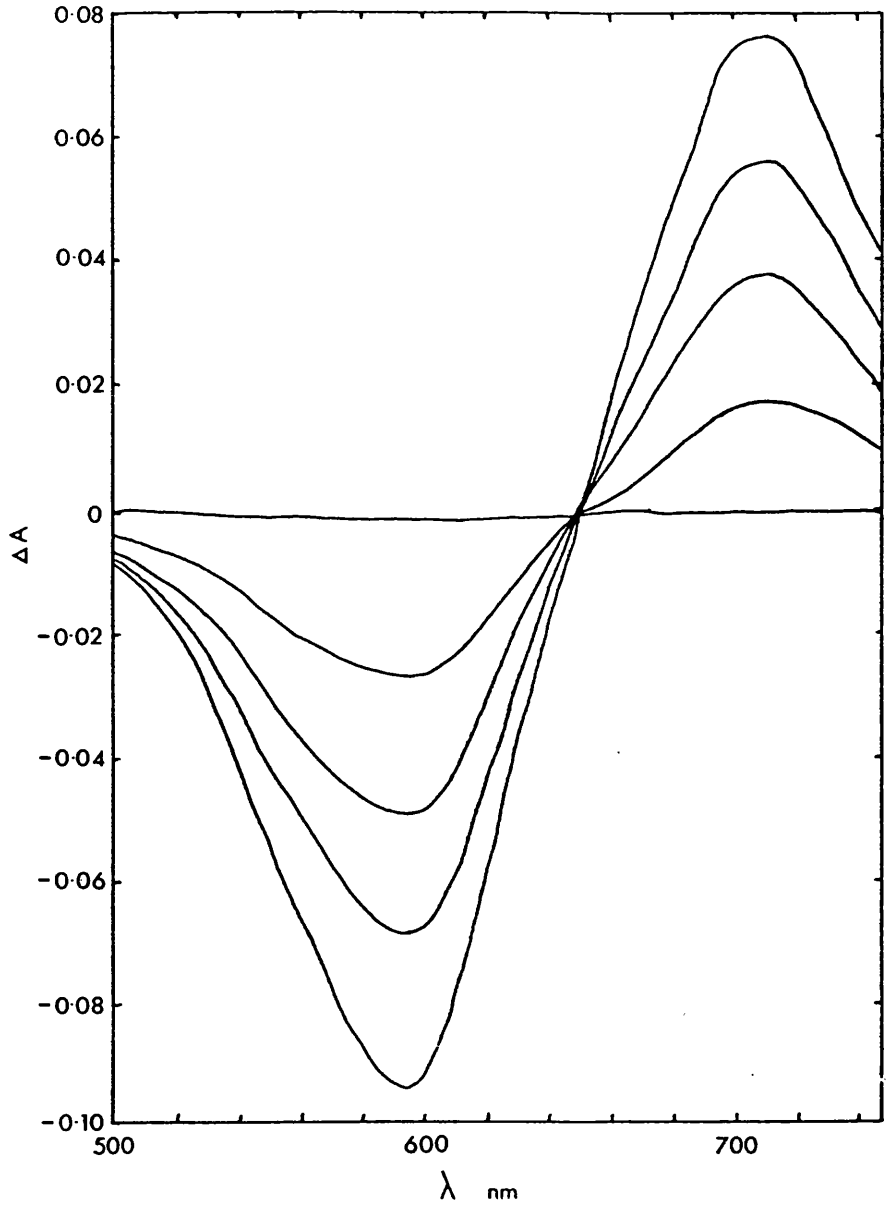

Figure 8.20

Difference spectra obtained when conjugate 5D5 was titrated with increasing concentrations of lysozyme. 2, 4, 6 and 12 μl 5mM lysozyme were added to 1ml 75μM (with respect to dye) 5D5 in 10mM tris 50mM NaCl pH8.0. The reference cuvette contained 1ml of the same conjugate solution in the same buffer to which water was added instead of lysozyme.

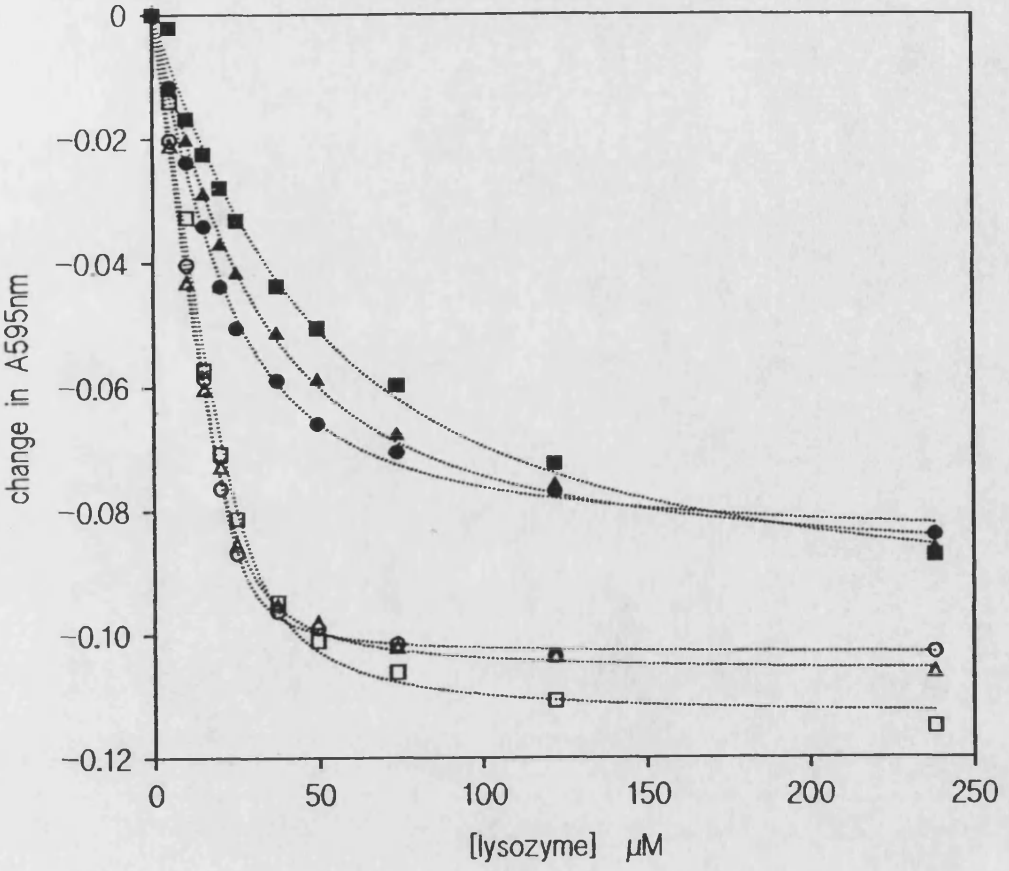

Figure 8.21

Graph of difference in absorbance at 595nm against lysozyme concentraton for titration of the 20D series of conjugates in 10mM tris 50mM NaCl pH8.0. Reference cuvettes contained the same conjugate solutions to which buffer was added.
72μM 20D2 (■), 75μM 20D3 (▲), 73μM 20D4 (●), 90μM 20D7 (□),
85μM 20D9 (△), 83μM 20D10 (○)
The broken lines are the fitted curves from which K_d and D_a were determined.

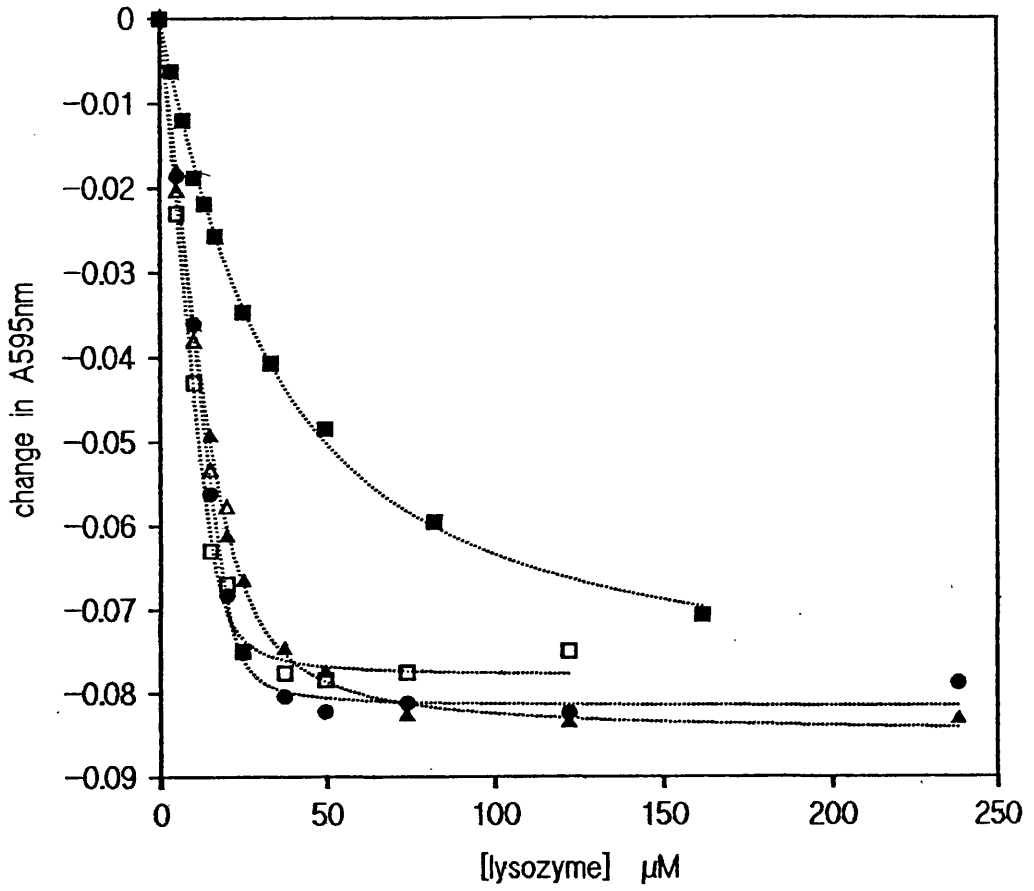

Figure 8.22

Graph of difference in absorbance at 595nm against lysozyme concentraton for titration of the 5D series of conjugates in 10mM tris 50mM NaCl pH8.0. Reference cuvettes contained the same conjugate solutions to which buffer was added.

75μM 5D1 (■), 74μM 5D3 (▲), 75μM 5D5 (●), 66μM 5D8 (□), 70μM 5D10 (△)

For 5D8 and 5D10 the lysozyme concentration where the symbols stop represents the point beyond which aggregation began to cause turbidity.

The broken lines are the fitted curves from which K_d and D_a were determined.

Plots of n and K_d against loading for the 20D and 5D series of conjugates are shown in figure 8.23 a and b and 8.24 a and b. The graphs of K_d against loading show an increase in affinity as the dye loading is increased. Both the graphs of n against loading are linear. The lines drawn are regression lines. From the gradients of the lines the proportion of dye participating in binding interactions with lysozyme at saturation is clearly constant at 28% and 27% respectively, regardless of dye loading.

At high dye/dextran ratios i.e. with 5D10 and also 5D8 at higher lysozyme concentrations, aggregation occured as the lysozyme concentration increased. This led to an increase in absorbance at 595nm. All of the conjugates formed gelatinous precipitates if left at 4°C for some time in the presence of lysozyme, suggesting that cross-linked aggregates eventually form in all cases but that the rate of formation is dependent on dye/dextran ratio and lysozyme concentration. Only with the most highly loaded dextran was precipitation clearly observable over the time course of a typical titration experiment. For this reason no data could be obtained for 5D10 from titration experiments, and the data points at high lysozyme concentrations were omitted from the curve fit of the data for 5D8.

Although spectral titration has been used sucessfully to measure binding of dyes to many proteins (eg. Thompson and Stellwagen, 1976; Subramanian and Kaufman, 1980; Skotland 1981), the technique was inapplicable to the measurement of the binding of free dye to lysozyme due to the rapid onset of aggregation resulting in turbid solutions as soon as the dye and lysozyme were mixed.

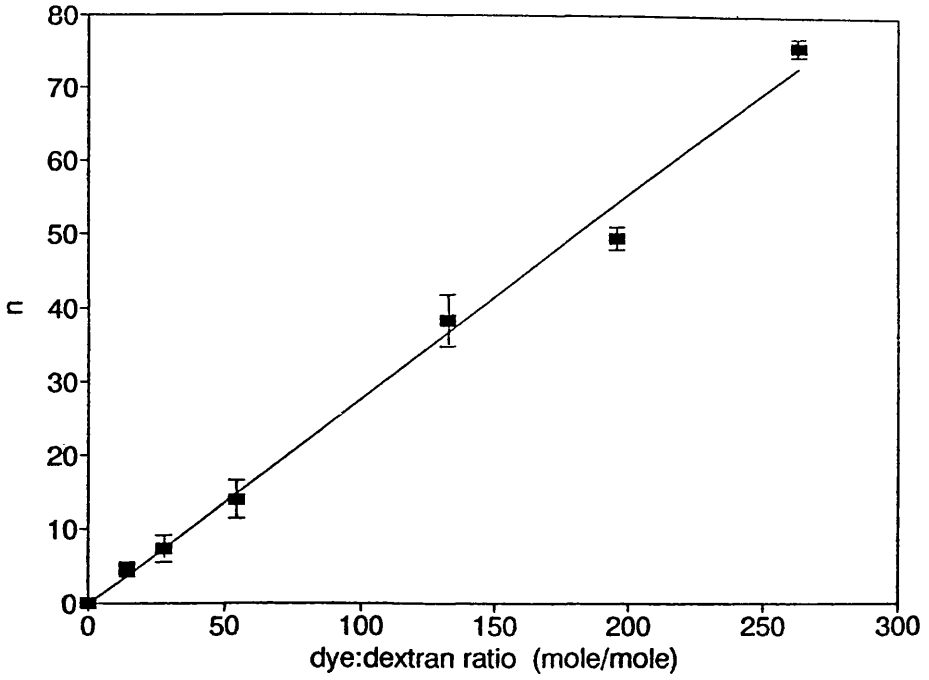

Figure 8.23a

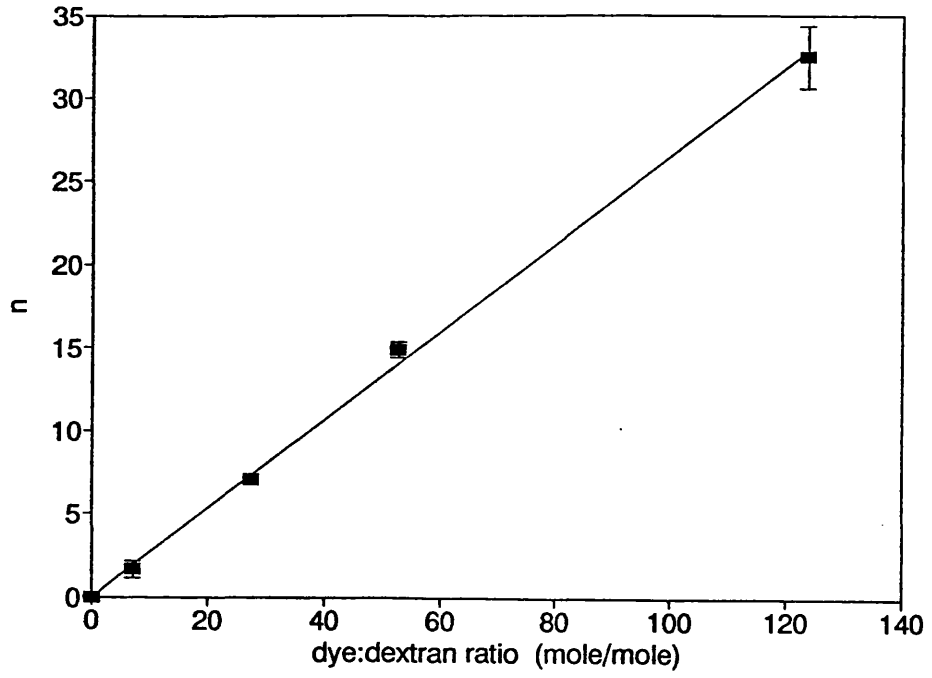

Figure 8.23b

Graphs of n against dye loading for a) the 20D and b) the 5D series of conjugates. The lines through the data are regression lines.

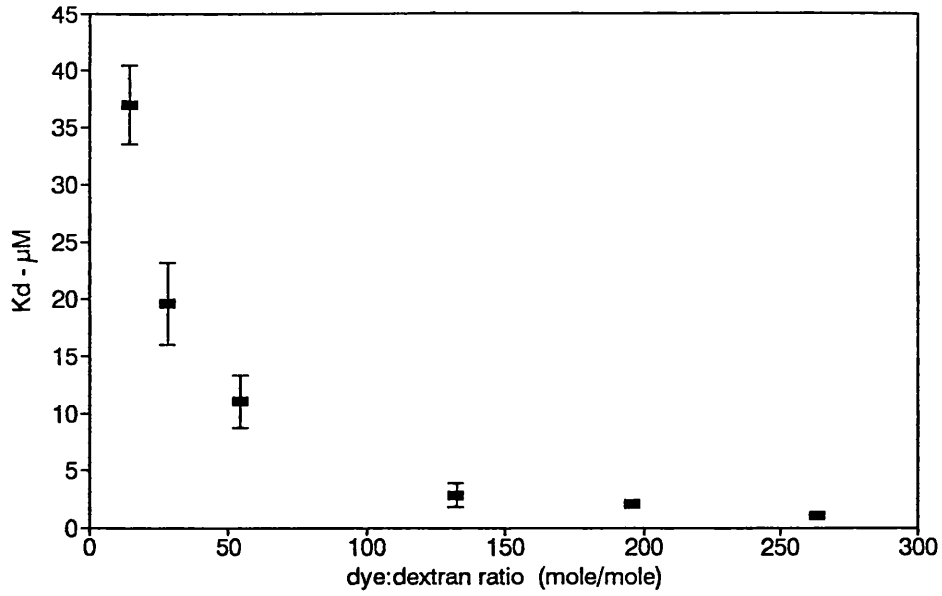

Figure 8.24a

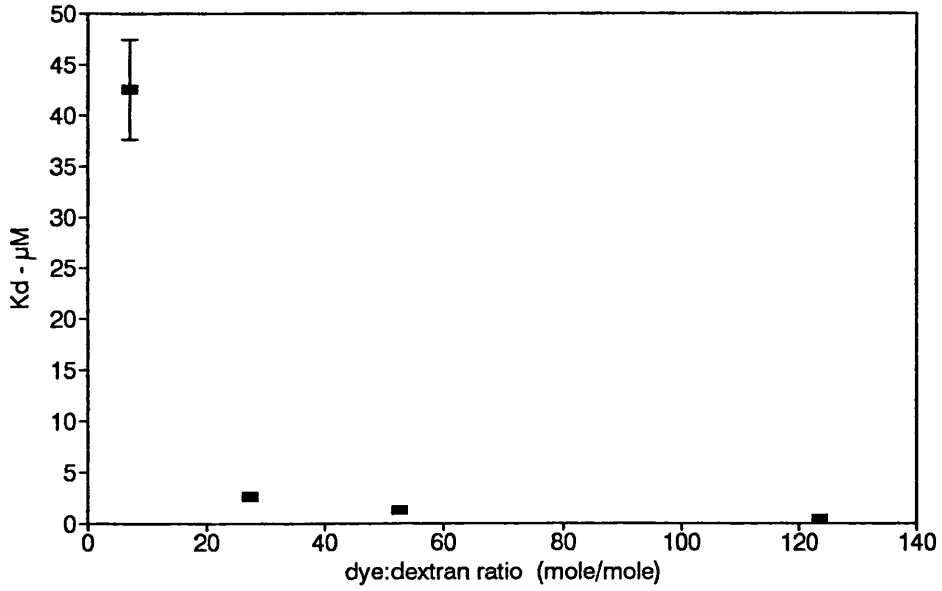

figure 8.24b

Graphs of K_d against dye loading for a) the 20D and b) the 5D series of conjugates.

8.3.2 The Effect of Buffer Composition and Concentration

To investigate the effect of ionic strength and type of buffer on the fraction of dye available to bind lysozyme at saturation, conjugates 20D3 and 20D10 were titrated in tris and phosphate buffers of varying concentration and also in 10mM tris buffer in the presence of different concentrations of NaCl. The titration curves are shown in figures 8.24 to 8.26. The values of % dye available (determined from D_a and dye concentration in the titration) and K_d determined by non-linear least squares curve fits of the data to equation 8.7 are summarised in table 8c.

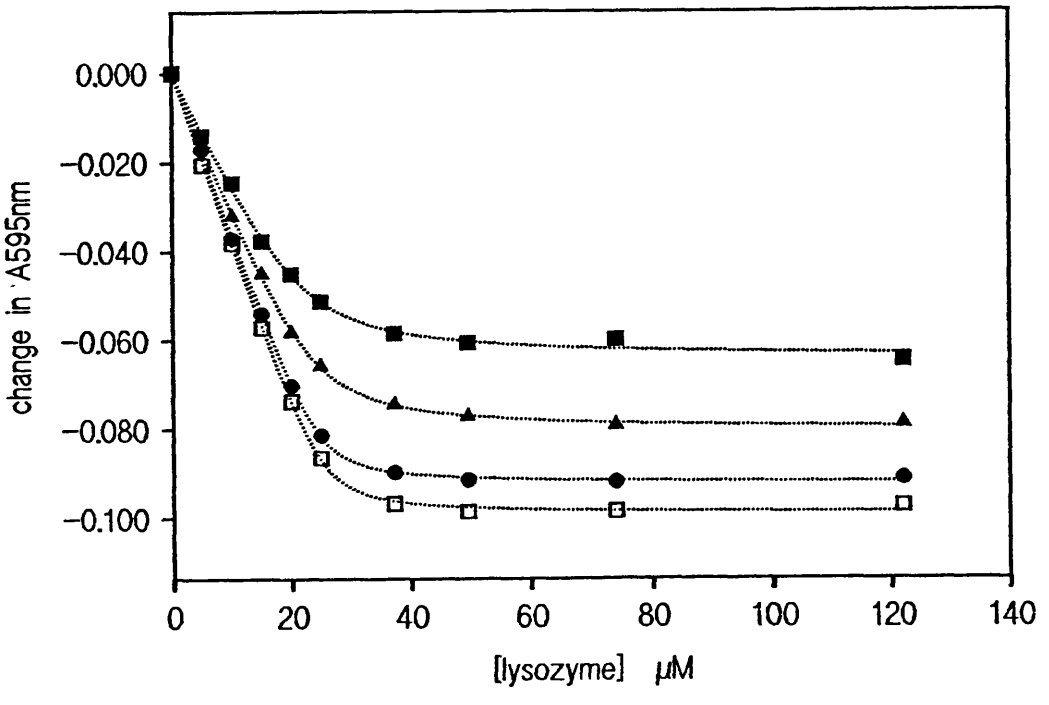

Figure 8.25

The effect of sodium chloride concentration on change in absorbance at 595nm against lysozyme concentration for titration of 70μM (w.r.t. dye) conjugate 20D10. The buffer was 10mM tris HCl pH8.0 containing: no NaCl (□), 10mM NaCl (●), 50mM NaCl (▲) and 100mM NaCl (■). The broken lines are curve fits using equation 8.7.

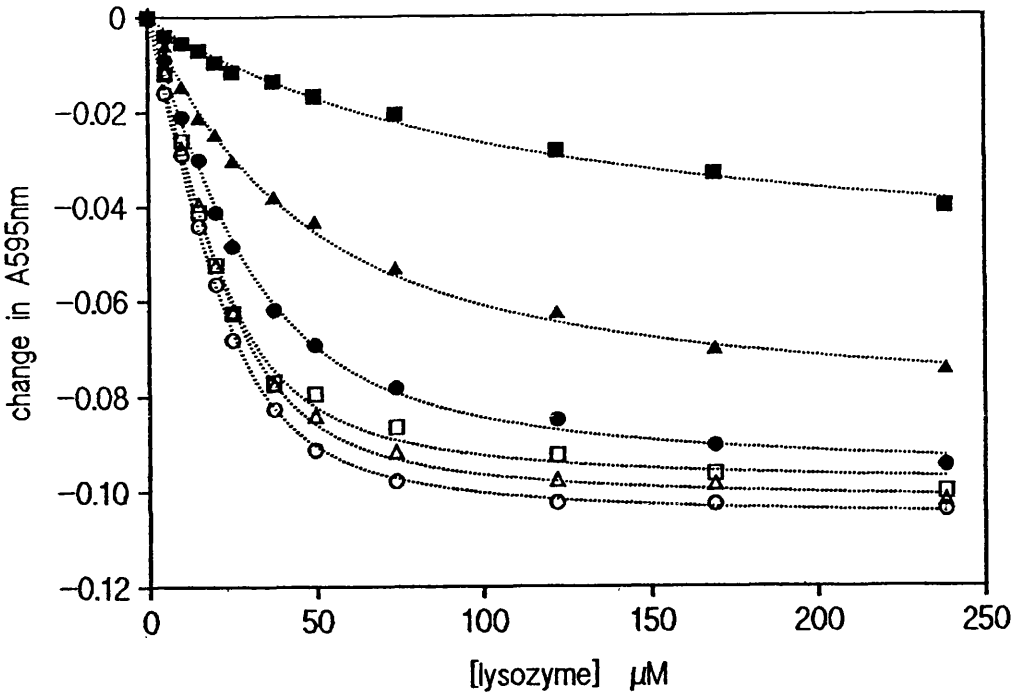

Figure 8.26a

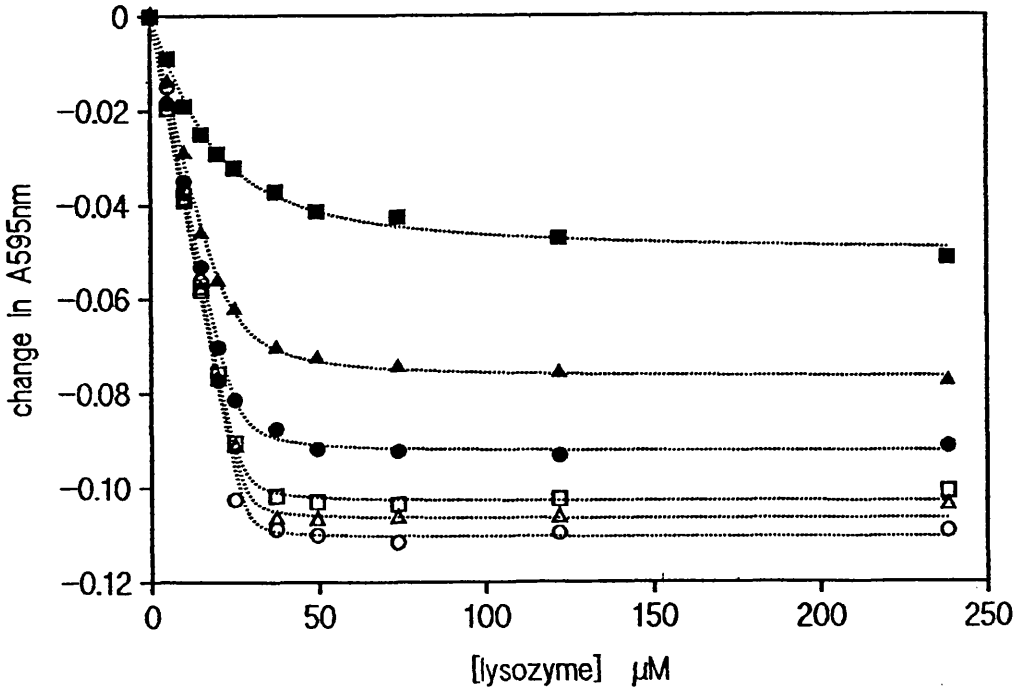

Figure 8.26b

The effect of tris buffer concentration on change in absorbance at 595nm against lysozyme concentration for titration of a) 73μM 20D3 and b) 70μM 20D10. The tris HCl pH8.0 concentrations were: 0.3M (■), 0.1M (▲), 0.03M (●), 0.01M (□), 0.003M (△), 0.0003M (○). The broken lines are curve fits using equation 8.7.

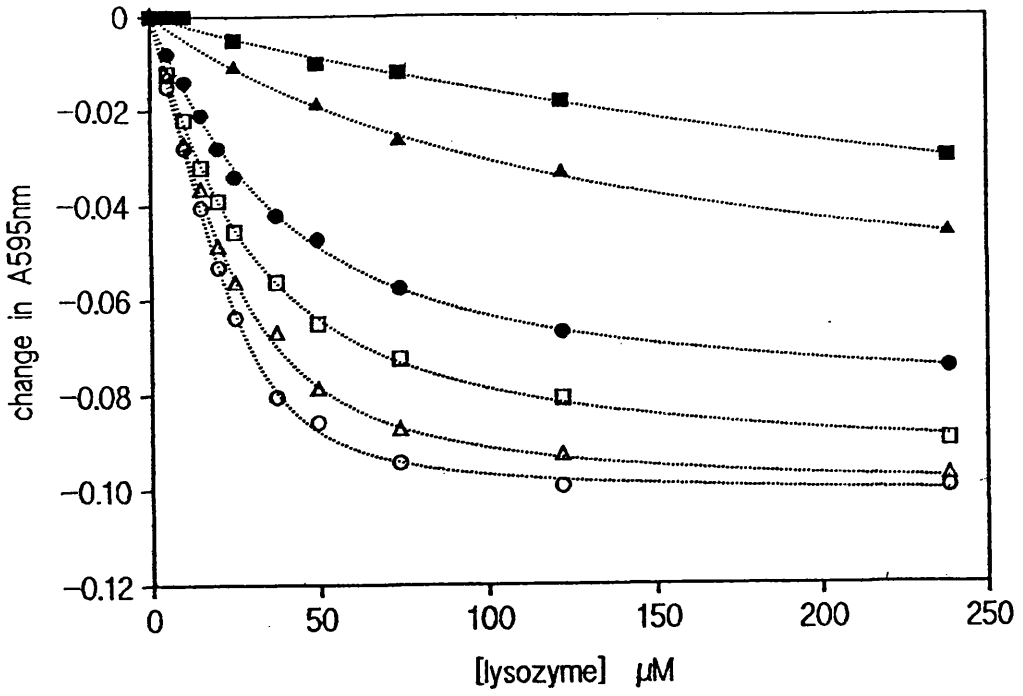

Figure 8.27a

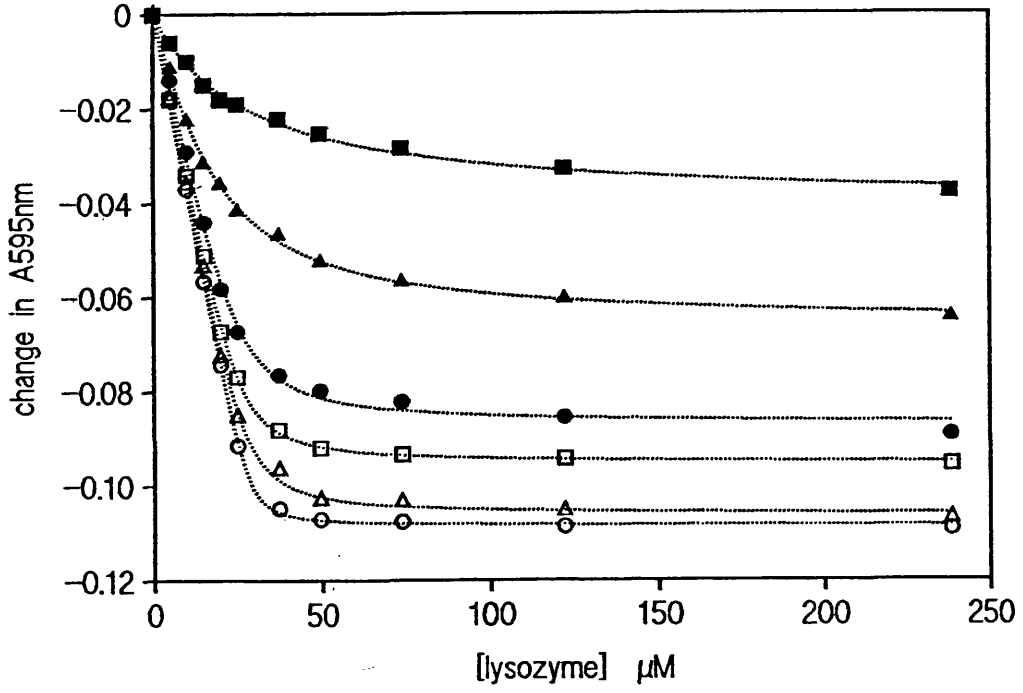

Figure 8.27b

The effect of phosphate buffer concentration on change in absorbance at 595nm against lysozyme concentration for titration of a) 73μM 20D3 and b) 70μM 20D10. The concentrations of sodium phosphate pH8.0 were: 0.3M(■), 0.1M(▲), 0.03M(●), 0.01M(□), 0.003M(△), 0.0003M(○). The broken lines are curve fits to equation 8.7.

buffer type and concentration	20D3		20D10	
	K_d	Dye bound	K_d	Dye bound
	μM	%	μM	%
tris HCl 0.3M	89.9	21.1	10.53	17.9
" 0.1M	27.5	32.7	1.44	32.3
" 0.03M	9.26	41.5	0.44	35.5
" 0.01M	4.43	37.2	0.22	37.5
" 0.003M	3.95	40.7	0.15	39.0
" 0.0003M	2.88	40.5	0.12	39.4
10mM tris HCl			0.20	35.9
" +10mM NaCl			0.40	35.1
" +50mM NaCl			1.21	33.5
" +100mM NaCl			1.90	31.0
phosphate 0.3M	362	30.1	21.40	15.0
" 0.1M	114	27.2	8.28	24.9
" 0.03M	25.5	30.9	1.91	36.2
" 0.01M	19.6	36.3	1.02	36.5
" 0.003M	8.9	35.2	0.92	38.6
" 0.0003M	3.8	41.6	0.27	40.3

Table 8c.

Summary of K_d values and percentage of dye participating in binding at saturation for titration of conjugates 20D3 and 20D10 in various buffers at different concentrations.

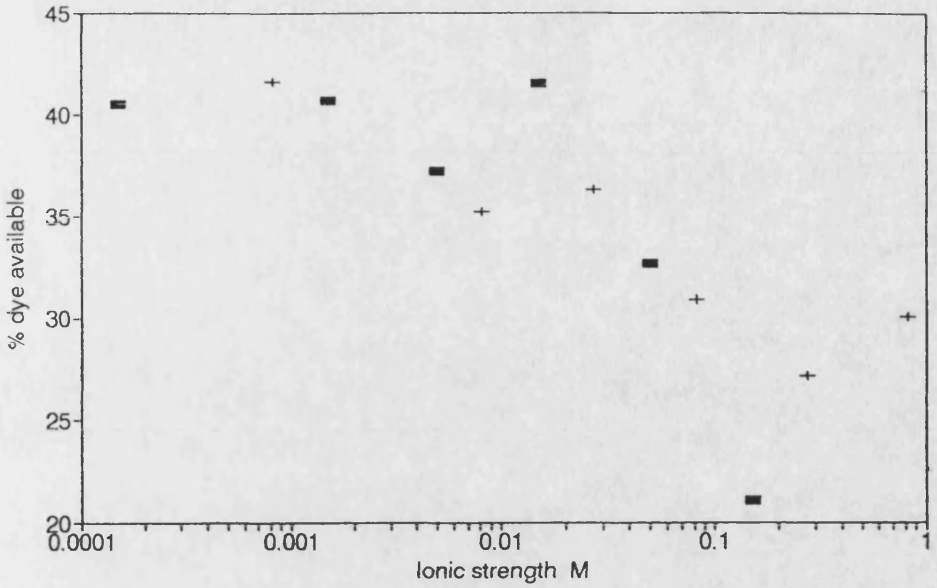

Figure 8.28a

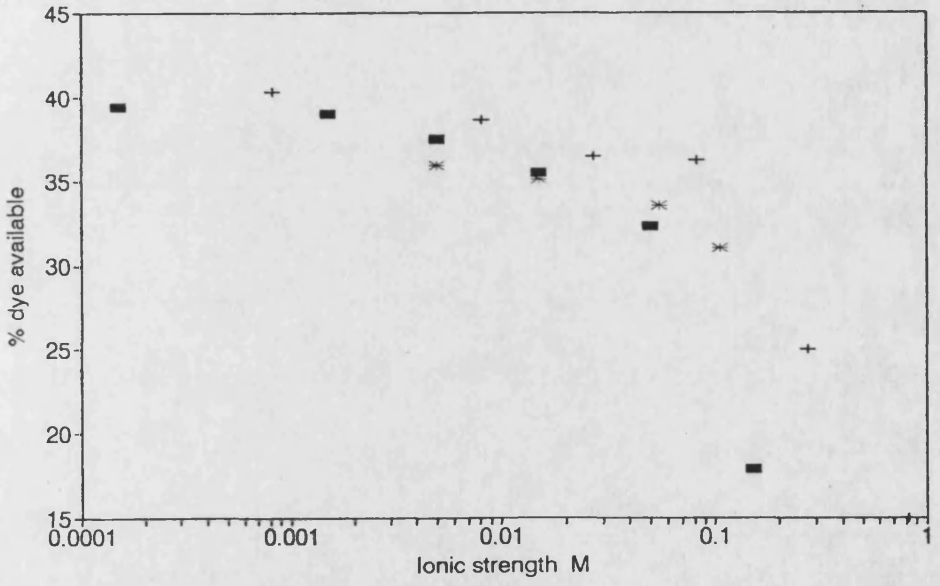

Figure 8.28b

Graphs of % dye available against ionic strength for a) conjugate 20D3 and b) conjugate 20D10. The buffers used were tris HCl (■), tris HCl + NaCl (★) and phosphate (+).

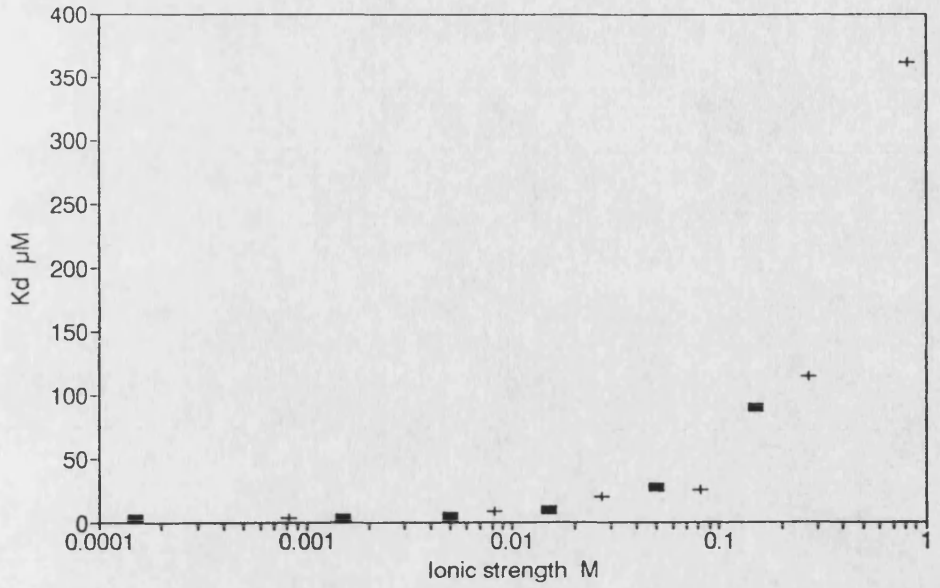

Figure 8.29a

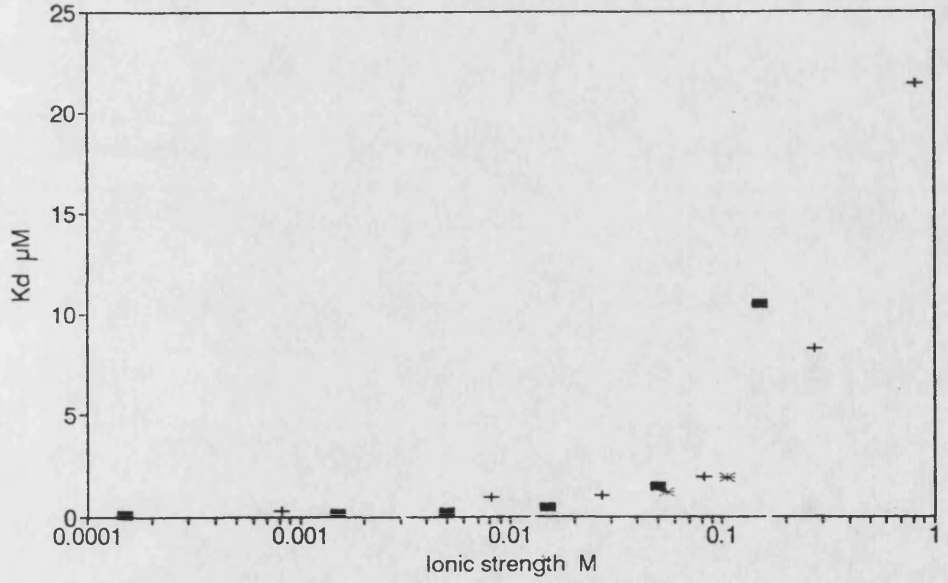

Figure 8.29b

Graphs of K_d against ionic strength for a) conjugate 20D3 and b) conjugate 20D10. The buffers used were tris HCl (■), tris HCl + NaCl (★) and phosphate (+).

8.4 The Effect of Salts and Organic Solvents on the Spectrum of Dye-Dextran Conjugates

Difference spectra for conjugate 5D10 in the presence of different concentrations of NaCl and dioxan are presented in figure 8.31. The spectra in the presence of NaCl have a double minimum at 600nm and 640nm. The spectra in the presence of dioxan are almost mirror images of those in the presence of NaCl, having a peak at 640nm and a shoulder at 600nm.

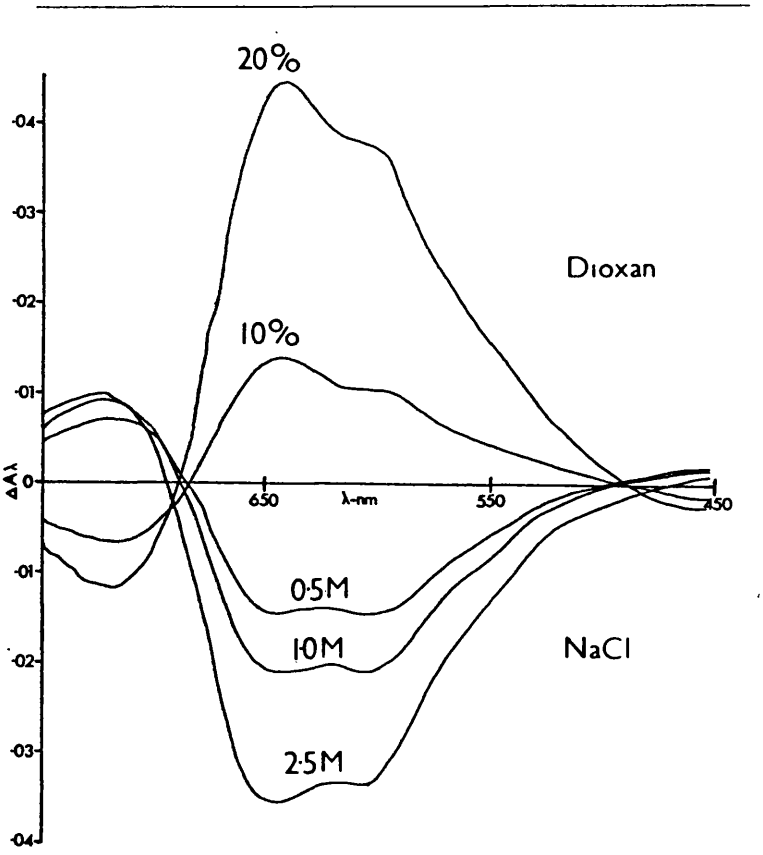

Figure 8.30

Difference spectra for conjugate 5D10 in the presence of different concentrations of NaCl and Dioxan. The reference cuvette contained 50μM 5D10 (with respect to dye) in 10mM trisHCl pH8.0. The experimental cuvettes contained 50μM 5D10 in 10mM trisHCl pH8.0 with the following additions: 0.5M NaCl; 1M NaCl; 2.5M NaCl 10% (v/v) dioxan; 20% (v/v) dioxan

8.5 The Kinetics of Protein Binding to Dye-Dextran Conjugates

Kinetic studies were conducted with both free dye and dye-dextran conjugate 5D5. The experimental conditions were similar to those used for equilibrium studies. The reaction time course was followed for a period of two seconds with data sampling at 4 x 10-3 s intervals to give a total of 500 points for each run. The results obtained are shown in figures 8.32 and 8.33. Each data set represents the average of two duplicate experiments.

The formulation of an integrated rate equation which describes D_b as a function of time can be substituted into equation 8.4 to give an expression which describes the progress curve.

$$\frac{dD_b}{dt} = k_1(D_a - D_b)(L_t - D_b) - k_2 D_b \qquad (8.9)$$

where k_1 is the "on" constant and k_2 is the "off" constant.

This equation can be integrated to give an algebraic expression relating D_b to time:

$$D_b = \frac{(bb - sx)(bb + sx) - (bb + sx)(bb - sx)\, e^{t.sx}}{2k_1(\, e^{t.sx}(bb - sx) - (bb + sx))}$$

$$\text{where} \quad bb = -k_1(K_d + D_a + L_t) \qquad (8.10)$$

$$sx = \sqrt{(bb^2 - 4.K_1.(K_d + D_a + L_t))}$$

$$t = time$$

This expression can be substituted into equation 8.4 to give the final equation which relates change in absorbance at 595nm to time. The data shown in figure 8.32 a and b was fitted using this equation and the lines of best fit are shown on the graphs.

The systematic deviation between predicted and experimental results shows that the simple rate model is unable to describe the data, which appear to indicate a combination of rapid initial reaction with a subsequently slower approach to

equilibrium. A possible explanation of this inadequacy is that the experimental data represents the sum of two coupled processes. It is well known that planar dye molecules undergo a 'stacking' interaction in aqueous solution (Federici *et al.* 1985; Stellwagen and Liu 1987), and it has been shown that the kinetics of dye/dye interactions can influence the apparent kinetics of the interaction of dye and macromolecule (Aubard *et al.* 1989). Hence in the system studied here, the rapid initial phase of the interaction could represent interaction of macromolecule with unstacked dye, while the subsequent reaction would be limited by the rate of 'destacking' of the interacting dye molecules. In a simplified form this could be described mathematically by a slight modification to equation 8.9 and the introduction of a second differential equation to describe the stacking interaction.

$$\frac{dD_b}{dt} = k_1(D_a - D_b - 2D_s)(L_t - D_b) - k_2D_b \qquad (8.11)$$

$$\frac{dD_s}{dt} = k_3(D_a - D_b - 2D_s)^2 - k_4D_s \qquad (8.12)$$

where k_3 is the formation constant for stacking, k_4 the breakdown constant for stacking and D_s the concentration of stacked dye (stacking assumed to be a dimerisation)

Non linear least squares estimates of these parameters were obtained by using a fourth order Runge-Kutta routine to solve equations 8.11 and 8.12 numerically over the reaction time course. The constant interval between recorded data points facilitated the comparison of computed with experimental data. The improved fit between model predictions and experimental data are shown in figure 8.33 a and b, with the parameter estimates obtained from both approaches summarised in table 8e.

		free dye		conjugate 5D5	
constant	units	simple	stacked	simple	stacked
D_a	M	2.65×10^{-6}	2.9×10^{-6}	3.49×10^{-6}	4.87×10^{-6}
k_1	$lmol^{-1}s^{-1}$	1.47×10^{4}	1.89×10^{4}	6.7×10^{3}	1.37×10^{4}
K_d	M	1.72×10^{-6}	4.7×10^{-5}	1.35×10^{-7}	4.19×10^{-5}
k_3	$lmol^{-1}s^{-1}$	-	1.3×10^{5}	-	4.58×10^{4}
k_4	s^{-1}	-	3.57	-	0.58

Table 8e

Comparison of the parameter estimates calculated from simple and stacked dye models fitted to kinetic data obtained for free dye and conjugate 5D5.

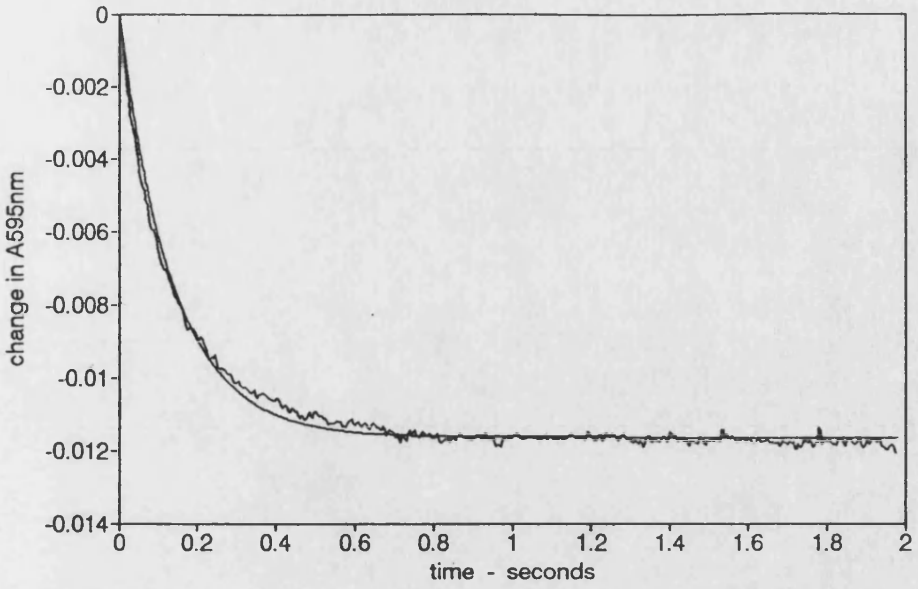

Figure 8.31a

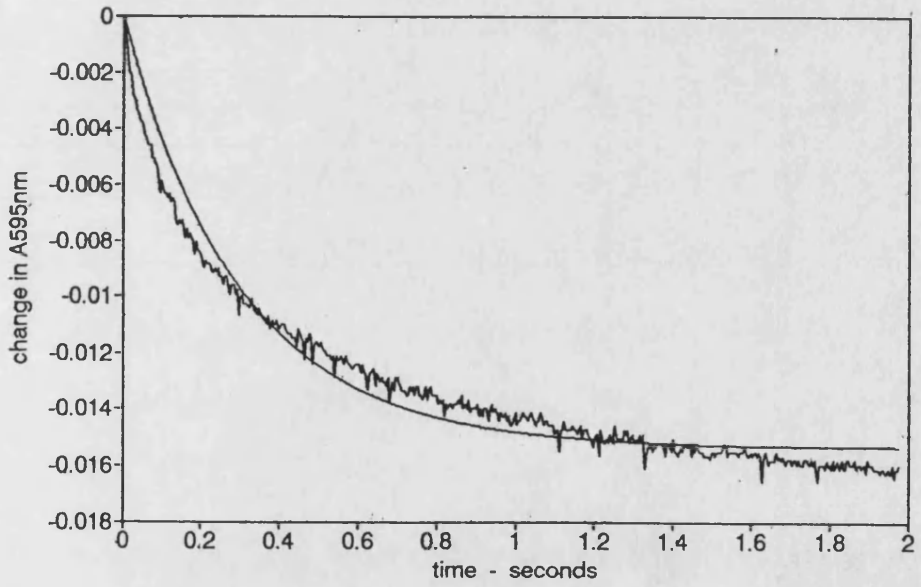

figure 8.31b

Graphs of change in absorbance at 595nm against time for a) 35μM free dye and b) 54μM 5D5 mixed with 500μM lysozyme (final concentrations) using a stop flow apparatus. The curves were generated by non-linear least squares curve fits of the data to equation 8.4 using equation 8.10 to determine D_b for each value of t.

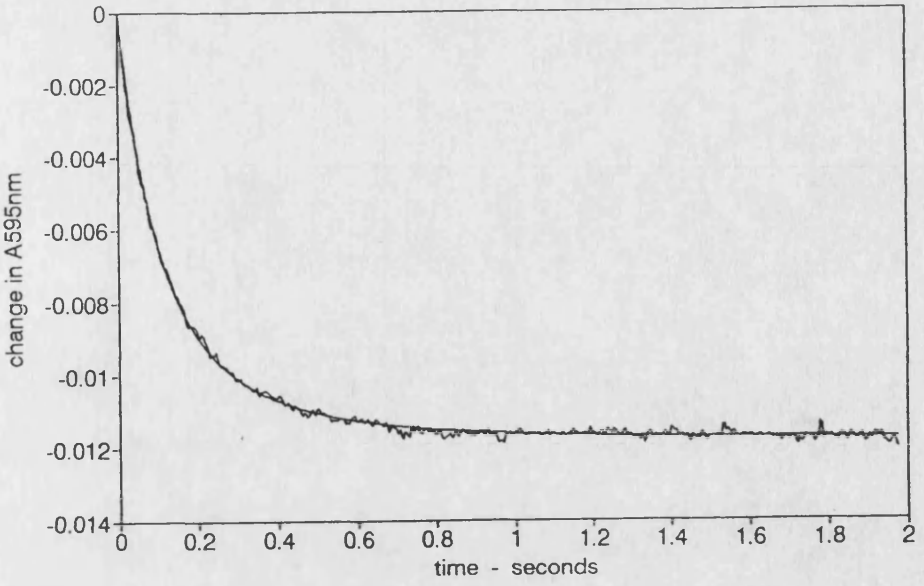

Figure 8.32a

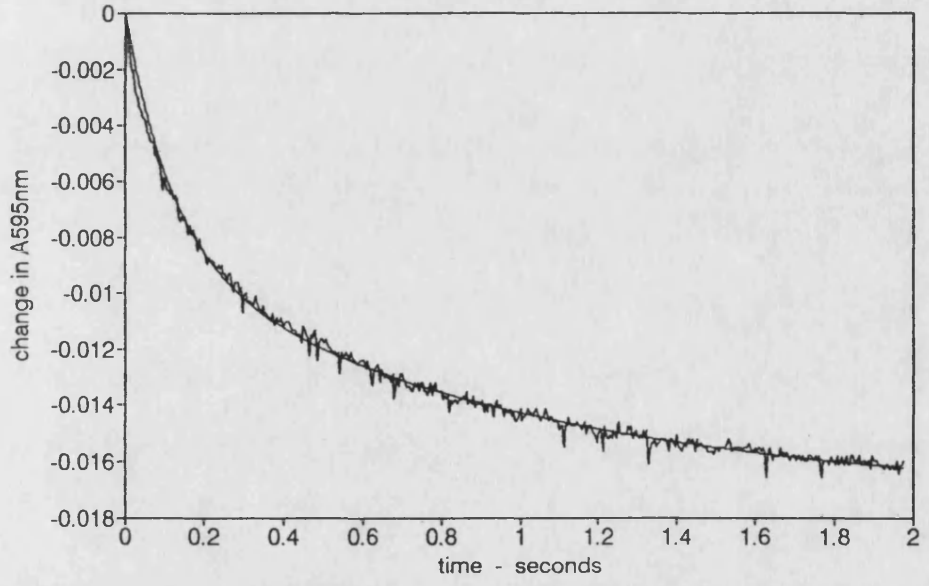

Figure 8.32b

The effect of fitting the data shown in figure 8.31 using the modified model (equations 8.11 and 8.12) taking account of dye stacking rather than the simple integrated rate equation. a) 35μM free dye; b) 54μM 5D5.

To investigate the dye precipitation phenomena which prevented the completion of equilibrium binding studies with free dye the stopped flow apparatus was used to follow the interaction over a 10 second time course. The result, shown in figure 8.33, clearly indicate the onset of precipitation after about 3 seconds.

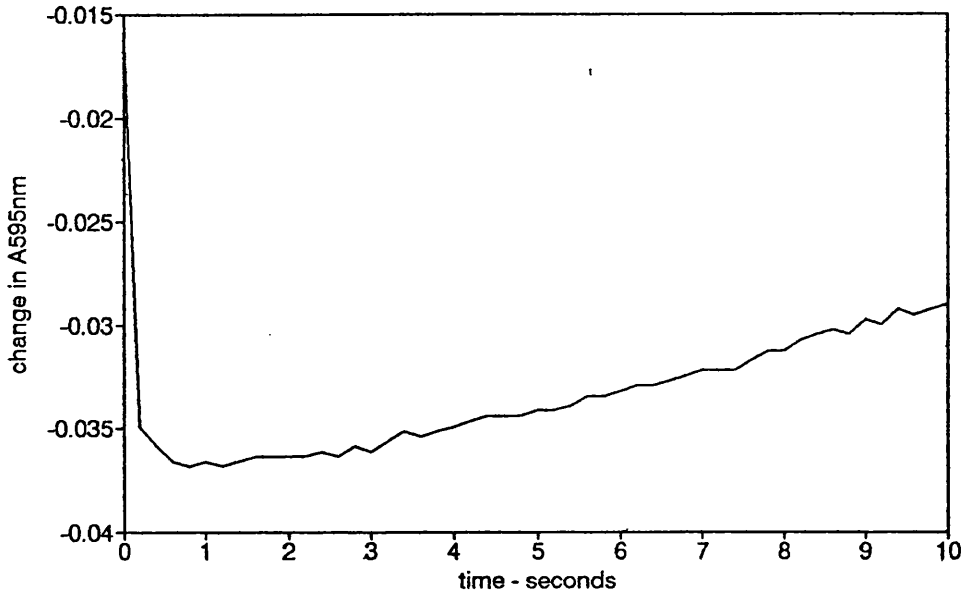

Figure 8.33

Graph of change in absorbance at 595nm against time for 35μM free dye mixed with 500μM lysozyme (final concentrations) showing the slow increase in absorbance due to aggregation which becomes evident about 3 seconds after mixing.

CHAPTER 9

PROTEIN BINDING TO DYE-DEXTRAN CONJUGATES

DISCUSSION

9.1 Characterisation of Dye-Dextran Conjugates

Due to the ambiguity present in much of the literature concerning binding of 'Reactive Blue 2' to proteins, the exact isomeric structure of the dye sample used in a particular set of experiments should be explicitly stated. For all the work presented in this thesis the same batch of Cibacron Blue 3G was used. The results presented in section 8.1.1 indicated that the dye contained only the ortho isomer of the sulphoanilino ring, together with a considerable amount of hydrolysed dye in which the reactive chlorine on the triazine ring had been replaced by a hydroxyl group. The sample also contained small amounts of several other components, both more and less hydrophobic than the intact dye. These were not identified so it is not known whether or not they contained active chlorotriazine rings. If they did they would couple to dextran, yielding a heterogeneous product but any such impurities would only make a small contribution to the total immobilised dye and would thus have little effect on the binding characteristics of the dye-dextran conjugates as a whole. Impurities not containing active chlorotriazine rings will not bind to dextran under the conditions of coupling used and will therefore be removed during washing of the dye-dextran conjugates.

Estimates of the dye:dextran ratios of the conjugates clearly indicate that intramolecular dye stacking occurs. In the solution conformations taken up by these conjugates there is obviously a considerable amount of interaction between bound dye molecules due to their proximity in the dextran microenvironment.

The insets to figures 8.6 and 8.7 indicate that, once a certain dye loading is reached, the ratio of the estimates at 257nm in water (affected by dye stacking) and 541nm in 6M HCl (independent of dye stackng) reaches a constant value, and is not affected by further increases in dye loading. This is surprising since stacking interactions would be expected to be favoured more at high loadings where the concentration of bound dye in the microenvironment of the dextran will be very high. That this is not so may be an indication that the distribution of bound dye on the dextran is not random. Since high concentrations of dye are used for the synthesis of the conjugates, a considerable amount of stacking of the free dye in solution would be expected. This could lead to clusters of dye molecules coupling to the dextran at closely grouped sites. Alternatively, the first few dye molecules bound could act as 'nucleation sites', interacting with free dye and inducing it to bind at sites in close proximity to the dye already bound. Since at the lowest loadings there is little apparent intramolecular dye stacking, the latter may be a more appropriate mechanism.

Another possible explaination is that the loading where the A257nm/A541nm ratio reaches a constant value represents the point where all (or the maximum possible) bound dye is in the stacked form. At this point Beers law would again be obeyed but with a new extinction coefficient representing stacked dye which is different to that for the free dye. Thus the ratio of the two measurements would become constant with the ratio representing the ratio of the two extinction coefficients.

The laser light scattering measurements indicate that as the dye-dextran ratios of the conjugates increase, the dye stacking interactions alter the solution conformation of the dextran, forming it into progressively more compact structures with lower hydrodynamic radii. This suggests that dye stacking interactions may occur between dye molecules immobilised some distance apart on the dextran chain, and not just

between near-neighbours. Formation of a more compact structure might also be expected to reduce the ease of access of proteins to immobilised dye. This will be discussed later with reference to the results of the kinetic experiments.

9.2 Quantitation of Protein Binding by Gel-Permeation Chromatography

Since the introduction of the gel-permeation method for measuring the binding of ligands to proteins by Hummel and Dreyer (1962), the method has been used extensively. Its major advantage is that it directly measures the ligand bound rather than relying on an indirect signal such as the change in conformation or environment of a 'reporter' chromophore. The disadvantages of the method include its relative slowness and the large amounts of protein that are required.

There are few reports in the literature for the use of this method with two interacting macromolecules although it was used by Waterson *et al.* (1973) to measure binding of tRNA to tRNA synthetase. It was thus of interest to demonstrate the feasibility of the technique in such circumstances. For this reason a small protein, lysozyme, and dye-dextran conjugates based on a dextran of high molecular weight (2×10^6 or 5×10^5) were chosen in order to minimise the problem of adequately separating the two species by gel-permeation chromatography. Figure 8.8 indicates that this could be adequately achieved by using a 50cm column of Sephadex G75. Binding isotherms were measured for a range of dye-dextran conjugates (figures 8.10 and 8.14) over the operationally achievable lysozyme concentration range. This range was limited by high absorbance and aggregation (see later discussion) at high concentrations, and by the stability and sensitivity of the U.V. detector at low concentrations, although this could have been extended by use of a more sensitive instrument.

The results obtained from the graphical analysis of data for the DCB20 series of conjugates (figure 8.10) clearly show that at least two types of interaction are

occurring. Although little can be said concerning the 'non-specific' interaction, the trends of the variation of the 'specific' binding parameters, $K_{0.5}$ and n, with ligand loading are clearly established. For high affinity binding $K_{0.5}$, values decrease with increasing dye loading, showing that increasing dye loading causes an increase in affinity. A similar effect was reported by Johansson and Joelsson (1987a) for the binding of phosphoglycerate kinase to a dye-dextran conjugate in an aqueous two-phase system. This increase in the strength of binding with increasing dye density could be explained by two mechanisms either or both of which may be occurring in this system. Once a lysozyme molecule has desorbed from a dye moiety, there is a higher probability of immediate interaction with another dye moiety in preparations with high dye:dextran ratios. This is due to the high local concentration of dye (relative to the bulk average) altering the equilibrium position within the microenvironment of the dextran molecule in favour of binding. The lysozyme molecule is 'trapped' by a number of neighbouring dextran-bound dye molecules between which it tends to be exchanged rather than diffusing back into the bulk solution. Alternatively, the initial 'specific' high affinity interaction may be reinforced by one or more additional interactions eg. ion pairs between dye sulphonate groups and surface lysine residues on lysozyme. The higher the dye concentration the greater the probability that dye molecules will be in the right orientation to achieve these secondary interactions. The flexibility of the soluble dextran will also aid this mechanism.

The finding that n is proportional to dye loading for loadings up to 101 moles dye per mole dextran indicates that the capacity of the high affinity saturable part of the system depends only on the total amount of dye present and is not affected by the physical proximity of the dye groups on the dextran molecules. At the highest loading used the region of proportionality appears to be exceeded and the fraction of dye molecules participating in binding drops from 30% to 24%. This was originally postulated (Mayes *et al.* 1990) to be due either to the onset of a degree of steric crowding limiting dye-lysozyme interactions, or to a reduction in the number of available dye molecules resulting from intranolecular dye stacking which was shown,

from the ligand loading estimations, to occur more at this dye density. A similar loss of proportionality was not observed when binding was measured by spectral titration, however, so it now seems more likely that the reduction in binding was due to some as yet unidentified artefact of the gel-permeation system.

The results of gel-permeation binding measurements on the DCB5 series of conjugates gave broadly similar results to those discussed above for the DCB20 series. The estimated value of $K_{0.5}$ decreased with increasing dye loading and n was again found to be proportional to loading with 31% of the immobilised dye available for the 'high-affinity' interaction. This is very similar to the fraction available on the dextran of M.W. 2×10^6 (30%). Hence the molecular weight of the dextran appears to have no influence on the fractional availability of covalently bound dye, at least in this four fold range. It would be interesting to see whether or not this is true over a much larger range of dextran molecular weights. The limitations of the gel permeation method prevent the use of smaller dextrans but the effect could easily be studied using the spectral titration method (see section 9.3.2).

The non-specific binding of lysozyme to dye appears to be a function of dye loading and may be due to a simple ionic interaction since the dye carries negative charges on its sulphonate groups and so will act as an ion exchanger at this pH. The magnitude of the total lysozyme binding to each conjugate reached about 50% of its theoretical maximum (assuming a monovalent interaction between dye and protein) at the highest lysozyme concentration used but showed no approach to saturation at this point. Fitting of a Langmuir isotherm over the complete range of lysozyme binding data for the FPLC experiments with the 5D series of conjugates gave an approximate estimate of 70% of the total dye available for some type of interaction with lysozyme at saturation. The high affinity 'specific' interaction accounts for about 30%, the other 40% being attributable to low affinity interactions.

A more detailed study of the binding of lysozyme to dye-dextran conjugates based on dextran of M.W. 5×10^5 was attempted using an FPLC system and a Superose 12HR column in the hope of obtaining clearer and more accurate data to demonstrate the

postulated biphasic binding behaviour. The results of this study were, however, disappointing. The main problem was caused by aggregate formation which resulted in increased back pressure and column blockage. This problem was not encountered with the conventional soft-gel system, probably due to the much larger interstitial spaces between the gel beads which allowed the aggregates to permeate through the column. In FPLC runs using high lysozyme concentrations, aggregation probably lead to a considerable loss of conjugate at the top of the column which could not then equilibrate with lysozyme. This would lead in turn to underestimates of lysozyme binding at high lysozyme concentrations which would tend to mask the biphasic binding behaviour. It is interesting to note that biphasic behaviour occurred most noticeably with conjugates having low dye:dextran ratios and was hardly apparent at all for the conjugates with very high dye:dextran ratios. This is consistent with the above explanation and also with observations concerning aggregation made during the spectral titration work.

The high-resolution of the FPLC system proved to be of little value for the model system used here due to the problems discussed above. However, in order to demonstrate the utility of the gel-permeation method in a more general case it was shown that the system was capable of resolving dextran conjugates based on dextran of molecular weight 2×10^6 and proteins with molecular weights up to at least 140000. This includes the majority of dehydrogenases and kinases, and thus allows the possibility of studying binding of such enzymes to nucleotide-polymer conjugates. Using such a system would make it possible to study the effects of ligand density on multiple interactions with oligomeric proteins since dehydrogenases are available ranging from monomers to hexamers. Data from kinetic studies has shown that LDH is inhibited by soluble polymers containing high NAD^+ loadings (Furukawa *et al.*, 1981) and it seems likely that this may be due to multiple binding of LDH to several sites simultaneously, effectively immobilising the enzyme and preventing access to further immobilised nucleotide. Since NADH binds more tightly than NAD^+ it may be that a few initial turnover steps of the enzyme generate sufficient NADH to effectively immobilise the enzyme. Such possibilities could be studied using a combination of binding studies with NAD^+ and NADH dextran conjugates and rapid

kinetic measurements to check for the initial burst of activity which would be predicted by the latter mechanism.

9.3 Protein Binding Measured by Spectral Titration

9.3.1 Spectra

The difference spectra between dye dextran-conjugates in the presence and absence of lysozyme showed some of the characteristics of both an 'ionic' effect and a hydrophobic effect i.e. the observed difference spectra had both positive and negative components. The shape of the spectrum in the presence of lysozyme, however, cannot be directly explained by an addition of the 'hydrophobic' and 'ionic' spectra shown in figure 8.30 since these are almost mirror images and would thus simply tend to cancel out. If the 'hydrophobic spectrum was shifted towards higher wavelength, however, a combined spectrum similar to that observed for lysozyme would be obtained. Such a spectral shift due to specific and intimate interactions between dye and protein seems quite possible. Subramanian (1989) published a difference spectrum for Cibacron Blue in the presence of low concentrations (μM) of spermine (a hydrophobic chain with amino and imino groups) which was very similar to that observed with lysozyme. Space filling models showed that the amino groups were well spaced to neutralise the dye sulphonate groups with the hydrophobic chain segments contacting the more hydrophobic regions of the dye. Hence it is tentatively proposed that the specific binding site for the dye on lysozyme is a region containing both positively charged groups interacting with dye sulphonate groups and hydrophobic groups interacting with one or more of the dye aromatic rings.

This interpretation of the interactions by which lysozyme and Cibacron Blue interact is consistent with conclusions drawn by Boyer and Hsu (1990) from studies of adsorption of lysozyme to Blue-Sepharose CL6B at different pH and ionic strength values.

9.3.2 Binding

The results from the gel-permeation experiments, which indicated that not all the immobilised dye was available to bind protein, necessitated the derivation of a model to describe the binding of protein in which D_t, the total immobilised dye concentration, did not appear. The resulting equation described the experimental data well, allowing K_d and D_a (and hence n) to be determined as a function of dye loading on the conjugate.

The advantage of the titration method over the gel-permeation method lies in its far greater speed and simplicity and the fact that no separation of bound and free protein is necessary. The bound protein can be independently measured due to the spectral signal which is generated when protein and ligand interact. This allows the possibility of using any dye-polymer conjugate of any desired molecular weight for binding studies, although in this work the same conjugates as for the gel-permeation experiments were used in order to allow direct comparison of the results. This potential was explored to some extent in the recent work of Johansson and Joelsson (1991), who characterised binding of protein to various dye polymer conjugates with the aim of predicting their performance in aqueous two-phase systems.

From the spectral titration data, n was found to be proportional to loading over the entire range of loadings used. This confirmed the findings from the gel permeation experiments that the maximum capacity depends only on the total amount of dye present and is not affected by the mutual proximity of the dye molecules on the dextran backbone i.e. there is no evidence of steric hindrance of binding. Results from the two methods show excellent agreement: Gel permeation gave values of 31% and 30% of total dye available for conjugates based on dextran of molecular weight 5×10^5 and 2×10^6 respectively, compared with 27% and 28% for spectral titration. With the gel permeation method I noted an apparent decrease in the proportion of dye available at a high loading of 208 moles dye per mole dextran and this lead to speculation that this might represent a degree of steric hindrance to binding. The titration results extend the range of dye:dextran ratios studied to higher values and

using this method no reduction in availability is observed right up to the point where the system reaches its practical limit due to aggregation. It therefore seems likely that the earlier result is an as yet unexplained artefact of the experimental system used.

Since steric hindrance of lysozyme binding by nearby bound lysozyme molecules has been discounted in this system, the observation that only about 30% of the dye was available for the high affinity interaction is presumably a reflection of dye orientation and positioning on the dextran backbone and possibly also the solution conformation of the dextran molecule itself. Liu and Stellwagen (1987) have reported an effect, sensitive to ionic strength, interpreted as alignment of conjugated dye molecules with the carbohydrate surface of Sepharose, placing them in an orientation unsuitable for specific interaction with protein. This may also be occurring with the dextran which has a similar chemical structure. Dye molecules coupled to the dextran near to branch points in the chain may be severely sterically crowded and inaccessible to protein molecules. The size of the ligand relative to glucose rings, and the low frequency of branch points in the structure, however, suggest that this would only make a small contribution to ligand inaccessibility.

Comparison of values for the fraction of total dye available for lysozyme binding to various blue dye matrices is complicated by the different conditions of buffer and ionic strength used which has a considerable effect on binding . Also, lysozyme binding to solid supports is much better described by a Freundlich isotherm rather than a Langmuir isotherm (Horstmann *et al.*, 1988; Livingstone and Chase, 1989; Boyer and Hsu,1990). This suggests that more than one binding mechanism is operating (a possibility discussed by Livingstone and Chase, 1989), with the Freundlich equation providing a reasonable empirical description of the binding as a whole. This would be consistent with the biphasic semi-log plots observed for binding of lysozyme to the dye-dextran conjugates. Fractional utilisation of ligand on solid supports would be more accurately compared with that of dye-dextran conjugates by comparing the fractional availability estimated for the whole binding curve rather than

just the high affinity part. Estimates for this from the FPLC gel-permeation experiments gave values of about 70% assuming a 1:1 interaction with lysozyme. This compares with values of about 40% for Procion Blue MX-R silica (Livingstone and Chase, 1989) and 50% for Cibacron Blue Sepharose CL6B (Boyer and Hsu, 1990). Such a reduction for Sepharose relative to the amount available on a soluble dextran conjugate is in line with expectation since the fractional accessibility of Sepharose CL6B for lysozyme is 0.75 (Pharmacia product information) i.e. about a quarter of the immobilised ligand might be unavailable due to physical inaccessibility assuming a uniform distribution. In order to confirm this, however, the measurements for the different systems would have to be repeated under identical operating conditions.

For porous matrices the value of 40-50% of dye participating in binding at saturation (assuming a monovalent interaction) compares with a value of only about 5% to 25% (depending on buffer conditions) for a different but similar sized protein, adenylate kinase, binding to Cibacron blue-F3GA Sepharose CL6B at a ligand density of 120μM (Liu and Stellwagen 1987). This represents a similar bulk average concentration to that at which the dye-dextran experiments were carried out. Such a result suggests that the nature of the protein and the mechanism of binding might also have a very profound effect on capacity independent of any physical limitations due to matrix structure.

The effect of ionic strength and the nature of the buffer were investigated for dye-dextran conjugates with high and low loadings. Changing the ionic strength over three orders of magnitude caused a three fold change in the percentage of dye available, compared with a ten fold change observed with Sepharose by Liu and Stellwagen (1987). The reduction in availability with increasing ionic strength is probably due to increasing ion pair formation between dye sulphonate groups and counter ions from solution. This will shield the charges and reduce the tendency for the sulphonate groups of adjacent dye molecules to repel and hence promote the dye stacking effect. Tris buffer was more effective in reducing dye availability than sodium phosphate. Maybe the sterically crowded cationic centre of tris provides more

effective charge shielding than the Na^+ cation, once an ion pair is formed.

Increasing ionic strength also had a considerable effect on the dissociation constant for the dye/lysozyme interaction. Increasing the ionic strength over four orders of magnitude caused a 100 fold increase in K_d. This indicates that ionic interactions make a considerable contribution to the stabilisation of the dye lysozyme complex. Ionic interactions are generally weakened by increases in ionic strength whereas hydrophobic interactions tend to be reinforced. Since the K_d increased this suggests that the ionic interactions predominate at this binding site.

Aggregates, which formed when the most highly loaded dye-dextran conjugates were titrated with lysozyme, could be readily dissolved by the addition of sodium hydroxide to a concentration of 10mM. This suggests that the interactions are ionic in nature and involve protonated basic groups which dissociate at high pH, presumably the lysine and arginine residues on the surface of the basic lysozyme, interacting with the dye sulphonate groups. Since both the molecules are polyvalent the potential for aggregate formation is considerable, and is rapid when free dye and lysozyme are mixed. That aggregate formation is very much slower with dye-dextran conjugates suggests that loss of rotational and translational freedom upon immobilisation of the dye may be highly significant to the kinetics of interaction. This has also been observed in the impaired kinetics of soluble immobilised coenzymes as enzyme substrates (Lee, 1978).

In a recent report by Birkenmeier and Kopperschlager (1991) triazine dyes were used to selectively precipitate a number of different proteins. Precipitation was found to vary depending on dye structure and pH, and by optimising conditions useful separations could be achieved. Most precipitations were achieved at acid pH values around 4. The precipitation of lysozyme observed here at alkaline pH is presumably a reflection of the unusually high isoelectric point of lysozyme. Thus, although dye-mediated protein aggregation proved to be highly inconvenient in this study it may prove to be quite a useful phenomenon, providing a cheap and rapid technique for downstream processing.

Morris and Fisher (1990) attempted to use Cibacron Blue linked to various polymers for the affinity precipitation of lactate dehydrogenase but failed to achieve any significant aggregation. This they attributed to a 'wrapping' effect i.e. multiple ligands on the same polymer chain occupying all the available sites on a protein surface, or at least making approach of another polymer chain sterically unlikely, such that inter-polymer cross bridging is disfavoured. This effect may well explain the inhibition of aggregation observed in the titration results.

It might be expected that 'wrapping' would become greater at high dye to dextran ratios where the local dye concentration in the dextran microenvironment is very high, but this is probably outweighed by the concomitant increase in dye molecules protruding outwards from a randomly coiled dextran molecule in solution. These are in a favourable position for inter-polymer cross bridging, and would lead to the observed rapid aggregation at very high dye to dextran ratios.

The results for the effect of loading on K_d follow the same trend as those obtained for the gel permeation method. The absolute values, however, show a 4 to 10 fold lower affinity when measured by the titration method. This may result from the theoretical basis of the titration method. It seems that only a specific intimate interaction between dye and protein causes a spectral shift. Simple ionic interaction gives no signal until the point where aggregation begins although it presumably occurs at concentrations far below this. In the titration experiments total lysozyme concentration (L_t) is the parameter which is controlled and not free lysozyme concentration as in the gel-permeation method. This means that free lysozyme has to be calculated from the difference between total and bound concentrations. Since the bound concentration only reflects specifically bound protein, this will cause an overestimate of the free lysozyme concentration if non-specific binding is occurring. This could lead to considerable errors at low total lysozyme concentrations where very little of the added protein remains unbound, and hence cause K_d to be overestimated. For a more specific interaction showing little tendency for simple ionic binding, such errors would probably be minimal.

Since simple ion-pair interactions do not appear to produce a spectral signal, comparison of the binding curves from the gel-permeation and spectral titration methods does not yield any information about the mechanism for the increasing apparent affinity of binding with increasing dye density. By repeating the experiments in a buffer of high ionic strength, however, it might be possible to largely iliminate simple ionic interactions. Under these conditions a large ligand density effect on the value of K_d could be interpreted as favouring the 'rapid cycling' rather than the 'multiple binding' mechanism. Whether the same mechanism would operate at both high and low ionic strength is unclear, however, so the value of such data is debatable.

For a system in which only binding is being considered, the mechanism of increased affinity with increasing ligand density is of interest only insofar as it might indicate rational approaches to optimisation. In a situation where reaction with coenzymically active ligands in a regeneration system is being considered, however, the mechanism could be of considerable importance. The multiple binding mechanism could lead to reduced rates at high ligand densities, if the enzyme-ligand association constant is high, due to enzyme immobilisation at particular sites. The rapid cycling mechanism, in contrast, might be beneficial, providing the ligand is also accessible to the regenerating enzyme, since the microenvironmental coenzyme concentration is effectively increased which should lead to an enhancement in rate. A detailed study of NAD^+ density effects on the activity of dehydrogenases with NAD^+-dextrans would hopefully resolve this question.

9.4 Implications for Aqueous Two-Phase Partitioning

The use of dye ligands in affinity based aqueous two-phase systems has received considerable attention due to the large changes in partition coefficient which can be achieved. To date most studies have used PEG/Dextran systems incorporating dye-PEG, which extracts proteins into the PEG phase. This is desirable since bulk protein generally partitions into the dextran phase. Extraction into the PEG phase can,

however, also be achieved using alternative polymers as the dye carrier (Johansson and Joelsson 1987b). Johansson and Joelsson(1987a) have shown that partition of dye-dextran conjugates is highly salt dependent, and that they can be directed to either phase depending on conditions. Such behaviour becomes more pronounced as dye loading increases. My study of the binding behaviour of dye-dextran conjugates has highlighted a number of properties of dye-dextran conjugates which suggest that they might be highly efficient in affinity based extraction.

i) Increasing dye loading on the dextran up to quite high levels has no effect on the dye availability, so a small amount of highly substituted dextran will bind just as much protein as a larger amount of less substituted dextran. This is important from an economic viewpoint since dextran is a major cost in these systems. Highly loaded dextrans can easily be steered into the PEG phase, improving separations and making product recovery simple.

ii) The size of the dextran had little effect on its binding properties over the four fold range studied. Use of high molecular weight dextrans as extractants offers the possibility of product separation by ultrafiltration and dye-dextran recycling.

iii) The dye-dextran microenvironment offers the possibility of enhanced operational affinity due to the 'rapid cycling' and/or 'multiple binding' mechanisms. This could be especially useful in systems with low intrinsic affinity, greatly improving the partition coefficient compared with a PEG system.

iv) The 'wrapping' effect would tend to reduce aggregation and consequent loss of material at the phase interface.

These possible benefits suggest that a detailed comparison of the performance and economics of dye-PEG and dye-dextran systems would be timely. Such a study should address the effect of dextran molecular weight and dye loading on protein extraction for a range of different proteins.

9.5 The Kinetics of Protein Binding to Dye-Dextran Conjugates

The results obtained from the preliminary kinetic evaluation serve to demonstrate the feasibility of the stopped flow technique for dye binding studies with ligand-polymer conjugates. The results were not well described by a simple extension of the equilibrium binding theory, and it appears that there is a second kinetically significant step involved.

The use of a more complex model, formulated to include the effect of dye stacking, leads to an improvement in the fit between predicted and experimental data. However, the introduction of two additional parameters would be expected to lead to an improved fit even if the model assumptions were incorrect. At this stage it can only be suggested that the modelling approach is consistent with the data, and the degree of improvement obtained with the more sophisticated model is greater with the dextran conjugated dye than with the free dye. This would be consistent with the hypothesis of dye clustering during preparation of the dye:dextran complex.

The laser light scattering results indicated that the dye-dextran structures became more compact as dye loading increased. It might thus be expected that the kinetics of binding to a conjugate with a high dye loading might be slower than that for a conjugate with a low loading, due to the larger amount of dye destacking and dextran chain rearrangement that would be necessary in order to reach equilibrium. If this is so it should be observable as a systematic change in the model parameters as the dye loading of the conjugates increases. This prediction clearly needs to be verified experimentally but unfortunately this could not be done for this thesis due to a lack of access to the necessary equipment.

The slow binding rate constant suggests that dye destacking might be a rate limiting step in the binding of proteins when using chromatographic supports with no pore diffusional limitations. Comparing the results of this study with those of Mao *et al.* for lysozyme binding to non-porous Cibacron Blue silica microparticles indicates that the results are similar. Mao *et al.* obtained values of 3.8×10^{-7} M and 8.6×10^{3}

$lmol^{-1}s^{-1}$ for K_d and k_1 respectively for the dye-silica compared with $1.35 \times 10^{-7}M$ and $6.7 \times 10^{3}lmol^{-1}s^{-1}$ for the soluble dye-dextran (using the results obtained from the fitting to the simple model ignoring dye stacking). It is interesting to note that Mao *et al.* found that their experimental breakthrough curves deviated systematically from those predicted by their model. The model fitted the initial part of the breakthrough curve well but failed to predict the observed 'tailing' as equilibrium was approached. It was noted that this effect was greater when silica particles with high ligand densities were used. This was attributed to heterogeneity of ligand distribution and steric hindrance but, in the light of the results presented here, it is tempting to speculate that the effect might be a result of dye stacking between neighbouring immobilised dye molecules. If this occurs then the kinetics of destacking will affect the approach towards equilibrium and would cause the observed 'tailing' effect.

Given the significantly slower interaction rate obtained with the dextran bound dye compared with the free dye, it would appear that the kinetics of the interaction and the underlying constraints are worthy of further more detailed investigation. For currently available chromatographic supports the kinetics of reaction at the surface tend to be very rapid relative to pore and film diffusion rates, except in HPLC systems as discussed above. In the emerging new generation of supports based on membranes, sponges, and beads containing 'flow through' as well as diffusive pores, this may no longer be true, and surface interaction rates may make a significant contribution to the kinetics of the overall binding process. Thus the kinetics of the protein immobilised ligand interaction may play an increasingly important role in the overall binding process and this will need to be reflected in the models of such processes.

REFERENCES

Akanuma H., Kasuga A., Akanuma T. and Yamasaki M. (1971) The Effective Use of Affinity Chromatography for the Study of Complex Formation of Bovine Carboxypeptidase B with Basic and Aromatic Amino Acid Analogues. *Biochem. Biophys. Res. Com.*, **45**, 27 - 33.

Ambard L. (1921) Amylase:its Estimation and the Mechanism of its Action. *Bull. Soc. Chim. Biol.*, **3**, 51 - 65.

Andersson L., Jornvall H. and Mosbach K. (1975) Preparative Purification of Homogeneous Steroid Active Isomer of Horse Liver Alcohol Dehydrogenase by Affinity Chromatography on an Immobilised AMP Analogue. *Anal. Biochem.*, **69**, 401 - 409.

Andrews P., Kitchen B.J. and Winzor D.J. (1973) Use of Affinity Chromatography for the Quantitative Study of Acceptor-ligand Interactions: the Lactose Synthetase System. *Biochem. J.*, **135**, 897 - 900.

Arsenis C. and McCormick D.B. (1964) Purification of Liver Flavokinase by Column Chromatography on Flavin-Cellulose Compounds. *J. Biol. Chem.*, **239**, 3093 - 3097.

Arsenis C. and McCormick D.B. (1966) Purification of Flavin Mononucleotide Dependent Enzymes by Column Chromatography on Flavin Phosphate Cellulose Compounds. *J. Biol. Chem.*, **241**, 330 - 334.

Aubard J., Schwaller M.A., Adenier A. and Dodin G. (1989) Kinetics and Thermodynamics of the Interaction of Dyes with Biological Macromolecules: In "Protein Dye Interactions: Developments and Applications", ed. Vijayalakshmi M.A. and Bertrand O., Elsevier: New York.

Axen R., Porath J. and Ernback S. (1967) Chemical Coupling of Peptides and Proteins to Polysaccharides by Means of Cyanogen Halides. *Nature*, **214**, 1302 - 1304.

Barnes L.D., Kuehn G.D. and Atkinson D.E. (1971) Yeast Diphosphopyridine Nucleotide Specific Isocitrate Dehydrogenase. Purification and some Properties. *Biochem.*, **10**, 3939 - 3944.

Barry S. and O'Carra P. (1973) Affinity Chromatography of Nicotinamide-Adenine Dinucleotide Linked Dehydrogenases on Immobilised Derivatives of the Dinucleotide. *Biochem. J.*, **135**, 595 - 607.

Beillmann , J-F , Samama , J-P , Branden C.I. and Eklund H. (1979) X-Ray Studies of the Binding of Cibacron Blue F3GA to Liver Alcohol Dehydrogenase. *E.J. Biochem.*, **102**, 107 - 110.

Beissner R.S., Quiocho F.A. and Rudolph F.B. (1979) Dinucleotide Fold Proteins: Interaction of Arabinose Binding Proteins with Cibacron Blue F3G-A. *J. Mol. Biol.*, **134**, 847 - 850.

Berg A. and Scouten W.H. (1990) Dye-Ligand Centrifugal Affinity Chromatography. *Bioseparations*, **1**, 23 - 31.

Bethell G.S., Ayers J.S., Hancock W.S. and Hearn M.T.W. (1979) A Novel Method of Activation of Cross-Linked Agaroses with 1,1'-Carbonyldiimidazole which gives a Matrix for Affinity Chromatography Devoid of Additional Charged Groups. *J. Biol. Chem.*, **254**, 2572 - 2574.

Birkenmeier G. and Kopperschlager G. (1991) Dye-promoted Precipitation of Serum Proteins. Mechanism and Application. *J. Biotechnol.*, **21**, 93 - 108.

Bohme H.J., Kopperschlager G., Schultz J. and Hofmann E. (1972) Affinity Chromatography of Phosphofructokinase using Cibacron Blue F3G-A. *J. Chromatogr.*, **69**, 209 - 214.

Boyer P.M. and Hsu J.T. (1990) Adsorption Equilibrium of Proteins on a Dye-Ligand Adsorbent. *Biotech. Techniques*, **4**, 61 - 66.

Bradford M.M. (1976) A Rapid and Sensitive Method for the Quantitation of Microgram Quantities of Protein Utilising the Principle of Protein-Dye Binding. *Anal. Biochem.*, **72**, 248 - 254.

Branden C.I. and Eklund H. (1980) Structure and Mechamism of Liver Alcohol Dehydrogenase, Lactate Dehydrogenase and Glyceraldehyde-3-phoshate Dehydrogenase: In "Dehydrogenases Requiring Nicotinamide Coenzymes", ed. Jeffery J., Birkhauser Verlag: Basel.

Brodelius P., Larsson , P-O and Mosbach K. (1974) The Synthesis of Three AMP-Analogues: N6-(6-Aminohexyl)- Adenosine 5'-Monophosphate, N6-(6-aminohexyl)-Adenosine2',5'-Bisphosphate and N6-(6-Aminohexyl)-Adenosine 3',5'-Bisphosphate and their Applications as General Ligands in Biospecific Affinity Chromatography. *Eur. J. Biochem.*, **47**, 81 - 89.

Buchmann A.F. and Carrea G. (1989) Synthesis and Application of Water-Soluble Macromolecular Derivatives of the Redox Coenzymes NAD(H), NADP(H) and FAD: In "Advances in Biochemical Engineering/Biotechnology **39**. Vertebrate Cell Culture II and Enzyme Technology.", ed. Feichter A., Springer Verlag: Berlin.

Buckmann A.F. (1988) Optimisation of the Synthesis of N(1)-(2-aminoethyl)-NAD(P) *Heterocycles*, **27**, 1623 - 1628.

Buehner M., Ford G.C., Moras D., Olsen K.W. and Rossman M.G. (1974) Structure Determination of Crystalline Lobster D-Glyceraldehyde-3-phosphate Dehydrogenase

J. Mol. Biol., **82**, 563 - 585.

Burton D.R., (1987) Structure and Function of Antibodies in "Molecular Genetics of Immunoglobulin" ed. Calabi F. and Neuberger M.S. Elsevier: Amsterdam.

Burton S.J., McLoughlin S.B., Stead C.V. and Lowe C.R. (1988) Design and Applications of Biomimmetic Anthraquinone Dyes 1. Synthesis and Characterisation of Terminal Ring Isomers of C.I. Reactive Blue 2. *J. Chromatogr.*, **435**, 127 - 133.

Caceci M.S. and Cacheris W.P. (1984) Fitting Curves to Data: The Simplex Algorithm is the Answer. *Byte*, May, 340 - 362.

Campbell D.H., Luescher E. and Lerman L.S. (1951) Immunologic Adsorbents (I). Isolation of Antibodies by a Cellulose-Protein Antigen. *P.N.A.S. U.S.*, **37**, 575 - 578.

Chaffotte A.F., Roucous C. and Seydoux F. (1977) Affinity Chromatography of Glyceraldehyde-3-Phosphate Dehydrogenase. *Eur. J. Biochem.*, **78**, 309 - 316.

Chaiken I.M. (1979) Quantitative uses of Affinity Chromatography. *Anal. Biochem*, **97**, 1 - 10.

Chambers G.K. (1977) Determination of Cibachron Blue F3GA Substitution in Blue Sephadex and Blue Dextran-Sepharose. *Anal. Biochem.*, **83**, 551 - 556.

Chen L.F. and Tsao G.T. (1976) Physical Characteristics of Porous Cellulose Beads as Supporting Material for Immobilised Enzymes. *Biotech. Bioeng.* **18** 1507 - 1516

Chen L.F. and Tsao G.T. (1977) Chemical Procedures for Enzyme Immobilisation on Porous Cellulose Beads. *Biotech. Bioeng.* **19** 1463 - 1473

Clonis Y.D. (1988) The Application of Reactive Dyes in Enzyme and Protein

Downstream Processing. *CRC Crit. Rev. Biotechnol.*, **7**, 263 - 280.

Colombo G., Hubert E. and Marcus E. (1972) Selective Alteration of the Regulatory Properties of Fructose 1-6 Diphosphatase by Modification with Pyridoxal 5'-Phosphate. *Biochem.*, 11, 1796 - 1801.

Cook R.A. and Koshland D.E. (1970) Positive and Negative Cooperativity in Yeast Glyceraldehyde 3- Phosphate Dehydrogenase. *Biochem.*, **9**, 3337 - 3342.

Cook R.A. and Sanwal B.D. (1969) Isocitrate Dehydrogenase (NAD Specific) from Neurospora crassa. *Methods Enzymol.*, **13**, 42 - 47.

Coultate T.P. and Dennis D.T. (1969) Regulatory Properties of a Plant NAD Isocitrate Dehydrogenase- The Effect of Inorganic Ions. *Eur. J. Biochem.*, **7**, 153 - 158.

Cox G.F. and Davies D.D. (1970) The Effect of pH on the Characteristics of the Binding of Nicotinamide Adenine Dinucleotide by Nicotinamide Adenine Dinucleotide Specific Isocitrate Dehydrogenase from Pea Mitochondria. *Biochem. J.*, **116**, 819 - 824.

Craven D.B., Harvey M.J., Lowe C.R. and Dean P.D.G. (1974) Affinity Chromatography on Immobilised Adenosine 5'-Monophosphate. A New Synthesis and some Properties of an N6-Immobilised 5'-AMP. *Eur. J. Biochem.*, **41**, 329 - 333.

Crothers D.M. and Metzger H. (1972) The Influence of Polyvalency on the Binding Properties of Antibodies. *Immunochem.*, **9**, 341 - 357.

Cruz Z.M., Tanizaki M.M., El-Dory H.A. and Bacila M. (1979) On the Nucleotide Binding Domain of Fructose-1,6-Bisphosphatase. *Arch. Biochem. Biophys.*, **198**, 424 - 433.

Cuatrecasas P. (1970) Protein Purification by Affinity Chromatography: Derivatisation of Agarose and Polyacrylamide Beads. *J. Biol. Chem.*, **245**, 3059 - 3065.

Cuatrecasas P. and Anfinson C.B. (1971) Affinity Chromatography. *Methods Enzymol.* **22** 345 - 378

Cuatrecasas P., Wilchek M. and Anfinson C.B. (1968) Selective Enzyme Purification by Affinity Chromatography. *P.N.A.S. U.S.*, **61**, 636 - 643.

Danner J., Somerville J.E., Turner J. and Dunn B.M. (1979) Multiple Binding Sites of Carboxypeptidase B: The Evaluation of Dissociation Constants by Quantitative Affinity Chromatography. *Biochem.*, **18**, 3039 - 3045.

Davies D.D. (1969) NAD-Specific Isocitrate Dehydrogenase from a Plant Source. Sigmoid Kinetics and Enzyme Stability. *Biochem. Biophys. Acta*, **191**, 719 - 721.

Dean P.D.G. and Qadri F. (1983) Affinity Chromatography on Immobilised Dyes: In "Solid Phase Biochemistry: Analytical and Synthetic Aspects", ed. Scouten W.H., John Wiley and Sons: New York.

Dean P.D.G., Johnson W.S. and Middle F.A. (1985) Affinity Chromatography: A Practical Approach, IRL Press: Oxford.

DeMaine M.M., Caperelli C.A. and Benkovic S.J. (1982) Fructose-Bisphosphatase, Zinc-Free, from Rabbit Liver. *Methods Enzymol.*, **90**, 327 - 329.

Dunn B.M. and Chaiken I.M. (1974) Quantitative Affinity Chromatography. Determination of Binding Constants by Elution with Competitive Inhibitors. *P.N.A.S. U.S.*, **71**, 2382 - 2385.

Dunn B.M. and Chaiken I.M. (1975) Evaluation of Quantitative Affinity Chromatography by Comparison with Kinetic and Equilibrium Dialysis Methods for

the Analysis of Nucleotide Binding to Staphylococcal Nuclease. *Biochem.*, **14**, 2343 - 2349.

Dunn B.M. and Gilbert W.A. (1979) Quantitative Affinity Chromatography of Alpha Chymotrypsin. *Arch. Biochem. Biophys.*, **198**, 533 - 540.

Easterday R.L. and Easterday I.M. (1974) Affinity Chromatography of Kinases and Dehydrogenases on Sephadex and Sepharose Dye Derivatives: In "Immobilised Biochemicals and Affinity Chromatography", ed. Dunlap R.B., Plenum Press: New York pp 123 - 134.

Eilat D. and Chaiken I.M. (1979) Expression of Multivalency in the Affinity Chromatography of Antibodies. *Biochem.*, **18**, 790 - 795.

Er-el Z., Zaidenzaig Y. and Shaltiel S. (1972) Hydrocarbon-Coated Sepharoses. Use in the Purification of Glycogen Phosphorylase. *Biochem. Biophys. Res. Com.*, **49**, 383 - 390.

Federici M.M., Chock P.B. and Stadtman E.R. (1985) Interaction of Cibacron Blue F3GA with Glutamine Synthetase: Use of the Dye as a Conformational Probe. 1. Studies Using Unfractionated Dye Samples. *Biochem.*, **24**, 647 - 660.

Furukawa S., Urabe I. and Okada H. (1981) Inhibition of Lactate Dehydrogenase Activity by Polymeric NAD Derivatives with Different NAD Densities. *Eur. J. Biochem.*, **114**, 101 - 104.

Gennis L.S. (1976) Negative Homotropic Cooperatiity and Affinity Heterogeneity: Preparation of Yeast Glyceraldehyde-3-Phosphate Dehydrogenase with Maximal Affinity Homogeneity. *P.N.A.S. U.S.*, **73**, 3928 - 3932.

Gilham P.T. (1971) The Covalent Binding of Nucleotides, Polynucleotides and Nucleic Acids to Cellulose. *Methods Enzymol.*, **21**, 191 - 217.

Grant N.H. and Robbins K.C. (1957) Porcine Elasease and Proelastase. *Arch. Biochem. Biophys.*, **67**, 396 - 403.

Hall D.A. (1957) Complex Nature of the Enzyme Elastase. *Arch. Biochem. Biophys.*, **67**, 366 - 377.

Han P.F. and Johnson J. (1982) Fructose-1,6-Bisphosphatase from Turkey Liver *Methods Enzymol.*, **90**, 334 - 340.

Harvey M.J., Lowe C.R., Craven D.B. and Dean P.D.G. (1974) Affinity Chromatography on Immobilised Adenosine 5'-Monophosphate 2. Some Parameters Relating to the Selection and Concentration of the Immobilised Ligand. *Eur. J. Biochem.*, **41**, 335 - 340.

Harvey M.J., Lowe C.R. and Dean P.D.G. (1974) Affinity Chromatography on Immobilised Adenosine 5'-Monophosphate 5. Some Applications of the Influence of Temperature on the Binding of Dehydrogenases and Kinases. *Eur. J. Biochem.*, **41**, 353 - 357.

Heyns W. and DeMoor P. (1974) A 3(17)-β-Hydroxysteroid Dehydrogenase in Rat Erythrocytes: Conversion of 5-α-Dihydrotestosterone into 5-α-Androstane-3β,17β-diol and Purification of the enzyme by Affinity Chromatography. *Biochem. Biophys. Acta*, **358**, 1 - 13.

Hjerten S. (1964) The Preparation of Agarose Spheres for Chromatography of Molecules and Particles. *Biochem. Biophys. Acta*, **79**, 393 - 398.

Hockenhull D.J.D. and Herbert D. (1944) Amylase and Maltase of Clostridium acetobutylicum. *Biochem. J.*, **39**, 102 - 106.

Hodgins L.T. and Levy M. (1980) Affinity Adsorbent Preparation. Chemical Features

of Agarose Derivatised with Tri-chloro-s-triazine. *J. Chromatogr.*, **202**, 381 - 390.

Hogg P.J. and Winzor D.J. (1985) Effects of Solute Multivalency in Quantitative Affinity Chromatography: Evidence for Cooperative Binding of Horse Liver Alcohol Dehydrogenase to Blue Sepharose. *Arch. Biochem. Biophys.*, **240**, 70 - 76.

Holbrook J.J. and Stinson R.A. (1970) Reactivity of the Essential Thiol Group of Lactate Dehydrogenase and Substrate Binding. *Biochem. J.*, **120**, 289 - 297.

Holmbergh O. (1933) Adsorption of Malt Amylase on Starch. *Biochem. Z.*, **258**, 134 - 140.

Holroyde M.J., Chesher J.M.E., Trayer I.P. and Walker D.G. (1976) Studies on the use of Sepharose-N-(6-Aminohexanoyl)-2-Amino-2-Deoxy-D-Glucopyranose for the Large Scale Purification of Hepatic Glucokinase. *Biochem. J.*, **153**, 351 - 361.

Horstmann B.J., Kenney C.N. and Chase H.A. (1986) Adsorption of Proteins on Sepharose Affinity Adsorbents of Varying Particle Size. *J. Chromatogr.*, **361**, 179 - 190.

Horvath C. (1988) High-Performance Liquid Chromatography - Advances and Perspectives, Academic Press Inc.: San Diego.

Horvath C. (1988) High-Performance Liquid Chromatography - Advances and Perspectives, Academic Press Inc.: San Diego. pp 178 - 187

Hubble J. (1987) Cooperative Binding Interactions in Affinity Chromatography: Theoretical Considerations. *Biotech. Bioeng.*, **30**, 208 - 215.

Hummel J.P. and Dreyer W.J. (1962) Measurement of Protein-Binding Phenomena by Gel Filtration. *Biochem. Biophys. Acta*, **63**, 530 - 531.

Ingebretsen O.C. and Sanner T. (1974) Properties of the Nicotinamide Adenine Dinucleotide-specific Isocitrate Dehydrogenase from *Blastocladiella emersonii* *Biochem. Biophys. Acta*, **358**, 25 - 32.

Inman J.K. and Dintzis H.M. (1969) The Derivatisation of Cross-Linked Polyacrylamide Beads. Controlled Introduction of Functional Groups for the Preparation of Special Purpose Biochemical Adsorbents. *Biochem.*, **8**, 4074 - 4082.

Jacoby W.B. and Wilchek M. (eds.) (1974) Affinity Techniques - Enzyme Purification: Part B. Methods Enzymol. **34** Academic Press: New York.

Johansson G. and Joelsson M. (1987) Affinity Partitioning of Enzymes using Dextran-bound Procion Yellow HE-3G. *J. Chromatogr.*, **393**, 195 - 208.

Johansson G. and Joelsson M. (1987) Effect of Polymer Structure on Affinity Partitioning of Lactate Dehydrogenase in Polymer-Water Two-Phase Systems. *J. Chromatogr.* **411** 161 - 166

Johansson G. and Joelsson M. (1991) Protein-lignad Interactions Studied on Bovine Serum Albumin with Free and Polymer-bound Cibacron Blue F3G-A as Ligand with Reference to Affinity Partitioning. *J. Chromatogr.*, **537**, 219 - 233.

Kalderon N., Silman I., Blumberg S. and Dudai Y. (1970) A Method for the Purification of Acetylcholinesterase by Affinity Chromatography. *Biochem. Biophys. Acta*, **207**, 560 - 562.

Karush F. (1987) The Affinity of Antibody: Range, Variability and the Role of Multivalence: In "Immunoglobins", ed. Littman G.W. and Good R.A., New York:Plenum Press. p89

Karush F. (1987) The Affinity of Antibody: Range, Variability and the Role of Multivalence: In "Immunoglobins", ed. Littman G.W. and Good R.A., New

York:Plenum Press. pp104 - 108

Kasai K. and Ishii S. (1975) Quantitative Analysis of Affinity Chromatography of Trypsin. *J. Biochem.*, **77**, 261 - 264.

Kay G. and Crook E.M. (1967) Coupling of Enzymes to Cellulose using Chloro-s-triazines. *Nature*, **216**, 514 - 515.

Klinov S.V., Sugrobova N.P. and Kurganov B.I. (1979) Regulation of Enzyme Activity in Adsorptive Enzyme Systems. The Influence of Dextran Sulphate on Catalytic Properties of Lactate Dehydrogenase (Isoenzyme M4). *Molek. Biologiya*, **13**, 559 - 567.

Kopperschlager G., Bohme , H-J and Hofmann E. (1982) Cibacron Blue F3G-A and Related Dyes as Ligands in Affinity Chromatography: In "Advances in Biochemical Engineering No. 25", ed. Fiechter A., Springer-Verlag: Heidelberg.

Kopperschlager G., Freyer R., Diezel W. and Hofmann E. (1968) Some Kinetic nad Molecular Properties of Yeast Phosphofructokinase. *F.E.B.S. Lett.*, **1**, 137 - 141.

Krassig H. (1985) Structure of Celluloas and its Relation to the Properties of Cellulose Fibres. In "Cellulose and its Derivatives: Chemistry, Biochemistry and Applications". Ed. Kennedy J.F., Phillips G.O., Wedlock D.J. and Williams P.A., Ellis Horwood: Chichester.

Kremer R.D. and Tabb D. (1989) Paper: the Beneficially Interactive Support Medium for Diagnostic Test Development. *International Laboratory*, **July** , 40 - 45.

Kuehn G.D., Barnes L.D. and Atkinson D.E. (1971) Yeast diphosphopyridine nucleotide specific isocitrate dehydrogenase. Binding of ligands. *Biochem.*, **10**, 3945 - 3951.

Kyprianou P. and Yon R.J. (1982) A Quantitative Study of the Biospecific Desorption of Rat Liver (M4) Lactate Dehydrogenase from 10-Carboxydecylamino-Sepharose *Biochem. J.*, **207**, 549 - 556.

Larsson , P-O and Mosbach K. (1971) Preparation of NAD(H) Polymer Matrix showing Coenzyme Function fo the Bound Pyridine Nucleotide. *Biotech. Bioeng.*, **13**, 393 - 398.

Lasch J., Koelsch R., Weigel S., Blaha K. and Turkova J. (1982) Final Affinity Support Characterisation: (In)Homogeneity, Stability of Ligand-Matrix Linkage: In "Affinity Chromatography and Related Techniques: Theoretical aspects/industrial and biomedical applications", ed. Gribnau T.C.J., Visser J. and Nivard R.J.F., Elsevier: Amsterdam.

Lee C-Y (1978) Study on the Properties of Dextran-Linked Adenine Nucleotide Derivatives. *J. Solid Phase Biochem.*, **3**, 49 - 56.

Lee C-Y , Lappi D.A., Wermuth B., Everse J. and Kaplan N.O. (1974) 8-(6-Aminohexyl)-Amino-Adenine Nucleotide Derivatives for Affinity Chromatography. *Arch. Biochem. Biophys.*, **163**, 561 - 569.

Lee C-Y , Lazarus L.H., Kabakoff D.S., Russell P.J., Jr , Laver M. and Kaplan N.O. (1977) Purification of Kinases by General Ligand Affinity Chromatography *Arch. Biochem. Biophys.*, **178**, 8 - 18.

Lerman L.S. (1953) A Biochemically Specific Method for Enzyme Isolation. *P.N.A.S. U.S.*, **39**, 232 - 236.

Leyton J.F., Chinelatto A.M., El-Dorry H.A. and Bacila M. (1980) Correlation of Inhibition of Fructose 1,6-Bisphosphatase by AMP and the Presence of the Nucleotide Binding Domain. *Arch. Biochem. Biophys.*, **202**, 168 - 171.

Lineweaver H., Jang R. and Jansen E.F. (1949) Specificity and Purification of Polygalacturonidase. *Arch. Biochem. Biophys.*, **20**, 137 - 152.

Lis H. and Sharon N. (1973) The Biochemistry of Plant Lectins (Phytohaemagglutinins). *Ann. Rev. Biochem.* **42** 541 - 574

Liu C., Ledger R. and Stellwagen E. (1984) Quantitative Analysis of Protein Immobilised Dye Interaction. *J. Biol. Chem.*, **259**, 3796 - 3799.

Liu Y-C and Stellwagen E. (1987) Accessibility and Multivalency of Immobilised Cibacron Blue F3GA. *J. Biol. Chem.*, **262**, 583 - 588.

Livingston A.G. and Chase H.A. (1989) Preparation and Characterisation of Adsorbents for use in High-Performance Liquid Affinity Chromatography. *J. Chromatogr.*, **481**, 159 - 174.

Lowe C.R. and Dean P.D.G. (1973) Affinity Chromatography of Lactate Dehydrogenase on Immobilised Nucleotides. *Biochem J.*, **133**, 515 - 520.

Lowe C.R. and Dean P.D.G. (1974) Affinity Chromatography, John Wiley and Sons: London.

Lowe C.R. and Dean P.D.G. (1974) Affinity Chromatography, John Wiley and Sons: London. pp 200 - 245

Lowe C.R. and Pearson J.C. (1984) Affinity Chromatography on Immobilised Dyes *Methods Enzymol.*, **104**, 97 - 113.

Lowe C.R., Burton S.J., Pearson J.C., Clonis Y.D. and Stead C.V. (1986) Design and Applications of Biomimmetic Dyes in Biotechnology. *J. Chromatogr.*, **376**, 121 - 130.

Lowe C.R., Harvey M.J., Craven D.B. and Dean P.D.G. (1973a) Some Parameters Relevant to Affinity Chromatography on Immobilised Nucleotides. *Biochem J.*, **133**, 499 - 506.

Lowe C.R., Harvey M.J., Craven D.B., Kerfoot M.A., Hollows M.E. and Dean P.D.G. (1973b) The Purification of Nicotinamide Nucleotide-Dependent Dehydrogenases on Immobilised Cofactors. *Biochem J.*, **133**, 507 - 513.

Lowe C.R., Harvey M.J. and Dean P.D.G. (1974) Affinity Chromatography on Immobilised Adenosine 5'-Monophosphate 3. The Binding of Glycerokinase and Lactate Dehydrogenase in Relation to Column Geometry and Dynamics. *Eur. J. Biochem*, **41**, 341 - 345.

MacGregor J.S., Annamalai A.E., Van , Tol A., Black W.J. and Horecker B.L. (1982) Fructose-1,6-Bisphosphatase from Chicken and Rabbit Muscle. *Methods Enzymol.*, **90**, 340 - 345.

Mao Q.M., Johnston A., Prince I.G. and Hearn M.T.W. (1991) High-Performance liquid Chromatography of amino Acids, Peptides and Proteins: CXIII. Predicting the Performance of Non-Porous particles in Affinity Chromatography of Proteins. *J. Chromatogr.*, **548**, 147 - 163.

Marchalonis J.J. and Edelman G.M. (1968) Isolation and Characterisation of a Hemagglutinin from *Limulus polyphemus*. *J.Mol. Biol.*, **32**, 453 - 65.

March S.C., Parikh I. and Cuatrecasus P. (1974) A Simplified Method for Cyanogen Bromide Activation of Agarose for Affinity Chromatography. *Anal. Biochem.*, **60**, 149 - 152.

Marcus F., Rittenhouse J., Chatterjee T. and Hosey M.M. (1982) Fructose-1,6-bisphosphatase from Rat Liver. *Methods Enzymol.*, **90**, 352 - 357.

Mayes A.G., Moore J.D., Eisenthal R. and Hubble J. (1990) Investigation of Binding Site Density: Effects on the Interaction Between Cibacron Blue-Dextran Conjugates and Lysozyme. *Biotech. Bioeng.*, **36**, 1090 - 1096.

Mendicino J. and Abou-Issa H. (1974) Cooperative Effects of AMP, ATP and Fructose 1,6-diphosphate on the Specific Elution of Fructose 1,6-diphosphatase from Cellulose Phosphate: In "Immobilised Biochemicals and Affinity Chromatography", ed. Dunlap R.B., Plenum Press: New York.

Mockrin S.C., Byers L.D., Koshland D.E. and Jr (1975) Subunit Interactions in Yeast Glyceraldehyde 3-Phosphate Dehydrogenase. *Biochem.*, **14**, 5428 - 5437.

Morris J.E. and Fisher R.E. (1990) Complications Encountered using Cibacron Blue F3G-A as a Ligand for Affinity Precipitation of Lactate Dehydrogenase. *Biotech. Bioeng.*, **36**, 737 - 743.

Mosbach K. (1972) AMP and NAD as "General Ligands". *Methods Enzymol.*, **34**, 229 - 242.

Mosbach K., Guilford H., Ohlsson R. and Scott M. (1972) General Ligands in Affinity Chromatography. Cofactor-Substrate Elution of Enzymes Bound to the Immobilised Nucleotides Adenosine 5'-Monophosphate and Nicotinamide-Adenine Dinucleotide. *Biochem. J.*, **127**, 625 - 631.

Mosbach K., Larsson , P-O and Lowe C. (1976) Immobilised Coenzymes. *Methods Enzymol.*, **44**, 859 - 887.

Mullon C., Saltzman W.M. and Langer R. (1988) Computer Based Visualisation for Quantitative and Qualitative Analysis of the Distribution of Matrix-Bound Proteins. *Biotechnology* **6** 927 - 929

Nichol L.W., Ogston A.G., Winzor D.J. and Sawyer W.H. (1974) Evaluation of

Equilibrium Constants by Affinity Chromatography. *Biochem J.*, **143**, 435 - 443.

Nichol L.W., Ward L.D. and Winzor D.J. (1981) Multivalency of the Partitioning Species in Quantitative Affinity Chromatography. Evaluation of the Site Binding Constant for the Aldolase-Phosphate Interaction from Studies with Cellulose Phosphate as the Affinity Matrix. *Biochem.*, **20**, 4856 - 4860.

Niekamp C.W., Sturtevant J.M. and Velick S.F. (1977) Energetics of the Cooperative and Noncooperative Binding of Nicotinamide Adenine Dinucleotide to Yeast Glyceraldehyde 3- Phosphate Dehydrogenase at pH6.5 and pH8.5. Equilibrium and Calorimetric Analysis over a Range of Temperature. *Biochem.*, **16**, 436 - 445.

Nilsson K. and Mosbach K. (1980) p-Toluenesulphonyl Chloride as an Activating Agent of Agarose for the Preparation of Immobilised Affinity Ligands. *Eur. J. Biochem.*, **112**, 397 - 402.

Nimmo H.G. and Tipton K.F. (1975) The Purification of Fructose 1,6-Diphosphatase from Ox Liver and its Activation by Ethylenediaminetetra-Acetate. *Biochem. J.*, **145**, 323 - 334.

Nimmo H.G. and Tipton K.F. (1975) The Allosteric Properties of Beef Liver Fructose Bisphosphatase. *Eur. J. Biochem.*, **58**, 575 - 585.

Nishikawa H. (1983) Introduction to Affinity Purification of Biopolymers: In "Solid Phase Biochemistry: Analytical and Synthetic Aspects", ed. Scouten W.H., John Wiley and Sons: New York.

Nishikawa H. (1983) Introduction to Affinity Purification of Biopolymers: In "Solid Phase Biochemistry: Analytical and Synthetic Aspects", ed. Scouten W.H., John Wiley and Sons: New York. pp 28 - 33

Nissani N., Koren R. and Perlmutter-Hofman B. (1983) Positive Cooperativity in

Binding by Albumin: the System Bovine Serum Albumin and Alizarin Yellow G Cobinding by Salicylic Acid. *Arch. Biochem. Biophys.*, **226**, 357 - 364.

O'Carra P., Barry S. and Griffin T. (1973) Spacer Arms in Affinity Chromatography: the Need for a More Rigorous Approach. *Biochem. Soc. Trans.*, **1**, 289 - 290.

O'Carra P., Barry S. and Griffin T. (1974) Interfering and Complicating Adsorption Effects in Bioaffinity Chromatography. *Methods Enzymol.*, **34**, 108 - 126.

Ohlsson R., Brodelius P. and Mosbach K. (1972) Affinity Chromatography of Enzymes on an AMP-Analogue. Specific Elution of Dehydrogenases from a General Ligand. *F.E.B.S. Lett.*, **25**, 235 - 238.

Porath J., Janson J.C. and Laas T. (1971) Agar Derivatives for Chromatography, Electrophoresis and Gel-Bound Enzymes I. Desulphated and Reduced Cross-Linked Agar and Agarose in Spherical Bead Form. *J. Chromatogr.*, **60**, 167 - 177.

Porath J., Laas T. and Janson J-C. (1975) Agar Derivatives for Chromatography, Electrophoresis and Gel-Bound Enzymes III. Rigid Agarose Gels Cross-Linked with Divinyl Sulphone (DVS). *J. Chromatogr.*, **103**, 49 - 62.

Ramadoss C.S., Luby L.J. and Uyeda K. (1976) Affinity Chromatography of Phosphofructokinase. *Arch. Biochem. Biophys.*, **175**, 487 - 494.

Ryan L.D. and Vestling C.S. (1974) Rapid Purification of Lactate Dehydrogenase from Rt Lver and Hepatoma: A New Approach. *Arch. Biochem. Biophys.*, **160**, 279 - 284.

Sakamoto H., Nukamura A., Urabe I., Yamada Y. and Okada H. (1986) Analysis and Improvement of the Synthesis of N6-(2-carboxyethyl)-NAD+. *J. Ferment. Technol.*, **64**, 511 - 516.

Sander E.G., McCormick D.B. and Wright L.D. (1966) Column Chromatography of Nucleotides over Thymidylate-Cellulose. *J. Chromatogr.*, **21**, 419 - 423.

Sarngadharen M.G., Watanabe A. and Pogell B.M. (1970) Purification of Rabbit Liver Fructose 1,6-Diphosphatase by Substrate Elution. *J. Biol. Chem.*, 245, 1926 - 1929.

Scatchard G. (1949) The Attractions of Proteins for Small Molecules and Ions. *Ann. N.Y. Acad. Sci.*, **51**, 660 - 672.

Schmidt , H-L and Grenner G. (1976) Coenzyme Properties of NAD+ Bound to Different Matrices through the Amino Group in the 6-Position. *Eur. J. Biochem.*, **67**, 295 - 302.

Schmidt J. and Raftery M.A. (1973) Purification of Acetylcholine Receptors from Torpedo californica Electroplax by Affinity Chromatography. *Biochem.*, **12**, 852 - 856.

Schwimmer S. and Balls A.K. (1949) Crystalline Alpha Amylase from Barley Malt *J. Biol. Chem.*, **179**, 1063 - 1074.

Scopes R.K. (1986) Strategies for Enzyme Isolation using Dye Ligand and Related Adsorbents. *J. Chromatogr.*, **376**, 131 - 140.

Scouten W.H. (1981) Affinity Chromatography: Bioselective Adsorption on Inert Matrices, John Wiley and Sons: New York.

Scouten W.H. (1981) Affinity Chromatography: Bioselective Adsorption on Inert Matrices, John Wiley and Sons: New York. pp 42 - 80

Scouten W.H. (1981) Affinity Chromatography: Bioselective Adsorption on Inert Matrices, John Wiley and Sons: New York. pp 109 - 162

Scouten W.H. (1981) Affinity Chromatography: Bioselective Adsorption on Inert Matrices, John Wiley and Sons: New York. pp 110 - 127

Sica V., Nola E., Parikh I., Puca G.A. and Cuatrecassas P. (1973) Affinity Chromatography and the Purification of Estrogen Receptors. *J. Biol. Chem.*, **248**, 6543 - 6558.

Sidebotham R.L. (1974) Dextrans: In "Adv. Carbohydr. Chem. Biochem. 30", ed. Tipson R.S. and Horton D., Academic Press: New York.

Sigma Chemical Catalogue (1989) p 910

Silman I.H. and Katchalski E. (1966) Water Insoluble Derivatives of Enzymes, Antigens and Antibodies. *Ann. Rev. Biochem.*, **35**, 873 - 908.

Sloan D.L. and Velick S.F. (1973) Protein Hydration Changes in the Formation of the Nicotinamide Adenine Dinucleotide Complexes of Glyceraldehyde-3-phosphate Dehydrogenase of Yeast. *J. Biol. Chem.*, **248**, 5419 - 5423.

Sober H.A. and Peterson E.A. (1954) Chromatography of Proteins on Cellulose Ion Exchangers. *J. Am. Chem. Soc.*, **76**, 1711 - 1712.

Stallcup W.B., Mockrin S.C., Koshland D.E. and Jr (1972) A Rapid Purification Proceedure for Glyceraldehyde 3-Phosphate Dehydrogenase from Bakers Yeast. *J. Biol. Chem.*, **247**, 6277 - 6279.

Starkenstein E. (1910) Uber Fermentwirkung and Deren Besiuflussung Durch Neutralsalze. *Biochem. Z.*, **24**, 210 - 218.

Steers E., Jr , Cuatrecasas P. and Pollard H.B. (1971) The Purification of Beta-galactosidase from Escherichia coli by Affinity Chromatography. *J. Biol. Chem.*, **246**, 196 - 200.

Stellwagen E. and Liu Y-C. (1987) Quantitative Considerations of Chromatography using Immobilised Biomimetic Dyes: In "Analytical Affinity Chromatography", Chaiken I.M., CRC Press: Boca Raton.

Stellwagen E. and Liu Y-C. (1987) Quantitative Considerations of Chromatography using Immobilised Biomimetic Dyes: In "Analytical Affinity Chromatography", Chaiken I.M., CRC Press: Boca Raton. pp 170 - 180

Stinson R.A. and Holbrook J.J. (1973) Equilibrium Binding of Nicotinamide Nucleotides to Lactate Dehydrogenase. *Biochem. J.*, **131**, 719 - 728.

Subramanian S. (1982) Spectral Changes Induced in Cibacron Blue F3GA by Salts, Organic Solvents and Polypeptides: Implications for Blue Dye Interaction with Proteins. *Arch. Biochem. Biophys.*, **216**, 116 - 125.

Subramanian S. (1989) Ionic and Apolar Interactions of Cibacron Blue F3GA with Model Compounds and Proteins: Application to Protein Purification: In "Protein-Dye Interactions: Developments and Applications", Vijayalakshmi M.A. and Bertrand O., Elsevier: New York.

Subramanian S. and Kaufman B.T. (1980) Dihydrofolate Reductase from Chicken Liver and Lactobacillus casei Bind Cibacron Blue F3GA in Different Modes and at Different Sites. *J. Biol. Chem.*, **255**, 10587 - 10590.

Sundberg L. and Porath J. (1974) Attachment of Group-Containing Ligands to Insoluble Polymers by Means of Bifunctional Oxiranes. *J. Chromatogr.*, **90**, 87 - 98.

Swaisgood H.E. and Chaiken I.M. (1987) Analytical Affinity Chromatography and Characterisation of Biomolecular Interactions. In "Analytical Affinity Chromatography" ed. Chaiken I.M., CRC Press: Boca Raton. pp 65 - 117

Tashima Y. and Mizunuma H. (1982) Fructose-1,6-bisphosphatase from Mouse and Rabbit Intestinal Mucosa. *Methods Enzymol.*, **90**, 357 - 365.

Taylor J.F. (1953) : The Isolation of Proteins. In "The Proteins Vol. 1 Part A", Neurath H. and Bailey K., Academic Press : New York pp 1 - 85.

Tesser G.I., Fisch H-U and Schyzer R. (1972) Limitations of Affinity Chromatography: Sepharose-Bound Cyclic 3' 5'- Adenosine Monophosphate. *F.E.B.S. Lett.* **23** 56 - 58

Thompson S.T., Cass K.H. and Stellwagen E. (1975) Blue Dextran-Sepharose: An Affinity Column for the Dinucleotide Fold in Proteins. *P.N.A.S. U.S.*, **72**, 669 - 672.

Thompson S.T. and Stellwagen E. (1976) Binding of Cibachron Blue F3GA to Proteins Containing the Dinucleotide Fold. *P.N.A.S. U.S.*, **73**, 361 - 365.

Travis J., Bowen J., Tewksbury D., Johnson D. and Pannell R. (1976) Isolation of Albumin from Whole Human Plasma and Fractionation of Albumin Depleted Plasma *Biochem. J.*, **157**, 301 - 306.

Trayer I.P., Trayer H.R., Small D.A.P. and Bottomley R.C. (1974) Preparation of Adenine Nucleotide Derivatives Suitable for Affinity Chromatography. *Biochem. J.*, **139**, 609 - 23.

Turkova J. (1987) Affinity Chromatography : J. Chromatogr. Library **12**, Elsevier: Amsterdam.

Turkova J. (1987) Affinity Chromatography : J. Chromatogr. Library **12**, Elsevier: Amsterdam. pp 155 - 189

Turkova J. (1987) Affinity Chromatography : J. Chromatogr. Library **12**, Elsevier:

Amsterdam. pp 189 - 195

Velick S.F., Baggott J.P. and Sturtevant J.M. (1971) Thermodynamics of Nicotinamide Adenine Dinucleotide addition of the Glyceraldehyde-3-phosphate Dehydrogenase of Yeast and Rabbit Skeletal Muscle. An Equilibrium and Calorimetric Analysis over a Range of Temperature. *Biochem.*, 10, 779 - 786.

Veronese F.M., Bevilacqua R. and Chaiken I.M. (1979) Drug-Protein Interactions: Evaluation of the Binding of Antipsychotic Drugs to Glutamate Dehydrogenase by Quantitative Affinity Chromatography. *Mol. Pharmacol.*, **15**, 313 - 321.

Waterson R.M., Clarke S.J., Kalonsek F. and Konigsberg W.H. (1973) Seryl Transfer RNA Synthetase from *E. coli*: Substrate Binding and Chemical Modification of Cysteinyl Residues. *J. Biol. Chem.* **248** 4181 - 4185

Watson D.H., Harvey M.J. and Dean P.D.G. (1978) The Selective Retardation of NADP+ Dependent Dehydrogenases by Immobilised Procion Red HE3B. *Biochem. J.*, **173**, 591 - 596.

Wermuth B. and Kaplan N.O. (1976) Pyriding Nucleotide Transhydrogenase from Pseudomonas aeruginosa: Purification by Affinity Chromatography and Physicochemical Properties. *Arch. Biochem. Biophys.*, **176**, 136 - 143.

Wilchek M., Miron T. and Kohn J. (1984) Affinity Chromatography. *Methods Enzymol.* **104** 3 - 53

Winzor D.J., Ward L.D. and Nichol L.W. (1982) Quantitative Considerations of the Consequences of an Interplay Between Ligand Binding and Reversible Adsorption of a Macromolecular Solute. *J. Theor. Biol.*, **98**, 171 - 187.

Yang , C-M and Tsao G.T. (1982) Affinity Chromatography: In "Advances in Biochemical Engineering No. 25", Fiechter A., Springer-Verlag: Heidelberg pp 19 -

42.

Yon R.J. (1988) Computer Modelling of Multivalent Affinity Partitioning. *Biochem. Soc. Trans.*, **16**, 542 - 543.

Yon R.J. (1988) A Re-examination of the Interaction between Aldolase and Phosphocellulose. *Biochem. Soc. Trans.*, **16**, 543 - 544.

Yon R.J. (1988) Co-operative Cluster Model for Multivalent Affinity Interactions Involving Rigid Matrices. *J. Chromarogr.*, **457**, 13 - 23.

Zittle C.A. (1953) Adsorption Studies of Enzymes and other Proteins. *Advan. Enzymol.*, **14**, 319 - 374.

APPENDIX

Publications and Presentations of the Results Contained in this Thesis

Publications

A.G. Mayes, J.D. Moore, J. Hubble and R. Eisenthal.
Investigation of Binding Site Density: Effects on the Interaction between Cibacron blue-dextran Conjugates and Lysozyme.
Biotech. Bioeng. **36** (1990) 1090 - 1096

A.G. Mayes, J. Hubble and R. Eisenthal.
Investigation of Liquid Phase Cooperative Binding Interactions on the Capacity of Insoluble Affinity Adsorbents. *J. Chromatogr.* **539** (1991) 245 - 254

A.G. Mayes, J. Hubble and R. Eisenthal.
Investigation of Binding Isotherms for Liquid Phase Immobilised Affinity Ligands using Spectral Titration. *Biotech. Bioeng.* (submitted)

Presentations

Biochemical Society Meeting: Bath, April 3rd, 1990

Poster *"Specific and Non-specific Binding Phenomena in Affinity Adsorption"*

3^0 Colloque du Groupe Francais de Bio-Chromatographie. Bio-Chromatography and Molecular Affinity: Dijon, France. May 22nd - 25th, 1990

Oral presentations *"Ligand Density Effects in a Model System: Interaction between Cibacron Blue-dextran Conjugates and Lysozyme"*
and *"Do Liquid Phase Cooperative Phenomena Influence Binding to Immobilised Ligands?"*

Investigation of Binding Site Density: Effects on the Interaction Between Cibacron Blue–Dextran Conjugates and Lysozyme

A.G. Mayes, J.D. Moore, and R. Eisenthal*
Biochemistry Department, University of Bath, Bath, BA2 7AY, United Kingdom

J. Hubble
School of Chemical Engineering, University of Bath, United Kingdom

Received October 18, 1989/Accepted March 3, 1990

Cibacron-blue–dextran conjugates have been produced with a range of ligand loadings using a dextran preparation of average molecular weight of 2×10^6. The equilibrium binding capacity of these ligand conjugates for lysozyme was determined using a gel permeation procedure to separate bound from free protein. The results obtained give clear evidence for at least two types of binding showing a marked difference in affinity. For the higher-affinity interaction the half-saturation constant decreases with increasing ligand loading. The number of dye molecules participating in binding is proportional to loading up to 154 mol dye/mol dextran but is reduced at the highest loading used (315 mol dye/mol dextran). This may be due to steric interference or to dye stacking reducing the number of dye molecules available for binding.

INTRODUCTION

As affinity chromatography becomes more widely used on a process scale, the optimization of binding site density becomes increasingly important for economic as well as operational reasons. Preliminary work on the effects of ligand density on the performance of affinity chromatography has been conducted by a number of workers and some underlying effects have been reported.[1,2]

From a simple consideration of the equilibrium between adsorbate and affinity ligand, it might be expected that increasing the ligand concentration should lead to an increase in both binding capacity and fraction of adsorbate bound for a given volume of affinity matrix. This suggests that the highest possible ligand concentration will give the most favorable binding equilibrium. In practice, however, the optimal ligand density may be below the maximum achievable due to the increase in nonspecific binding interactions which occurs at high ligand densities. These arise from ion-exchange and hydrophobic interactions. The consequence of nonspecific binding is to reduce the purity of the product obtained, and possibly to reduce the capacity (where nonspecific interactions swamp the affinity effect). An additional practical drawback is the increased difficulty in regenerating supports showing nonspecific binding.

In studies on the availability of ligands for binding, Liu et al.[3] found that less than 2% of the ligand in a 0.12 m*M* Reactive Blue 2 Sepharose column could adsorb rabbit muscle lactate dehydrogenase. They concluded that this reflected a high proportion of adsorbed dye that was not available for binding, and discounted steric factors as a major contributing factor. This suggests that great attention must be paid to the synthesis and characterization stage of the resin preparation. The importance of high ligand density is particularly apparent for separations where the dissociation constant for the interaction is high, but the results of Liu and Stellwagen[4] show that high ligand densities have little advantage if much of the ligand is in the wrong orientation.

In studies aimed at process development, it has been found that while increases in ligand density lead to increases in equilibrium binding capacity, the kinetics of the interaction can be significantly impaired.[5] This effect has been attributed to differences in ligand distribution throughout the porous support particles used; i.e., with light ligand loadings only the external regions of the support particle are substituted such that diffusional paths within the bead will be short. It is clear that a similar effect should be observed when only a small fraction of the capacity of beads with a higher ligand density is utilized. This was demonstrated by Eveleigh and Levy,[5] who showed that increasing the flow rate of adsorbate through a fixed bed lead to reductions in both capacity and cycle time. Further evidence for the significance of diffusional resistances was provided by Fowell and Chase[6] who showed that a column prepared

* To whom all correspondence should be addressed.

Biotechnology and Bioengineering, Vol. 36, Pp. 1090–1096 (1990)

CCC 0006-3592/90/01101090–07$04.00

with low ligand concentrations performed better than one prepared with more highly substituted material diluted with unsubstituted support.

The limited amount of experimental data suggests that a systematic study of ligand density optimization is of central importance to the development of affinity chromatography. Clearly, the chemical effects of ligand immobilization and the physical diffusional limitations imposed by the use of porous support particles both have a significant effect on the apparent performance of an affinity chromatography resin. To improve our understanding of the differing factors affecting the affinity interaction, we need to be able to study ligand density effects in the absence of diffusional limitations.

We now report the use of the Cibacron-blue–lysozyme interaction as a model system to study these effects. This system was first reported by Chase[7] as a model system for studying the kinetics of adsorption in affinity chromatography and has since been used in other quantitative chromatographic studies.[8] In the present study, dextran–Cibacron-blue conjugates have been produced by a method modified from that of Bohme et al.[9] These conjugates can easily be synthesized in a range of dye:dextran ratios, making them an ideal liquid phase probe for the study of affinity interactions. The experimental system adopted utilizes a modified Hummel and Dreyer technique[10–12] whereby a Sephadex G-75 column is equilibrated with a buffered solution of lysozyme. The dye–dextran conjugate dissolved in the same equilibration solution is loaded on to the column, and eluted with more equilibration buffer. The conjugate binds lysozyme thus reducing the concentration of free lysozyme in the applied sample. As the dye–dextran conjugate, together with its bound lysozyme, moves down the column it continually comes into contact with lysozyme at the column equilibration concentration so it continues to adjust its equilibrium, removing more lysozyme as it does so. This leaves behind a region of lysozyme depletion which travels down the column more slowly due to the size of free lysozyme permitting it to enter the gel pores. Eventually the conjugate reaches a point where it has established equilibrium with the column equilibration concentration of lysozyme so no more lysozyme is removed. By measuring the absorbance at a suitable wavelength, a peak containing the dye–dextran conjugate and bound lysozyme can be detected at the void volume of the column followed by a plateau corresponding to the absorbance of the lysozyme in the equilibration buffer and then a trough, extending to the elution volume of lysozyme, representing protein that has been bound to the dye dextran conjugate.

With reference to the molar extinction coefficient of the protein and the flow rate, the area of the trough can be used to quantify the amount of lysozyme bound by the loaded dye-dextran conjugate. The concentration of free lysozyme, $[L_f]$, is defined to be the concentration of lysozyme in the column equilibration buffer since this is the concentration of lysozyme with which the dye–dextran conjugate has equilibrated at the point where peak and trough separate. The amount of dye dextran conjugate in the sample loaded is known. The experiment is repeated at a range of lysozyme concentrations. Data analysis can then be carried out to calculate the dissociation constant, K_d, and the maximum number of lysozyme molecules which can be bound per dye–dextran conjugate molecule, n. This value can then be compared with the number of dye molecules coupled to the dextran to determine the proportion of dye molecules which can interact with lysozyme simultaneously.

The Hummel and Dreyer method has often been used in the study of protein–ligand interactions[11,13,14] where the ligand is a small molecule. The method as used in the context of this work is novel, because both the "ligand" and "macromolecule" in these experiments are macromolecules. As the lysozyme molecules are smaller than the dextrans, the column in these experiments was equilibrated with lysozyme, and small sample volumes containing the Cibacron-blue–dextran conjugates were loaded.

MATERIALS AND METHODS

Materials

Lysozyme (grade VI from chicken egg white), dextran of nominal average molecular weight of 2×10^6 and medium grade Sephadex G-75 were purchased from Sigma Chemical Co. (Poole, Dorset, UK). Cibacron blue 3G was purchased from Ciba (Manchester, UK). All other reagents were of Analar grade and were purchased from British Drug Houses (Poole, Dorset, UK).

Methods

Coupling of Cibacron Blue to Dextran

The coupling was performed by a method modified from that of Bohme et al.[9] A solution of 20 g dextran in 600 mL water was mixed with solutions of 2 g Cibacron blue in 200 mL water and 20 g Na_2CO_3 in 200 mL water. The mixture was then stirred at 45°C while samples of 100ml were withdrawn at various time intervals. After 75 h another 2 g Cibacron blue was added to the mixtures. An equal volume of ethanol was added to each sample which was then allowed to stand at −20°C for at least 60 min. The precipitate was spun down and the pellet resuspended in 50 mL water. The precipitation and resuspension procedure was repeated a further two times. The final resuspension of the dextran–Cibacron-blue conjugates was in 40 mL water. These concentrated aqueous solutions were stored at 4°C with a few crystals of sodium azide to inhibit the growth of microorganisms.

On the basis of gel filtration experiments, no low-molecular-weight material of high absorbance was

present in the conjugate solutions. This indicated that the free dye was separated from that bound to dextran by the preparation method. Similar analysis showed that no release of dye occurred over a two-month storage period and that the conjugates were stable two months after production.

Dye loadings on the conjugates were calculated by two methods. In the first method, the loading was estimated from dry-weight determinations together with absorbance measurements at 257 nm for solutions of the conjugates and solutions of dextran alone. Dye stacking in solution was found to cause a decrease in absorbance at 257 nm so all measurements were made using diluted samples with concentrations below 5 μM where the effect of intermolecular dye stacking was found to be minimal. The extinction coefficient of dextran (molecular weight of 2×10^6) at 257 nm was found to be 0.5 mM^{-1} cm^{-1}; thus, the contribution of dextran to the overall absorbance of the conjugate at 257 nm is very small. In calculating ligand loading by this method, it is assumed that the extinction coefficient of Cibacron blue at this wavelength (32 mM^{-1} cm^{-1}) is unaltered by the coupling procedure.

In the second method, dye loading was estimated by acid hydrolysis using the method of Chambers.[15] Spectra in 6M HCl were measured using a Cecil CE588 spectrophotometer scanning from 390 to 750 nm. Comparison of spectra before and after hydrolysis revealed an isosbestic point at 541 nm. This was used to measure dye loading without the need to hydrolyze the sample, thus avoiding the problem of assessing when hydrolysis was complete. The absorbance of diluted solutions of free dye was proportional to concentration up to at least 100 μM at 541 nm. Concentrations were calculated using an extinction coefficient of 2.75 mM^{-1} cm^{-1} (determined using free dye under the same conditions).

Hummel and Dreyer Experiments

A column (50 × 0.66 cm i.d.) was packed with Sephadex-G75 under gravity. This matrix was chosen because Cibacron blue does not interact with the dextran matrix under the experimental conditions, and the pore size allowed adequate separation of lysozyme (molecular weight of 1.45×10^4) and the conjugates (average molecular weight $>2 \times 10^6$); the latter were completely excluded and eluted at the void volume of the column. The column was equilibrated with "running buffer" (50 mM NaCl, 10 mM Tris, and lysozyme as appropriate adjusted to pH 8.0 with HCl) until a stable plateau was observed on a chart trace (at least two column volumes of running buffer were required). Typical flow rates were 20–25 mL/h. Column temperature was maintained at 24°C by the use of a water jacket and a thermostatically controlled recirculating water bath. Running buffers were degassed by helium sparging and pre-equilibrated to the column temperature before use. The samples for loading were prepared by diluting aqueous dye–dextran conjugate solutions with an equal volume of double-strength buffer which contained lysozyme at twice the concentration of that in the equilibration buffer. The dye–dextran conjugate sample was loaded using a precalibrated injection loop of 36.25 μL volume. The column eluate was passed through a quartz flow cell in a spectrophotometer connected to a chart recorder, with absorbance monitored at 280 nm. From the chart trace, extinction coefficient of lysozyme (see below) and the flow rate, troughs could be integrated to determine the amount of bound lysozyme.

An operational extinction coefficient for lysozyme was determined by equilibrating the column with running buffer in the absence of lysozyme and then in the presence of a known concentration of lysozyme. The difference between the baseline and the plateau on the chart trace could then be used to relate pen displacement and lysozyme concentration in subsequent measurements.

RESULTS

Coupling of Cibacron Blue to Dextran: Ligand Densities

Figure 1 shows the ligand density (as mol dye/mol dextran) plotted against reaction time for Cibacron blue coupling to dextran of average molecular weight of 2×10^6. As expected, the rate of increase in ligand loading declines with time as all the free reactive Cibacron blue is consumed. A proportion of the reactive dye reacts with the water in the solution rather than with the dextran, but high loadings were nevertheless achieved by the method used. Commercially available Blue Dextran (Pharmacia) contains approximately 8% dye by mass,

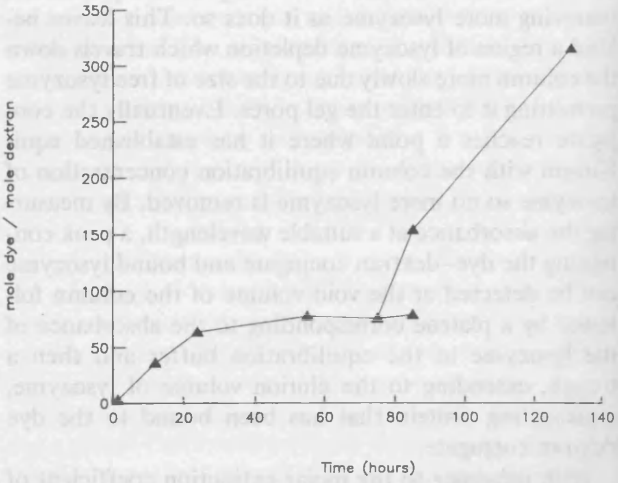

Figure 1. Time course for the reaction between Cibacron blue 3G and dextran of 2×10^6 average molecular weight in 20 g/L sodium carbonate at 45°C. Aliquots were removed at the indicated times and coupling estimated by dry weight and absorbance measurements after removal of unbound dye (see the methods section). The branch point indicates the addition of fresh dye.

a figure exceeded by the highest loadings produced in this work.

Dye loading was determined by two methods in order to check for the possible presence of intrachain dye stacking which could lead to a change in the apparent extinction coefficient of the conjugated dye. At high loadings, dye molecules may be forced into proximity when coupled to dextran and this could lead to dye stacking due to local high concentrations even at low bulk average concentrations where stacking of free dye would be negligible. Thus, determination of dye loading from the absorbance of dilute solutions (<5 μM) of dye–dextran conjugates at 257 nm gives an estimate of loading assuming that there is no intramolecular dye stacking. Measurement at 541 nm in 6M HCl gives an estimate which is unaffected by dye stacking so comparison of the two values for each conjugate gives an indication of the degree of dye stacking at each dye loading. Comparison of the two methods showed that the results varied by less than 3% for all loadings except the highest where the measurement in 6M hydrochloric acid gave a dye-to-dextran ratio 18% higher than the measurement at 257 nm. This suggests the presence of considerable intramolecular dye stacking in this sample. The higher value was used in subsequent calculations.

Hummel and Dreyer Experiments

Trough areas were calculated by measuring the deviation of the trace from the stable plateau line at 2-mm intervals and integrating using the trapezium rule. A typical eluate trace is shown in Figure 2. Conjugates prepared from dextran of 2×10^6 average molecular weight with average loadings of 36.3, 63.7, 81, 154, and 315 mol dye/mol dextran were chosen for the binding experiments. Each of the dye–dextran conjugates was used in seven runs at lysozyme equilibration concentrations of 0.5, 0.25, 0.125, 0.0625, 0.0208, 0.0104, and 0.0052 mg/mL.

The amount of lysozyme bound to each conjugate at each concentration of free lysozyme was calculated using the formula:

$$\text{Bound lysozyme} = \frac{L_f A \text{FR}}{\text{CS} \times \text{PLATEAU}} \text{ mol}$$

where L_f is the molar concentration of lysozyme in running buffer; A is the area of trough (mm^2); FR is the flow rate in (h^{-1}); CS is the chart speed in (mm/h); and PLATEAU is the difference in mm between baseline in the absence of lysozyme and plateau in the presence of lysozyme.

In these experiments the amount of dye used in each run was kept constant so the amount of dye–dextran conjugate varied in inverse proportion to its dye loading. Control experiments were run in which the dextran concentration was also kept constant by the inclusion of appropriate amounts of blank dextran. These indicated that the total dextran concentration had no effect on lysozyme binding in the range used here [0.07–0.5% (w/w)]. In the absence of dye ligands, no binding was observed between dextran and lysozyme even at the highest dextran concentration examined [5% (w/w)].

Scatchard plots[16] of $r/[L_f]$ vs. r (where r is the number of mol lysozyme bound/mol dye dextran conjugate) for each of the dye–dextran conjugates were all clearly curved (concave upwards). A typical plot is shown in Figure 3. It is tempting in such circumstances to assume that the system contains two discrete populations of binding sites and to fit straight lines to the data points at the two extremes of the curve and extrapolate to obtain the values of K_d and n. As pointed out by a number of authors,[17–19] this is an incorrect treatment of the data and the values obtained do not represent true values of

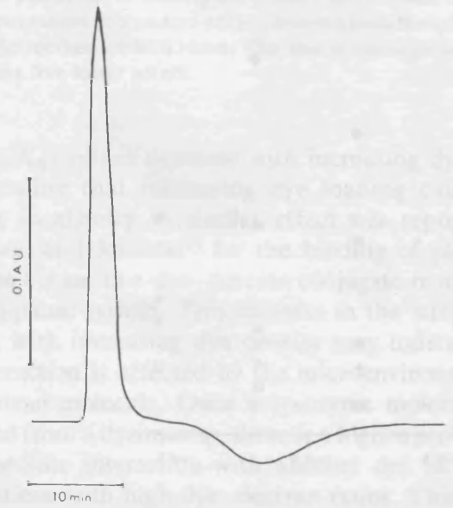

Figure 2. A typical chart trace from a gel permeation binding experiment. Dye-dextran conjugate with a loading of 81 mol dye/mol dextran at a concentration of 100 μM (expressed in terms of dye) in the presence of lysozyme (62.5 mg/L) at 24°C. The flow rate was 23.1 mL/h; absorbance was monitored at 280°C.

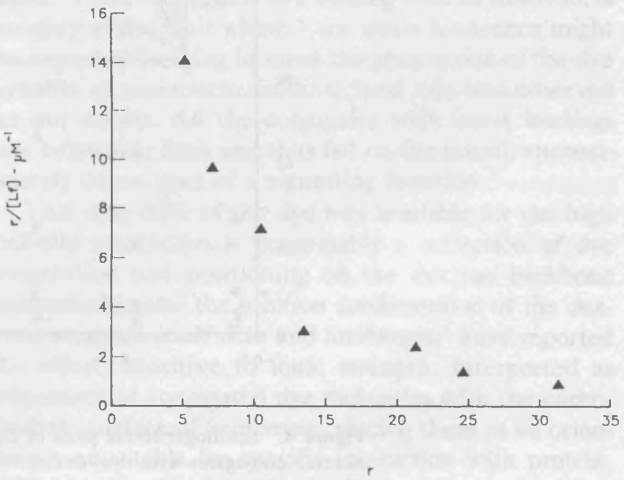

Figure 3. Scatchard plot of binding data for the dye–dextran conjugate with a loading of 81 mol dye/mol dextran.

K_d and n but complicated functions of site parameters, which are unsuited to binding constant evaluation except in simple well-defined cases.

As recommended by Klotz,[20] the data were plotted as semilogarithmic graphs and are shown in Figure 4. These graphs clearly indicate the presence of high affinity "specific" saturable sites and lower affinity "nonspecific" sites which showed no approach to saturation over the range of ligand concentration studied. Data points corresponding to the saturable part of the binding curves (Fig. 4, inset) were used to determine operational values for the half saturation constant $K_{0.5}$ (a dissociation constant) and the value of n, together with their standard errors, using a computer program based on the method of Wilkinson[21] (a nonlinear least-squares fit to a hyperbolic function). These values are plotted against the ligand loadings of the corresponding dye–dextran conjugates in Figures 5 and 6. From Figures 5 and 6 it is apparent that specific binding capacity is directly proportional to the dye loading on the dextran up to a loading of 154 mol dye/mol dextran, i.e., the fitted line passes through the origin. The gradient of the line indicates that approximately 20% of the total conjugated dye is available for specific binding. At the highest loading (315 mol dye/mol dextran), the proportionality no longer holds and the fraction of conjugated dye available for binding is 20% less than that observed for the other dye–dextran conjugates studied. Statistical analysis indicates that the difference between n observed at the highest loading and that calculated from the linear relationship is statistically significant ($P < 0.01$). The relationship of specific binding affinity to dye loading is more complex, but a general decrease of $K_{0.5}$ with increasing loading is apparent. It should be stressed that these are operational constants and do not represent the true values of K_d and n because of the contribution made by the lower affinity system.

DISCUSSION

The objective of this work was to produce soluble dye–dextran conjugates with a range of ligand densities, to characterize these, and to investigate their potential as a liquid phase model system for studying affinity interactions. The coupling procedure used recovered in the best case nearly 60% of the dextran and more than 40% of the dye used in its production. In practice, this was perfectly acceptable for a laboratory-scale synthesis and no attempt was made at optimization. The loading reaction was limited by the availability of dye due to the competing reaction of dye with hydroxyl ions in solution. After 48 h at 45°C, the reactive form of the dye was depleted and additional dye was added at this point to produce higher loadings.

Having obtained dye–dextran conjugates over a range of loadings a method was needed to allow the determination of equilibrium binding. The soluble nature of the system and the molecular size of the compounds involved precludes the use of equilibrium dialysis, or other conventional separation techniques. As an alternative the use of the Hummel and Dreyer method was investigated and shown to be successful.

The results obtained from the graphical analysis clearly show that at least two types of interaction are occuring. Although little can be said concerning the "nonspecific" interaction, the trends of the variation of the "specific" binding parameters, $K_{0.5}$ and n, with ligand loading are clearly established. For high affinity

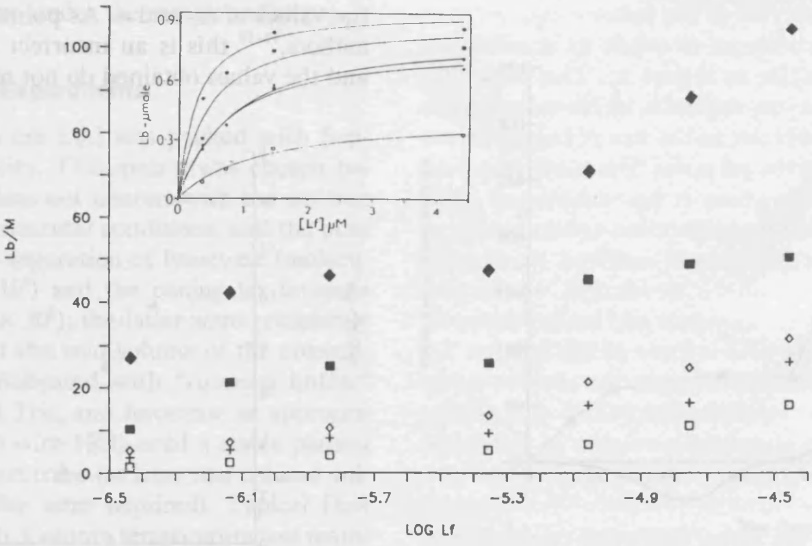

Figure 4. Semilogarithmic plots of L_b/M vs. log $[L_f]$ for binding of lysozyme to dye–dextran conjugates with dye–dextran ratios of: (□) 36.3, (+) 63.7, (◇) 81, (■) 154, and (◆) 315 mol dye/mol dextran at 24°C. Inset shows graphs of L_b vs. L_f for the saturable part of the binding curves. The solid line through each set of data was generated using the values of $K_{0.5}$ and n obtained from curve fitting to a hyperbolic adsorption isotherm.

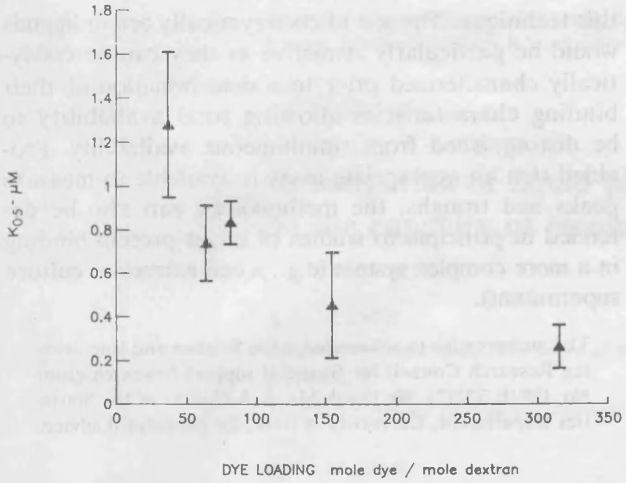

Figure 5. The effect of binding site density on the value of $K_{0.5}$. The graph shows means ± standard errors obtained from the estimation of $K_{0.5}$ by the method of Wilkinson.

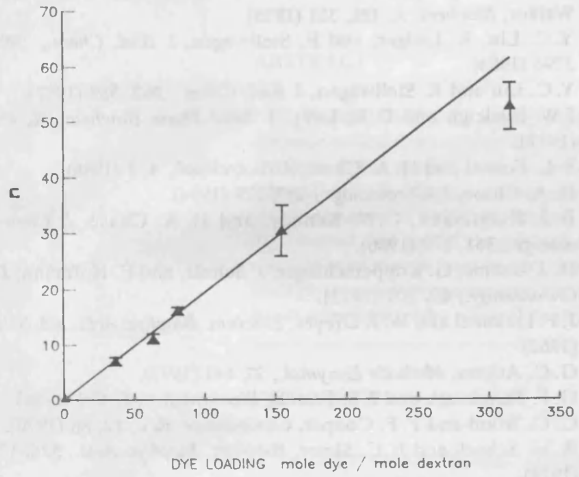

Figure 6. The effect of binding site density on the value of n. The graph shows means ± standard errors obtained from the estimation of n by the method of Wilkinson. The line is the regression line through the five lower points.

binding, $K_{0.5}$ values decrease with increasing dye loading, showing that increasing dye loading causes an increase in affinity. A similar effect was reported by Johansson and Joelsson[22] for the binding of phosphoglycerate kinase to a dye–dextran conjugate in an aqueous two-phase system. This increase in the strength of binding with increasing dye density may indicate that the interaction is affected by the microenvironment of the dextran molecule. Once a lysozyme molecule has desorbed from a dye moiety, there is a higher probability of immediate interaction with another dye moiety in preparations with high dye: dextran ratios. This is due to the higher local concentration of dye (relative to the bulk average) altering the equilibrium position within the microenvironment of the dextran molecule in favor of binding, i.e., the lysozyme molecule is "trapped" by the dextran bound dye molecules. Thus up to a critical limit, the microenvironmental effects may outweigh the tendency of steric hindrance to reduce the strength of binding.

The finding that n is proportional to dye loading for loadings up to 154 mol dye/mol dextran indicates that the capacity of the saturable part of the system depends only on the total amount of dye present and is not affected by the physical proximity of the dye groups on the dextran molecules. At the highest loading used the region of proportionality is exceeded and the fraction of dye molecules participating in binding drops from 20 to 16%. This may be due either to the onset of a degree of steric crowding limiting dye–lysozyme interactions, or to a reduction in the number of available dye molecules resulting from intramolecular dye stacking which was shown, from the ligand loading estimations, to occur at this dye density.

The results of Male et al.[23] provide an interesting comparison with those presented here. They presented trypsin binding data for a range of soluble polyacrylamide polymers made by copolymerizing acrylamide and *N*-acryloyl-*m*-aminobenzamidine at monomer ratios of 1:200 up to 1:5 acrylamide:*N*-acryloyl-*m*-aminobenzamidine ratios. For the 200:1 ratio, the theoretical trypsin binding limit was reached, i.e., all ligands were simultaneously binding protein. At 100:1, only half the sites were occupied and the proportion continued to decline such that at a 5:1 ratio only 6% of ligands were occupied. For a 5:1 ratio, the average distance along the polyacrylamide backbone between ligands is only about 1.5 nm—less than the radius for trypsin—so it is not surprising that considerable steric hindrance is apparent. For the 100:1 ratio, where steric hindrance was observed, the distance between ligands is about 25 nm or 13 times the radius of trypsin. A similar consideration of our conjugates indicates that even the most highly derivatized one has only one ligand for every 39 sugar residues or one for every 20 nm of backbone. This is about 13 times the Stokes radius of lysozyme. Thus, the highest dye loading used in this work is roughly at the limit where some steric hindrance might be expected (bearing in mind the greater size of the dye relative to aminobenzamidine), and this was observed in our results. All the conjugates with lower loadings are below this limit and thus fall on the initial, approximately linear, part of a saturating function.

That only 20% of the dye was available for the high affinity interaction is presumably a reflection of dye orientation and positioning on the dextran backbone and possibly also the solution conformation of the dextran molecule itself. Liu and Stellwagen[4] have reported an effect, sensitive to ionic strength, interpreted as alignment of conjugated dye molecules with the carbohydrate surface of Sepharose, placing them in an orientation unsuitable for specific interaction with protein. This may also be occurring with the dextran which has a similar chemical structure. Dye molecules coupled to the dextran near to branch points in the chain may be

severely sterically crowded and inaccessible to protein molecules.

The value of 20% of dye participating in binding at saturation (assuming a monovalent interaction) compares with a value of only about 5% for a similar sized protein (adenylate kinase) binding to Cibacron-blue–F3GA-Sepharose CL6B at a ligand density of 120 μM. Although the buffer compositions are different in the two systems, they should have similar effectiveness in lowering dye availability due to the alignment effect, according to data presented by Liu and Stellwagen.[4]

The nonspecific binding of lysozyme to dye appears to be a function of dye loading and may be due to a simple ionic interaction since the dye carries negative charges on all its sulphonate groups and so will act as an ion exchanger at this pH. The magnitude of the total lysozyme binding to each conjugate reached about 40% of its theoretical maximum (assuming a monovalent interaction between dye and protein) at the highest lysozyme concentration used but showed no approach to saturation at this point. It is possible that total saturation of all dye molecules might eventually be achieved with a high enough concentration of lysozyme.

The results obtained show that, even without the complications of pore diffusional limitations associated with the use of macroporous supports, optimization of ligand density in affinity supports is complicated by ligand density and distribution considerations. The experimental system demonstrated here provides a convenient way of assessing ligand density effects, and can in principle be extended to any affinity interaction. Although the resolving power of the chromatographic setup used in this study was insufficient to permit the use of proteins larger than lysozyme, preliminary studies with a Superose 12HR column on a Pharmacia FPLC system have indicated that this technique can be extended to larger proteins, namely bovine serum albumin (molecular weight of 6.7×10^4) and yeast alcohol dehydrogenase (molecular weight of 1.44×10^5). In order to achieve complete resolution of peaks and troughs with these proteins the dye–dextran conjugate must be fractionated by gel permeation chromatography or membrane filtration to remove lower-molecular-weight material prior to use in Hummel and Dreyer experiments. As pointed out by Sebille and Thaud,[24] HPLC methods also offer the advantages of economy of scale and time in such studies and greatly increase the range of protein–ligand interactions that can be studied by this technique. The use of coenzymically active ligands would be particularly attractive as they can be catalytically characterized prior to a determination of their binding characteristics allowing total availability to be distinguished from simultaneous availability. Provided that an appropriate assay is available to measure peaks and troughs, the methodology can also be extended in principle to studies of target protein binding in a more complex system (e.g., a cell extract or culture supernatant).

The authors wish to acknowledge the Science and Engineering Research Council for financial support (research grant No. GR/E 32717). We thank Mr. A. J. Collins of the Statistics Department, University of Bath, for his helpful advice.

References

1. M. J. Harvey, C. R. Lowe, D. B. Craven, and P. D. G. Dean, *Eur. J. Biochem.*, **41**, 335 (1973).
2. M. J. Holroyde, J. M. E. Chesher, I. P. Trayer, and D. G. Walker, *Biochem. J.*, **151**, 351 (1976).
3. Y. C. Liu, R. Ledger, and E. Stellwagen, *J. Biol. Chem.*, **259**, 3796 (1984).
4. Y. C. Liu and E. Stellwagen, *J. Biol. Chem.*, **262**, 583 (1987).
5. J.W. Eveleigh and D. E. Levy, *J. Solid Phase Biochem.*, **2**, 45 (1977).
6. S. L. Fowell and H. A. Chase, *J. Biotechnol.*, **4**, 1 (1986).
7. H. A. Chase, *J. Chromatogr.*, **297**, 179 (1984).
8. B. J. Horstmann, C. N. Kenney, and H. A. Chase, *J. Chromatogr.*, **361**, 179 (1986).
9. H. J. Bohme, G. Kopperschlager, J. Schulz, and E. Hofmann, *J. Chromatogr.*, **69**, 209 (1972).
10. J. P. Hummel and W. J. Dreyer, *Biochim. Biophys. Acta.*, **63**, 530 (1962).
11. G. C. Ackers, *Methods Enzymol.*, **27**, 441 (1973).
12. G. F. Fairclough and J. S. Fruton, *Biochemistry*, **5**, 673 (1966).
13. G. C. Wood and P. F. Cooper, *Chromatogr. Rev.*, **12**, 88 (1970).
14. R. M. Scheek and E. C. Slater, *Biochim. Biophys. Acta.*, **526**, 13 (1978).
15. G. K. Chambers, *Anal. Biochem.*, **83**, 551 (1977).
16. G. Scatchard, *Ann. NY Acad. Sci.*, **51**, 660 (1949).
17. J. G. Norby, P. Ottolenghi, and J. Jensen, *Anal. Biochem.*, **102**, 318 (1980).
18. I. M. Klotz and D. L. Hunston, *Biochemistry*, **10**, 3065 (1971).
19. K. Zierler, *Trends in Biochemical Sciences*, **14**, 314 (1989).
20. I. M. Klotz, in "Protein Function—A Practical Approach," T. E. Creighton, Ed. (IRL Press, Oxford, 1989), pp. 25–55.
21. Wilkinson G. N., *Biochem. J.*, **80**, 324 (1961).
22. G. Johansson and M. Joelsson, *J. Chromatogr.*, **393**, 195 (1987).
23. K. B. Male, J. H.T. Luong, and A. L. Nguyen, *Enzyme Microb. Technol.*, **9**, 374 (1987).
24. B. Sebille and N. J. Thaud, *J. Chromatogr.*, **167**, 159 (1978).

Journal of Chromatography, 539 (1991) 245–254
Elsevier Science Publishers B.V., Amsterdam

CHROM. 22 873

Investigation of liquid phase cooperative binding interactions on the capacity of insoluble affinity adsorbents

A. G. MAYES
Biochemistry Department, University of Bath, Claverton Down, Bath BA2 7AY (U.K.)
J. HUBBLE*
School of Chemical Engineering, University of Bath, Claverton Down, Bath BA2 7AY (U.K.)
and
R. EISENTHAL
Biochemistry Department, University of Bath, Claverton Down, Bath BA2 7AY (U.K.)

ABSTRACT

Experimental data is presented to support the theoretical prediction of an enhancement of adsorption arising from a positively cooperative liquid phase interaction between a multivalent adsorbate and free ligand. The results obtained with glyceraldehyde 3-phosphate dehydrogenase show a 4-fold increase in adsorption to 5′-adenosine monophosphate cellulose in the presence of 3 μM nicotinamide adenine dinucleotide compared with that obtained in the absence of cofactor. Although the magnitude of the effect, and the optimal free ligand concentration do not correspond to those predicted in the original model, the discrepancies may at least in part be accounted for by a maldistribution of immobilised ligand, leading to multiple cooperative interactions between adsorbate and affinity matrix. This can be qualitatively predicted by an extension to the original model.

INTRODUCTION

Separation techniques based on affinity adsorption have great potential for the production of high value, high purity bioproducts. This results from the high degree of selectivity and the consequently large purification factors which can be achieved. However, as affinity adsorption is adopted as a process scale operation the optimisation of empirically developed laboratory-scale methodology becomes important for maximising yield and quality of the end product.

Although much effort has been directed towards optimisation of the solid phase, *i.e.*, investigation of ligand immobilisation chemistry and the effect of both the length and nature of spacer arms, there appears to have been little consideration given to the possible contribution of the liquid phase to the overall performance of a system, for example the possible gains achievable by using free ligand in the liquid phase to enhance the binding of a positively cooperative enzyme to the solid phase.

The property of positive cooperativity, whereby proteins show sigmoid ligand binding isotherms is a fairly common feature of multimeric proteins in free solution.

0021-9673/91/$03.50

The performance and capacity of affinity adsorbents is strongly influenced by the affinity of the protein for the immobilised ligand. It therefore seems likely that adding free ligand to positively cooperative protein in the presence of immobilised ligand will increase the affinity of the protein for all available ligand and hence lead to tighter binding of protein to matrix ligand. This hypothesis was examined quantitatively in computer simulations by Hubble [1], which suggested that significant gains could be achieved in an appropriate system. In this paper we report attempts to obtain experimental evidence for this behaviour and compare the results with the theoretical predictions obtained from computer simulation.

MATERIALS

N^6-(6-aminohexyl)AMP, N^6-(6-aminohexyl)NAD^+, long fibrous cellulose powder, glyceraldehyde 3-phosphate dehydrogenase (GAPDH), glyceraldehyde 3-phosphate diethyl acetal and NAD^+ were obtained from Sigma (Poole, Dorset, U.K.).

Free glyceraldehyde 3-phosphate was liberated from the diethyl acetal (Sigma) by heating an aqueous solution in the presence of Dowex 50 H^+ resin, and was assayed using GAPDH and NAD^+ to check for complete hydrolysis of the acetal. This was stored in aliquots at $-20°C$ until required.

Sepharose 4B came from Pharmacia (Uppsala, Sweden). All other chemicals were of analytical grade.

METHODS

Preparation of nucleotide matrix derivatives

Sepharose 4B or long fibrous cellulose was activated with cyanogen bromide using the method of March *et al.* [2]. The final wash was with 0.1 *M* sodium bicarbonate pH 8.9 (buffer A). Matrix was resuspended in an equal volume of buffer A and sufficient N^6-(6-aminohexyl)AMP or N^6-(aminohexyl)NAD^+ added to give the desired concentration of matrix ligand. This was agitated gently for 16 h at 4°C. The matrix was washed with buffer A and the washings retained for spectrophotometric determination of unbound ligand. The washed matrix was added to 1 *M* ethanolamine and left at room temperature for 2 h to block any remaining reactive groups, then washed with water, 1 *M* sodium chloride and water again before storage at 4°C as a moist cake. Ethanolamine–Sepharose was prepared by activation followed by immediate blocking with ethanolamine.

Ligand bound to the matrices was estimated by calculation of the difference between ligand added and ligand remaining in the washings. Absorbance was measured at 267 nm and a molar absorptivity of 17.7 $mM^{-1}cm^{-1}$ used for calculations [3]. Ligand bound to Sepharose was also estimated by direct spectroscopy of a 10% suspension of matrix in glycerol–water (50:50, w/w) using a similar suspension of underivatised Sepharose as a blank. The wavelength maximum and molar absorptivity of the coupled ligand were assumed to be the same as for the free ligand. The two methods showed close agreement.

Coupling was consistently found to be 94–96% for Sepharose and 50–60% for cellulose.

Nucleotide removal from GAPDH

Nucleotides were removed by charcoal treatment using the method of Gennis [4]. Treated GAPDH had an A 280 nm/A 260 nm ratio of about 2 and was stored as an ammonium sulphate suspension at 4°C until required.

Assay of GAPDH

GAPDH was assayed at pH 8.5 and 25°C in 1 ml of a buffer containing (final concentrations) 50 m*M* sodium pyrophosphate, 5 m*M* EDTA, 10 m*M* sodium dihydrogen orthophosphate, 0.1 *M* potassium chloride, 10 m*M* cysteine, 1 m*M* NAD^+, and 1 m*M* D-glyceraldehyde 3-phosphate (2 m*M* DL racemate) which was added last to initiate the reaction. Enzyme (about 0.005 I.U.) was preincubated for 8 min in the assay buffer to ensure complete reduction of active site thiol groups. Increase in absorbance at 340 nm was followed using a Cecil 272 UV spectrophotometer fitted with a jacketed cuvette holder. Temperature was maintained using a recirculating water bath and cuvettes were left for 15 min to equilibrate prior to use.

Equilibrium batch adsorption

A quantity of matrix equal to 4 ml settled volume was added to 20 ml 50 m*M* sodium pyrophosphate buffer pH 8.5 containing 1 m*M* 2-mercaptoethanol and 1 m*M* EDTA. The total volume was measured and the suspension added to a water jacketed vessel maintained at 25 ± 0.3°C, stirred with an overhead stirrer to minimise physical matrix degradation. A known amount of GAPDH was added and allowed to equilibrate for about 10 min.

A 100-μl sample was withdrawn, spun briefly to sediment the matrix and 20-μl samples of supernatant removed for triplicate enzyme assays. The total added ligand concentration in the vessel was increased by adding a small volume of NAD^+ solution and the system allowed to re-equilibrate for 8 min before repeating the cycle. This was continued until the desired range of added ligand had been covered.

The concentration of free enzyme is found from the assays so, knowing the total amount of enzyme initially added and the system volume (recalculated after each cycle), bound enzyme can be calculated from the enzyme mass balance for each concentration of added ligand.

RESULTS AND DISCUSSION

Fig. 1 shows the simulated effect of free ligand concentration on GAPDH adsorption using theory developed by Hubble [1] and literature values for the binding constants [4]. In contrast Fig. 2a–c shows plots of bound enzyme/total enzyme against log added NAD^+ from batch adsorption experiments using AMP–Sepharose matrices with different ligand densities. In order to keep the bulk average matrix ligand concentration comparable the volume of the highest ligand density AMP–Sepharose used was lower than that used in the other two experiments. As might be expected the fractional binding in the absence of free NAD^+ (arbitrarily plotted at −6.5) increased with increasing ligand density but the predicted enhancement of binding on adding free NAD^+ was not apparent under the experimental conditions adopted for any of the matrix ligand densities tested. Similar results were obtained for NAD^+–Sepharose matrices (data not shown).

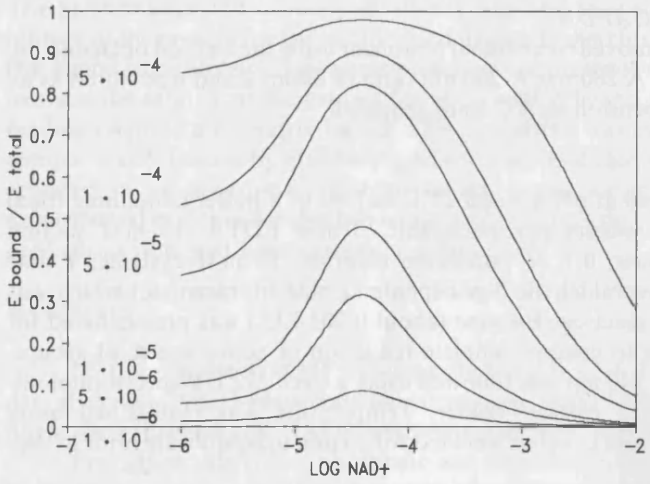

Fig. 1. The predicted effect of matrix ligand concentration on the relationship between free ligand concentration and the fraction of enzyme bound for glyceraldehyde 3-phosphate dehydrogenase. The affinity constants used were derived from the data of Gennis [4]. $K_1 = 2.6 \cdot 10^3$, $K_2 = 1.5 \cdot 10^4$, $K_3 = 1.9 \cdot 10^5$, $K_4 = 5.7 \cdot 10^3\ M^{-1}$. The matrix ligand concentrations were: $1 \cdot 10^{-6}$, $5 \cdot 10^{-6}$, $1 \cdot 10^{-5}$, $5 \cdot 10^{-5}$, $1 \cdot 10^{-4}$, $5 \cdot 10^{-4}\ M$.

The data obtained using AMP cellulose is shown in Fig. 3. Due to the low levels of binding observed in this system the scatter of points in individual experiments was greater than for the Sepharose experiments since the magnitudes of the changes in bound enzyme were similar to the magnitudes of the errors. All the individual experiments suggested that some enhancement of binding was occurring, with control experiments using blank cellulose and ethanolamine-derivatised cellulose showing no

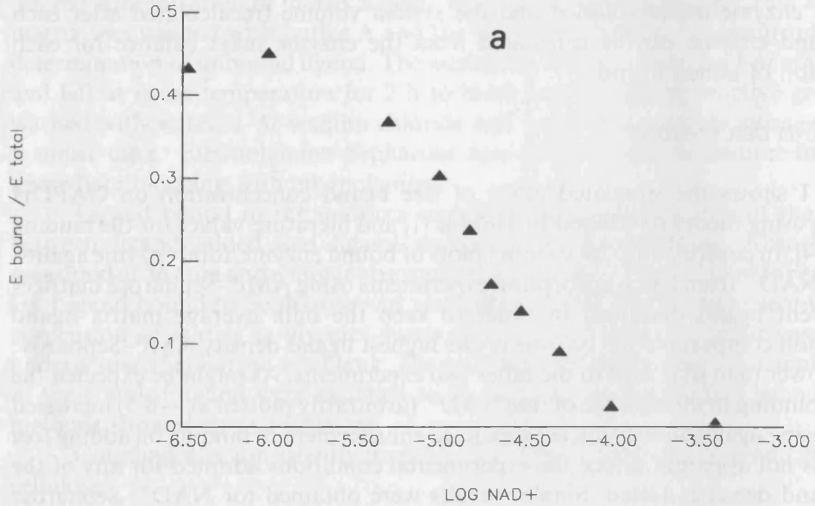

Fig. 2.

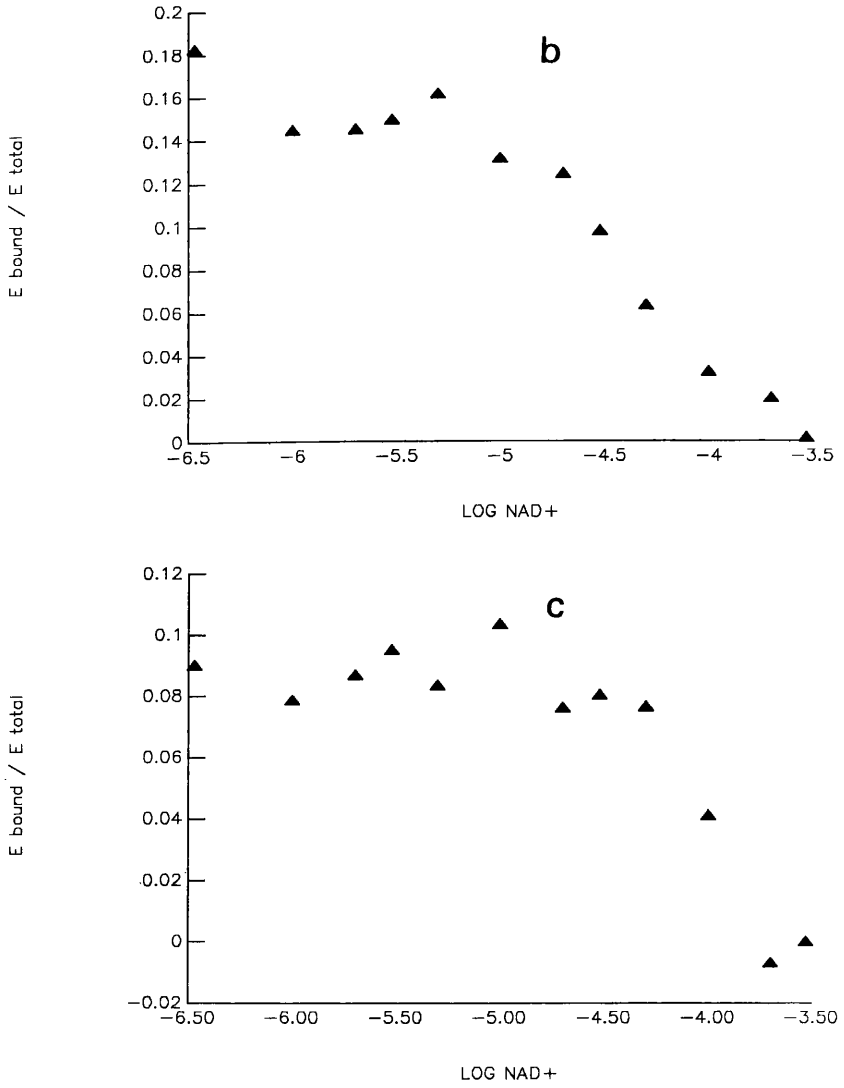

Fig. 2. Effect of added NAD^+ on the fraction of enzyme (GAPDH) bound to AMP-Sepharose. (a) High density: bulk average ligand concentration $1 \cdot 10^{-4}$ *M*. Matrix volume 6.5% of total. Matrix ligand concentration $1.5 \cdot 10^{-3}$ *M*. (b) Medium density: bulk average ligand concentration $9.3 \cdot 10^{-5}$ *M*. Matrix volume 18% of total. Matrix ligand concentration $5.2 \cdot 10^{-4}$ *M*. (c) Low density: bulk average ligand concentration $2.5 \cdot 10^{-5}$ *M*. Matrix volume 18% of total. Matrix ligand concentration $1.4 \cdot 10^{-4}$ *M*. Values for no added NAD^+ are arbitarily plotted at −6.5.

effect. On combining the data from several runs with AMP cellulose the enhancement is quite clearly seen (Fig. 3). An approximately 4-fold increase in binding was apparent on adding free ligand and this compared well with that predicted for the bulk average matrix ligand concentration used. In two other respects, however, the data were not comparable with the predicted behaviour. The fractional binding of enzyme to matrix

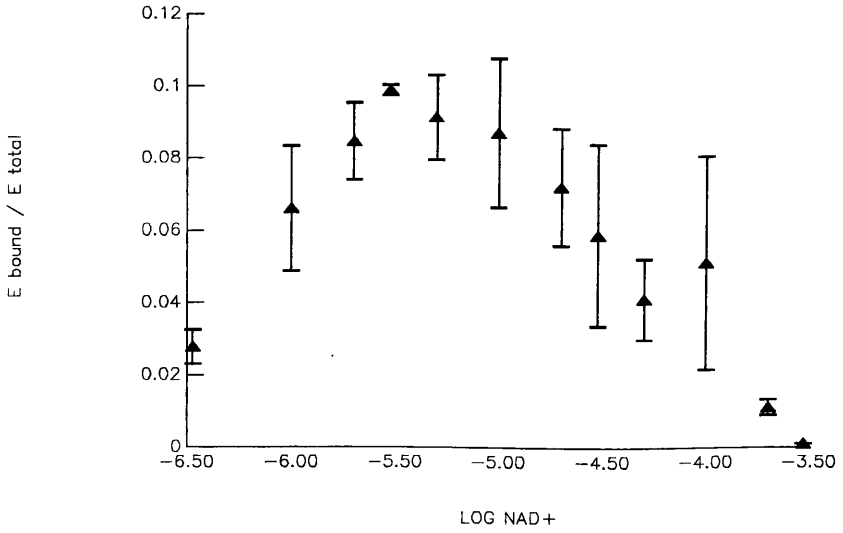

Fig. 3. Effect of added NAD^+ on the fraction of enzyme bound for GAPDH binding to AMP cellulose. The bulk average ligand concentration was $7.8 \cdot 10^{-5}$ *M* and the matrix volume = 20% of total (matrix ligand concentration $3.9 \cdot 10^{-4}$ *M*). Values plotted are means ± standard errors ($n = 3$). Values for no added NAD^+ are arbitarily plotted at −6.5.

ligand was about 10-fold lower than predicted. This observation probably results from restrictions imposed on ligand accessibility by the support matrix, and/or changes in binding constants arising from the chemical effects of immobilisation. The second deviation from the theoretical prediction is that the maximum observed binding enhancement occurs at a lower free ligand concentration. This can in part be explained by the effects of immobilised ligand maldistribution.

The difference in the behaviour of the cellulose and Sepharose matrices probably arises as a result of their different physical structures and consequent differences in the pattern of derivatisation. Sepharose beads are approximately spherical with a size range of 60–140 μm. Fibrous cellulose approximates to cylinders of length 100–250 μm and diameter about 25 μm. Sepharose 4B beads are known to be porous with pore sizes 80–230 nm, averaging about 170 nm [5]. The porosity of the cellulose used is unknown due to batch to batch variation of this natural product. It is generally composed of porous "amorphous" regions, with greater porosity than cross-linked polysaccharides like Sepharose 4B interspersed with compact "microcrystalline" regions [6]. Thus both matrices used should be freely permeable to both small molecules and GAPDH. Hence it does not appear that differences in accessibility could be a major contributor to the different behaviour of cellulose and Sepharose matrices.

The diffusional path length to the centre of a particle is up to 6 times longer for Sepharose assuming similar degrees of contortion in both matrices. Since both activating chemicals and coupling ligands must diffuse into the particle from the liquid phase it is likely that the end product will not be a uniformly derivatised particle but one with a "shell" of high ligand density at the surface and a concentration gradient running to a minimum at the centre of the particle. The shorter the path length the less

pronounced this would be expected to be. The result of this will be that the cellulose matrix will have a more uniform ligand distribution, more closely approximating the bulk average concentration than will the Sepharose matrix where the majority of the ligand will be concentrated towards the external surface of the beads. This would have two possible repercussions.

(1) The Sepharose matrix will behave as one with a higher ligand density thus tending to swamp out the cooperative effect.

(2) The higher ligand density in the Sepharose matrix will lead to an increased probability of multivalent interactions between protein and immobilised ligand.

This behaviour has been observed for a number of proteins with multiple binding sites [7–9]. A bivalent interaction will have a higher affinity constant than a monovalent one and if this is greater than or equal to the enhanced affinity of enzyme molecules partially saturated with free ligand then this will also swamp out any enhancement which might have been achieved due to the cooperative effect.

The effect of localised high concentrations of matrix ligand together with the consequences of multivalant interaction between macromolecule and resin can be qualitatively considered using an extension to the model described by Hubble [1]. In the original theoretical assessment of liquid phase cooperativity the assumption was made that with low matrix ligand densities only monovalent interactions would be possible between adsorbate and support. However, if localised high concentrations of immobilised ligand occur the possibility of multivalent interactions between enzyme and support cannot be discounted. The original model can easily be extended to consider all theoretically possible interactions between a tetravalent enzyme and both free and immobilised ligand. The broader model can be used to give a qualitative indication of the effects that these multivalent surface interactions might be expected to have on observed binding enhancements.

Development of the revised model leads to the formulation of fourteen equilibria describing interactions between individual complex species. For interaction with soluble ligand:

$$[E][L] \overset{K_1}{\rightleftharpoons} [EL]$$

$$[EL][L] \overset{K_2}{\rightleftharpoons} [EL_2]$$

$$[EL_2][L] \overset{K_3}{\rightleftharpoons} [EL_3]$$

$$[EL_3][L] \overset{K_4}{\rightleftharpoons} [EL_4]$$

A similar set of equilibria can be formulated for the interactions of E with immobilised ligand (M) using association constants $K_{m1} - K_{m4}$. Binding between enzyme and both soluble and immobilised ligand can be described in terms of six further association constants:

$$[EM][L] \overset{K_{l1}}{\rightleftharpoons} [EML]$$

$$[EML][L] \overset{K_{l2}}{\rightleftharpoons} [EML_2]$$

$$[EML_2][L] \overset{K_{l3}}{\rightleftharpoons} [EML_3]$$

$$[EM_2][L] \overset{K_{l4}}{\rightleftharpoons} [EM_2L]$$

$$[EM_2L][L] \overset{K_{l5}}{\rightleftharpoons} [EM_2L_2]$$

$$[EM_3][L] \overset{K_{l6}}{\rightleftharpoons} [EM_3L]$$

Fractional binding of enzyme to the affinity support can be described in terms of:

$$Y_m = \frac{\Sigma[EM_i] + \Sigma[EM_iL_j]}{[E] + \Sigma[EL_j] + \Sigma[EM_i] + \Sigma[EM_iL_j]}$$

where i denotes number of sites bound to immobilised ligand and j denotes number of sites bound to free ligand (for a tetramer $1 \leqslant (i + j) \leqslant 4$).

This equation can be expressed in terms of the equilibrium concentrations of L and M together with appropriate products of the individual association constants. Where the association constants are known this relationship can be used to predict the effect of free ligand concentrations on fractional binding as previously described. However, the more general form allows the effect of permitting progressively more complex multiple interactions between enzyme and adsorbate to be predicted. An example of a prediction of this type is given in Fig. 4 using the same association

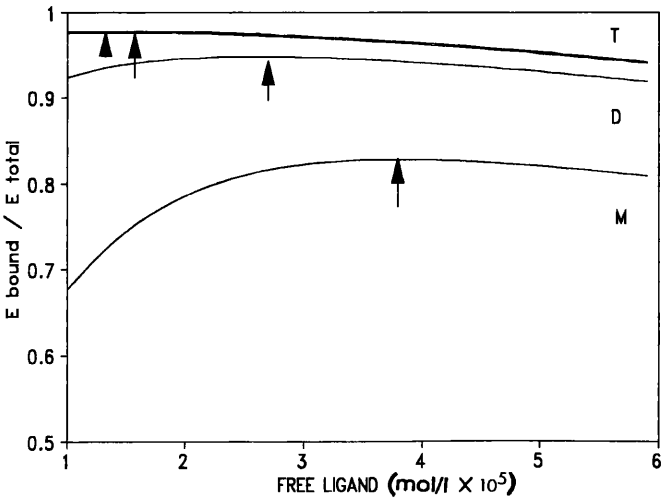

Fig. 4. The predicted effect of multivalent interactions between enzyme and matrix ligand on the relationship between free ligand concentration and fractional binding (association constants as for Fig. 1, bulk average ligand concentration $5 \cdot 10^{-5}$ M). M denotes monovalent interaction, D divalent and T tri- and tetravalent. Arrows denote the free ligand concentration giving maximal fractional binding.

constants for GAPDH as detailed for Fig. 1. The curves obtained as the number of permitted interactions with immobilised ligand is increased from 1 to 4 clearly show a shift towards a lower optimal free ligand concentration together with a masking of the enhancement effect. This was clearly observed in the Sepharose experiments where masking of enhanced binding prevented the identification of an optimum free ligand concentration.

The optimum free ligand concentration in the cellulose experiment was lower than that predicted, indicating perhaps, that even in this case some multivalent interactions were occurring.

No quantitative observations can be made at this stage concerning the levels of binding (which should increase if multivalent interactions are occurring), since the levels observed are much lower than those predicted. This may be due to changes in the intrinsic affinity constants for the interaction of protein with immobilised ligand relative to free ligand, as a result of the immobilisation process. Analysis is further complicated as onlyl a proportion of the immobilised ligand molecules will be in sufficiently close proximity to allow multiple simultaneous interactions with the enzyme. It does, however, clearly demonstrate the trends produced by multiple interactions.

CONCLUSIONS

The results presented demonstrate the occurrence of a liquid phase modification of adsorption capacities arising from the cooperative interaction of free ligand with a multivalent macromolecule. The effect observed is unlikely to be of significance in currently available affinity supports given that it is only observed under conditions of low immobilised ligand density and sub-optimal pH for binding (GAPDH shows optimal binding at about pH 7, but shows no cooperativity in the liquid phase at this pH). However, as both theoretical predictions, and the experimental results presented here suggest that cooperative effects are masked by high localised concentrations of immobilised ligand, it is possible that more significant capacity enhancements might be observed with the soluble supports used in aqueous two-phase partition [10].

In formulating the theoretical relationships described we have only considered the intrinsic cooperative properties of the adsorbate molecule. A more rigourous modelling approach would be needed to take account of the surface cooperative effects as described by Yon [11]. These arise from an increased valency of interaction even where there is no intrinsic molecular cooperativity. The concept of cooperative surface interactions resulting from immobilised ligand "clusters" in orientations suitable for multivalent interactions with a multimeric enzyme has been used to describe the binding of aldolase to phosphocellulose [11,12]. The increased apparent affinity arising from multiple surface interactions is an additional factor which will tend to mask the consequences of liquid phase cooperativity and lead to deviations from the response predicted by simple models. In generating the predictions used in this work we have assumed that the association constants between enzyme and insoluble ligands are similar to those describing the interactions with soluble ligands. Clearly this is a gross simplification even in the case of monovalent interactions with the support. When polyvalent interactions are possible determination of appropriate surface association constants becomes extremely complicated and requires much further work if accurate predictive models are to be developed.

ACKNOWLEDGEMENT

The authors wish to acknowledge the financial support of the British SERC (Grant No. GR/E 32717).

REFERENCES

1 J. Hubble, *Biotechnol. Bioeng.*, 30 (1987) 208–215.
2 S. C. March, I. Parikh and P. Cuatrecasus, *Anal. Biochem.*, 60 (1974) 149–152.
3 D. B. Craven, M. J. Harvey, C. R. Lowe and P. D. G. Dean, *Eur. J. Biochem.*, 41 (1974) 329–333.
4 L. S. Gennis, *Proc. Natl. Acad. Sci.*, 73 (1976) 3928–3932.
5 A. Demiroglou, W. Kerfin and H. P. Jennissen, in T. W. Hutchens (Editor), *Protein Recognition of Immobilised Ligands*, Alan R. Liss, New York, 1989, pp. 71–82.
6 *Whatman Technical Bulletin IE2*, 48–54.
7 D. Eilat and I. M. Chaiken, *Biochemistry*, 18 (1979) 790–794.
8 P. J. Hogg and D. J. Winzor, *Arch. Biochem. Biophys.*, 240 (1985) 70–76.
9 Y.-C. Liu and E. Stellwagen, *J. Biol. Chem.*, 262 (1987) 583–588.
10 J. M. Harris and M. Yalpani, in H. Walter, D. E. Brooks and D. Fisher (Editors), *Partitioning in Aqueous Two-Phase Systems*, Academic Press, Orlando, FL, 1985, p. 590–620.
11 R. J. Yon, *J. Chromatogr.*, 457 (1988) 13–23.
12 R. J. Yon, *Biochem. Soc. Trans.*, 16 (1988) 53.